

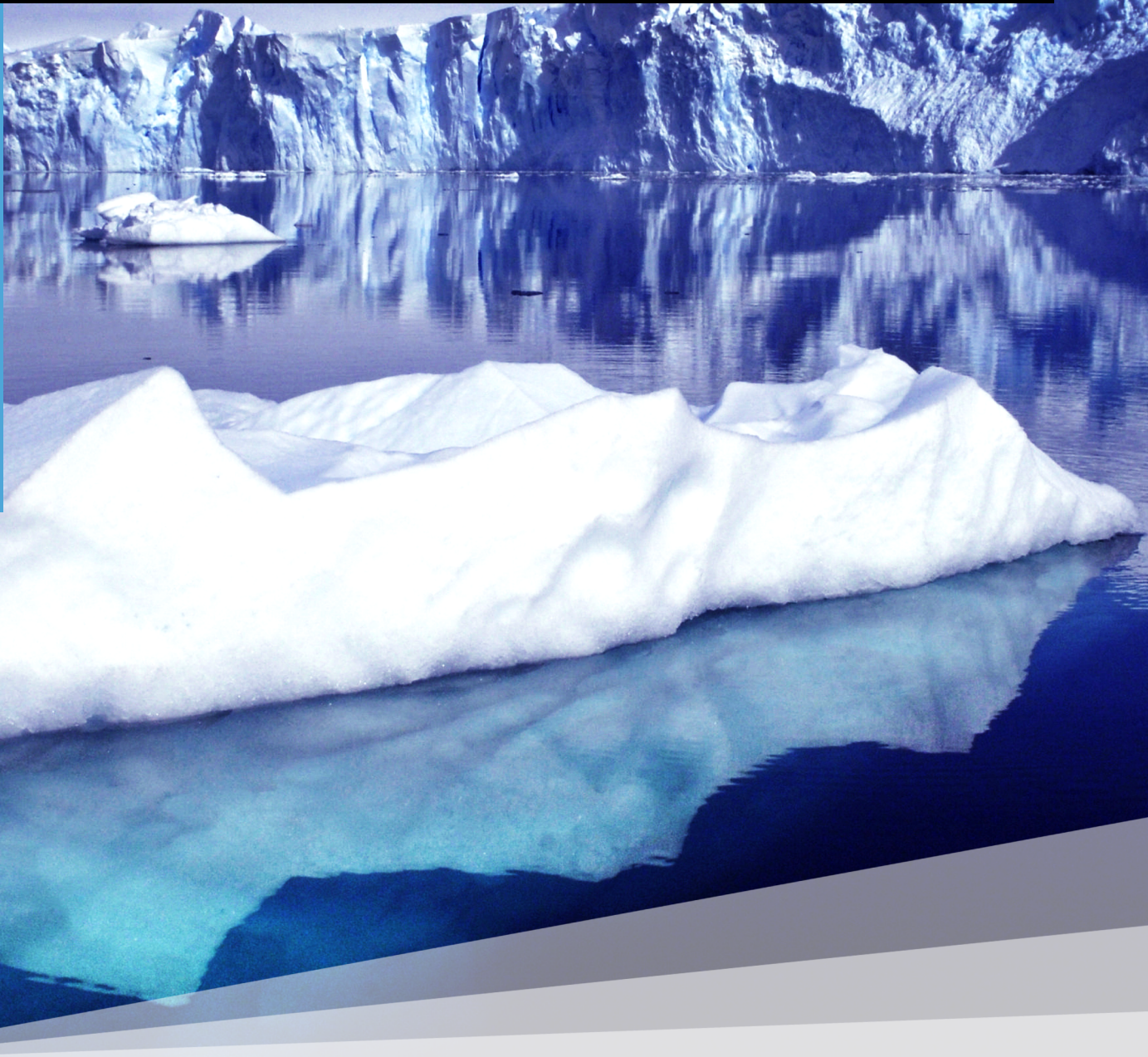
Antarctic Wind Turbines: Windpulse

Design Synthesis Exercise: Group 20

Marthijn Bontekoning	4100867	Stephan Niemansburg	4036883
Sebastien Callens	4152743	Jelle Reinders	4140087
Delphine De Tavernier	4175719	Sofia Ribeiro	4283074
Susan Haasdijk	4031571	Nienke Tange	4013824
Andreas Koshias	4086147	Maaïke Weerdesteijn	4157427

Final Report

Design Synthesis Exercise



Preface

The TU Delft has created a Design Synthesis Exercise (DSE) in order to give the students more project experience in designing. It is the task of the project group to fulfil the requirements of the DSE and come to the best design. This is the final report and it contains the results of the DSE, along with the explanation of the main design decisions. For more technical information and trade-offs the reader should consult the appendices.

This DSE is based on the Project Guide Design Synthesis Exercise 2013-2014 by N. Timmer [1] and this file is used as the main reference for this document. The deliverables of the project were adjusted in agreement to this document, instead of the general requirements of the DSE.

We would like to thank our tutor and coaches, Nando Timmer, Daphne Stam and Weiling Zheng for their guidance and help. Furthermore we would like to thank the British Antarctic Survey for making their wind and temperature data and reports on geology freely available.



DSE Group 20
June, 2014

Summary

This report presents the results of the design phase of the DSE Spring 2014 of the TU Delft. The mission statement of this project is stated as: *The DSE group of the TU Delft will design a wind energy system to meet the power demand of the Signy Research Station in a sustainable way.*

Signy Research station has been occupied since 1947 at which mainly biological research is performed. The island has been declared an important bird area and may not be disturbed in any situations. The research centre on Signy Island is located at the waterfront. It therefore has a maritime climate in the summer, but a continental climate in the winter, due to icing of the surrounding water. The temperature varies between $-38\text{ }^{\circ}\text{C}$ and $10\text{ }^{\circ}\text{C}$, with winds reaching speeds up to 58 m/s mainly from a Southern direction.

The main configuration that was deemed to be the optimum design of the wind turbines given the Antarctic environment and energy purpose was found to be the horizontal axis wind turbine (HAWT). The HAWT design is a lift driven device and as such the most commonly implemented wind turbine system around the world. The main designed system components of the wind energy system designated for Signy Island can be defined as the wind turbines, the battery system and the back-up system.

Based on an intensive analysis, the total amount of required power is estimated to be 50 kW which will be produced by 3 turbines each producing 17 kW . For each turbine, the main components of the rotor, nacelle and tower are designed where the largest attention is put on the most risky components. The designed wind turbine is a variable pitch/variable speed downwind oriented turbine with a diameter of 8.8 m . The airfoil shaped rotor blades have an optimum twist and chord distribution and are internally supported by stiffening elements which are able to withstand all forces exerted on the blades. The blades are made out of a hybrid composites using flax and bio-based epoxy. The rotation of the blades is converted into electrical energy by use of the shaft and a permanent magnet direct drive generator cooled with a passive cooling system. These parts are protected from the environment by a nacelle housing which creates the least amount of drag. The bedplate made of highly recyclable steel alloys transfers the loads of the other components into the tower. A tapered 8.8 m tower is supporting the complete rotor and is designed in such a way that it can handle all load cases. A rock anchor foundation fixes the wind energy system to the ground with 8 anchors with a length of 2 m . The wind turbine design was subjected to fatigue and vibrational analysis as well as an intensive verification and validation.

By adding special features to the turbine, the system is suited to the Antarctic environment. The bird impact is minimized by using one solid black blade and two blank blades to reduce the effects of motion smear. To account for the extremely low Antarctic temperatures, an electric pulse de-icing system is implemented to keep the blades free from ice formation. Due to the height of the wind turbines they are vulnerable to the effects of direct lightning strikes which is dealt with by installing a lightning system. The design is completed by adding sensors used to provide environmental and operational information.

The batteries, back-up electrical generation system and cabling are vital in the provision of power from the system electrical system to the research station. Lead acid batteries with a capacity of 1600 kWh are selected as energy storage system. In case of emergency, the currently present Diesel generator will be used as back-up system which is advised to be replaced in the future by a hydrogen fuel cell system to have a complete zero emission imago. Through the use insulated of cables, the produced energy will be transported to the research station with a power loss smaller than 3% .

Sustainability, environmental impact and cost have been the driving criteria while setting up the manufacturing, transportation and erection plan. Also, the operational aspect of the wind turbine system, as well as the maintenance and logistics has to comply with these aspects. The turbines can only be maintained once a year and are inoperative during the whole winter period.

The electricity cost of the wind energy system designed for the Signy station is estimated to be 0.1402 €/kWh using the total project cost and the annual energy production. Since the energy system is not assumed to make profit and benefits from the high wind conditions, the price per kWh is rather low compared to the competitors available on the market.

Nomenclature

α	Angle of attack [°]	f_K	Ultimate strength [Pa]
β	Twist angle [°]	G	Shear modulus [Pa]
γ	Rotational position of the blade [°]	I	Moment of inertia [$kg.m^2$]; Breaking time
γ_f	Load safety factor [-]	J	Second moment of inertia [m^4]
γ_m	Material safety factor [-]	K_n	Southwell coefficient [-]
θ	Pitch angle [°]	K_t	Stiffness of the shaft [Pa]
θ_T	Optimum twist angle [°]	$K_{x,y,z}$	Curvature about principal axis [m^{-1}]
$\theta_{P,0}$	Blade pitch angle at the tip [°]	l	Length [m]
λ	Tip speed ratio [-]	M	Moment of force [$N.m$]
ρ	Density [kg/m^3]	m	Mass [kg]
σ	Normal stress [N/m^2]	N	Number of blades [-]
σ_d	Design stress [N/m^2]	n_i	Counted number of fatigue cycles [-]
ϕ	Flow angle [°]	P	Power output [kW]
Ω, ω	Rotational speed [rad/s]	P_d	Power Demand [kW]
ω_n	Natural frequency [rad/s]	Q	Torque [$N.m$]
A	Area [m^2]	q	Shear flow [N/m]
AEP	Annual energy production [kW]	R	Radius [m]
a	Axial induced factor [-]	R_c	Resistance per meter [Ω/m]
a'	Tangential induced factor [-]	s_i	Stress level associated with counted cycles
B	Number of blades [-]	T	Trust [N]; Braking torque [$N.m$]
b	Width of skin between consecutive booms [m]	T_d	Design life of the turbine [s]
C_d	Drag force coefficient [-]	t	Thickness [m]
C_l	Lift force coefficient [-]	u_z	Tip deflection [m]
C_n	Normal force coefficient [-]	V	Voltage [V]
C_P	Power coefficient [-]	V_0	Wind velocity [m/s]
C_t	Tangential force coefficient [-]	V_{in}	Cut-in speed [m/s]
c	Drag constant [-]	V_{out}	Cut-out speed [m/s]
F	Prandtl tip loss factor [-]	W	Weight [kg]
$f(V)$	Probability of a certain wind speed [-]		

Contents

Summary	i
Nomenclature	ii
List of Figures	5
List of Tables	8
1 Introduction	9
2 Environmental Analysis	10
2.1 Topography	10
2.2 Climate and Temperature	10
2.3 Wind Resource	11
2.4 Elevation	12
2.5 Ground Characteristics	12
2.6 Wildlife	13
2.7 Flora	13
3 Requirements & Functional Evaluation	14
3.1 Functional Evaluation	14
3.2 Requirement Analysis	15
4 Contingency Management	16
4.1 Schedule Monitoring	16
4.2 Resource Monitoring	16
5 Lay-out Wind Energy System	17
5.1 Base Design	17
5.2 Power Rating & Number of Turbines	18
5.3 Location & Configuration	19
6 Technical Risk Assessment Plan	20
6.1 Process and System Risks	20
6.2 Consequences of Failure	21
6.3 Statistical Analysis: Risk Map	22
6.4 Safety	23
7 Sensitivity Analysis	24
7.1 Velocity	24
7.2 Temperature	25
7.3 Power Demand	25
7.4 Soil Variation	26
8 Environmental Solutions	27
8.1 Bird Impact	27
8.2 De-icing System	28
8.3 Lightning System	29
9 Power and Directional Control	30
9.1 Power Control	30
9.2 Directional Control	31

10 Blade Design	32
10.1 Airfoil Shape	32
10.2 Number of Blades	33
10.3 Geometric Blade Layout	33
10.4 Internal Blade Design	34
10.5 Material	36
11 Nacelle Design	38
11.1 Generator	38
11.2 Cooling System	39
11.3 Structure	39
11.4 Braking System	41
11.5 Rotor Hub	41
11.6 Shell and Cone	41
12 Tower and Foundation Design	43
12.1 Tower Structure Type	43
12.2 Tower Material Type	43
12.3 Tower Sizing for Bending	43
12.4 Tower Sizing Buckling and Compressive Stress Considerations	45
12.5 Tower Deflection	45
12.6 Foundation Type	45
12.7 Foundation Sizing	46
13 Vibration & Fatigue	47
13.1 Vibrational Characteristics	47
13.2 Fatigue	47
14 Verification & Validation	49
14.1 Verification and Validation of Subsystems	49
14.2 Validation of Wind Turbine	53
15 Energy Supply System	55
15.1 Battery Design	55
15.2 Back-up System Selection	55
15.3 Grid Connection Cabling	56
16 System Communication & Hardware and Software Interface	57
16.1 System Communication	57
16.2 Hardware and Software Block Diagrams	58
17 Integration Plan	59
17.1 Manufacturing Plan	59
17.2 Transportation Plan	60
17.3 Assembly and Erection Plan	62
18 Operations, Maintenance and Logistics	64
18.1 Performance Monitoring System	64
18.2 Operations of System	64
18.3 Maintenance of System	65
18.4 Logistics	66
19 Sustainability Implementation and Environmental Impact	67
19.1 Sustainable Development Strategy	67
19.2 Optimised Carbon Footprint	68
19.3 Noise and Visual Impact in Environment	70
19.4 Sustainability Comparison	71
20 Project Cost & Electricity Cost	73
20.1 Levelised Project Cost	73
20.2 Annual Energy Production	74
20.3 Electricity Cost	74

21 Market Analysis	76
21.1 Levelized Cost of Electricity	76
21.2 Wind Turbines Competitors	76
21.3 Sales Market	77
22 Project Design & Development Logic	78
23 Conclusion	79
Bibliography	80
Appendix A Requirements & Functional Evaluation	86
A.1 Functional Break-down Structure (FBS)	86
A.2 Functional Flow Diagram (FFD)	87
A.3 Requirements Discovery Trees (RDT)	88
A.4 Requirements	89
A.5 Requirements Compliance Matrix	91
Appendix B Gantt Chart	92
Appendix C Lay-out Wind Energy System	93
C.1 Trade-off Wind Energy Configuration	93
C.2 Summary Wind Energy System	93
C.3 Power Rating & Number of Turbines	93
Appendix D Risk Analysis	95
D.1 Risk	95
D.2 System Risks	95
D.3 Component Failure Likelihood	96
D.4 Distance Achieved by Fragments During a Catastrophe	97
Appendix E Investigation on De-icing Systems	98
E.1 Black Coating	98
E.2 Special Coating	98
E.3 Electrical Heating	98
E.4 Hot Air	98
E.5 Inflatables	99
E.6 Pulse Electro-thermal De-icing	99
E.7 Trade-off	100
Appendix F Blade Design	101
F.1 Airfoil Trade-off	101
F.2 Airfoil Selection	103
F.3 Rated Velocity	104
F.4 Chord Distribution	105
F.5 BEM Code	105
F.6 Blade Geometry and Loading	106
F.7 Stress Calculations	107
F.8 Deflection Calculations	109
F.9 Blade Materials	110
F.10 Material Selection	110
F.11 Temperature Effects	111
Appendix G Nacelle Design	113
G.1 Bedplate & Shaft Design	113
G.2 Generator Trade-off	115
G.3 Brake and Disk	116

Appendix H Tower and Foundation Sizing	118
H.1 Tower Structure Type	118
H.2 Tower Material Type	118
H.3 Forces, Moments and Load Cases	120
H.4 Load Cases	121
H.5 Bending Stress	121
H.6 Buckling Load	122
H.7 Static Compressive Stress	123
H.8 Tower Deflection	123
H.9 Geotechnical Research	124
H.10 Rock Foundation Types	124
H.11 Rock Foundation Sizing	124
Appendix I Vibrations	126
Appendix J Verification and Validation	128
J.1 Rotor Blades	128
J.2 Nacelle	129
J.3 Tower	129
Appendix K Energy Supply System	130
K.1 Battery Type Options	130
K.2 Back-up Energy System	131
K.3 Cabling	131
K.4 Electronics	132
K.5 Energy Supply Control Strategy	133
Appendix L Hardware & Software Diagram	135
Appendix M Maintenance Task List	138
Appendix N Project Cost & Electricity Cost	139
N.1 Capital Cost	139
N.2 Annual Energy Production	140
Appendix O Model Flow Charts	141
Appendix P 3D Catia	143

List of Figures

2.1	Map of part of Antarctica and the South Orkney Islands	10
2.2	Average temperature Signy Island at the research station between 1992 and 1995	11
2.3	Variance in average temperature Signy Island at the research station between 1992 and 1995	11
2.4	Average wind direction Signy Island at the research station between 1992 and 1995	11
2.5	Average wind speed Signy Island at the research station between 1992 and 1995	11
2.6	Elevation map of Signy Island according to the Antarctic Digital Database (ADD) with a 10 m accuracy	12
2.7	Rock map Signy Islands according to the Antarctic Digital Database (ADD)	13
4.1	Contingency progress during project	16
5.1	Horizontal axis wind turbine [2]	17
5.2	Airborne turbine [3]	17
5.3	Vertical axis wind turbine [4]	17
5.4	Jet engine turbine [5]	17
5.5	Typical weekly load profile in kW of the Signy Research Station measured at 30 second intervals [6] .	18
5.6	Wind energy system location	19
6.1	Annual failure frequency of wind turbine system	21
6.2	Risk map visualisation	23
8.1	Four of the eight patterns tested on bird impact [7]	27
8.2	Pulse electro-thermal de-icing system	28
8.3	External and internal charge transfer [8]	29
9.1	Sketch of an upwind and downwind wind turbine configuration	31
10.1	Wortmann airfoils selected for the blade	32
10.2	Chord distribution from 20% of the root until the tip	33
10.3	Twist distribution from 20% of the root until the tip	33
10.4	Power versus wind speed	34
10.5	Pitch angle versus wind speed	34
10.6	Internal structure of blade showing the stiffening elements	35
10.7	Schematic representation of the internal box sections	35
10.8	Thickness distributions of internal box, black stars indicating final distribution. First thickness distribution represents the distribution after stress design. Second thickness distribution represents the distribution after updating the design for deflection	36
10.9	Von Mises stress throughout the internal box.	36
11.1	Direct drive generator schematic	38
11.2	Height of the upper part of the hole	39
11.3	Result of bedplate optimisation	40
11.4	Result of optimisation	40
11.5	Generator and brake system	41
11.6	The nacelle and subsystems	42
12.1	Radius against height of tower using discrete segments for post-cut-out load case	44
12.2	Thickness against height of tower using discrete segments for post-cut-out load	44
12.3	Stress against height of tower using discrete segments for post-cut-out load case	44
12.4	3D Stress visualisation along tower height using discrete segments for post-cut-out load	44
12.5	Stress against height of tower using discrete segments for pre-cut-out load case	44
12.6	3D Stress visualisation along tower height using discrete segments for pre-cut-out operation	44
12.7	Tower deflection using mean radius for post-cut-out load case	45
12.8	Tower deflection using mean radius for pre-cut-out operation	45
12.9	Rock anchor foundation [9]	46
12.10	CATIA render of the foundation	46

13.1	Campbell diagram, minimum rotational speed 10 m/s	47
14.1	Polars of NACA64418 (tip) at a Reynolds number of 270,000 for Rfoil data, measurement data and corrected Rfoil data	50
14.2	Polars of FX84W218 (root) at a Reynolds number of 700,000 for Rfoil data, measurement data and corrected Rfoil data	51
14.3	Velocity versus power for the tool data and manufacturer data	51
14.4	Graphical results of optimisation	52
14.5	Validation data for the mass of a single blade versus the rotor diameter. Blue dots indicate reference turbines, dotted lines represent relations derived from [10]. The orange marker indicates the designed turbine	54
14.6	Validation data for the top and bottom diameter versus the rotor diameter. Dots indicate reference turbines, with the dotted lines representing the trendlines.	54
14.7	Validation data for the power versus the rotor diameter. Blue dots indicate reference turbines, with the dotted line representing the trendlines.	54
16.1	System communication	57
17.1	Spiral welding technique for turbine towers [11]	60
17.2	BAS research ships	61
17.3	Transportation media	62
17.4	Wind turbine erection	63
19.1	Distance from station and sound pressure level as function of rotational speed	71
19.2	Normalised shadow of turbines [12]	72
20.1	Key elements of costs of wind energy	73
20.2	Cost break-down of the wind turbine components	74
21.1	Competitor map placed with respect to rated power and price per kilowatt hour [13] [14] [15] [16] [17]	77
22.1	Post-design phases activities	78
B.1	Gantt chart	92
D.1	Damage on a wind turbine	97
E.1	Temperature on the blade	99
E.2	Inflatable de-icing system that can be implemented on the wind turbine	99
E.3	Pulse electro-thermal de-icing system	100
F.1	Polars of tip airfoils for clean configuration at $Re = 456388$	102
F.2	Polars of tip airfoils for rough configuration at $Re = 456388$	102
F.3	Polars of root airfoils for clean configuration at $Re = 879902$	102
F.4	Polars of root airfoils for rough configuration at $Re = 879902$	103
F.5	Airfoil curves for the root part of the blade at $Re = 879902$ in clean and rough configuration	103
F.6	Airfoil curves for the tip part of the blade at $Re = 456388$ in clean and rough configuration	103
F.7	Polars of FX84W218 at a Reynolds number of 700000 for Rfoil data, measurement data and corrected Rfoil data	104
F.8	Schematic representation of the structural box dimensions	106
F.9	Normal stress throughout the internal box (Pa), for the design loads considered. Blade twist and deflections are also included.	108
F.10	Shear stress throughout the internal box (Pa), for the design loads considered. Blade twist and deflections are also included.	108
F.11	Z-deflection of blade under design loads with safety factor 2. The zero-value on the x-axis corresponds with the blade tip.	109
F.12	Von Mises stress throughout the internal box (Pa), for the loads sustained at maximum wind speed of 75 m/s with blades pitched towards the wind. Blade twist and deflections are also included.	109
F.13	Orientation of principal axes	109
F.14	Blade cost for small wind turbine blade with different Carbon/Flax ratio's. [18]	111
G.1	Maximum Von Mises stress acting on each section	114

G.2	Impression of the bedplate	114
G.3	Maximum Von Mises stress acting on the shaft	115
G.4	Generators in trade-off [19]	115
G.5	Disk brake layout [20]	116
H.1	Yield strength of structural steel S355 at temperatures 20 °C - 950 °C [21]	119
H.2	Modulus of elasticity of structural steel S355 at temperatures 20 °C - 950 °C [21]	119
H.3	Forces acting on wind turbine	120
H.4	Forces and moments on a tower segment	122
H.5	Simplified model of tower for deflection analysis with Castigliano's Theorem	124
H.6	Rock foundation types	125
I.1	Campbell diagram	127
J.1	Deflection of a beam with constant stiffness and a uniform loading	129
J.2	Visual representation of the booms of the cross-section	129
K.1	Permanent magnet synchronous generator electrical scheme [22]	132
K.2	Energy storage system	133
L.1	Overview of energy production until rated velocity L.1a and after rated velocity L.1b	135
L.2	Overview of cooling system	136
L.3	Overview of de-icing system	136
L.4	Overview of brake system	136
L.5	Batteries & back-up system	137
N.1	Costs throughout lifetime	140
N.2	Wind speeds at the Signy station	140
O.1	Blade computational model flowchart	141
O.2	Nacelle (left) and tower (right) computational model flowchart	142
P.1	3D CATIA Model	143

List of Tables

2.1	Maximum and minimum temperatures and maximum and average wind speeds for 1992-1995	11
7.1	Key factors used for the sensitivity analysis	24
7.2	Changes on rotor, nacelle and tower design when the velocity is changed	24
7.3	Changes on noise, maintainability and cost of the project when the average velocity changes	24
7.4	Changes on rotor, nacelle and tower design when the power demand changes	25
7.5	Changes on noise, maintainability and cost of the project when the power demand changes	25
10.1	Rotor blade characteristics	34
10.2	Relevant parameters for internal blade box	36
11.1	Parameters generator	39
15.1	Battery sizing	55
15.2	Cable length and thickness	56
19.1	Total carbon footprint	70
20.1	Total cost	75
C.1	Trade-off table design options	93
C.2	References turbine sizes	94
C.3	Total power, number of turbines and power per turbine for reference research stations	94
D.1	Annual failure frequency	96
F.1	Error applied on the Rfoil data for the tip, root and middle airfoil	104
F.2	Properties of the different materials considered [23], [24], [25], [26] [18]. The composites have a fiber volume fraction of 60%. The cost values were averaged from available ranges and can differ for each manufacturer. They should be considered as relative values for cost.	110
F.3	Resulting designs for the different materials. The energy consumption values result from analysing different types of blades as described by [27]. The values are to be considered relatively for comparison of the different materials. No values were available for Aluminium 2024-T3. The value for glass blade was based on comparisons described by [18] The composites have a fiber volume fraction of 60%.	111
G.1	Optimisation results I-beam	114
G.2	Trade-off CS and DD	115
G.3	Parameters generator	117
H.1	Advantages and disadvantages of lattice tower and tubular tower	118
H.2	Low temperature steel alloys properties [28]	119
I.1	Tower natural frequency	127
I.2	Natural frequencies	127
J.1	Verification data between the developed and provided BEM code	128
J.2	Comparison numerical and analytical results structural blade analysis	128
J.3	Comparison numerical and analytical results structural bedplate analysis	129
J.4	Comparison numerical and analytical results tower analysis	129
K.1	Battery properties [29]	130
K.2	Cabling	132
M.1	Preventive maintenance of the wind turbine subsystems	138
N.1	Wind turbine component cost	139

1. Introduction

The Antarctic region, covering twenty percent of the Southern Hemisphere, is a priceless asset to the world with its unique wildlife and can provide great insight for all those studying climate change and the climate systems of the Earth. The Arctic regions are very important for regulating the climate and sea level rise, as they hold a huge reservoir of water. Due to its importance, thousands of scientists and supporting staff live and work in research stations at various locations in Antarctica. One of these research stations is the Signy Research Station located on Signy Island. The station has been occupied since 1947 and mainly biological research is performed. For the research operations, a proper energy source is required.

The objective of the Design Synthesis Exercise (DSE) of the TU Delft is to design an Antarctic wind energy system to power the Signy Research Station, controlled by the British Antarctic Survey (BAS), in an environmentally friendly way and by withstanding the harsh climate of Antarctica. The final wind turbine system design, named *Windpulse*, is presented in this report.

In Chapter 2, an analysis of the environment is done, which plays an important role in the design process of the wind turbine. It covers the topography, climate, temperature, wind, elevation, wildlife and flora of Signy Island. In Chapter 3, the requirements are checked with a compliance matrix and the functions of the system are evaluated. In Chapter 4, an update to the contingency management plan is presented. In Chapter 5, the design options considered, the power rating, number of turbines and the location and configuration of the wind turbines system are covered. In Chapter 6, the project and system risks and its consequences are discussed. In Chapter 7, the sensitivity analysis of the wind turbines system is presented. In Chapter 8, environmental solutions regarding icing of the blades and bird impact are described. In Chapter 9, the power control as well as the directional rotation control systems are covered. In Chapter 10, 11 and 12, the rotor blade design, nacelle design and tower and foundation design are dealt with, respectively. In Chapter 13, the fatigue characteristics and vibration characteristics of the system are described. In Chapter 14, the verification and validation procedures for the rotor, nacelle and tower design are covered. In Chapter 15, the energy supply system consisting of the battery system, back-up system and grid connection cabling are described. In Chapter 16, the system communication and hardware and software interfaces are presented. In Chapter 17, the manufacturing, transportation and erection plans are covered. Once the turbine is erected, it can start its operational lifetime. In Chapter 18, the operations, maintenance and logistics are discussed. In Chapter 19, the sustainability implementation and impact on the environment, including the carbon footprint of the system are presented. In Chapter 20, the electricity cost and project costs are described. In Chapter 21, the market analysis and comparison with equivalent wind energy systems are presented. In Chapter 22, the project design and development logic are discussed, covering which steps need to be taken in the future to finalise this wind energy system design.

2. Environmental Analysis

In order to design a wind energy system designated to provide energy for a research station comparable to the size of the Signy Research Station at Signy Island of the British Antarctic Survey (BAS), environmental aspects need to be taken into account. In Section 2.1 the topography of Signy Island is described. Section 2.2 covers general information on the climate at Signy Island. The wind speed and directions are elaborated upon in Section 2.3. The elevation of the island is discussed in Section 2.4. Section 2.5 deals with the ground characteristics. The wildlife and flora are discussed in Section 2.6 and Section 2.7, respectively.

2.1 Topography

Signy Island is an island of the South Orkney Islands, within the Antarctic region, situated in the South Atlantic Ocean. The South Orkney Islands lie on the southern limb of the Scotia Ridge. Signy Island is located at a latitude of $60^{\circ}43'$ S and a longitude of $45^{\circ}37'$ W. Figure 2.1 presents a map of a part of Antarctica and a closer view on the South Orkney Islands where Signy Island is located. The red square and orange square represent the Signy Research Station on Signy Island controlled by Great Britain and the Orcadas Base on Laurie Island controlled by Argentina, respectively. Laurie Island is not covered by this project. Signy Research Station is located in Factory Cove, Borge Bay, close to the waterfront where the surface is characterised by a rock bottom.

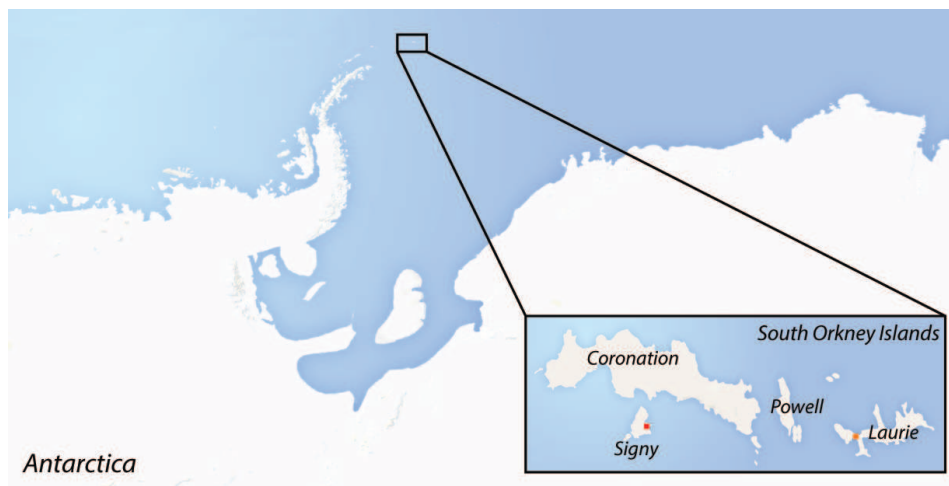


Figure 2.1: Map of part of Antarctica and the South Orkney Islands

2.2 Climate and Temperature

Signy is usually covered with ice and attached to the continent of Antarctica by ice. This makes the climate more continental than if it was not connected. Signy deals with strong winters with low temperatures and clear skies. The brightest sunniest days occur in November and December with increased levels of UV light. The summer is from November to March. The high icy plateaus on the island remain even in high summer times when the climate of Signy becomes more a maritime climate and the ice packs retreat. Low clouds cover the sky and cause frequent, but no heavy rainfall. Since Signy lies north of the Antarctic circle, it is never subjected to 24 hour days or nights. The Sun is below the horizon for a minimum of 4-5 hours at midsummer. [30]

Temperature data is obtained from the British Antarctic Survey Signy Research Station [31]. This research station has been a summer only station since 1996 [32]. The wind energy system to be designed is meant to provide energy the year around. Thus the temperature, and the humidity determine what external conditions the wind energy system has to survive. Therefore the temperature variation for the entire year is needed. This temperature data is only available before 1996, when the station was occupied the entire year. For the most accurate data every hour of the day for an entire year the temperature data is measured and covers the years 1992, 1993, 1994 and 1995. The represented temperature data below is the average dry-bulb temperature. Dry-bulb temperature is the measured air temperature by a thermometer which should be shielded from sources of radiant heat. It is considered the most direct measurement

of air temperature. [33] Figure 2.2 shows the average temperatures per month between 1992 and 1995. The maximum average temperature is reached in summer in February and in December. A significant drop in temperature occurs in midwinter. The absolute maximum and minimum temperatures are found in Table 2.1. The variance in average temperature for each month for the years 1992 to 1995 is shown in Figure 2.3. There is a large variance in average temperatures, from 1.6 °C in January to 9.0 °C in September. In the wind energy design, a sufficient safety factor needs to be incorporated regarding maximum and minimum temperature, due to the large variations in temperature.

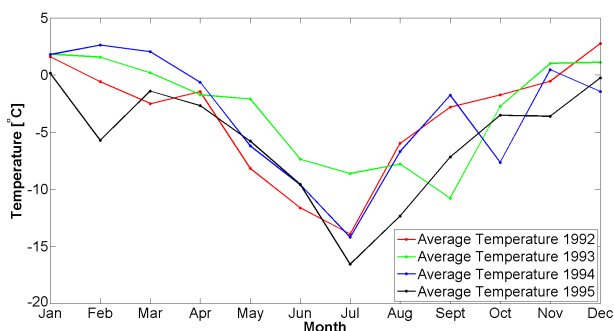


Figure 2.2: Average temperature Signy Island at the research station between 1992 and 1995

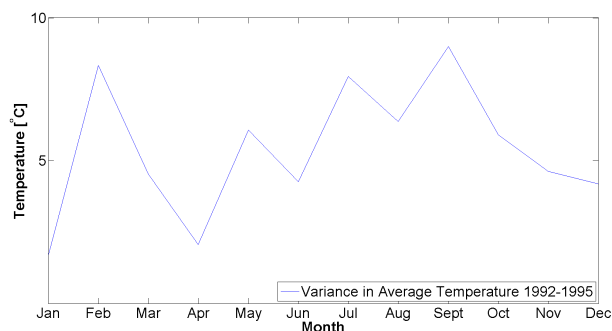


Figure 2.3: Variance in average temperature Signy Island at the research station between 1992 and 1995

2.3 Wind Resource

The wind data is also obtained from the British Antarctic Survey Signy Research Station and covers the years 1992, 1993, 1994 and 1995 for the same reasons mentioned above. The average wind directions and the average wind speeds of every month of the year have been plotted for the four subsequent years. From Figure 2.4 it can be seen that the wind directions vary between south, south-east and west direction. Zero degrees in Figure 2.4 is defined as wind coming from the north. Figure 2.5 shows that Signy is extremely windy. The averages vary between 10 m/s and 23 m/s. The magnitudes of the extreme wind speeds are found in Table 2.1. The average wind speed taken over each year is slightly increasing with time. The extreme winds in November 1995 have a large contribution to this trend. However, since it is data of only over 4 years, this trend may not be existing.

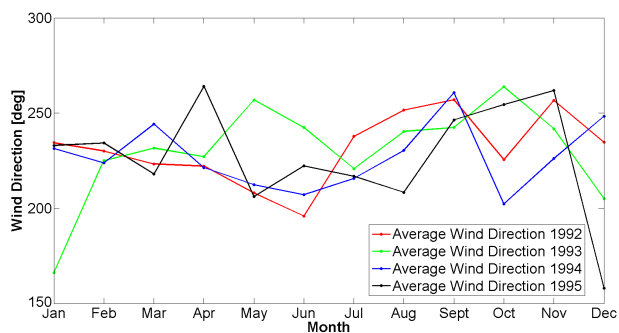


Figure 2.4: Average wind direction Signy Island at the research station between 1992 and 1995

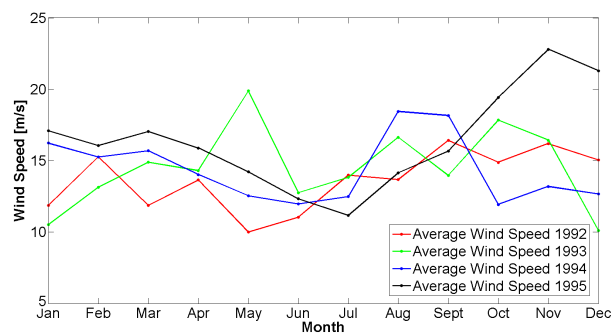


Figure 2.5: Average wind speed Signy Island at the research station between 1992 and 1995

Table 2.1: Maximum and minimum temperatures and maximum and average wind speeds for 1992-1995

Year	Maximum temperature in °C	Minimum temperature in °C	Maximum wind speed in m/s	Average wind speed in m/s
1992	10	-28	51	13.7
1993	10	-27	49	14.5
1994	10	-37	58	14.4
1995	8	-38	56	16.4

2.4 Elevation

Signy Island covers an area of 19.9 km^2 . The island stretches 6.4 km north to south and 4.8 km along the southern coast. The highest peak on the island, Tioga Hill, reaches a height of 276 m . Other summits rise to a height of over 245 m . The hill tops are generally flat or gently convex. The main upland part forms a plateau covered with a thin layer of permanent ice. Around the coasts of Signy Island there is lowland, with an elevation generally lower than 30 m above sea-level. At the north-western part of the island the terrain consists of drift-covered slopes below 90 m . Offshore rocks and small islets lower than 20 m above sea-level are characteristic for the west coast. [34]

A detailed overview of the elevation of Signy Island is shown in Figure 2.6a and the elevation map of the area surrounding the Signy Research Station is shown in Figure 2.6b, both obtained from the Antarctic Digital Database (ADD). The values in the maps are given in meters. Each line starting at the coast indicates an increase in elevation of 10 m . Where the lines are closer to each other, the landscape is characterised by steeper slopes. The Signy Research Station is represented with the red square.

The elevation at the Signy Research Station is of special importance, since the wind energy system will be placed relatively close to the station. Placing the wind energy system far away from the station would increase the length of the cable that transports the energy to the station and thus the costs. Also, it would have a negative influence on the maintainability and transportation of the system due to the hills that summit land inwards of the station and the remoteness of the land in general. From Figure 2.6b it can be seen that the area surrounding Signy Research Station is relatively flat. The elevation increases when going land inwards.

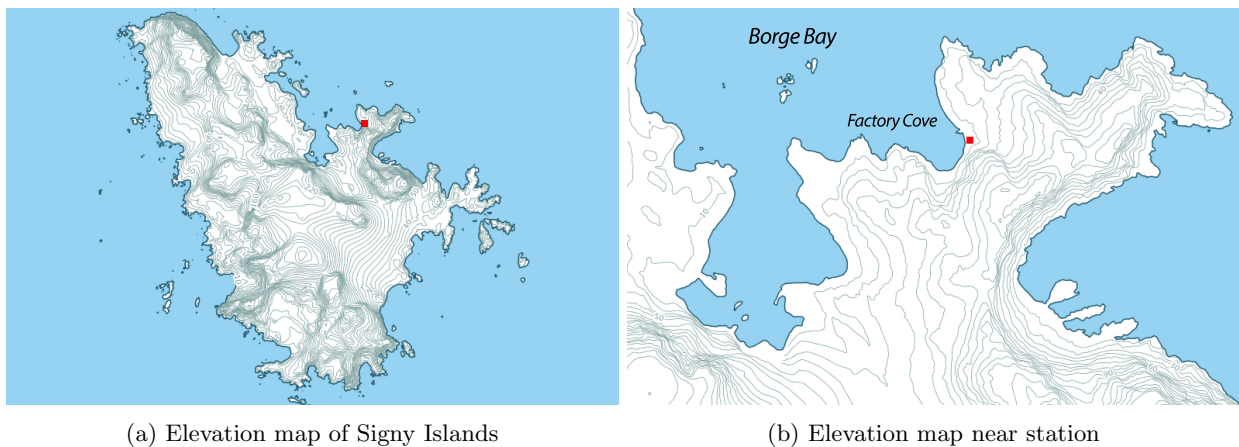


Figure 2.6: Elevation map of Signy Island according to the Antarctic Digital Database (ADD) with a 10 m accuracy

2.5 Ground Characteristics

An overview of the rock bottom on Signy Island is shown in Figure 2.7a and the rock map of the area surrounding the Signy Research Station is shown in Figure 2.7b, both obtained from the Antarctic Digital Database (ADD). The Signy Research Station is again represented with the red square. The brown area indicates the shallow rock bottom. The white area indicates the ice cap, where sometimes the rock bottom protrudes the ice cap. Signy Research Station is located near the coast in Borge Bay on a rock bottom. This is convenient for the foundation design of the wind energy system, since the ice cap is subjected to movement while the rock bottom is stagnant.

Over one-third of Signy Island is covered with a permanent ice cap. The solid rock floor protrudes through the ice cap, since it is a thin cap. There is relatively little movement between the two main glaciers, the Orwell Glacier and the McLeod Glacier due to small drainage basins. Most ice tongues that drain the central plateau are relatively stagnant. The lowlands, where Signy Research Station is located, are ice-free during summer. During winter there can be a layer of ice of over 1 m near the research station. The rocks exposed on the island are quartz-mica-schists, amphibolites and marbles.

Quartz-mica-schist is a highly anisotropic metamorphic rock. Landslides occur in schistose rocks due to the inherent weak nature of the schistose planes. This presents geotechnical challenges in construction projects. The anisotropic strength and deformation properties of the rocks need to be taken into account for a safe and reliable design. The properties of the quartz-mica-schist would introduce a challenge in the foundation design. Luckily these rocks mainly

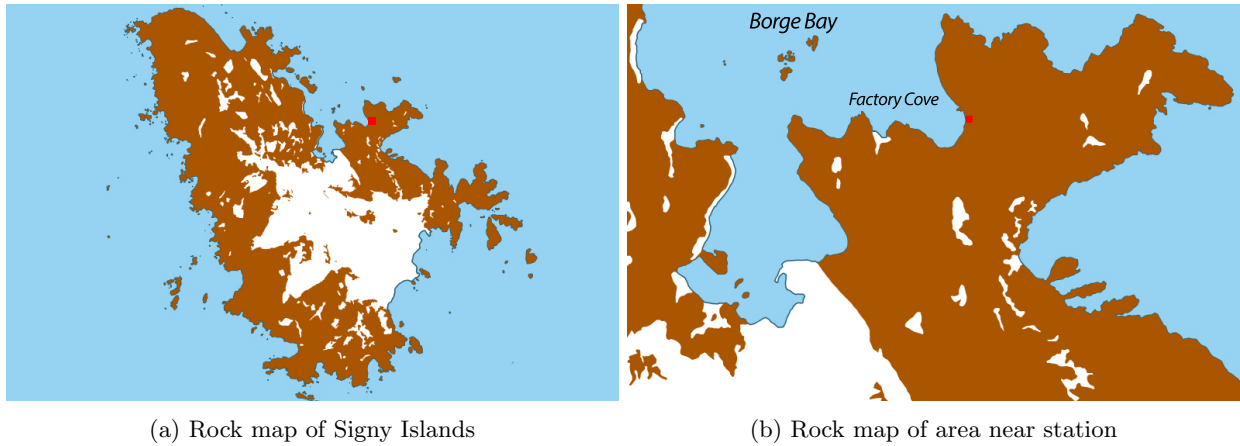


Figure 2.7: Rock map Signy Islands according to the Antarctic Digital Database (ADD)

form the bottom of Signy Island in the south-west and south-east, and not in east where the station is located. The amphibolites form the rock bottom in the ice-free part of the central plateau of the island. Outcrops of marble are present at the west and east side of the island, west from Borge Bay, as well as on higher grounds in the north. Amphibolites are dominant in the rock bottom of the area near Signy Research Station at Factory Cove. Therefore, it is important to have a comprehensive understanding of the characteristics and properties of amphibolites. [34], [35], [36]

The ground beneath the sea close to the station at Factory Cove consists of sand and gravel [37]. The rock bottom above sea-level is mainly characterised by amphibolite. Amphibolite is a metamorphic rock. Metamorphic rocks are shaped by pressure, heat and chemical processes while buried deep in the Earth's surface. Amphibolites have a density of approximately 3.0 g/cm^3 and a porosity of 2.0%. The compressive strength is 250 MPa [38]. Amphibolite has a high hardness and is therefore suitable as structural foundation. [39]

2.6 Wildlife

Marine predators are the dominant inhabitants of Signy. Penguins cover the largest population of the seabirds. The Gentoo, Ad'lie and Chinstrap penguin breed on the island in such extensive colonies that the island is identified as an Important Bird Area (IBA) by Birdlife International. There are twelve other species that breed on Signy and there are a number of species observed that breed on islands nearby. The main predator of the penguin is the seal, of which there are over 20,000 on Signy Island. The only seal that pups on Signy is the Elephant seal. The Weddell seals pup on the sea-ice and other species of seal are observed on the ice floes to hunt penguins. Large number of fish are found near Signy. The underwater habitats consist of both hard and soft bottom areas. Amphipods, anemones, sea squirts, tube worms, brachipods, limpets, starfish, sponges and sea cucumbers are especially common. One type of insect that can survive the freezing is the wingless fly. It was accidentally brought to Signy and it has spread to an area of over 7500 m^2 and occurs in densities of up to several thousand per m^2 . [30]

2.7 Flora

Mosses, liverworts and lichen cover large surfaces of the Signy Island. The mosses mostly occur on the lowlands and may become 2 m thick and over 5000 years old. Fur seals have destroyed large parts of the moss banks where it is replaced by green algae. The two types of flowering plants are the Antarctic hairgrass and the Antarctic pearlwort. [30] All flora and fauna are protected by the protocol on Environmental Protection to the Antarctic Treaty and environmental impact should be kept at a minimum. [40]

3. Requirements & Functional Evaluation

In this chapter the requirement analysis and functional evaluation, realised in the baseline report, will be summarised. The functional evaluation was used to understand what is expected of the system to be designed and can be found in Section 3.1. A requirement analysis was performed in order to make sure the requirements of all the stakeholders are met when the design is finished and can be found in Section 3.2.

3.1 Functional Evaluation

The functional evaluation has a top-level perspective. It only treats the *functions* of the system. It does not, however, provide or hint to a specific solution. For the functional break-down structure and the functional flow diagrams depicting this chapter, the reader is referred to Appendix A. The high level functions including brief expansions are stated below.

Provide Energy: The ultimate goal of the system is to provide energy to the station and is thus the top level of the functional evaluation. To achieve this goal the systems should be able to produce energy, withstand loads, store energy and transport energy.

1. **Energy Production:** Within this function both the extraction and conversion of energy from wind to electrical power as well as the control flow of the energy produced is encompassed.

- (a) *Extract Energy:* In order to produce energy, firstly it is necessary to extract energy of the wind.
- (b) *Convert Energy:* The system must be able to convert the extracted wind energy into electrical energy.
- (c) *Control Energy Production:* The production of energy must be a controllable process in order to keep the production between acceptable limits.

2. **Withstand Loads:** The structure has to withstand the loads originated by its aerodynamic functions and wind interactions but also from other external and internal loads grouped under the "Non-Aerodynamic Loads" heading.

- (a) *Withstand Aerodynamic Loads:* The structure should be able to withstand aerodynamic loads created by both pressure differentials and vibrations caused by the rotation of the blades.
 - i. *Withstand Pressure Loads:* The system must withstand loads created by the pressure differentials.
 - ii. *Withstand Aerodynamic Vibrations:* The system must be able to withstand vibrations caused by the movement of the system that is created by its aerodynamic functions and interaction with the wind.
- (b) *Withstand Non-Aerodynamic Loads:* The system must be able to support and withstand all non-aerodynamic loads, including but not limited to structural impacts, structural weight and weather.

- i. *Control for Structural Safety:* The system must have a means of control to ensure structural integrity from possible failure threats and allow for safe execution of possible maintenance tasks.
- ii. *Withstand Non-Weather Impacts:* The structure has to withstand or prevent impacts caused by wildlife such as birds.
- iii. *Support Weight:* The structure should support the weight of the entire system.
- iv. *Withstand Weather:* The system must be able to withstand the effects of all forms of weather that it will be exposed to in its environment.

- A. *Prevent Corrosion:* The system must not allow corrosion to instigate failure.
- B. *Support Weight Increase:* The system must be able to support the possible increases and fluctuations of weight caused by ice and precipitation build up.
- C. *Withstand Precipitation Impacts:* The system should be able to withstand precipitation impacts such as hail, ice pellets, and graupel.
- D. *Withstand Temperature Changes:* The system must be able to withstand both quasi-static compression and expansion effects, such as thermal coefficient differences between materials, but also possible dynamic effects such as fatigue growth due to temperature changes.
- v. *Withstand Non-Aerodynamic Induced Vibrations:* The system has to be able to withstand non-aerodynamic induced vibrations, within/induced by mechanical components, and within/induced by electrical components.

3. **Store Energy:** The energy should be gathered in a storage system and regulated.
4. **Transport Energy:** To provide electrical power to the station, the electrical energy should be transported from the system that produces energy to the storage and from the storage to the station.
 - (a) *Transport to Storage:* The system must enable transport of energy from point of creation to the storage system.
 - (b) *Transport from Storage:* The system must enable transport of energy from the storage system to the station.

3.2 Requirement Analysis

Before determining the stakeholders of the project, first its mission station is repeated: *The DSE group of the TU Delft will design a wind energy system to meet the power demand of the Signy Research Station in a sustainable way.* All requirements are used to realise this mission.

3.2.1 Stakeholders

The *client* was defined as the British Arctic Survey (BAS) of the *British Government* which recognises the *Arctic Treaty Party*. This treaty party, of which it is stakeholder itself, sets rules and guidelines for activities on Antarctica. Other environmental agencies, such as Greenpeace are also considered stakeholders. In addition the *researchers* also have vested interests in Antarctica. But the project also has consequences to the *research community* as a whole, because it facilitates the research and its outcomes on Signy Island. Finally, possible *investors* and the *support team*, taking care of the maintenance, are considered stakeholders to the project.

3.2.2 Requirements

Using requirements discovery trees, see Appendix A.3, all necessary requirements are captured. A dichotomy was made between technical requirements and constraining requirements. For the full list of requirements, the reader is referred to Appendix A.4. In this section only the driving and killer requirements are stated. For the requirement compliance matrix, see Appendix A.5.

Driving Requirements

- **REQ-CO-4:** The wind energy system shall leave no visible trace above the surface of the Antarctic continent after its end-of-life.
- **REQ-CO-5:** A waste management plan shall be constructed for the entire life cycle of the wind energy system.
- **REQ-CO-6:** The wind energy system shall have a carbon footprint with a CO_2 equivalent smaller than the current power system averaged over its entire life cycle.
- **REQ-TE-1:** The wind energy system shall be able to continuously meet the power demand of the Signy Research Station.
- **REQ-TE-12:** The wind energy system shall have an energy storage system capable of providing power at 65% of the average power for three consecutive days.
- **REQ-TE-15:** The maintenance of the wind energy system shall be limited to one major session per year.

Killer Requirements

- **REQ-CO-3:** The wind energy system shall adhere to the legal constraints and regulations imposed by the Protocol on Environmental Protection to the Antarctic Treaty.
- **REQ-CO-7:** The total cost of the wind energy system shall not exceed € 500,000, excluding battery systems.
- **REQ-TE-2:** The structure shall withstand the aerodynamic loads obtained at an average wind speed of 15 m/s with gusts of maximum 75 m/s during its entire lifetime.
- **REQ-TE-3:** The structure shall withstand a temperature range of minimum -50° and maximum 20° during its entire lifetime.

4. Contingency Management

In the beginning of the project a contingency management plan was presented. In this report an update will be given and it will be shown that a sufficient margin is left for further development. The contingency plan was focused on schedule and resource monitoring. It followed the planning of the Gantt chart (see Appendix B) of the project plan, as requirement *REQ-CO-8* states.

4.1 Schedule Monitoring

It was chosen before to use a simplified version of Earned Value Management (EVM). This entails comparing planned deliverables versus received deliverables during the project. This was done on daily bases at the end of every working day. The Gantt chart in Appendix B was used as a guidance for the planning. No significant problems were encountered with this planning. Most of the time the group was on schedule and therefore had more time for writing the report. Also, the required time for each task fitted well in the planned time. Only little extra time outside the scheduled hours was needed to meet the deadlines thanks to an efficient working environment and good communication.

4.2 Resource Monitoring

Due to the multi-component nature of the system and interconnected properties of the components, a simplified Technical Performance Measurement (TPM) was chosen as a monitoring system of the resources. The only two resources leading to multiple iterations were mass and thrust. The other resources could be implemented more easily.

Mass: The mass of the subsystems was the main driver of iteration between the subcomponents of the turbine. In Figure 4.1a the development of this parameter can be seen. It can be seen that the mass was predicted too high in the beginning. Mainly, because most of the available reference data was focused on larger turbines. In week 7 it was discovered that a safety factor of 10 was needed to comply with fatigue requirements. The mass of the foundation is excluded from the mass contingency management, since it did not show fluctuations.

Drag: The drag is the horizontal force acting on the tower. The force is dependent on the rotor diameter and the size of the nacelle. Optimisations have been performed, resulting in a decreasing drag force, see Figure 4.1b. Thrust was also considered but was found to be negligible in comparison.

Power Generation: As can be seen in Figure 4.1c the power was most of the time quite stable. In the beginning it was not yet decided that the required power would be divided between three turbines. In the last weeks the effect of the cables and yaw system was included, showing a decrease in power.

Fatigue Characteristics: The fatigue characteristics were not taken into account the first weeks of the project. After an analysis on this was done, it was concluded that a safety factor of 10 was needed to comply with constraints. This resulted in a higher mass of the structure.

Maintainability: All parts were designed while taking maintainability into account. No iterations were needed to improve maintainability.

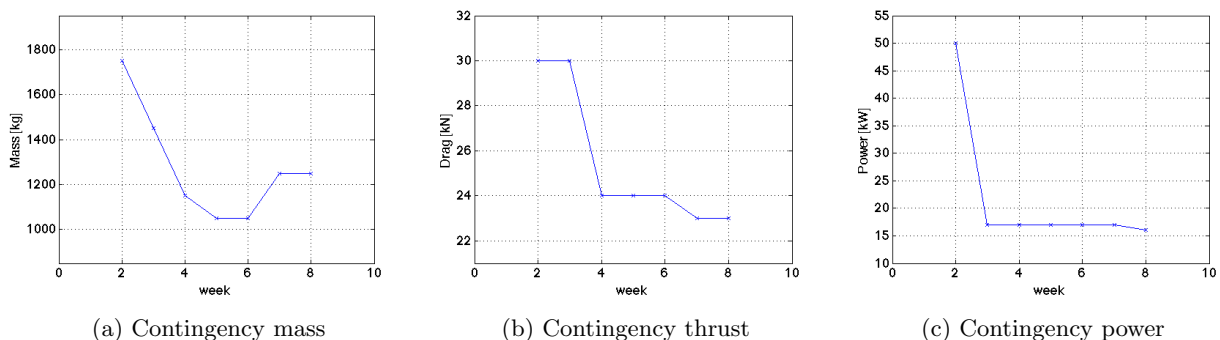


Figure 4.1: Contingency progress during project

5. Lay-out Wind Energy System

Since Signy Island is one of the most windy locations in the world, the free available wind is a perfect source to base the energy production on to power the research station. Wind energy systems appear in different shapes and configurations. By performing a trade-off, a base design is selected on which the whole design process is established in Section 5.1. Additionally in Section 5.2, the final power rating and the amount of energy producing systems are discussed. Finally, the main subsystems are shortly introduced together with their relative location with respect to each other in Section 5.3.

5.1 Base Design

After detailed design trade-off, the configuration selected to operate within the hostile Antarctic environment was that of a horizontal axis wind turbine (HAWT). The HAWT design selected is a lift driven device and as such is the most commonly implemented wind turbine system around the world [41] [42]. This configuration was deemed to be the optimum design given the environmental conditions and defeated vertical lift, vertical drag designs, airborne turbines and jet engine turbine configurations in the detailed trade-off phase. The trade-off table can be found in Appendix C.1.



Figure 5.1: Horizontal axis wind turbine [2]



Figure 5.2: Airborne turbine [3]



Figure 5.3: Vertical axis wind turbine [4]



Figure 5.4: Jet engine turbine [5]

In terms of feasibility and reliability the HAWT was seen as the best choice of all the options. This was because the HAWT design has already been successfully implemented in Antarctica and has been applied numerous times in various configurations all around the world [41] [42] [43]. Due to the wealth of experience associated with this design being implemented on such a vast scale, in addition to the steady refinement of design methodology within the wind energy sector, the HAWT is deemed to be the safest choice in terms of reliability. Furthermore in terms of size, the HAWT design leads to a smaller design solution than equivalent power drag driven devices. This is due to having a higher maximum theoretical efficiency. Only the airborne and jet engine devices can be seen as being capable of being made smaller due to the higher wind speeds which they can experience. However, such devices are considered to be in the experimental phase and as such performed significantly worse in terms of reliability, feasibility and maintainability. Moreover in terms of maintainability of the system, the HAWT is seen to perform well. This is because maintenance check procedures have been well established for such systems due to the large scale implementation of the technology. The vertical axis systems are considered more easily checked as they tend to have their generators on the ground. However such designs have had greater fatigue concerns [44]. In terms of costs, the HAWT is seen to be the best due to its wide scale production, benefiting from the experience curve resulting in a reduction of cost each year [45]. Finally, in terms of sustainability and environmental concerns the vertical axis systems are seen to produce less noise than the HAWT system. However due to noise naturally caused by the large wind speeds found at the Signy location this is not seen as a prohibitive factor [46]. Also the HAWT is seen to have a relatively low carbon footprint due to the refined manufacturing processes associated with it as stated above.

In conclusion the lift driven HAWT system was taken to form the basis of the design with further configuration changes applied during the detailed design of the turbine as described in preceding chapters. An overview of the complete turbine set-up along with vital subsystems is shown in Appendix C.

5.2 Power Rating & Number of Turbines

The design of the wind energy system to provide power to the Signy Research Station is intensively influenced by the required power rating and the number of turbines. Therefore, it is important to make a good estimation at the beginning of the design. In this section, the obtained power rating will be discussed followed by the selection of the number of turbines.

5.2.1 Power Rating

Currently the Signy station is only operative during summer and has a capacity of 8 persons. However, in the future the station can be expanded to accommodate more people and become operative during the whole year. The wind energy system will thus be sized considering the future perspective. Combining the reference stations and the current installed and used power, an initial estimate of the required wind power is made to be 50 kW taking into account losses.

Different research stations spread over the whole Antarctic continent are investigated. The installed power of the Belgian, Great-Britain, German and Australian station are used to make the power estimation for the Signy station. The installed power varies from 100 to 250 kW and is shown in Appendix C.3. The electrical load of the equipment is coupled to a seasonal and daily occupation. Additionally, the loading is also influenced by the station size and the present number of crew members. The more researchers occupying the station, the more power is needed to be produced. The recently built Belgian station is of special interest for this project mainly based on its size and zero emission strategy, and thus serves as one of the major references. 100 kW of power is installed for a maximum crew size of 48 persons. The reference scientific polar station Princess Elisabeth Antarctica, became operative in 2009. The station is the first polar base that combines eco-friendly generation unit, clean and efficient energy use and optimisation of the station's energy consumption. Two renewable sources, solar and wind, provide the zero emission Princess Elisabeth Antarctica station of free energy.

Figure 5.5 shows a typical weekly load profile during a manned period of the current existing Signy Research Station measured at 30 second intervals. It displays the power consumption corresponding to a crew size of 8 persons. It is clear that large fluctuations are present between the intervals. However, the general behaviour displays 7 clear highs and lows corresponding to day and night. The average loading can be estimated to be around 17 kW. The British Antarctic Survey is contacted regarding the actual power demand and the installed power at the Signy station. The Signy station is currently powered by a 40 kW Diesel generator of which 75% is used during normal operations.

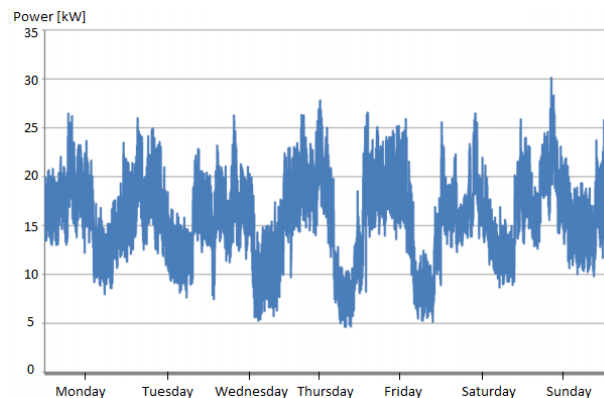


Figure 5.5: Typical weekly load profile in kW of the Signy Research Station measured at 30 second intervals [6]

5.2.2 Number of Turbines

The estimated power of 50 kW can be produced by one large turbine or by multiple small turbines. For this project, it turned out that 3 turbines each producing 17 kW is preferred based on reference Antarctic research stations and a exerted trade-off.

In Appendix C.3, the total power, number of turbines and the power produced by one turbine is shown in a summary table for multiple reference research stations. For the smaller research centres generally smaller wind turbines are used than for the large stations. The power produced by one turbine lies between 6 and 30 kW. From the trade-off, it came out that 3 turbines is a great balance. The selection of number of turbines is supported by the following factors:

- **Redundancy:** A maximum of 17.5 kW can be missed resulting in a minimum of 65% of the rated power. This cannot exceed the power that can be lost if one turbine is not operating.
- **Maintenance:** When using multiple turbines, more and smaller parts should be inspected during each maintenance session. However, the components of the turbines are more easily accessible when utilising smaller systems.
- **Manufacturing:** More material is required when multiple turbines are used. This results in a more costly and less sustainable design. However smaller machining tools, such as molds and autoclaves, are required to manufacture the parts.
- **Transportation:** A large system would require complicated transportation. When using three turbines, a standard container can be used.
- **Installation:** When choosing a single turbine, only one turbine has to be installed. However, small systems need less technology to assemble.
- **Electrical Components:** For each turbine, electrical parts are required. These parts are costly, even small power components.

5.3 Location & Configuration

When considering the wind energy system designed for Signy Island, the various system components can be defined as the wind turbines, the condition monitoring system, the battery system, the research station and the back-up system. In the subsequent chapters of the report these subcomponents will be handled. The placement of the various energy subsystems effects how the components interact with each other and the environment, both during construction and normal operations. The location of the system components relative to each other can be seen in Figure 5.6.

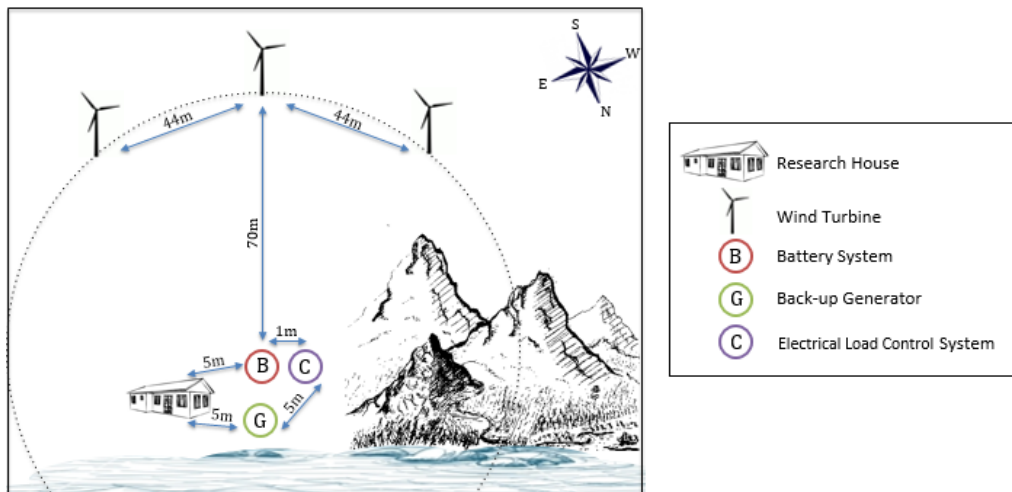


Figure 5.6: Wind energy system location

The research station is directly connected to the battery and the back-up system, with the electrical configuration. The battery system, determined in Section 15.1, is placed in an isolated room located 5 m away from the research station. The back-up diesel generator, found in Section 15.2, is also placed at a distance of 5 m from both the research station and the monitoring system. Due to the noise requirement found in Section 19.3 the turbines are placed 70 m from the research station. In order for the turbines to independently operate and to not negatively interfere with each other they are placed at a distance of 44 m apart, 5 times the radius of the turbines. [47] [48] [49] The turbines are situated to the south of the research station. This is because to the east of the station the land available spans less than the required distance, thus violating the noise requirement. Furthermore, the station is situated on a north facing coast and as such there is no landmass further north where the turbines can be placed. Finally, to the west of the station there is a steep hill, making placing turbines on there impractical for construction reasons. In addition, placing the turbines on top of the hill would increase the required cable length and thus increase the costs and the power losses, it would decrease the structural safety of the cable if placed going up and down the steep side of the hill and would interfere more with the environment due to the extra cable and insulation placement across the island. In addition as the wind generally comes from the south, south-east and south-west directions, as expanded in Section 2.3, placing the wind turbines south of the station allows for the spectrum of the wind directions to be captured by the energy system.

6. Technical Risk Assessment Plan

In order to fully evaluate if a design is a suitable system solution, designs must also be assessed on the various risks that are imposed due to their specific implementation. The definition risk can be defined as the *uncertainty of attaining a specific goal or requirement*" [50]. Risk can also be seen to stem from the interaction of the likelihood of failure and the severity/consequence of a given failure, which can be represented visually in the form of a risk map. The likelihood of failure relates to the probability that a given concept or component will fail, which generally related with the level of maturity of the given technology, while the severity of failure is seen as how a given failure type effects the mission requirements. It must be noted when making a risk analysis, that maintainability possibilities of the system should also be considered. In this chapter, the technical risks of the wind energy system will be discussed. Section 6.1 encompasses a discussion of the possible process and system risks, followed subsequently by Section 6.2 on system and environmental consequence of a failure. The chapter is concluded by a quantitative visualisation of the risk analysis in the form of a risk map. This chapter in conjunction with subsequent chapters on manufacturing (Chapter 17) and the power control characteristics of the system(Chapter 9) cohesively form the Reliability Availability Manufacturing and Safety (RAMS) of the wind turbine system design.

6.1 Process and System Risks

The risks which may occur during the lifetime of the wind energy system can be categorised in process or system risks. The process risks contain the production, transportation, assembly and maintenance. In the system risks, the likelihood of failure for the wind energy system components are discussed.

6.1.1 Process Risks

During the entire life-time of the wind energy system, different processes have to be performed which each consist of risks. The risks corresponding to the production, transportation, assembly and maintenance of the turbine are discussed below.

- **Production Risks:** During manufacturing, production lines/methods should minimise the risks to the system, such as through the minimisation of production defects. Although risks will always be present, it is assumed that production risks will be higher for concepts that have not yet been produced, unless concepts have specific production risk advantages within their design. It should also be noted that different components will differ in production risks simply because designs will have limited options for production technique they are able to utilise due to geometry and/or materials selected. For the tower and nacelle structural elements, it is of vital importance during the alloying process that the material meets the required chemical composition with low levels of residual elements otherwise the structural performance will be lower than required in the cold climate. Due to the hand lay-up process used in producing the blades, special attention must be focused on the placement of the lay-up for correct fibre orientation in order to create an omnidirectional composite. Even slight misalignment of the lay-ups will result in drastic loss of material properties leading to failure of the components. Furthermore during resin application ensuring that no voids are created is again of vital importance for the structural performance of the composite.
- **Transportation Risks:** Considering the size and weight of the system, the transportation is an important part of getting the system operational. Transportation risks include the possible vibrations induced into the parts and the damage that can be caused from the various transfer of parts during transportation. As the various subcomponents are shipped in large vessels, induced vibrations are unlikely to be a problem. The most problematic segments of transportation are the loading and off loading of components. This is especially true when considering off loading the components onto the final smaller work boat where damage from knocks may occur if the waters are not calm or the attention of the crew members lapses during the process. Furthermore due to the smaller nature of the workboat as compared to the larger ships used for transportation, induced vibrations can become more of a problem and as such special care must be taken with bounding the tower components.
- **Assembly Risks:** Once the parts are in Antarctica they need to be assembled. The assembly process adds risks to the system itself. Such risks include possible crack formations, deformations, or even complete failure of parts if extremely complex system assembly processes are needed. As the vertical gin pole tower raising system is used for erection, special care must be taken so as not to induce loads on the system which will cause permanent deformations and as such lead to sub par performance or failure of the system during normal

operations. The risks included in using such a system include the possibilities that the tower is not adequately supported during raising. Furthermore erection and assembly should be avoided during times of adverse weather conditions, such as storms, however such risks are still present if there are sudden gust of winds during planned assembly operations.

- Maintenance Risks:** These include all risks to the system, be it to the electrical systems, structural components, or any other components, due to the execution of maintenance tasks. These risks increase with increasing complexity of maintenance tasks and the frequency at which these maintenance tasks must be carried out. There is a risk that major system components can be damaged during maintenance if maintenance is carried out carelessly or in adverse weather conditions, and as such must be planned and carried out with extreme care. Such risks carry significant burden as they can result in damage of parts which cannot be replaced until subsequent maintenance activities and as such result in large turbine downtime.

6.1.2 System risks

The likelihood of failure for the system components can be seen in Figure 6.1 with a discussion of values found below. The reader is advised to refer to Appendix D for additional discussions on risks.

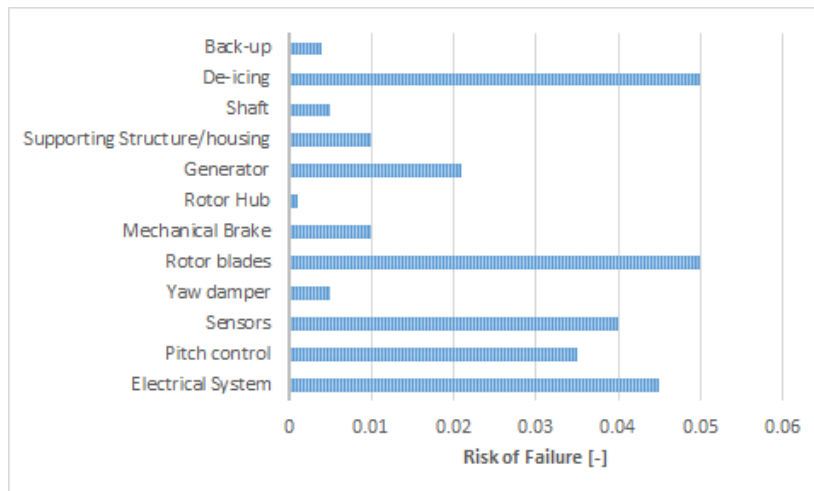


Figure 6.1: Annual failure frequency of wind turbine system

The values shown in Figure 6.1 are estimated using multiple sources of wind turbine failure rate data combined with extrapolations for the given wind turbine design [51] [52] [53] [54] [55]. The values are adapted in order to more accurately reflect the size of the wind turbine in question as many sources give indications for larger wind turbines where failure rates are higher [56]. In addition, due to the reduced complexity of using a passive yaw system, the rate of failure of the yaw mechanism is considered lower than that of traditional active yaw systems. Moreover as a direct drive system is used, greatly reducing the complexity of the drive train, a lower probability of failure is estimated, as reflected by the low failure frequency value of the shaft. On the other hand the use of a direct drive generator increases the risk of generator failure due to the level of maturity of the technology being less than that of traditional turbine generators. Due to the harsh environmental conditions present on Signy Island, including low temperatures and high winds, the estimates of failure for the blades and supporting structure are on the higher end of the spectrum as opposed to traditional turbines. This is also due to the fact that the blades use an innovative combination of materials and as such the level of maturity of the materials are seen as less than their conventional counterparts. However as can be seen in the subsequent risk map, this is not of issue in terms of risks. It should be noted however that although the values reflect the average annual failure frequency over the whole lifetime, such values change depending on the age of the turbine. This is backed by empirical evidence showing that the failure frequency of components during the first year of operation are close to zero as opposed to the same systems during the end of their lifetime [56]. This suggests that failures can be mitigated with extensive maintenance activities, keeping components close to their manufactured state, and as such the annually planned maintenance activities will be used to minimise the frequency of failures.

6.2 Consequences of Failure

The risks of failure in one of the processes or components may have large consequences on the rest of the system or on the Antarctic environment. The possible consequences of an occurring failure are enumerated below:

- **System Failure:** A failure of one of the turbine components might imply that a complete turbine fails. Since three turbines are designed due to redundancy, the consequences of one failed turbine should not need to be categorised to be really severe. With one turbine off, there is still enough energy available for the basic needs of the station inhabitants and researchers.
- **Human Safety:** During operation and all stages before, the wind energy system might not bring humans in danger. At Signy station, researchers are living close to the turbine site. If one of the turbines fails, it is important that the researchers do not experience life-threatening events.
- **Wildlife Safety:** Not only the human safety should be insured but also the safety of the wildlife. At Signy Island, the wildlife is observed and thus an interruption with the normal behaviour of the wildlife has to be avoided. Also due to failure, this might not become the case. For example, fire might drive the wildlife away resulting in the loss of the utility of the station.
- **Emission:** During transportation and production some emissions are present which will increase if extra parts need to be manufactured and transported. This is an unlikely consequence of failure since the aim of the project is to be as sustainable as possible and to have a zero emission energy source.
- **Noise Disturbance:** If some of the energy system components fail an increase in noise might occur. This consequence might influence the wildlife and humans living on Signy Island. Humans are really sensitive for noise which might make the life on Signy unacceptable. The animals might leave the Island if they are too disturbed in their daily life.
- **Waste:** Failures during production, assembly and transportation implies most of the time waste of material. If a component is not useful by for example made inaccurately, a new part should be manufactured. If parts have to be remade, the sustainability of the system also decreases.
- **Cost:** Failure of parts always results in higher costs. Parts might be replaced or parts should be remade. Additional material and working hours have to be paid, increasing the product cost. If the turbines are not running, no energy is produced which means that the system is not producing its estimated annual energy production (AEP). This will consequently lead to an increasing energy cost. Since Signy Island is a remote location, an inspection on-site or a transportation to that location is not easy nor priceless. To use an individual transportation method, a high cost price will be assigned to this.

6.3 Statistical Analysis: Risk Map

Within this section a visual representation of operational failure risks will be presented through the use of a risk map. The risk of each separate component is estimated by combining the likelihood of failure with the severity/consequence of a given failure. Such reference data is deemed important in order to give insight into areas which may need extra attention to meet maintenance and failure requirements *REQ-TE-15*. The risk map is formed using statistical information on failures of conventional wind turbines adjusted to correspond to the Antarctic wind energy situation.

It is interesting to see that most components are found within the lower risk area (bottom left), and no components are found in the high risk area (top right). This is due to the fact that the designed wind turbines are designed in such a way to minimise risk. Additionally a lot of information and experience is available for a horizontal axis wind turbine, even in the Antarctic environment. In fact, a component with extreme failure consequences has a very small probability and vice versa. This highlights an important design methodology, where the designers have chosen to use higher quality parts for components which would cause significant consequences, and thus reduce risk. The most risky components are the electrical system consisting of the cables, transformer and converter, the generator, the mechanical brake and the back-up system. A visual representation of the risk map can be found in Figure 6.2. The risks associated with the components are separated into three major groups in relative terms, low, medium, high, represented by the colour differences in the risk map, going from light to dark respectively.

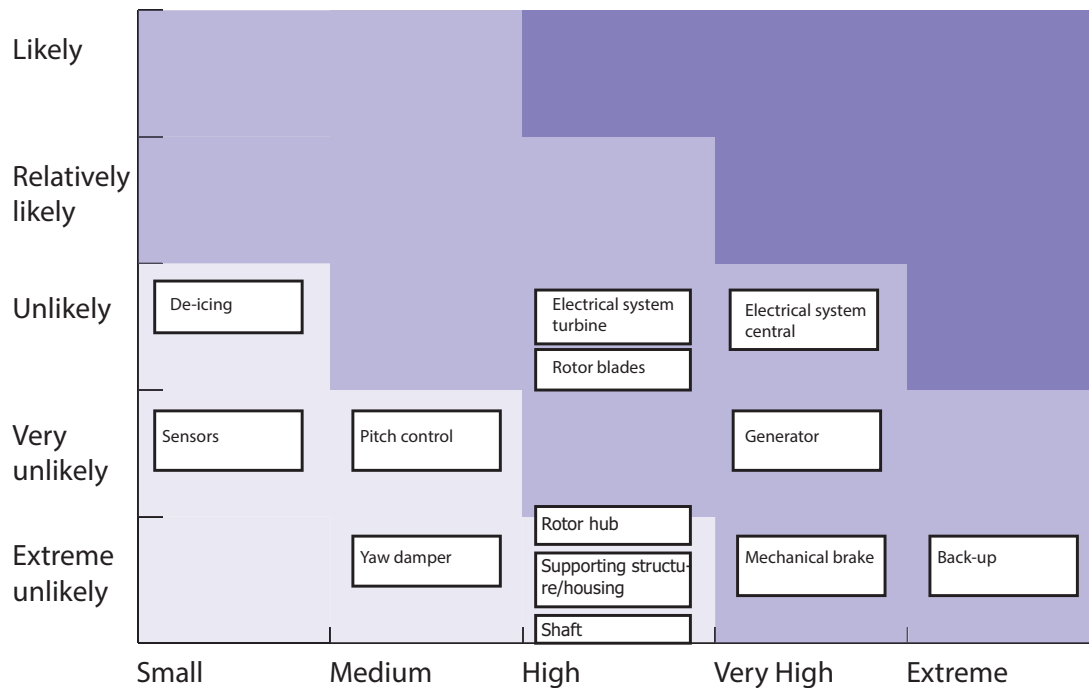


Figure 6.2: Risk map visualisation

6.4 Safety

The safety of the wind turbine system is closely related to the risks. A widely used definition of safety is *'the freedom from hazards to human and equipment'* [57]. For the Signy research station this definition should also include the freedom from hazards to flora and wildlife.

The main hazard is structural failure of the system. This can damage the flora, wildlife and research facilities. In the design method of all these components a safety factor of 10 is applied. Moreover, for the weather condition the worst case scenario is used to calculate all the stresses. Calculations were conducted to ensure no fragments of the wind turbine would reach the research station or cause damage in case of failure and can be found in Appendix D.4 thus fulfilling *REQ-CO-11*. In addition redundancy is applied to even lower the safety risks. One of the main important safety considerations are the brakes. Two types of brakes are applied, both fail-safe, to ensure an emergency stand still when needed. Furthermore all materials are chosen such that there will be no health issues for the scientists or wildlife. The resin of the blade and shell material can be toxic. However when the production is executed in the right way there will be no consequences. During the production a vacuum bagging is used to ensure no health issues during the curing. When the blades and shell are finished there will be no safety issues of the material any more. At the end-of-life disposal all the wind turbine parts except the foundation are removed from the island to guarantee the safety after usage. The batteries are made from lead acid and lead can be extremely toxic. That is why the batteries will be in an insulated area. This will prevent the batteries to crack due to the cold and will also be to ensure the safety of the environment.

In conclusion the wind turbine system is designed in a way that the researchers, equipment, wildlife and flora are protected from hazards. This is done by applying both safe life and fail-safe design methodologies, through the use of safety factors, conservative worst case calculation values, in conjunction with redundant components.

7. Sensitivity Analysis

In this chapter the performed sensitivity analysis is presented. Sensitivity analysis is defined as "the study of how the uncertainty in the output of a mathematical model or system (numerical or otherwise) can be appointed to different sources of uncertainty in its inputs" [58]. The sensitivity of the design will represent the effects that changing certain input parameters have on the requirements and the ability to meet the requirements. In the following sections a sensitivity analysis is performed for important parameters as velocity, power demand, temperature and soil variation and their effect on the requirements related to sustainability (that incorporates the carbon footprint and noise), maintainability and cost. The sensitivity of the design is evaluated to changes in these parameters of 25%. The reference values of the design can be found in Table 7.1.

Table 7.1: Key factors used for the sensitivity analysis

<i>Rotor+Nacelle</i>	<i>Tower</i>	<i>Total</i>
Diameter of rotor: 8.8 <i>m</i> Wing box mass: 9 <i>kg</i> Mass of rotor & nacelle: 509.7 <i>kg</i>	Mass: 738.5 <i>kg</i> 0.0763 < Radius (<i>m</i>) < 0.3189	Mass: 1248.2 <i>kg</i> Cost: € 642,000

7.1 Velocity

The design was evaluated on changes to velocity by simulating a change in rated velocity of 25% both above and below the reference value. The results of this analysis can be seen in Tables 7.2 and 7.3, followed by a discussion on the design changes.

Table 7.2: Changes on rotor, nacelle and tower design when the velocity is changed

<i>Input</i>	<i>Rotor+Nacelle</i>	<i>Tower</i>
25% increase in <i>V</i>	Diameter of Rotor: 7.9 <i>m</i> Wing box mass: 5.7 <i>kg</i> Mass of rotor & nacelle: 508.7 <i>kg</i>	Mass: 710.2 <i>kg</i> 0.074 < Radius(<i>m</i>) < 0.307
25% decrease in <i>V</i>	Diameter of rotor: 9 <i>m</i> Wing box mass: 10.7 <i>kg</i> Mass of rotor & nacelle: 517.8 <i>kg</i>	Mass: 744.6 <i>kg</i> 0.077 < Radius(<i>m</i>) < 0.322

Table 7.3: Changes on noise, maintainability and cost of the project when the average velocity changes

<i>Input</i>	<i>Noise [%]</i>	<i>Mass [%]</i>	<i>Cost [%]</i>
25% increase in <i>V</i>	-5.5	-2.4	-0.6
25% decrease in <i>V</i>	1.1	1.1	0.2

As can be seen from the above results, as the rated velocity increases the required blade diameter to achieve the same power output decreases by 11% to 7.9 *m* and this causes a change in blade mass. Due to the lowered rotor mass the nacelle mass decreases. However this decrease is only 0.2% as the generator is the main contributor to the nacelle mass. There is a bigger drop in tower mass. However as through the reduction of blade size, the dominant factor is the drag force at survival speed which decreased and as such the tower radius can also decrease. When combining the effects it can be seen that a total decrease of mass of the system is equal to roughly 2.5%. It should be noted that this percentage would likely increase during more detailed design phases due to the snowball effect, were smaller components such as connectors and singular components could be sized more accurately to reflect the mass decrease [57]. For a decrease of rated velocity, the same principles apply as those stated above, with shifts in diameters and masses in the opposite direction. The results of these shifts are stated in Table 7.2 and Table 7.3.

The noise level is calculated at 70 *m* from the station. In terms of noise, an increase in rated velocity resulted in a bigger change in noise level than a decrease in velocity, see Equation 19.1. This is due to the fact that noise is linked to rotor diameter and the magnitude of change of rotor diameter for the two cases is different. This in turn stems from the fact that only rated velocity is changed and the other parameters of the power curve are not changed leading to

such a result. Once the maximum allowable noise at the station of 40 $dB(A)$ is reached, the distance between the wind turbine farm and the station has to be increased, not the noise requirement. Thus for a decrease in noise level the wind turbines must be placed further away, this requires increasing the cable length and higher power losses, although these are small for such changes.

In terms of maintainability, such small changes in design parameters are unlikely to cause any modifications in maintenance procedures and cost changes, and as such is not sensitive to these changes. The same can be said for such changes in terms of sustainability, although having a smaller or larger rotor diameter will impact the environment in terms of visibility and manufacturing carbon footprint, such small changes are negligible. Only if the rated velocity increase or decrease are extreme both sustainability and maintenance would come into play, where different procedures and manufacturing techniques should be concerned.

The cost are directly related with the production, manufacturing and material cost. A linear relation can be found with the amount of material used to each part: rotor, nacelle, tower and foundation. A relation between production costs and the amount of materials used was made for each part in order to calculate the changes on the total cost. It is logical that for an increase in velocity the total costs decrease by only a small amount because all the materials costs had decreased while the generator, back-up system and batteries had remain the same, which are the main cost contributors. In the same way when the velocity decrease is 25% the cost also increase due to overall increase of materials. Due to small changes in cost the requirement defined is still considered valid.

7.2 Temperature

When increasing the temperature with 25% the air density decreases from 1.3185 kg/m^3 to 1.2982 kg/m^3 and when decreasing the temperature with 25% the air density changes to 1.3201 kg/m^3 . The influence of this difference is very small; the variance on the blade radius is lower than 5 cm and so the noise is approximately the same. Also the loads are very close to the ones taken in the design and so the cost of the wind turbine is only slightly different. The maintainability sessions during the year will not need to be changed.

For a large increase in temperature (average temperature of 10 $^{\circ}C$) the cost of the project would be lower. This is because the resins used for the composites materials and also the steel and others metals used would be cheaper due to its higher availability on the market. A much higher temperature will also have a beneficial effect on the foundation design, since the isolation material for the concrete can be decreased lowering the material use. The need of a de-icing system would disappear as well, making the production easier and less costly.

7.3 Power Demand

The design was also evaluated on changes to the power demand by simulating a change in the required installed power capacity of 25% both above and below the reference value. The results of this analysis can be seen in Tables 7.4 and 7.5, followed by a discussion on the design changes.

Table 7.4: Changes on rotor, nacelle and tower design when the power demand changes

<i>Input</i>	<i>Rotor</i>	<i>Nacelle</i>	<i>Tower</i>
25% increase in P_d	Diameter: 9.5 m Wing box mass: 10.4 kg	Mass: 623.9 kg	Mass: 757.4 kg $0.0780 < \text{Radius}(m) < 0.3273$
25% decrease in P_d	Diameter: 7.9 m Wing box mass: 5.5 kg	Mass: 407.7 kg	Mass: 709.7 kg $0.074 < \text{Radius}(m) < 0.307$

Table 7.5: Changes on noise, maintainability and cost of the project when the power demand changes

<i>Input</i>	<i>Noise [%]</i>	<i>Mass [%]</i>	<i>Cost [%]</i>
25% increase in P_d	3.9	10.7	12.8
25% decrease in P_d	-5.5	-10.5	-12.5

When analysing the results for changes in power, it can be seen that when the required power increases by 25%, the rotor diameter increases by 8%. This in turn causes an increase in mass of the nacelle. However, this increase in mass is mainly due to the fact that a larger generator must be used and as such has a larger mass. The combined effects of both a larger total mass and an increase in drag, due to larger blades, results in a tower weight increase of roughly 3%

and a change in root radius of 10 *mm*. The total mass change of the system is then equal to 10% mainly due to the increase in generator weight. Again it should be noted that the percentages are likely to increase due to the snowball effect when components go into a more detailed design phase [57]. The same principles hold true for a required power decrease, however with changes of parameters in the opposite directions.

In terms of noise both power changes cause similar percentage changes in noise level however the small differences are explained by the non-linear changes on the rotor diameter. When considering the increased noise level on the original requirements, it can be seen that the wind turbines must be placed further away from the research station due to these changes. This will in turn also cause an increase in cable length and also increased power losses. On the other hand when considering the decreased noise level, it can be said that the wind turbine farm can be placed closer the station, reducing the cable length and power losses.

In terms of maintenance again for such relatively small changes, the maintenance procedures will not change. However, if the design would be subjected to larger changes, causing a significant change in generator size, both maintenance procedures and costs would be subjected to an increase. This is especially true in the case that the required power changes in orders of magnitude, due to the link of higher component failure with higher turbine size/power rating [56]. On the other hand, there is a much more significant link with required power changes and sustainability of the design. Firstly the required battery storage capacity needs to be increased, this increases the carbon footprint of the whole system. Furthermore although the back-up generator currently used would be able to handle a 25% increase of required power output, if this number were to increase more, a larger back-up generator would be required, which also increases to both the carbon footprint and the costs. In addition when more power is required, the carbon emissions from the back-up generator would also increase as it is linked to the *kWh* required.

The cost of the project changes significantly for 25% of increase and decrease on the power demand. These differences are explained in part by the small changes on the manufacturing and production costs on the blades, nacelle and tower, due to difference in diameter of the rotor, but the most significant contribution is because the size of the batteries and generator has to be adapted. Although the increased turbine costs still meet the current turbine cost requirements, further increases in the required power output would require the cost limit placed on the wind turbine to be changed.

7.4 Soil Variation

If the soil turns out to be of a different type, the foundation of the design will have to be adapted. However this is very unlikely as both amphibolite rock bottom and other rock bottoms found in the Antarctic location are very good for foundation purposes. If the design were to be adapted to another location, where the soil is not rock, the foundation type should be different. For softer soils, spread footing is the best option. This option requires more material thus will be less sustainable. This option is widely used which implies lower costs and as such provides some benefits. Maintainability will be the same because both foundation types do not require much maintenance during the turbine lifetime. If the soil strength is lower than expected a larger foundation is needed with more concrete, anchors and steel. This will of course result in both increases in costs and a decrease in sustainability, and as such the foundation design is sensitive to this parameter.

8. Environmental Solutions

The wind turbines are located in a very specific environment. The wind turbines should cope with the harsh climate and at the same time, the turbines should not affect the surrounding untouched nature. In this chapter, several solutions are presented to cope with these matters. In Section 8.1 the method to decrease the bird impact is presented. Section 8.2 shows the system to cope with the icy environment and Section 8.3 presents the lightning system.

8.1 Bird Impact

Birds can have difficulty seeing structures, therefore collision of birds with wind turbines occur. The concern about bird strikes increases on Signy Island since the goal of research is to find out more about the behaviour of birds, but also because the Antarctic Environmental Protocol has to be conformed. This protocol states that every institution entering the Antarctic's should work with a minimum environmental impact [40]. Twelve flying birds species breed on Signy Island and 27 species visiting the island have been recorded [59]. However, in order to design a solution that prevents bird strikes into wind turbines, the view field of birds need to be researched.

8.1.1 View of Birds

The visual information birds extract from their environment is different from the visual information extracted by humans for the same circumstances. The retina, physiological optics, visual fields and the visual information processing for primates and birds differ. One explanation for avian collisions with wind turbines is that birds cannot simultaneously survey the ground for prey and monitor the horizon to avoid obstacles. But this explanation seems unlikely for the following three reasons. Birds can keep good acuity in peripheral vision. They have two foveal regions. Their fovea is responsible for sharp central vision. Birds can keep objects at different distances simultaneously in focus on the retina. Another explanation is the reduced visibility of the blades due to motion smear. An image of an object becomes blurred as the object moves with increasing speed. Motion smear occurs at the tip of rotor blades of wind turbines and increases when the observer moves closer to the wind turbine. When the observer is too close to the wind turbine that the retina cannot process the information of the velocity of the blades, the blades will become transparent. [60], [7]

8.1.2 Bird Impact Solutions

There are two options to reduce the effects of motion smear to reduce avian collisions into wind turbines. One solution is to make use of UV-light or near-UV-light. However, research on the reduction of avian collisions using UV-light is currently being conducted and results have not yet been made available. The second solution is to maximize the time between successive stimulations of the same retinal region. This can be accomplished by painting patterns on the blades. The colour and spatial patterning of the background has a major impact on the visibility, as well as the angle of approach of the bird. A research has been performed on which type of pattern is the most effective. Eight patterns have been tested, of which four are presented in Figure 8.1. It was concluded that one solid black blade and two blank blades are twice as visible than three black blades, for a three-bladed wind turbine and this is the most effective of the patterns tested. Additionally, painting one blade black is the simplest to produce which makes it also the most cost-effective, so this method will be used. [7]

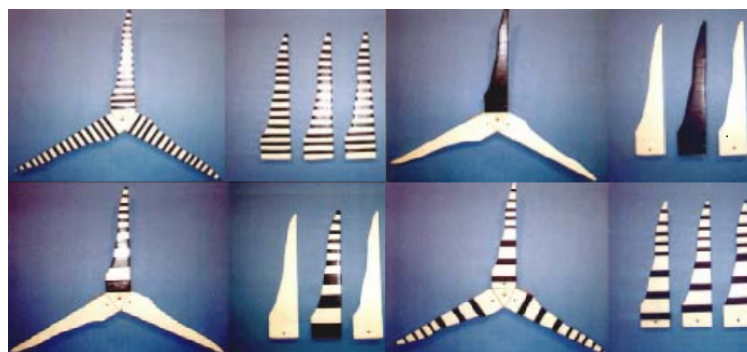


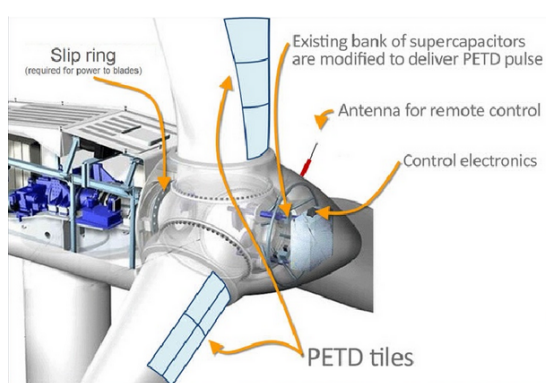
Figure 8.1: Four of the eight patterns tested on bird impact [7]

8.2 De-icing System

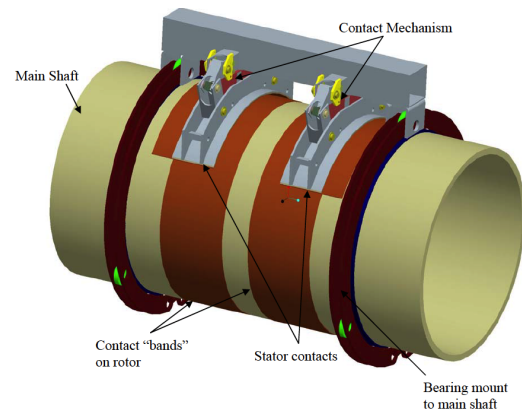
The humidity of the air in Antarctica is very low and so it is not expected that ice will be attached to blades of the wind turbines. However, even a small amount of ice causes a large perturbation on the airflow. The pressure gradient on the leading edge is increased and with this the drag forces increase and early stall occurs, which should be avoided. Therefore a de-icing system is implemented on the Windpulse.

Several de-icing systems were considered, such as black coating, special coating, hot air provided by heat losses of the generator, inflatable leading edges, electrical heating and pulse electro-thermal de-icing (PETD). The description of each can be found in Appendix E. The PETD system uses a millisecond-long electrical pulse directly applied to an ice-covered surface through a conductive layer applied to the leading edge of each blade, see Figure 8.2a. This method will be implemented because it is the most efficient system with low power consumption [61]. The full trade-off of the different systems can also be found in Appendix E.

Special attention should be paid to the electricity supply of the de-icing system because of the rotating turbine. A capacitor bank needs to be installed in the rotor to deliver the electrical pulse directly to the conductive layer on the leading edge of the blade, see Figure 8.2b.



(a) PETD system overview [62]



(b) Capacitor bank in the blade [63]

Figure 8.2: Pulse electro-thermal de-icing system

Besides higher thermal and electrical conductivity, the layer material should present low Young's modulus in order to stretch or compress with the flexing of the blade and should withstand lightning strikes. The materials that are suitable for these requirements are copper, silver and aluminium. Silver and copper are certainly the ideal choice with respect to conductivity. However, the price is much higher than for the other options. Although copper presents almost the same conductivity of silver, it does not present high strength and it is sensitive to corrosion. Finally, aluminium is a low cost material with relatively good conductivity, strength and resistance to corrosion and so this is chosen for this purpose [63]. The series 7xxx of aluminium alloy present high resistance to corrosion and was developed for operations at lower temperatures being widely used for aviation purpose [64]. The thermal conductive layer at the leading edge will be made of 7079 aluminium alloy for being one of the most common type and so, one of the cheapest [65].

To detect the amount of ice on the blades, a sensor has to be installed. The most commonly used sensor is an electromechanical sensor that operates as a vibrating rod. If there is no ice, the vibration rod resonates at its natural frequency. But if it has a coating of ice the additional weight slows down the vibrations, which changes the frequency. When the frequency change is detected, this is converted into ice weight and ice thickness, and subsequently used to set the ice-alert signal after a predetermined thickness has accumulated on the blade. Unfortunately, such complex assemblies have lots of precision internal parts that are costly to manufacture and hard to assemble. They are very sensitive, and require a high-speed ambient air stream in order to work properly. In order to counter the problem the following sensors were considered: an optical sensor, a microwave-based ice sensor, a sensor that measures the difference between the capacitance of two adjacent metal plates and a piezoelectric sensor that measures the difference of weight on the blade [66].

An optical sensor is already widely used on commercial and military aviation. The microwave-based ice sensor is not yet completely developed. Sensors that measure the difference between capacitance have a complex installation and a piezoelectric sensor is not accurate enough due to vibrations induced by gusts and general deflections. For these

reasons it was determined that the optical sensor is the best option for the Windpulse. The ice optical sensor consists of a small, easy to install sensor head that is situated on the top of the nacelle. The sensor allows ice formation directly on its optical surface, defining the relative accumulation rate. There are four states: no-ice, ice-alert, more-ice and saturation-ice. By knowing the growth ice ratio, the ice on the blades can be predicted. On the other hand, as sunlight heats and melts the accumulated ice the state sequence reverses itself [66].

8.3 Lightning System

Due to the height of the wind turbines they are vulnerable to the effects of direct lightning strikes. On average a wind turbine is hit by a direct lightning strike every year and so the necessity to create a system that addresses this problem arises. [67]

The most likely lightning attachment points are the blades, air terminal (lightning rods), the nacelle or protuberances near the top of the structure. Upon being hit, the entire structure becomes a part of the lightning discharge path; from the attachment point to the ground the lightning current will flow through the lowest-impedance paths available, inducing sufficient currents and voltages to damage vulnerable materials and electronic components. A lightning strike on the wind turbine produces electricity, which is dissipated into the ground through the rotor blade, the nacelle, the tower and the foundation earth electrode in the way explained further in this section.

8.3.1 Blade

The rotor blade tip is the highest point of the wind turbine and therefore it has the highest risk point during thunderstorms. The chosen material for the blade is a hybrid composite. This presents poor conductivity, and so a direct strike could cause severe damage. To protect a non-metallic blade, a good conducting path linking the tip of the blade to the root has to be created. An internal wire is installed on the blade, while the external path will be made by the aluminium layer created for the de-icing system, as can be seen on the Figure 8.3. Since lightning dissipation takes place on the blade root and not through the hub and the rotor bearings, the damage on the electrical parts is prevented.

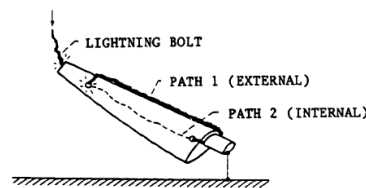


Figure 8.3: External and internal charge transfer [8]

8.3.2 Nacelle

Once the current arrives at the root of the blade, the dissipation of the lightning current from the rotor to the nacelle takes place through a spark gap, which is formed by lightning rods on the nacelle and an aluminium ring on the rotor blade. On the back of the nacelle shell there is also a lightning rod to protect the nacelle and the measuring equipment. Within the nacelle, the lightning current is conducted to the bonding bar inside the tower via a slip ring system made of flexible copper cable.

8.3.3 Tower

The chosen material for the tower is steel and so the tower itself is the conductive material that conducts the current to ground level. Notwithstanding, the foundation is made of concrete, a non-electrical conductive material, as a result the discharge should be made outside the foundation (directly in the ground). Four brackets are welded to the tower, four wires that are insulated but not at both ends connect the brackets to the rock anchors that discharge the energy.

9. Power and Directional Control

This chapter describes the techniques applied to control the output power of the wind turbine as well as the directional rotation. First the reasons for having a power control strategy will be discussed, after which the specific method and mechanisms for control are explained, in Section 9.1. Section 9.2 elaborates on the directional control of the wind turbine and justifies the choice for a downwind rotor.

9.1 Power Control

The power available in the wind is proportional to the air density, the rotor swept area and the wind speed cubed. This means that the available power rapidly increases with increasing wind speed. However, the output power of a wind turbine is limited for high wind speeds by the induced loads on the rotors and mechanical power train, as well as the rated power of the generator. It is very important to not exceed this rated power since this might trigger an imbalance between the rotor and generator torque, causing an acceleration of the blades. In addition to the power control above rated wind speed, it is also possible to control the power at lower wind speeds in order to obtain the optimum output.

In general, the output power of the wind turbine can be controlled by controlling the generator speed, the blade angle of attack or the angle of the entire turbine with respect to the wind direction (yawing or furling). Control of the generator speed will be used on the wind turbine considered in this report, to allow operation at optimum tip speed ratio for a range of wind speeds below V_{rated} . The required rotational speed will be obtained by measuring the torque at a given time and relating this to a desired rotational speed, as shown in Appendix L. For the power control above rated wind speed the decision was made to control the blade angle rather than the angle of the turbine with respect to the wind direction. This is because the angle of attack control is widely used on wind turbines and provides a more accurate control of power. Additionally, pitching the blades can serve as aerodynamic braking in case of emergency and is needed to reduce the loads when the blades are in the parked position above cut-out speed. See Section 9.2 for more about the directional control.

The blade angle control of the designed wind turbine shall be done actively, by pitching the blades towards the wind direction (pitch-to-feather). By doing so, the angle of attack of the blades is reduced for higher wind speeds, leading to lower forces hence lower produced power. With respect to passive stall control, where the blade stalls at high wind speeds to reduce power, the active control can provide a constant power output, P_{rated} , for wind speeds above V_{rated} . This is beneficial for the annual energy production and is the common control strategy for the current wind turbines. It would also be possible to pitch the blades actively towards stall at higher wind speeds. However, with this strategy it is difficult to obtain the same constant rated power output above V_{rated} as with pitch-to-feather control. Another argument that can be made against both stall-inducing strategies is the unpredictable flow behaviour that occurs after stall. It might be that aerodynamic hysteresis effects cause the flow to reattach at very low angles of attack, meaning that the wind turbine will produce less power if the wind speeds decrease again beyond the point where the airfoil stalls. [68]. The required pitch angle can be obtained by measuring the torque and relating this to the required pitch angle, as was done for the first part of the power curve and the rotational speed.

The active pitch control will be obtained by means of an actuator connected to a mechanism for rotating the blades about the pitch axis. On smaller wind turbines, pitching is sometimes achieved by using the centrifugal force and flyweights attached to the blades. However, this system relies on an ever increasing rotational speed, which is not the case in the current design. As will be explained later, the rotational speed is limited to approximately 15 rad/s for noise constraints, hence centrifugal pitch systems cannot be applied on this turbine. In addition to that, the centrifugal systems are very sensitive to mass imbalances, which can occur in Antarctica due to ice-accumulation. Although older designs made use of hydraulic actuators for the pitch system, the market has turned towards the use of electromechanical systems due to their compactness, high reliability, lower maintenance costs and environmentally safe use (no leakage possible) [69]. Especially for the small wind turbine considered in this report and the harsh environment it operates in, the low maintenance and high reliability outweigh the slightly lower initial costs and higher obtainable force of the hydraulic systems. Additionally, the oil in the hydraulic system may become very viscous at the low temperatures in Antarctica, resulting in higher friction, lower pressure and eventually congelation of the fluid [70].

The pitch control mechanism will transform the linear motion from the electromechanical actuator to a rotation of all three blades simultaneously. The chosen option to do this is by having the actuator, which is located in the nacelle and powered by the generator, push a small rod through the middle of the main shaft forwards and backwards. This rod will in turn rotate three levers with a torsional spring in order to pitch the blades. The torsional springs provide a fail-safe design since they rotate the blades automatically into the wind (full furl) in case the actuator fails. Other possible mechanisms include having the actuator located inside the hub itself. However, the power supply of the actuator then becomes difficult due to the constant rotation of the motor(s), implying the use of e.g. slip rings for transferring electrical power and thus adding complexity.

9.2 Directional Control

For an optimised power output, it is important that the turbine rotor is always perpendicular to the incoming wind speed. If not, the effective rotor diameter is decreased resulting in less output power. The method to perform directional control heavily depends on whether the turbine configuration is upwind or downwind.

For the Windpulse, a downwind turbine is selected to be the most suitable. A downwind turbine has its rotor behind the nacelle (see Figure 9.1). Downwind turbines have the important advantage that the rotor blades may be made more flexible since it is less likely that the blades hit the tower. More flexible blades result in less expensive blades which can be placed closer to the tower and lower stresses occurring on the tower during high or gusty wind conditions. More forces are transferred directly to the blades instead of the tower. However, this flexibility also refers back to more fatigue problems. The basic drawback from the downwind configuration is the reduction in wind speed due to the rotor passing through the wind shade of the tower which may also increase fatigue loads on the turbine. The Antarctic turbines presented in this report are designed in such a way that they are able to handle these loads. On the other hand, the downwind rotor is advantageous in that it allows a wind sensor to be installed ahead of the rotor. This makes it possible to obtain data on wind direction free of disturbance, resulting in precise pitch control. While for an upwind configuration a difficult yaw system is required, for a downwind a passive yaw mechanism can be used. If the rotor and nacelle have a suitable design that makes the nacelle follow the wind passively, the nacelle itself can be used as windvane, as is the case for this turbine. [71] [72]

Since cables are connected to the generator to lead the produced current away, a system to untwist the cables should be added to the passive yaw system. Because at Signy Island the wind is almost unidirectional, the decision was made to limit the rotation of the turbine. If the angle range is limited to 180 degrees, the rotor will be able to point 85% of the time perpendicular to the wind. Based on the measurement data of the wind speeds at Signy Island, a simulation is made showing the influence on the annual energy production when limiting the angular range. This limitation will consequently result in a decrease in the annual energy production of 3%. However, this loss and thus a small increase in electricity price definitely outweighs the cost of an active yaw system.

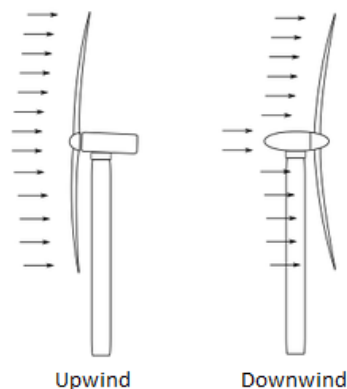


Figure 9.1: Sketch of an upwind and downwind wind turbine configuration

10. Blade Design

In this chapter the final blade design is presented. The geometric blade properties as well as the internal blade structure are determined and the methods to end up with these results are shortly introduced in Sections Section 10.3 and 10.4, respectively . Section 10.1 justifies the airfoil shape. The number of blades are covered in Section 10.2 and Section 10.5 discusses the material choice for the blades.

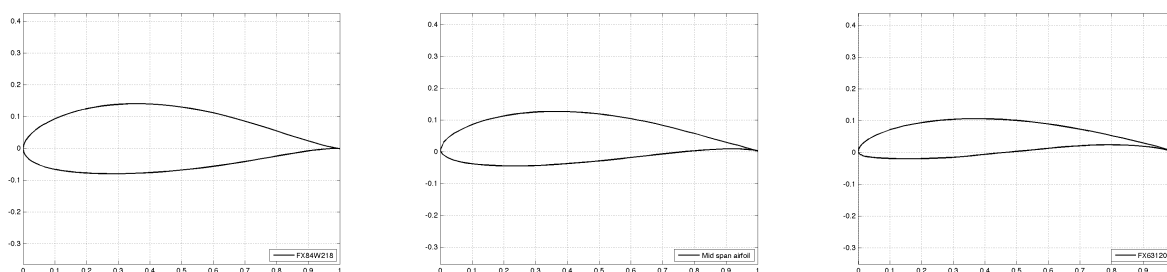
10.1 Airfoil Shape

For the selection of the blade airfoil, the blade is divided up into the tip part, middle part and the root part for which different airfoils are selected. Due to the different aerodynamic and structural behaviours, various requirements are set for the selection of the geometric characteristics of each part.

The shaft part of the blades has no aerodynamic demands so a circular cross-section is selected. Caused by the high loading of the blade towards the root, the root part of the blade requires high strength. This strength at the root can be obtained by increasing the distance between the bottom and the top skin of the airfoil. However, the airfoils with high relative thickness present high drag, hence they are not desired for the tip design and thus a different airfoil is needed for the tip blade design. At the tip a high maximum lift over drag ratio, high angle of stall, posterior smooth stall, low noise and insensitivity to roughness is required. The middle airfoil should be a balance between the tip and root design characteristics and it is important that the different airfoils are geometrically compatible. Therefore only one airfoil family is selected such that the airfoils can smoothly change into each other. A trade-off is made between different families that are commonly used for aviation and maritime application (NACA, Wortmann and Eppler), but also airfoils specially designed for wind turbine blades (S8, DU, FFA and Ris ϕ). The trade-off can be found in Appendix F.1.

For the Antarctic turbine with approximately 5 meter blade length, the FX63120 is selected for the tip and the FX84W218 for the root. The middle airfoil has consequently been extracted from the 3D drawings, having a smooth transition from the tip to chord airfoil. The shape of the selected airfoils are visualised in Figure 10.1. The Wortmann airfoil family has a high maximum C_l/C_d ratio. This is reflected in a good stall behaviour for the tip and a later stall for the root. Compared to the other families, the Wortmann airfoil used for the tip part of the blade is relatively insensitive to a Reynolds change within the large operating range of Reynolds numbers. At the operational Reynolds number, the selected airfoils are roughness insensitive. For the tip the maximum thickness occurs at 30.8% and for the root the maximum thickness is present at 33.9% of the chord. An airfoil with the maximum thickness far away from the leading edge will experience a decrease in the pressure gradient at the leading edge when exposed to ice or dust. This leads to the fact that transition and stall occur later than expected; for the airfoil with maximum thickness at a large distance of the leading edge the streamlines still follow the airfoil shape without creating high adverse pressure gradients.

To gather the airfoil data, Rfoil is used. However, the software is not able to produce accurate enough results. Therefore Rfoil is validated with measurement data after which a correction is implemented on the software data to make them more realistic. This process and the C_l and C_d values are shown in Appendix F.2.



(a) Root airfoil FX84W218

(b) Middle airfoil

(c) Tip airfoil FX63120

Figure 10.1: Wortmann airfoils selected for the blade

10.2 Number of Blades

To decide on the best choice for the number of blades, three configurations are considered during a trade-off by comparing their own advantages and disadvantages; a two, three or four bladed horizontal axis wind turbine. Many variables are affected by the number of blade selection, such as rotational speed, efficiency, weight, drag, cost and so on. Most modern wind turbines are three bladed designs and tend to lead in the world's market. The three bladed horizontal axis wind turbine came out of this analysis to be the most suitable configuration for this project. For most of the criteria, the three bladed rotor is the optimum balance between two and four bladed configurations.

Each blade disturbs the air for the following blade. This influences the lift and drag working on a blade. For a three bladed turbine the influence of one blade on the other remains acceptable. The tip speed ratio for a three bladed turbine is only 82% of the two bladed turbine. High rotational speeds are a disadvantage regarding noise and results in a smaller range of operating at optimum tip speed ratio. The loads resulting from the BEM-code, based on Blade Element Momentum theory, differ significantly for the different configurations. The higher the number of blades, the smaller the normal and tangential forces that are working on the turbine blades. The loads of a three bladed turbine seem to be preferred considering the required structural box thicknesses and length. No teetering hub is required for the obtained configuration and the stability is significantly better than for the other considered designs. The reason is that at the very moment when the uppermost blade bends backwards, because it gets the maximum power from the wind, the lowermost blade passes into the wind shade in front of the tower. [73] Also for the vibrations, the selected configuration seems to have better properties resulting in less fatigue issues. The visual impact on humans is also confirming the decision. The human eye is really sensitive to rotating parts. Most of the time, multiple wind turbines are placed close to each other which do not necessarily have the same rotational speed. Studies have proven that the asynchronous rotation of multiple even-bladed turbines is visually unpleasant while the out of phase rotation of odd-bladed turbines is less notable.

10.3 Geometric Blade Layout

With the airfoil and number of blades known, the geometrical blade layout is determined. At the end of this chapter the blade length, chord distribution and twist distribution are obtained. Also the corresponding power output and pitch angle for each velocity are shown.

To start this process, the rated velocity is determined. The values of the rated wind velocity at which a wind turbine will produce its maximum average power has to be determined. The method for determining the optimum rated wind velocity was based on the wind speed probability density function occurring at Signy Island explained in Appendix F.3. For the wind turbine of this project, the rated velocity is calculated to be 10.16 *m/s*. The corresponding cut-in and cut-out speed are 3.5 and 30.5 *m/s* based on reference [74].

To minimise the loss of kinetic energy due to wake rotation, an optimum chord distribution exists. The method to determine this distribution is based on the theoretical Betz limit. From that same method, the optimum twist distribution is computed. A visualisation of the results can be found in Figure 10.2 and 10.3. The used equations can be found in Appendix F.4.

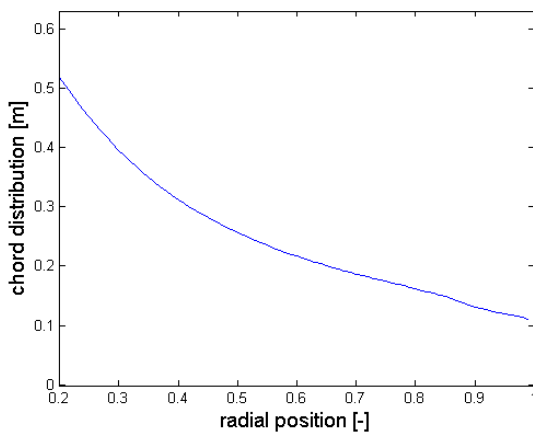


Figure 10.2: Chord distribution from 20% of the root until the tip

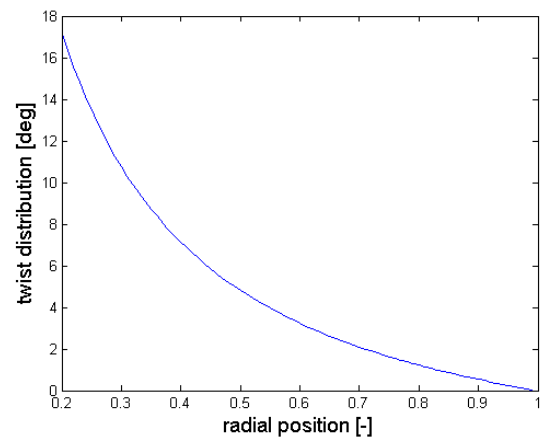


Figure 10.3: Twist distribution from 20% of the root until the tip

To determine the best combination of the rotor diameter for the three bladed configuration, the main used tool is the Blade Element Momentum model. With this BEM-model it is possible to calculate the steady loads and thus also the thrust and power for different settings of wind speed, rotational speed and pitch angle. The explanation of this method is discussed in detail in Appendix F.5. The procedure to determine the best combination of number of blades and rotor diameter consists of multiple steps and uses the airfoil data, chord and twist distribution as main inputs.

The first step in determining the rotor diameter is to calculate the optimum power coefficient, which is the highest obtainable value. The C_p values are calculated by varying the wind speed (and thus the tip speed ratio λ) and pitch angles θ_p . From all these combinations the maximum value for the power coefficient is chosen and the corresponding λ and θ_p are defined.

With these numbers in mind, the diameter of the rotor plane is selected based on one main requirement: the rated power should be reached at the estimated rated velocity. This implies that the average rated power is maximum and that the turbine is not over- or under-designed. The best diameter/blade combination is selected by using the BEM-code. The code is run for only the rated velocity and calculates the corresponding power. In Table 10.1 the resulting values for the diameter, pitch angle, tip speed ratio and maximum power coefficient are shown.

Table 10.1: Rotor blade characteristics

# Blades [-]	Rotor Diameter [m]	Optimum λ [-]	Optimum θ_p [°]	Optimum C_p [-]
3	8.8	8.25	-2.5	0.53

For the power output, it would be beneficial to run constantly at optimum tip speed ratio and pitch angle. However, the wind turbine rotational speed range and the maximum power are limited. The turbine will operate at optimum tip speed ratio until the speed at which ω_{max} of 15 *rad/s* is reached. The rotational speed will thus increase linearly, holding λ at the optimum value. As soon as ω_{max} is reached, λ will decrease again. Due to vibrational reasons explained in Section 13.1, the minimum rotational speed is limited to 10 *rad/s*. To limit the power, the pitch regulated control system was considered to change the pitch angle. Until the rated velocity the pitch angle will be kept constant at its optimum value and for the high wind speeds, the matching pitch angle corresponding to the rated power should be found. To do this, the BEM-code is adapted to run over a range of pitch angles and extended to find the correct θ_p . A visual representation of the power curves and the pitch angle variations for a velocity range between cut-in and cut-out speed can be found in Figure 10.4 and 10.5, respectively.

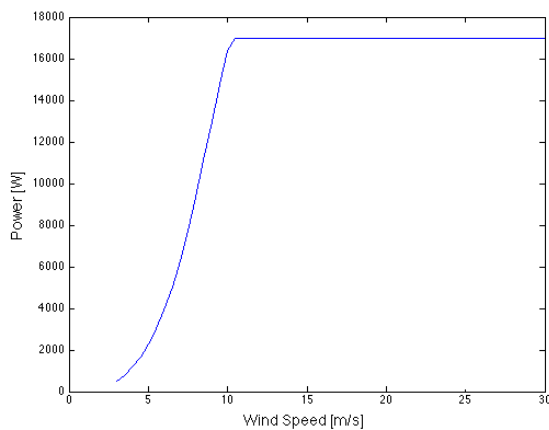


Figure 10.4: Power versus wind speed

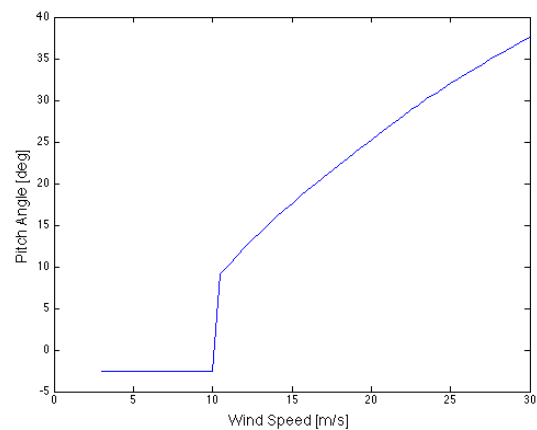


Figure 10.5: Pitch angle versus wind speed

10.4 Internal Blade Design

Wind turbine blades are constantly exposed to a variety of distributed loads that act in different directions. First of all, the lift and drag forces induced by the aerodynamic shape of the blade are decomposed into the normal and tangential loads. Additionally, the blade mass exerts a loading that is different for every rotational position. Finally, the centrifugal force due to the rotation is considered. The combination of these loads results in stresses in the blade and causes it to deflect. Their time and position varying behaviour also induces vibrations in the structure.

In order to reinforce the aerodynamic shape of the blade to cope with the high loadings, the majority of wind turbine manufacturers use internal stiffening elements that provide the necessary strength and stiffness. For the design

presented in this report, an internal box structure as shown in Figure 10.6 is applied due to its superior torsion performance with respect to e.g. a single spar. The tapered box will consist of three main elements, as displayed in Figure 10.7: the blade itself with a linearly increasing width from the tip, which is consequence of the applied chord distribution, the section of the shaft with linearly decreasing width and finally the straight shaft at the root. As a result of the aerodynamic design, the box is given a twist along the length.

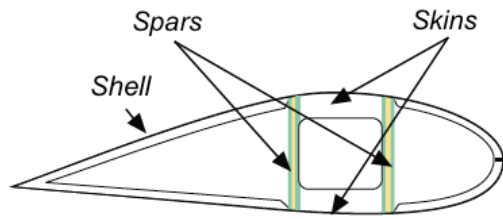


Figure 10.6: Internal structure of blade showing the stiffening elements

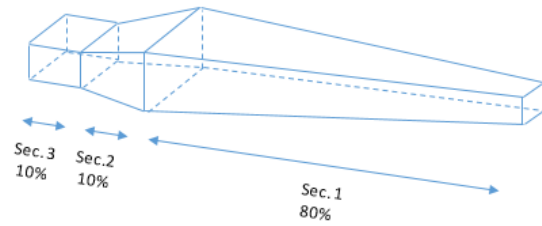


Figure 10.7: Schematic representation of the internal box sections

The internal box forms the main structural element of the blade and is therefore carefully designed to limit the maximum stresses and deflections below the allowed values. Additionally, the resulting eigenfrequencies are calculated to create an understanding of the constraining frequencies that cause resonance. First, a numerical tool was constructed to find the required skin and spar thicknesses of the box that confined the maximum Von Mises stress in the three sections of Figure 10.7 below the allowed value of 150 MPa . The maximum allowed value is dictated by material choice and fatigue issues, explained in Chapter 13. The thicknesses were found by calculating the maximum forces, bending moments and torques on several discrete positions along the box and consequently obtaining the stresses. The thickness distribution that satisfied the stress constraint and yielded the lowest weight was then selected. Also note that width and height of the box was adjusted appropriately to obtain the required stiffness without influencing the airfoil characteristics. Using the bending moments on the section, the deflections of the beam were also calculated and the design was modified to restrict the tip deflection from exceeding the predefined limit of 50 cm out-of-plane. The stresses and deflections were not only checked for the maximum operational case, but also for the case of parked blades with a 75 m/s wind speed as *REQ-TE-2* states. This analysis revealed that the best position to park the blades is by pitching them so that the tip has a 0° angle of attack, which gives a tip deflection of 0.2 m and a maximum stress well below the allowed value. Finally, the first flapwise and first edgewise eigenfrequencies were calculated by iterating between applied forces and resulting eigenfrequency. Appendices F.7 and F.8 elaborate on the specific methods used to design the beam and the design decisions made during the process.

Figure 10.8 displays the final thickness distribution of the box after designing it for stresses and deflections. The red stars display the thicknesses that would suffice if the beam was only designed to cope with the applied stresses, while the black stars indicate the final thicknesses after restricting the deflections as well. As visible from the figure, the spars and skins have the same thicknesses, which is beneficial for manufacturing, and the overall thickness distribution was kept simple: the first section of Figure 10.7 has an increasing thickness and the shaft sections show a constant thickness. Figure 10.9 shows the Von Mises stress throughout the box after finalizing the design. The twist angle and deflections are also included. The red and blue colours indicate the high and low stress values respectively. It is clear that the stresses are highest along the leading edge of the blade, in positive x-direction, and increase towards the root. This is due to the high bending stress at the leading edge caused by the combination of normal and tangential forces in positive z- and positive x-directions respectively. In addition to that, the shear stress at the front spar is highest, mainly due to the contribution of the torque. The legend in Figure 10.9 reveals that the maximum stresses, which occur in each of the three sections of the blade, are never higher than the allowed value of 150 MPa . The out-of-plane deflection, in z-direction of the tip is also lower than 50 cm , which was the predetermined limit. This value was based on deflection angles for reference wind turbines [75]. Although the designed wind turbines will be downwind types, it is still important to limit this deflection since a high deflection causes the effective rotor diameter to decrease and will lead to large vibrations when the blade passes behind the tower. In appendices F.7 and F.8 more detailed figures are shown to clarify the stress distributions and deflections.

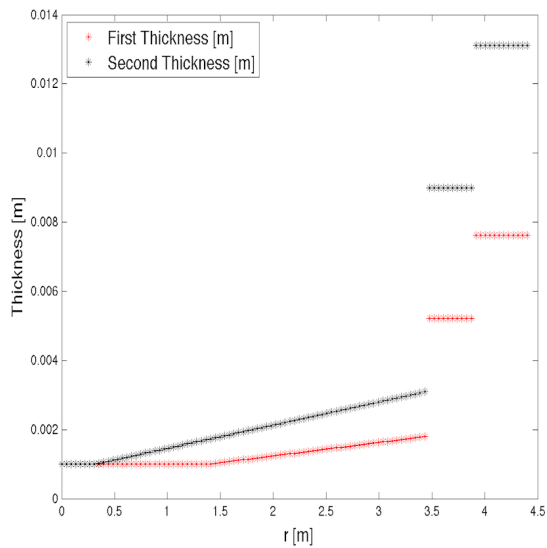


Figure 10.8: Thickness distributions of internal box, black stars indicating final distribution. First thickness distribution represents the distribution after stress design. Second thickness distribution represents the distribution after updating the design for deflection

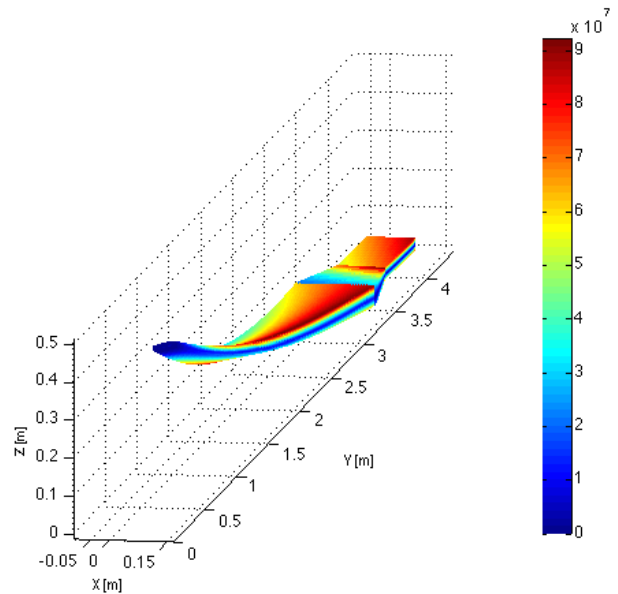


Figure 10.9: Von Mises stress throughout the internal box. Red and blue colours indicate high and low stress levels respectively. Blade twist and deflections are also included.

The relevant parameters for the final box design are shown in Table 10.2. In addition to the geometric parameters that ensure a robust design capable of handling the stresses and deflections, the two lowest eigenfrequencies of the structure are also provided.

Table 10.2: Relevant parameters for internal blade box

<i>Parameter</i>	<i>Minimum Value</i>	<i>Maximum Value</i>
Thickness [mm]	1	13.1
Box Width [cm]	5.22	20.73
Box Height [cm]	1.3	5.18
Box Mass [kg]	-	9.6
Von Mises Stress [MPa]	0	92.12
	<i>X-direction</i>	<i>Z-direction</i>
Tip Deflection [cm]	13.88	49.93
	<i>Flapwise</i>	<i>Edgewise</i>
First Eigenfrequency [rad/s]	5.13	15.04

10.5 Material

In this section, the chosen materials to construct the blades are discussed. Firstly, the choices made for the internal box will be explained, after which the aeroshell material is described. More information on this matter is also provided in Appendix F.9.

10.5.1 Internal Box

When dealing with composites, it is impossible to ignore the mutual relationships that exist in the trinity of materials, manufacturing and design. Thus when a material is investigated, it is important to consider how this material affects the design itself as well as the production method. For the internal box of the blade four material types were considered, all of them currently being used on small wind turbines: Aluminium (*Al* – 2024 – *T3*) and Glass-, Carbon- and Natural-Fibre Reinforced Polymers (respectively GFRP, CFRP, NFRP). After analysing these different possibilities, the decision was made to use a hybrid composite consisting of 60% Carbon and 40% Flax fibres together with a 53% bio-based epoxy. The justifying numbers and the decision process are presented in Appendix F.9, but the essence of the choice lies in the trade-off between cost and sustainability.

With the material properties shown in Table F.2 of Appendix F.9, the different designs belonging with each material were obtained. As explained in the appendix, the Aluminum design already turned out to be infeasible after designing it for stresses since the material thickness at the root needed to be higher than the actual height of the box. In addition to the stress design, the flexural stiffness of the different designs also had to be altered to account for the tip deflection requirement. As described in the appendix, the Glass fibre and Flax fibre blades required too radical aerodynamic design changes (changing the airfoil thickness would be needed since the material thickness at the root is otherwise too high) in order to meet the tip deflection requirement, leaving the carbon fibre blade as the remaining possible option. Glass fibre composites might not be suitable for this design, however the material is widely used on large scale wind turbines. One explanation for this is the fact that the loads on the blades do not increase at the same rate as the stiffness does when upscaling the blades from a small to a large wind turbine. Due to the larger cross sections, large wind turbine blades will most likely have a higher relative flexural stiffness as compared to the small turbine blades of this design. In fact, the moments of inertia increase with the third power of the box thickness and width. This contributes to the flexural stiffness of the blades.

Although the Carbon fibre design satisfied the requirements and has a relatively low cost (even lower than Glass fibre, if that design was considered feasible), it still has a high environmental impact and requires a large amount of energy to be produced, as shown in table F.3 of Appendix F.9. Based on studies presented in [27] and [18] and on the results presented in table F.3 of Appendix F.9, a hybrid composite consisting of 60% Carbon and 40% Flax fibres was determined to be the best compromise between performance, cost and environmental impact. As stated earlier, a bio-epoxy resin was chosen for the composites. According to [76], the properties of the SuperSap 53% bio-epoxy are comparable to the properties of conventional non-bio resins. Using a bio-resin also contributes to lowering the environmental burden of the composite, as explained in the appendix. An epoxy was chosen since it has better adhesive properties, superior mechanical properties, better resistance against fatigue and microcracking and reduced degradation from water ingress [77].

With respect to the cold environment in which the wind turbines operate, it has to be stated that little research is done towards the performance of composites in low temperatures since the main research focus lies on high temperature effects [78]. However, some research is done into the behaviour of GFRP's and CFRP's in cryogenic temperatures. The general conclusion of this research is that the mechanical properties of composites are not affected by low temperatures and can even increase with decreasing temperature (e.g. shear strength). The low temperatures have a negligible effect on the fibres, regardless of the moisture content, but can reduce the toughness of the matrix material and can have consequences on the formation of micro-cracks due to residual stresses. Appendix F.9 provides more information on the effects of cold temperatures, but the final conclusion that was drawn is that the fibres will pose no problems at all and that epoxy will be the best choice for resin due to the good resistance against microcracking and water ingress.

10.5.2 Aeroshell

The function of the aeroshells is to provide the required aerodynamic shape to the blades and to protect the internal structure from external influences such as UV light and erosion [76]. In order to avoid buckling and maintain the aerodynamic profile, the aeroshells mainly need to be stiff and low-weight. Therefore, the shell will be constructed with sandwich structures, with a core material that has a reinforcing laminate on each side, as well as an external coating.

Since the laminates will be thin and do not have to carry the main loads, carbon fibres were substituted by glass, mainly because they are inexpensive, durable and less brittle than carbon fibres. The latter aspect is important to resist impacts occurring on the blades. The resin will be the same as the one for the internal box (a 53% bio-based epoxy) for manufacturing ease. For the light-weight core that will be placed in between the glass fibre laminates, end-grain balsa will be used. This material is inexpensive, widely used, has good specific properties and is derived from a renewable source (fast-growing balsa-tree). Other options that were considered are styrene acrylonitrile (SAN), polyvinyl chloride (PVC) and polyethylene terephthalate (PET) [79]. Although these other cores are easier to use with resin infusion and are lighter, they are generally also more expensive and can have lower mechanical properties, to such an extent that twice as much material is needed than with balsa, also all these materials can sustain very low temperatures without large difference on mechanical properties.

Finally, the surface of the wind turbine blade is painted with a special gelcoat to protect the composite material, specifically the chosen resin, from damage originating from environmental exposure as UV-radiation and humidity that cause corrosion of the blade. Epoxy gelcoat was chosen since it meets these requirements with a low cost and since it is widely used on blades of wind turbines. For the leading edge besides this coating, a plate of aluminium will be placed, as stated in Section 8.2. The aeroshells will consist of a 1 mm outer glass laminate, a 2 mm balsa core and a 1 mm inner glass laminate. With these thicknesses, the aeroshell weight becomes 10.4 kg given the total blade a weight of 20.1 kg.

11. Nacelle Design

In this chapter the detailed design of the nacelle will be presented. The nacelle connects the blades with the tower. Therefore the design must process the inputs of the blades and generate the inputs needed for the tower design. The windy and cold climate of Signy Island makes the maintenance of the nacelle and the blades more difficult for the experts to work at a rough 9 meters height. Therefore, it is strived for as least as possible components in the nacelle. The generator and the braking system will be up in the nacelle, but the electronics will be placed in a well-insulated housing at the root of the tower.

The generator converts the kinetic energy into electrical energy and the type that will be installed is discussed in Section 11.1. In Section 11.2 the cooling system for the generator is defined. The structure that transfers the loads from the rotor to the tower is shown in Section 11.3 and the braking system is shown in Section 11.4. Section 11.5 shows the hub characteristics and Section 11.6 shows the designed outer shape of the nacelle.

11.1 Generator

The generator is the main electrical component of the nacelle and converts the rotational energy of the shaft into electrical energy. In general, variable speed and constant speed operating wind turbines exist and the corresponding generators are variable speed and constant speed generators, respectively.

For the Signy Research Station, both maintenance and reliability are important criteria. These factors weighed the most in the trade-off between the direct drive and the constant speed generator. The winner of this trade-off is the direct drive generator and the most important reason for this is the absence of a gearbox. In low temperature climates gearboxes are the most troublesome part of the turbine. Additionally, less moving parts are required which is beneficial in the Antarctic climate [80]. The full trade-off can be found in Appendix G.

Permanent magnets or electromagnets are available for direct drive generators. A permanent magnet is an object made from a material that is magnetized and creates its own persistent magnetic field. This means that it always has a magnetic field and will display a magnetic behaviour at all times. An electromagnet is made from a coil of wire which acts as a magnet when an electric current passes through it. Often an electromagnet is wrapped around a core of ferromagnetic material like steel, which enhances the magnetic field produced by the coil [81]. Permanent magnets will be implemented because these are more cost efficient, generate no heat, they are more compact and lighter and require minimum maintenance [82] [83]. The latter reason weighs the most in the decision for installing permanent magnets for the direct drive generator.

For the preliminary sizing of the generator an estimate is made of the weight and other parameters of the permanent magnet direct drive generator. This estimate, shown in Table 11.1, is based on existing permanent magnet generators. The manufacturers [84] [85] [86][87] of these generators can customise the generators to the requirements.

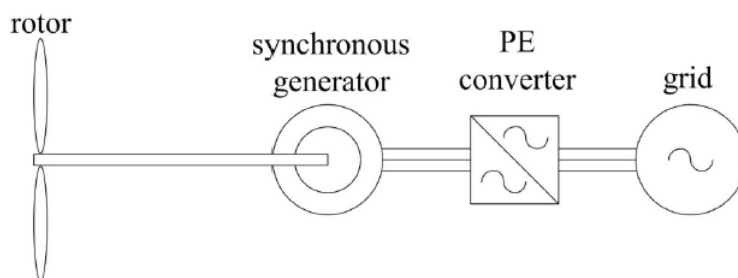


Figure 11.1: Direct drive generator schematic

Table 11.1: Parameters generator

<i>Parameter</i>	<i>Values</i>
Generator type	Permanent magnet synchronous direct drive generator
Rated angular velocity	143 <i>rpm</i>
Rated power	17 <i>kW</i>
Diameter	550 <i>mm</i>
Generator width	400 <i>mm</i>
Mass	378 <i>kg</i>

The starting torque of this wind turbine will approximately be 10 *Nm* and the efficiency of the generator will be higher than 95%. The preliminary generator layout is shown in Figure 11.1.

11.2 Cooling System

The generator produces a large amount of heat. To prevent the generator and surrounding components from overheating, a cooling system will be integrated. The environment on Signy Island, being characterised by very low temperatures and high wind speeds, allows the use of a passive cooling system and making use of it results in lower losses in power and in minimum noise. The nacelle shell will have a hole with variable diameter on the front side and one fixed hole on the hub. Due to the shape of the nacelle the air will flow through the interior of the shell, cooling the generator. The bottom part of the nacelle will have a fixed hole from which the cumulated water can exit. When the wind turbine is shut down during winter, the opening will be entirely closed. The cooling system can be visualized in Figure 11.6.

The bottom front of the nacelle presents a semi-circle of 5 *cm*, while the upper part is a rounded plate with the shape of semi ellipse with minor semi-axes of 5 *cm*. The height of this top plate is controlled by the servo of the electric motor in order to have the temperature inside of the nacelle always at 30°. The height of the hole, for each temperature and velocity, is calculated assuming conservation of mass and energy on the control volume (the volume of air inside of nacelle). Moreover it is assume that the generator produces 850 *W* of heat (5% of 17000 *W*) and can be found in Figure 11.2.

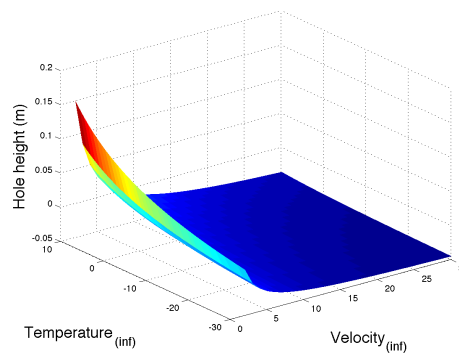


Figure 11.2: Height of the upper part of the hole

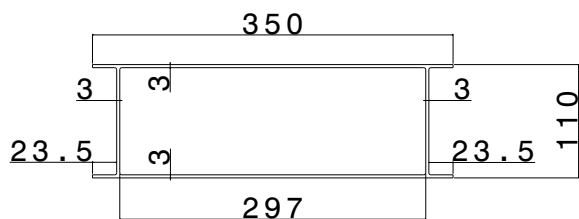
11.3 Structure

The structure will be designed to withstand the loads of the present components and to transfer the loads of the rotor to the tower. The rotor hub, the shaft and the bedplate are the structural components that carry the largest loads. The bedplate is the main structural component that transfers the loads from the rotor to the tower and will be the base for the other components. The bedplate is designed to withstand the static loads and is presented in Section 11.3.1 together with the design of the shaft. The braking system is selected at the end of this section.

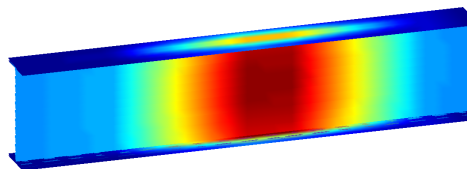
11.3.1 Bedplate

The bedplate is the most important structural part of the nacelle design. It transfers the loads of, among others, the rotor, hub and generator into the tower. In view of simplicity and level of possible optimisation, it was chosen to use

I-beams for this structure. After an analysis of the torque acting on the bedplate, it was determined that the two I-beams would be connected to each other in order to create a torsion box. See Appendix G.1 for the actual bedplate design process and manufacturing plan and figure 11.3a for the result. The total mass of the bedplate is 6.5 kg and the maximum Von Mises stress is 57.7 Mpa.



(a) Front view of bedplate with dimensions in mm



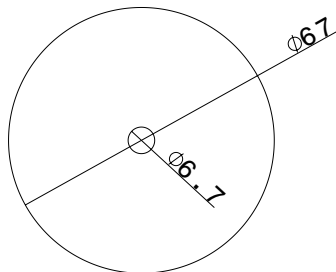
(b) Stress visualisation over single I-beam (red indicates the highest stresses). The rotor is located to the left of the graph.

Figure 11.3: Result of bedplate optimisation

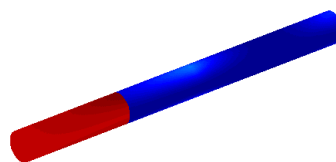
Figure 11.3b shows the stress distribution over the I-beam. The bedplate is connected to the tower just behind the middle of the beam. It can be seen clearly that the stress reaches its highest point, just before the loads are transferred into the tower. The stress concentration at the right end of the I-beam is to overcome the moment of the shaft acting on the generator.

11.3.2 Shaft

The shaft is the part that passes the rotational energy of the rotor to the generator. The main loads on the shaft are the torsions of the rotor and generator, but also of the brake when active. Furthermore, shear force of the weight of the rotor, shear forces of the bearings and the normal force due to drag on the rotors are present. The shaft was designed for the worst load case, which is at maximum rotational speed with brakes full active. The design was performed in a similar way as the bedplate. A program was developed that searches for the lightest solution possible within the given boundaries. Since the forces acting on the shaft are similar to the bedplate a similar program was made, see Appendix G.1. Figure 11.4b shows the result of the optimisation. As can be seen in Figure 11.5a, the shaft sprouts into a bigger diameter at the end of the shaft. This is needed in order to let the stresses of the hub flow into the shaft. The mass is 22 kg and the maximum Von Mises stress is 43 Mpa. The limiting case for the shaft design is the full braking case. Figure 11.4b shows the braking situation where the red part is the location of the brakes, so this is where the maximum Von Mises stress acts, and the blue part is inside the generator and the stress has a value of around 35 Mpa.



(a) Front view of shaft with dimensions in mm



(b) Stress distribution over shaft in case of braking (red indicates highest stresses).

Figure 11.4: Result of optimisation

11.3.3 Material

The material of both the bedplate and the shaft should withstand the heavy loads of the rotor and it should not lose its mechanical properties in the cold environment of Signy. Steel alloys are considered a suitable material because of high strength for low costs and special types of steel exist that can withstand the cold temperatures. Moreover, steel is a highly recyclable material. The A537 Class 1 (Grade A) steel alloy is selected, which is the same material that is used for the tower and the trade-off of different steel types can be found in Section H.2. The yield stress of this material is 345 MPa which is high enough for coping with the stress induced on the bedplate and shaft including a safety factor.



Figure 11.5: Generator and brake system

11.4 Braking System

The safety system should contain two types of brakes in order to be fail-safe according to the regulation DS-472 of the Danish Energy Agency [88]. The pitch system is the aerodynamic brake of the wind turbine and in emergency cases a rotor brake, which is a mechanical brake, will be needed to stop the rotor. This brake will also be used to enforce a standstill during the maintenance operations. A disk brake is the most common option for these purposes. The disk brake itself can be bought off-the-shelf, however the disk should be designed and attached to the shaft. It is a pneumatic brake which can be operated manually or by an electrical signal. See Figure 11.5b for an impression of the brake system.

The maximum braking time of 15 s leads to a braking torque on the shaft to be 250 Nm . See Appendix G.3 for the detailed calculations. In order to reduce the weight of the brake system, a trade-off has been performed between the size of the disk and the weight of the needed brake. As can be seen in Appendix G.3, the maximum braking force of the disk brake selected is 2.6 kN . [20] This yields a required disk radius of 10 cm with the given required torque. The material of the disk was selected to be spheroidal graphite, because of its high heat capacity characteristics. The mass of the disk is calculated to be 1.56 kg .

11.5 Rotor Hub

The rotor hub is one of the highly stressed components of wind turbine [89]. At the rotor hub, the rotor blades are connected to the shaft. The hub should withstand all loads acting on the blades, both static and dynamic. For a three or four bladed rotor a fixed hub can be used. Since the wind turbines have three blades, the this type will be implemented. The material of the hub shall carefully be selected on high loads and the fatigue life of the material. A spherical hub will be implemented made of A537 Class 1 (Grade A) steel, since this type can withstand the cold temperatures and can withstand high stresses, as explained in H.2. Three holes for the blades are required. The blades are connected to the hub through slip rings allowing the pitch angle to be changed by the pitch control system. The hub is bolted to the perforated end of the shaft, explained in Section 11.5. This allows easy assembly on the site. The diameter of the hub will be 0.31 m and the mass is determined to be 15 kg [90].

11.6 Shell and Cone

The shell has two main functions, the protection of the environment with creating the least amount of drag. Since the wind turbine should cope with the extreme environment and the wind turbine is down-wind, care needs to be taken when designing the shell shape. To cope with the harsh environment, the type of material should be resistant against

these situations, which will be elaborated on further in this section. The shape is based on airfoil geometries to achieve a laminar airflow for the wind turbine blades. Then, an egg-shaped volume is designed since this can follow the airfoil geometry and is sufficiently stiff to cope with the induced stresses. Furthermore, as is explained in Section 11.2 an opening in the nacelle is made for the cooling of the generator. The shell is required according to *REQ-TE-14*, that is shall be able to be unfolded for maintenance, so the components are either attached to the bottom or to the upper part. The cone fulfils similar functions as the shell, protection of the hub and the pitch control system and it should not create turbulent airflow. The shape follows the shape of the shell, so the airflow is not disturbed. The mass of the shell is 12 kg.

Material

Glass fibre is an often used material for shells and cones of the nacelle. The shell does not carry the heavy loads and serves as protection of the components in the nacelle. The material should cope with the required temperature difference of $-50\text{ }^{\circ}\text{C}$ outside and $20\text{ }^{\circ}\text{C}$ at the inside. Furthermore, the outer surface should be smooth for optimal airflow. Composite materials were considered since these are light weight with sufficient strength. Glass fibre is selected over carbon fibre because glass fibre is less costly, less brittle and it is sufficient to withstand the prevailing stresses. The glass fibre is combined with flax fibres. Flax fibre is a sustainable material as is explained in Section 10.5.1. The composition is 60% E-glass fibre and 40% flax fibre. This is considered the best composition considering cost, stiffness and sustainability. Polyester will be used as resin. Epoxy does have better mechanical qualities, of which fatigue resistance. However, the shell will not suffer from fatigue to that much extent as the blades and polyester has sufficient mechanical properties. Moreover, it presents smooth finishing. No sandwich structure core will be implemented since this the shape of the shell is complex, so the manufacturing costs will rise. Sufficient stiffness is obtained by increasing the thickness of the composite material.

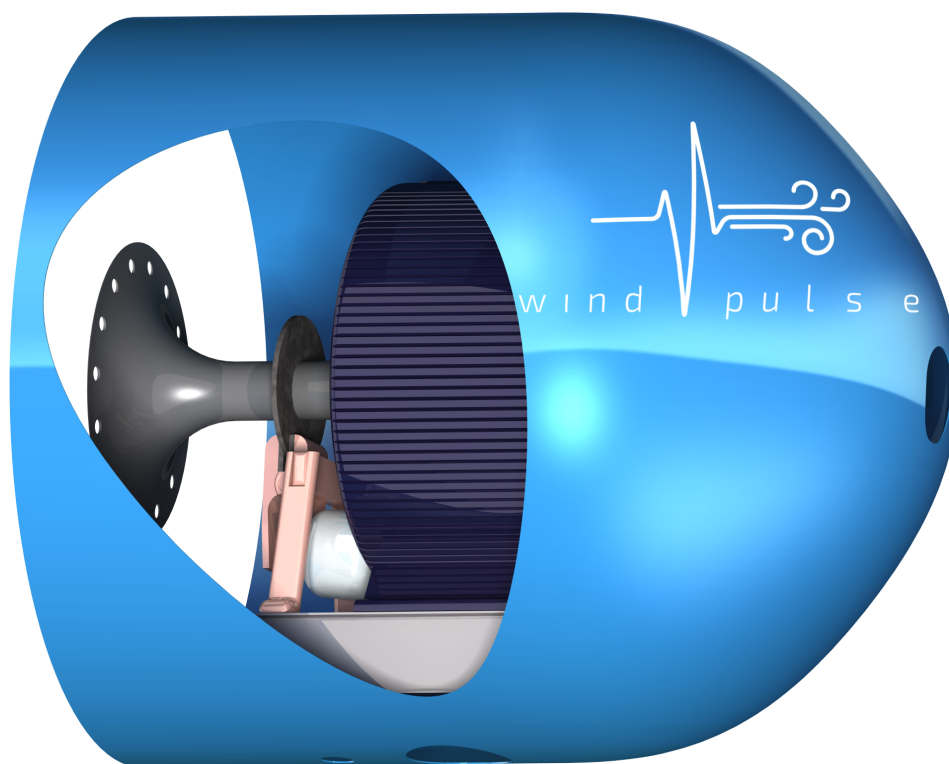


Figure 11.6: The nacelle and subsystems

12. Tower and Foundation Design

Within this chapter the sizing results for the tower and foundation design will be presented. Section 12.1 covers the structure type, Section 12.2 the tower material, Sections 12.3 and 12.4 the tower sizing for bending, buckling and compressive stress and Section 12.5 the tower deflection. The foundation type and sizing are presented in Section 12.6 and 12.7, respectively.

12.1 Tower Structure Type

A tubular structure was selected as the basic tower structure type. One of the dominant reasons for picking a tubular structure as opposed to a truss structure was because it was seen to interact the least with the wildlife by not offering places for birds to sit and thus minimising the interference with the scientific observation mission of the Signy station. Furthermore, due to the extreme weather condition ranges, a single piece tubular structure was seen as the best solution to avoid possible structural problems with expansion and contraction of the tower, and simultaneously allow for insulation of the electrical cables required for power transfer. For a complete overview of the tower type trade-off, the reader is referred to Appendix H.1.

12.2 Tower Material Type

Due to the fact that the tower will be exposed to extreme negative temperatures in the Antarctica, a material able to handle such temperatures needs to be selected. The material selected was a cold temperature steel alloy, designated A537 Class 1 (Grade A), capable of operating at temperatures up to minus 60 °C [28], so the required minimum of minus 50 °C is met. Such a material was selected due to the numerous decades of industrial use of steel, and thus the acquired manufacturing knowledge associated with the material [91] [92]. Moreover, steel provides a high strength to weight ratio for its costs as shown by the fact that more than 90% of wind turbine towers use steel for their construction [93] [94] [95]. A dominant reason for selecting such a material was because of the highly recyclable and sustainable nature of steel with steel being recycled at its currently theoretical maximum [96]. By using steel, which does not lose its material properties upon being recycled, 642 kWh of energy, equivalent to 1.8 barrels of oil can be saved with every ton of steel recycled [97]. The yield stress of the material is 345 MPa and has a Young's modulus of 200 GPa [28]. For a complete overview of the considerations on material the reader is referred to Appendix H.2.

12.3 Tower Sizing for Bending

The tower was sized in order to withstand the loads it would be exposed to during operations in Antarctica. Two load cases were considered, pre-cut-out conditions, and post-cut-out survival speed conditions. Sizing of the tower for bending stress was conducted with a weight minimisation optimisation process. The thickness, radius and stress distributions are shown in Figures 12.1, 12.2, 12.3, 12.4, for the most critical load case which was found to be the post-cut-out case. It can be seen that due to the very large wind conditions that are experienced in Antarctica, the tower radius is much larger than it would be if placed in a more moderate environment. The modelling of the forces and loads can be found in Appendix H.3 and the specific method used for bending stress sizing is described in Appendix H.5. It should be noted that the fluctuations found in the graph are due to discretisation of the tower, and for given infinite number of segments, with infinite radii possibilities such fluctuations would not be present.

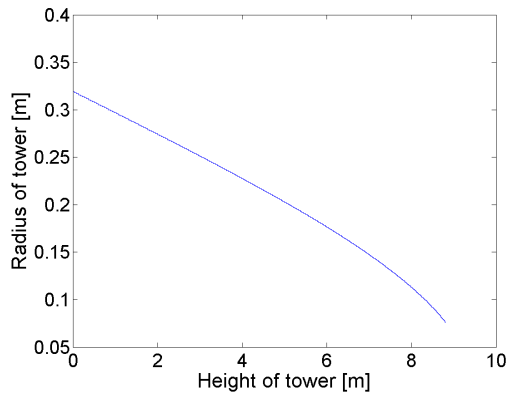


Figure 12.1: Radius against height of tower using discrete segments for post-cut-out load case

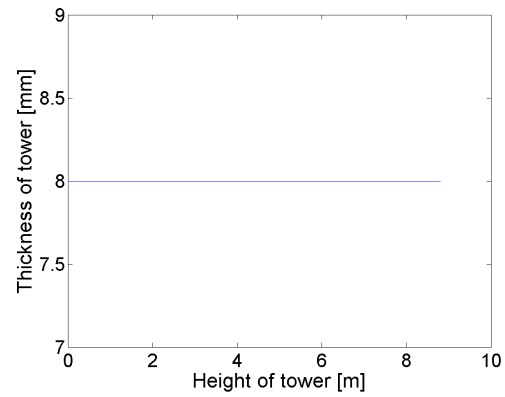


Figure 12.2: Thickness against height of tower using discrete segments for post-cut-out load

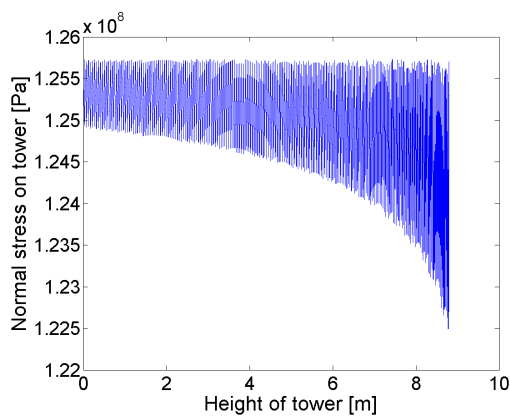


Figure 12.3: Stress against height of tower using discrete segments for post-cut-out load case

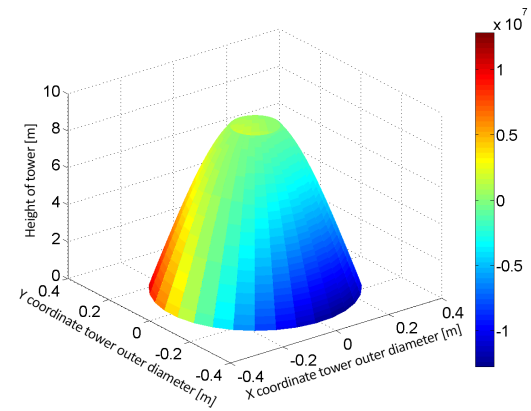


Figure 12.4: 3D Stress visualisation along tower height using discrete segments for post-cut-out load

As can be seen by the results, the lowest weight solution is that of constant minimum thickness and increasing tower radius from top to bottom. In Figure 12.4 the stress distribution of the pre-cut-out operational range is shown. Due to sizing for the very large wind speeds experienced on Signy Island, the stresses on the tower during normal operations are much lower. The tower height was taken to be 8.8 m, twice the size of the blade length, in order to avoid any aerodynamic interference from the ground and provide the blade enough clearance from collisions with animals on the island. Although the tower is optimised with the above radius distribution, a linear changing radius distribution will be used for easier manufacturing. The distribution will have a top radius of 0.077 m and a bottom radius of 0.319 m. The reader can find additional information on the computational model programming flow in Appendix O.

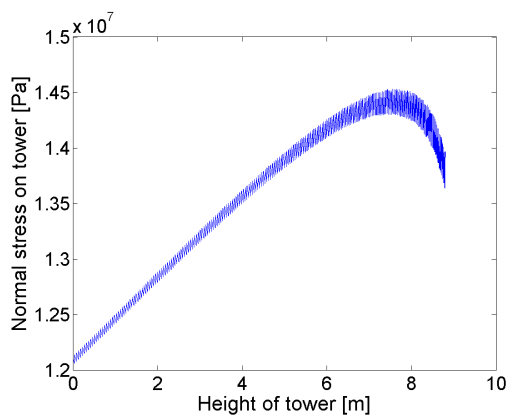


Figure 12.5: Stress against height of tower using discrete segments for pre-cut-out load case

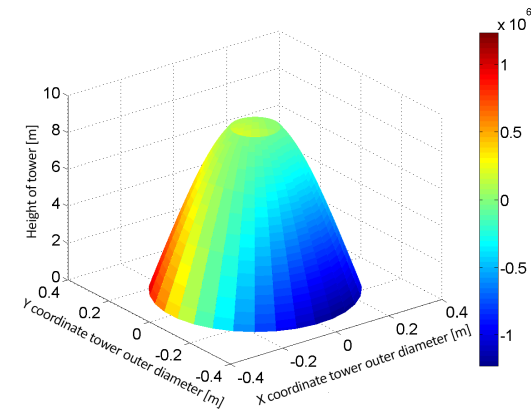


Figure 12.6: 3D Stress visualisation along tower height using discrete segments for pre-cut-out operation

12.4 Tower Sizing Buckling and Compressive Stress Considerations

In addition to the tower being sized for bending stresses, buckling and compressive stresses were also considered. The methods for calculating the required thickness for buckling can be found in Appendix H.6. The computational method for calculating compressive stresses can be found in Appendix H.7. The required thickness for buckling is found to be $6.6337 \cdot 10^{-4} m$ and the compressive stresses on top and bottom were found to be lower than the maximum allowable yield stress. This result indicates that the required thickness for withstanding buckling and the compressive stresses on the tower are lower than the required thickness for bending stresses and maximum allowable yield stress, respectively. Thus it is seen that the bending stress load case is the dominant one and so the tower size is as described in Section 12.3.

12.5 Tower Deflection

The tower deflection was calculated by using both engineering beam theory and Castigliano's method. The mean radius and mean thickness were used for calculations using beam theory, and a linear distribution was used for Castigliano's method. The full descriptions of the two methods can be found in Appendix H.8. The deflection is seen to be $0.097 m$ at survival speed load case and seen to be $0.011 m$ during normal operational wind speed range through the Castigliano's method. The deflection is seen to be $0.141 m$ at survival speed load case and seen to be $0.017 m$ during normal operational wind speed range through the beam deflection theory method. As can be seen both methods give similar values and as such can be used to show the validity of the methods. The methods result in a difference due to the fact that Castigliano's method approximates a linear distribution. Figure 12.7 and 12.8 show the calculated deflection of the tower.

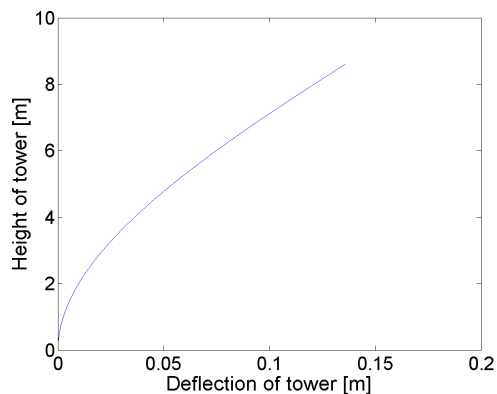


Figure 12.7: Tower deflection using mean radius for post-cut-out load case

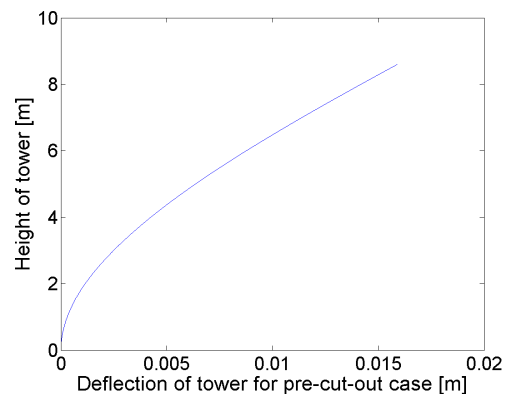


Figure 12.8: Tower deflection using mean radius for pre-cut-out operation

12.6 Foundation Type

The foundation is the component that is below the ground surface and ensures that the wind energy system is fixed to the ground. The foundation is the most heavily loaded element of the wind turbine system and thus it has to be the most robust component. There is a high overturning moment compared to the weight of the structure of the wind turbine. Therefore, the foundation does more work of withstanding the introduced moments due to the wind force than the structure itself.

The wind turbine is placed on a location with shallow bedrock of amphibolites. This is a metamorphic rock and thus very strong. The geotechnical research on the bedrock is stated in Appendix H.9. The options for the foundation type are the rock socket and rock anchor foundations. For the rock socket a large amount of rock needs to be excavated to implement the foundation. Due to the large footprint of the rock socket, the rock anchor foundation is used. The trade-off for the foundation type is stated in Appendix H.10. A rock anchor foundation is used which is suitable for shallow bedrock and relies on the strength of the rock. This foundation has a small footprint and can easily be covered up at the end-of-life of the wind turbines as is required. Therefore, a rock anchor foundation is sustainable. The tower connection to the foundation is an anchor bolt cage [98]. The rock anchor foundation that is going to be implemented is shown in Figure 12.9. Appendix H.10 presents in more detail the rock socket and rock anchor foundation and why the rock anchor is used. The implementation of the foundation on Signy Island is elaborated upon in Section 17.3. For the concrete a surface active agent is added to the mixture to protect it from freezing and thawing damage. Many

closely spaced small air bubbles are created in the concrete, that function as expansion chambers that relieve pressure [99].

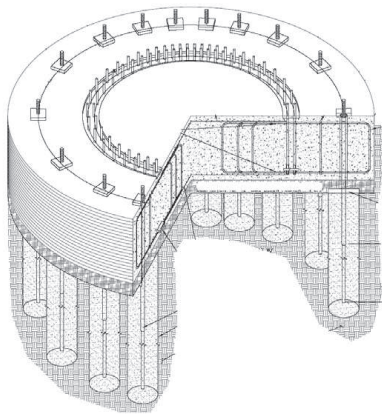


Figure 12.9: Rock anchor foundation [9]

The principle of the rock anchor foundation is multiple self-drilling anchors drilled into the rock bottom with a concrete cap on top of the anchors. The gap between anchors and cap allows post-tensioning and retensioning of the anchors. The gap in between the cap and the anchors is filled with soil. Due to the extreme environment the anchors will be tensioned twice a year, at the start and at the end of the summer season, instead of annually under normal conditions [100]. Pre-stressed anchors have several benefits. The essence of pre-stressing is that it will hold its design load before the final construction is completed. Steel elongation only occurs when the service load exceeds the pre-stressed load of the bolt. The fatigue failure is minimised, since the periodic stretching and relaxing are eliminated. Due to the pre-stressed condition the anchor will not elongate through the grout column and therefore cracks in the grout will not occur. This leads to anchors that are well protected against corrosion. [101]

12.7 Foundation Sizing

The anchor bolt cage diameter is 0.94 m , the same diameter as the tower bottom diameter plus 15 cm at each side for the tower flange at the bottom where the tower is connected to the anchor bolt cage. The diameter of the foundation is 1.28 m , twice the tower bottom diameter. 8 rock anchors with a length of 2 m and a cross-sectional area diameter of 25 mm are used for each turbine foundation, determined from the analysis presented in Appendix H.11, based on rock mechanics. The depth of the concrete cap and thus the height of the anchor bolt cage is 0.6 m , based on reference wind turbine foundations [9]. [102] [103] [104] [105] [106]

The CATIA render of the foundation can be seen in Figure 12.10.



Figure 12.10: CATIA render of the foundation

13. Vibration & Fatigue

In this chapter the vibrational and fatigue characteristics are examined. In Section 13.1 the Campbell diagram is generated to check for resonant conditions and Section 13.2 elaborates on how fatigue is taken into account during the design process of the wind turbine.

13.1 Vibrational Characteristics

The vibrational characteristics of the wind turbine will be visualised using a Campbell diagram. The Campbell diagram of a wind turbine allows to check for coincidence of vibration sources with natural resonances. Based on this diagram it is possible to define frequency exclusion ranges. For the full calculation of all the elements in the Campbell diagram, the reader is referred to Appendix I.

As can be seen in Figure 13.1, no resonant conditions occur. This is managed by keeping the minimum rotational speed limited to 10 *rad/s*. This change in operation only affects the AEP to decrease by 0.2%.

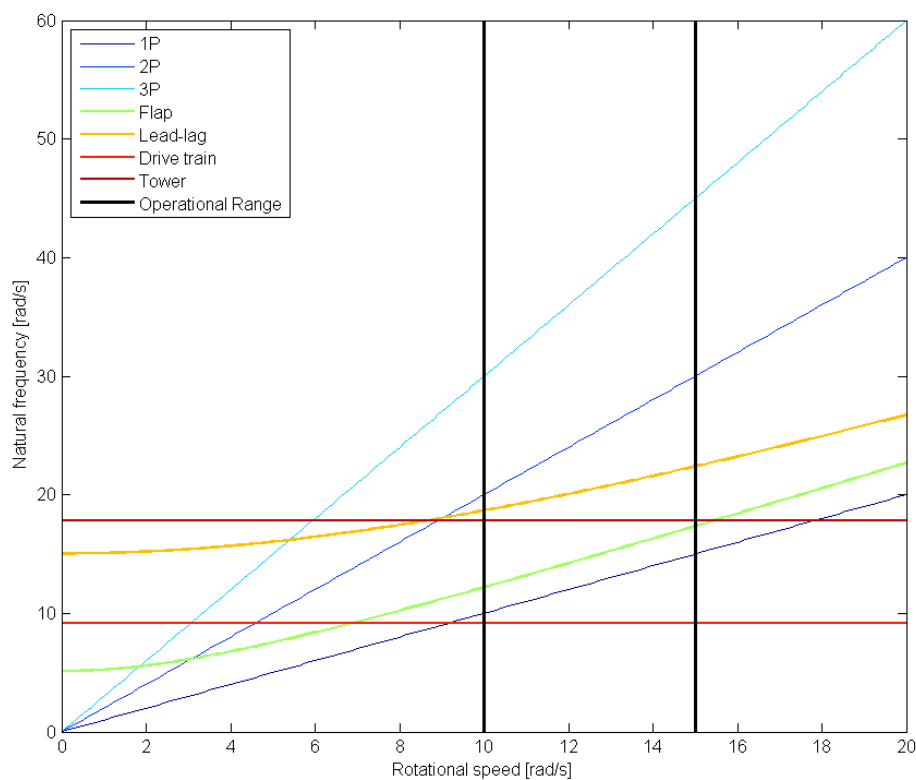


Figure 13.1: Campbell diagram, minimum rotational speed 10 *m/s*

13.2 Fatigue

External and operational conditions cause cyclic loadings on the wind turbine. These repeated loads on the different components can cause microscopic cracks and due to the continuous cyclic loading the crack size will grow and finally reach a critical size which results in structural failure of the system. [107]

To optimally take into account fatigue failure of the design, the load cycle needs to be known accurately and applied to the structure and analysed in a Finite Element (FE) program. In this case only measurement data is available for hourly wind speeds on one particular location which would be insufficient for a thorough analysis. The lack of data

combined with the limited time and expertise makes it at this stage of the design process impossible to perform a FE analysis.

The presence of fatigue however can not be neglected during the current design phase. Therefore fatigue is taken into account by complying with the regulations regarding fatigue design stated in the "Design requirements for small wind turbines" [108]. These requirements state in order to take into account fatigue failure, the Miner's rule can be used. This rule calculates the accumulated damage during the lifetime of a wind turbine. For the turbine to survive the fatigue loads, this damages should be smaller than or equal to 1 as shown in Equation 13.1.

$$Damage = \sum_i \frac{n_i}{N(\gamma_f \gamma_m s_i)} \leq 1.0 \quad (13.1)$$

With n_i the counted number of fatigue cycles, s_i the stress level associated with the counted cycles including the effect of both mean and cyclic range, N the number of cycles to failure as a function of stress obtained from the S-N curve, γ_f and γ_m the safety factors for loads and materials respectively. The counted number of fatigue cycles can be calculated with Equation 13.2.

$$n = \frac{Bn_{design}T_d}{60} \quad (13.2)$$

With T_d being the design life of the turbine in seconds. However at this stage the S-N curves for the specific materials used are not available. In that case, the design requirements stipulate to account for the fatigue in the design stress, as shown by the following equation:

$$\sigma_d \leq \frac{f_k}{\gamma_m \gamma_f} \quad (13.3)$$

In Equation 13.3 f_k is the ultimate strength, γ_m the partial safety factor for fatigue and γ_f is the partial safety factors for loads. The design requirements demand γ_m to be equal to 10 to account for fatigue if no S-N curves are available. γ_f is equal to 1.35 for the load calculations.

The method of applying a safety factor of 10 on the design stress to account for fatigue is applied to all the relevant parts in the wind turbine that could experience fatigue. By applying this safety factor for fatigue design requirement *REQ-TE-8* has been met. This is due to the fact that no repair to the structure must be conducted for fatigue during its lifetime since this design methodology is implemented.

14. Verification & Validation

To prove the reliability of the tools used in the design process, verification and validation should be performed. This chapter will elaborate on the specific methods used to check whether the tools correctly solve the applied problem and whether the chosen problem corresponds to reality. Section 14.1 covers the verification and validation of the separate subsystems. In Section 14.2, a validation of the entire wind turbine is provided by comparing it with reference wind turbines. In this way, more confidence can be obtained in the final design described in this report.

14.1 Verification and Validation of Subsystems

In this section, the verification and validation of the tools for all the subsystems will be described. Verification is the process of checking whether the constructed program functions correctly and consists of two parts, named code verification and calculation verification. The code verification was done to check whether the numerical code is implemented correctly. This was done by verifying the correct use of formulas, units and sign conventions. In the calculation verification, the goal becomes to further determine whether the numerical model solves the problem right and calculates the output values in a correct way. During this process, unit and system tests are performed for each subsystem. The verification of each subsystem (rotor blades, nacelle, tower) is treated below. If the errors are within limits, one can say that the program is successfully verified.

To answer the question whether the numerical tools are solving the right numerical problems, the results are validated against existing and reliable data. One can say that the better the experimental data fits the numerical results, the better the numerical model predicts the reality. A successful validation will result in extra confidence in the numerical program. However, since reliable data was not available for all the tools, some programs could not be validated separately. The possible validations of the numerical codes is discussed in the corresponding subsections.

14.1.1 Rotor Blades

In the rotor blades design two main tools are used. The aerodynamic numerical tool is mainly based on the BEM-code and is able to compute the power curve. The structural tool consists of stress and deflection calculations of the inner box of the wind turbine blades. To prove that the tools are working properly, a verification and validation is performed. Although the codes are made general, at some conditions, the tools are not able to run and thus provide answers. Some of the code singularities are listed below:

- Chord calculations unit the tip
- Too small lift and drag coefficient range (required for interpolation)
- Discretisation in unequal sections
- Thickness factor of zero
- Material thickness should not exceed the box dimensions

The aerodynamic BEM code is verified by comparing the results of the developed tool with the results of an externally provided code from Delft University of Technology. During the test, the tip speed ratio, thrust and power are compared for a certain geometrical input and for a range of velocities. A two-bladed turbine with a diameter of 1.2 *m*, no blade twist and a NACA 0012 airfoil is used to perform the verification. The differences between the two codes averaged over the velocity range, is not exceeding 5%. In Table J.1 in Appendix J, the resulting values from the test can be found. The still present differences can be explained by the fact that different assumptions are made. The developed code slightly overestimates the torque and power. A BEM-code initially assumes that the force from the blades on the flow is constant in each annular element and no radial dependency is present. In the created code a Prandtl's tip loss factor and Wilson-Walker 1984 CT-correction is used. However, it is unclear how the provided tool is dealing with these assumptions. It was detected that the TU Delft tool is extrapolating the data while the developed tool is only able to interpolate the airfoil data. Therefore only velocities at which no part of the blade is stalled are used. The actual aerodynamic design tool uses the BEM-code for different input values to select an optimum combination. The selection procedure is manually checked to see if this process is working as expected. Since the provided code is obtained from a very reliable source and since the results are as initially foreseen, it can be concluded that the developed BEM-code is working correctly based on the negligible errors.

The numerical tool that was used to design the internal box for was verified by checking the solutions provided by the code against an analytical solution. This was done by considering one section of the blade at 2.02 *m* of the tip. To

facilitate the analytical calculations, quadratic distributions of P_n and P_t were assumed with maximum values of 250 and 75 N/m respectively. In addition to that, the twist angle of the blade was set to zero. Before doing the actual comparison between numerical and analytical results, several sanity checks were performed. For example, the blade should not be tapered if the root and tip chord are set equal, or the top part of the blade should be in compression. No peculiarities were discovered from the sanity checks. For the unit tests, the geometric properties, load calculations, stress computations and deflections (with constant loading and stiffness) were verified. Afterwards, the accumulated errors were taken into account to perform the full system test. Table J.2 displays the results from the verification of the numerical tool. A visual representation of the deflections with both numerical and analytical methods is provided in Appendix J, as well as the positions of the booms along the cross section. It is readily visible that the errors between the tool and the analytical calculations are all very small for the unit tests. The differences in cross sectional area and moments of inertia are easily explained by the structural idealisation that was implemented. The boom calculations take into account the corner skins twice leading to a slightly higher cross sectional area and a higher moment of inertia. Because the load and moment calculations show such a small error, it can be concluded that the assumption that the P_n and P_t loads vary linearly within each section is acceptable. The same counts for the stress comparisons that were done in the unit tests. Only the shear flow shows differences, since a simplification is applied when using booms. The σ and q values for the system test show the effect of the accumulated errors. It makes sense that the tool predicts lower stresses, since it overestimated the moments of inertia slightly. The final errors in the system test are assumed to be acceptable since they are lower than 7% and are taken into account during the design by applying safety factors according to the design requirements for small wind turbines [108]. Thus it can be concluded that the tool correctly solves the applied physical problem and is hence properly verified.

The lift and drag data of the airfoils is extracted from the software Rfoil. Measurement data are much more accurate to obtain the lift and drag coefficients. However for the operational Reynolds numbers of the project wind turbine no measurement data is available. Before relying on the Rfoil program, validation is performed by comparing real measurement data with the software data. The comparison of the data for the root airfoil is performed with the FX84W218 airfoil at a Reynolds number of 700,000. Since no data was available for the tip airfoil, the aerodynamically similar airfoil NACA64418 is used at a Reynolds number of 270,000. When comparing the two data sets of the tip and root airfoil, first of all it is clear that the drag is underestimated. Also, the slope of the lift curve slightly deviates. Important to note is that the Rfoil deviation at the thick root airfoil is significantly larger than the thin airfoil at the tip. When using the Rfoil data during the design, a correction is added to the airfoil data to make it more accurate. In Figure 14.1 and 14.2 a visual presentation of the validation process is shown.

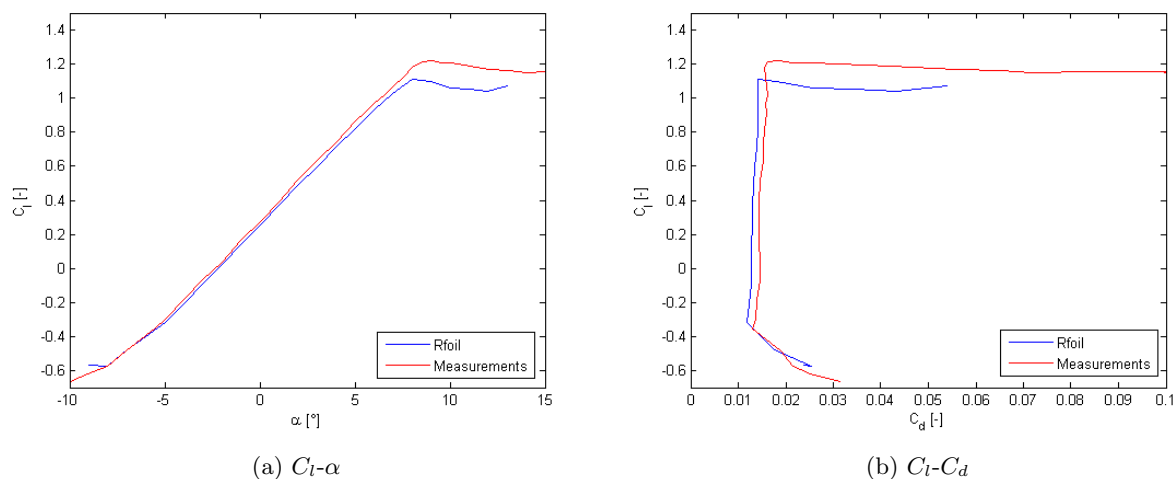


Figure 14.1: Polars of NACA64418 (tip) at a Reynolds number of 270,000 for Rfoil data, measurement data and corrected Rfoil data

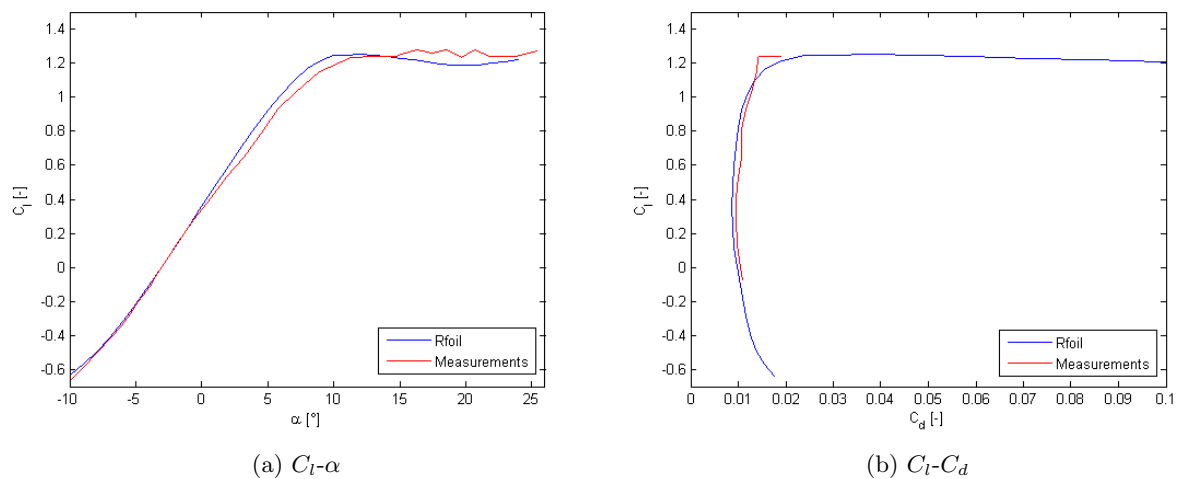


Figure 14.2: Polars of FX84W218 (root) at a Reynolds number of 700,000 for Rfoil data, measurement data and corrected Rfoil data

Not only the airfoil data proving software Rfoil has to be validated, but also the reliability of the BEM-code should be proven. For the validation, the turbine *Jonica Impianti* is considered [109]. This Italian 20 kW rated horizontal axis wind turbine has a diameter of 8 m and has a maximum rotational speed of 200 rpm. The turbine has 3 blades and is pitch controlled. The cut-in and cut-out wind speed of this turbine are 2.5 m/s and 37.5 m/s respectively. The geometrical properties are implemented in the developed code while the power curve is consequently compared to the power curve provided by the manufacturer. The considered turbine has no twist and the chord distribution is obtained by upscaling the optimum distribution such that the tip and root chord correspond to the reality. In Figure 14.3, the velocity versus power for the tool and manufacturer data is shown. The tool is slightly overestimating. As already found during the verification process, the reality is slightly off from the calculated results. In fact this only means that in real operations, the rated power is reached at a slightly higher velocity, implying a lower annual energy production. After completing the validation, the developed product can be trusted with higher confidence.

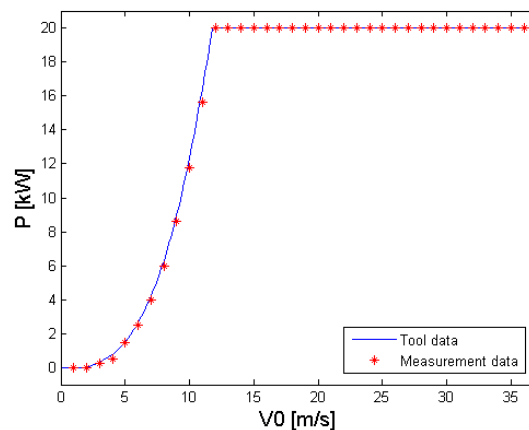


Figure 14.3: Velocity versus power for the tool data and manufacturer data

14.1.2 Nacelle & Tower

Some of the units used in the programmes of the bedplate, shaft and tower are relatively simplistic. Therefore they do not need an elaborate verification. The basis arithmetic operations performed inside these blocks are already checked when writing the code. For the bedplate and shaft programme these units are *Static Relations, Moments of Inertia, Von Mises Stress, Buckling Check and Weight*. For the tower program the *Static Relations, Loads on Section, Dimensions, Weight* got the same approach. These units are verified by changing the inputs in size and sign and performing a sanity check on the output. In all cases the units passed these tests. In the next sections the units not covered above will be treated. There are no complete reference data to perform a proper and complete validation of the tower, bedplate and shaft. In the next design phase it is suggested to perform a Finite Element Analysis on the designs, followed by a full-scale test model to validate the design more extensively for all three components. With these

planned activities it is possible to validate the vibrational characteristics, the stresses, fatigue, structural behaviour on the cold temperatures and the deflection of the tower. Some code singularities are listed below:

- The tower height needs to be divided up into at least 2 sections for the tower tool to be able to run.
- Limitations needs to be put on the maximum and minimum radius of the tower in order for the tower tool to run.
- For the bedplate- and shaft tool boundaries have to be set for sweeping over the dimensional properties.

Nacelle

See table J.3 in Appendix J for a more precise verification of the units.

Discretise: This unit breaks up the I-beam and shaft into discretised points where the stresses need to be calculated. Its inputs are the geometry of the shaft or I-beam and the required maximum distance between two points. It was checked if the output of the unit indeed has this maximum distance between two points and if the points are spaced evenly. The unit reacted correctly to increasing flange sizes, heights and lengths. Finally, the amount of points in the discretisation is checked.

Loads on Section: All the loads acting on the bedplate and shaft are considered to be distributed loads. The force of the generator weight for example, is distributed over the width of the generator feet. It was verified if this distribution is performed correctly over the given widths. After this the other inputs, e.g. forces and their locations, are verified. It was checked if the forces act at the right location, using force and moment diagrams. The errors made in this are zero with respect to the analytical model.

Figure 14.4 shows the shear forces, normal forces and bending moments acting on each section of the I-beams for a given set of inputs. The normal force consists of the drag force of the rotor. The shaft transfers the normal forces to the generator that transfers the loads to the tower. So the normal force will start to increase at the location of the generator, at 0.11 m . The tower has a width of 0.20 m in this analysis and is runs from 0.13 m until 0.33 m . At 0.13 m , the tower appears and causes the slope to change of sign and decreases until the end of the tower at 0.33 m . Behind this location, the slope increases again until the end of the generator, at 0.51 m .

The shear forces includes the weights of the components on the bedplate and the normal force of the tower. The brake has a very small weight compared to the other components, so only a very small variation of the shear force line is seen at 0.05 m . At 0.11 m , the first bearing is placed that results in a steep decrease at that location. The normal force of the tower works upwards, so the steepness is reduced from 0.13 m until 0.31 m since bearing 1 does not reach further. The second bearing experiences an upwards shear force so a steeper line is expected from 0.31 m until 0.33 m . Bearing 2 is the only contribution until 0.51 m , so a constant increasing line runs until the end of the bedplate. The moment diagram follows directly from the shear force diagram, since the moment line is the integral of the shear force line. This can be seen from moment diagram 14.4b. Because this analysis shows that the implementation of the code is correct, it is therefore considered verified.

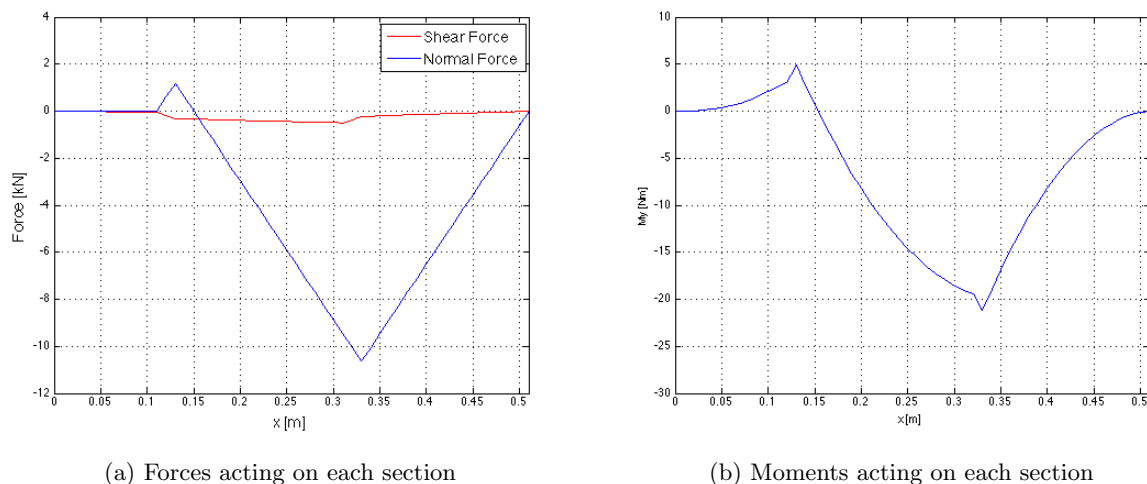


Figure 14.4: Graphical results of optimisation

Tower

Drag on Tower: The drag on the tower is dependent on the geometry of the tower and the wind speed. It is therefore verified if the block of code uses the right geometry values for the relevant section. The input for the calculations of the drag on the tower are the outputs given by the numerical model in an earlier stage. If these values are used to calculate the drag by hand on the middle segment of the tower it gives a 0% difference when compared to the numerical calculated value.

Buckling: The code block calculating whether the required thickness to withstand buckling is lower or higher than the calculated thickness, is checked in the same manner as the code block of *drag on tower*. When comparing the numerical solution for buckling thickness with the value obtained from the analytical calculations a difference of 0.25% is found. This small offset can be explained by rounding errors.

Deflection: The deflection is calculated analytically and compared to the numerical solutions. The difference between the two is 4.3%. This difference can be explained by the discretisation of the deflection over the entire tower in the numerical model. The numerical model calculates the deflection for each section and adds it up to the top of the tower, whereas the analytical model uses the entire beam and therefore takes the tower as one section.

Static Compressive Stress: The static compressive stress calculations are checked in the same manner as the code block of *drag on tower*. There is a zero percentage difference, this is as expected since the same formulae and inputs are used and the numerical model is not discretised.

Natural Frequency: The natural frequency in the numerical model is calculated for 3 different positions and not discretised. Therefore, when comparing the numerical solution for the natural frequency with the analytical calculations for the same input values the difference between the solutions is 0%.

14.2 Validation of Wind Turbine

In order to ensure confidence in the developed design and prove its reliability on the market, the wind turbine can be compared with reference turbines. To this extent, data from existing horizontal axis designs is gathered and collected in scatterplots showing the relations between two parameters e.g. power and diameter. The reference data comes from the Catalogue of European Urban Wind Turbine Manufacturers [109]. By then evaluating the performance of the wind turbine with respect to these reference devices, conclusions can be drawn on whether or not the designed turbine is viable in reality. In addition to that, this procedure also serves as a validation of the interaction between all the tools and can also provide more insight into the validity of separate tools.

Figures 14.5, 14.6 and 14.7 display the gathered data from the reference turbines as well as the datapoint corresponding to the designed turbine. The blue dots in Figure 14.5 indicate the masses of a single blade plotted against the rotor diameter for several comparable small wind turbines. The two dotted lines are not the trendlines belonging to these points, but were extrapolated from relations given in [10]. The orange triangle represents the final design described in this report. It is clear from this figure that the blades of the design have a lower weight than the blades of the reference turbines. This is the consequence of choosing the Carbon/Flax material for the internal box design, while the blades of the reference turbines in Figure 14.5 were all constructed out of Glass fibre composites. However, the mass of the designed blade coincides with the relation for Carbon fibre blades from [10] and is thus assumed to be logical and reliable. Additionally, the structural design of the blade can be considered valid to some extent since the weight is a direct consequence from the structural design. Figure 14.6 displays the validation data for the tower diameter with respect to tower height, with the dotted lines representing the trendlines through the data points. As for the blade weight, the tower diameters of the designed turbine are in line with the reference data, which supports the idea that the calculations were performed correctly and all the required aspects of the tower design were considered.

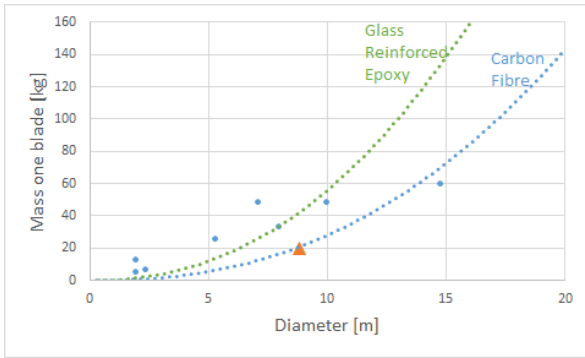


Figure 14.5: Validation data for the mass of a single blade versus the rotor diameter. Blue dots indicate reference turbines, dotted lines represent relations derived from [10]. The orange marker indicates the designed turbine

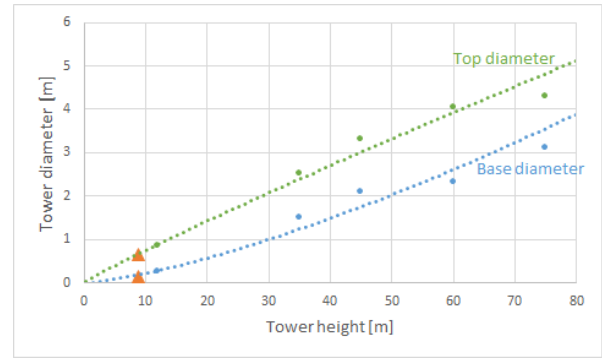


Figure 14.6: Validation data for the top and bottom diameter versus the rotor diameter. Dots indicate reference turbines, with the dotted lines representing the trendlines.

One of the most important parameters to properly validate is the diameter of the designed turbine. Figure 14.7 shows the power of multiple reference turbines versus the diameter. If the designed turbine would show a significant deviation from the general trend between power and diameter, it would have a much lower reliability to be viable in reality. However, the orange marker in Figure 14.7 clearly indicates that the designed turbine exactly adheres to the general power-diameter relation constructed with reference data, hence the diameter of the turbine (and the rated power) is assumed to be valid.

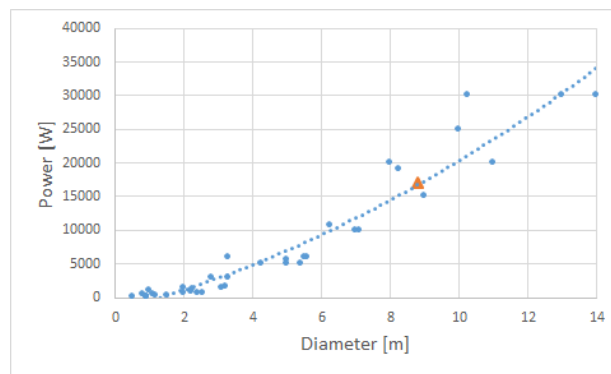


Figure 14.7: Validation data for the power versus the rotor diameter. Blue dots indicate reference turbines, with the dotted line representing the trendlines.

15. Energy Supply System

Within this chapter the final design for the batteries, back-up electrical generation system and cabling will be presented. These systems are vital in the provision of power from the system electrical system to the research station. The battery sizing and type can be found in Section 15.1, with back-up system selection and cabling found in Sections 15.2 and 15.3 respectively.

15.1 Battery Design

For the design of the energy storage system lead acid, as opposed to lithium or nickel based batteries was selected as the battery of choice. One of the dominant reasons for selecting this type of batteries were the low costs per *Wh* of 0.17 dollars [29]. Furthermore as they account for 40-45% of all battery sales worldwide [110] and have a well established recycling process, bringing the recycling rate of such batteries to more than 97% [111] [112], and as such lead acid batteries are a safe and sustainable choice for such storage systems. Due to the expected cycling of the system, deep-cycle, VRLA maintenance free batteries will be used in order to achieve a longer lifetime with least maintenance possible [113]. For a trade-off of the various battery types and aspects considered, the reader is referred to Appendix K.1.

The battery system is required to provide 65% of installed power for an extended period of time to the station (*REQ-TE-12*). Two size options are presented, with future clients to select one for their specific purposes. One option provides energy for one day and as such would require the back-up system to be turned on on average around 30 times a year. This option is the recommended choice as it provides a balance between costs and sustainability. The second option provides energy for three days with the generator needed to be turned on on average 4 times a year, and may be an option for clients who wish to minimise carbon emissions at a higher cost. The design results of the two options are presented below in Table 15.1. It should be noted that in order to increase the lifetime of the batteries the maximum depth of discharge is limited to 50%, and thus the battery capacity must be twice as large as the usable energy.

Table 15.1: Battery sizing

	<i>1 Day Energy Option</i>	<i>3 Day Energy Option</i>
Energy Capacity [<i>GJ</i>]	5.70	17.20
Energy Capacity [<i>kWh</i>]	1600	4800
Mass [<i>t</i>]	39	118
Cost [<i>\$</i>]	270,000	810,000
Back-up Generator On [<i>days/year</i>]	30	4

The battery system will be located in an insulated enclosure with heating elements which can be used to keep the operating temperatures above the minimum -20 °C operating temperature if required. The heating elements in the enclosure can also be used as an energy dumping load explained in Appendix K.5 which describes the load control strategy. Although such an enclosure is more costly and will need to be attached to the research station, the costs of specialist cold resistant batteries would be significantly higher, with a three day equivalent system of Li-SOCL costing more than six million dollars. Further confirmation of lead acid batteries being a viable and implementable choice in the Antarctic environment can be found by considering the Belgium Antarctic station where lead acid batteries are implemented successfully as an energy storage system [114].

15.2 Back-up System Selection

In the case the battery system does not have enough energy stored to meet demand at any given time or in the case of emergencies, a back-up power system must be selected. Three types of back-up systems were considered, namely diesel, bio-fuel and hydrogen fuel cell systems. A summary of the three systems can be found in Appendix K.2. When evaluating possible designs for costs, reliability and sustainability, it emerged that converting the diesel (Marine Gas Oil) generator, currently used as the primary source of energy on the BAS station, to a back-up generator setup would be the best option. Using the current generator would reduce costs, as no new generator would be purchased, also saving on transportation and installation of a new system. Furthermore, such generators are very reliable, as can be seen by the use of such generators as primary energy sources, and so a good choice for an emergency system [115]

[116] [117]. Moreover although such a system still causes green house gas emissions, by using the currently stationed generator, the green house gases that would be used to produce and transport a new generator can be offset [118] [119]. In addition reusing the generator would promote the "Reduce, Reuse, Recycle" motto of waste management hierarchy and as such promote a sustainable future [120]. The generator currently stationed is a 40 kW generator and as such can be used both to meet peak power and provide a margin for possible increase. Hereby, both *REQ-TE-6* and *REQ-TE-9* are met. It is the recommendation of this group that a hydrogen fuel cell system should be explored for future replacement of the generator, when the cost of storing and producing hydrogen have reduced, and the technology has reached a level of maturity to safely and reliably be implemented as both a back-up system and a energy storage system. Such a future change is recommended in order to create an emissions free energy system for the Signy station.

15.3 Grid Connection Cabling

In order to connect the different electrical systems, cabling is needed. Several components can be identified and their distances to the control unit can be found in Table 15.2 in addition to the required thickness of the cables. The distance of the wind turbine to the control unit is a constraint of the noise requirement. It should be noted that there is also a cable running from the back-up generator directly to the station in case of emergencies or failures in the rest of the electrical system. However this generator is already installed at the station and as such is not analysed in this section.

All cables are made from copper, instead of aluminium. This is because copper has better conductivity, better thermal properties and better resistance to corrosion than aluminium [121] [122]. Although aluminium costs less (however exact difference fluctuates with commodity markets), the advantages of copper in the Antarctic environment in terms of maintainability/resistance to damage, in addition to the afore mentioned reasons, outweigh these costs [121] [123].

The cabling to and from the controller will run in an insulated tube on the ground. No overhead cables are used to ensure less interference with the bird population and to protect the cables from the large winds experienced on the island [124]. Underground cabling is not considered economically feasible due to the rock bottom at Signy and environmentally damaging due to the permanent deformation of the rock in the case of implementation [125]. For the full calculation of the cable thicknesses, the reader is referred to Appendix K.3. It should be noted that an extra cable along each connection line will be placed for redundancy, thus avoiding a system shutdown in case of cable malfunction.

Table 15.2: Cable length and thickness

	<i>Distance [m]</i>	<i>Cable thickness [mm]</i>
Wind turbine Generator - Transformer	10	4.6
Wind Turbine transformer - Controller	70	6.5
Controller - Battery	1	8.3
Battery - Station	5	8.3
Back-up - Controller	5	7.3

16. System Communication & Hardware and Software Interface

The flow of data through the system and to and from the environment will be presented in a communication flow diagram in Section 16.1. The required sensors are included in this section. The flow of data consisting of hardware and software of the wind energy system will be explained in Section 16.2.

16.1 System Communication

As can be seen in the communication flow diagram in Figure 16.1, there are three systems present; the wind turbine system, the power supply system and the sensor system. The cabling and condition monitoring system are the main connectors. The communication flows through these different systems.

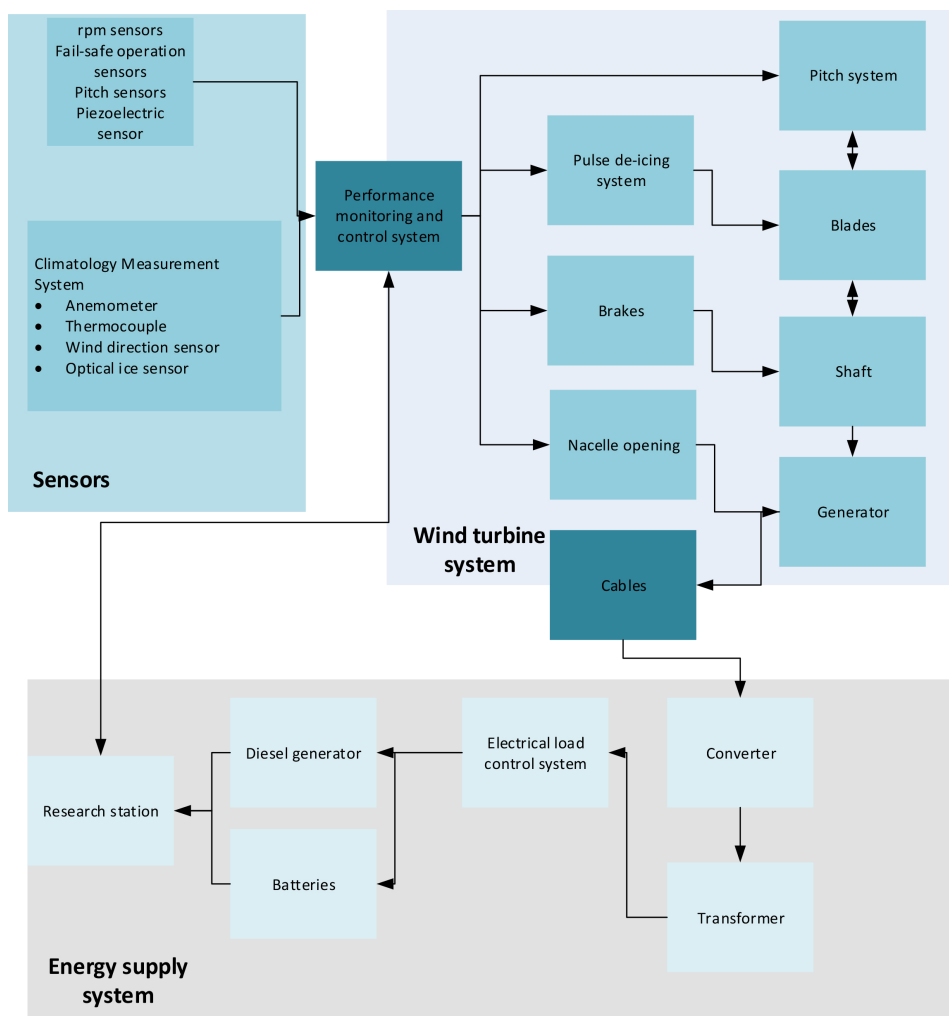


Figure 16.1: System communication

The sensors are used in this design in order to provide the system itself with information about the environment and its operations and as such they need to be protected against the environment in order to obtain reliable data. The sensors that will be implemented are given below.

Wind Direction Sensor and Anemometer: This instrument measures both wind direction and wind speed. An anemometer is responsible for measuring the wind speed. The wind direction sensor measures the direction of the wind. Since the yawing of the wind turbine is limited to 170° , the wind direction needs to be measured to check whether a power drop corresponds to a wind direction outside the allowable yaw angles. This sensor is placed on top of the wind turbine, so it must be protected against the ice to obtain reliable data. Moreover, the wind turbine has a downwind configuration and so the anemometer will operate in undisturbed flow. The sensor that will be implemented is specifically developed for extreme cold climate and it has an active heating function integrated. When the temperatures are below 0°C , the heating will be switched on [126]. The power consumption is 50 kW , this is not significantly high. The wind speed measurement of the anemometer will not be used for accurate control applications (like pitch or rotational speed control).

Blade Pitch Sensor: This sensor will measure the angular displacement of the blade with respect to a reference point in the rotor hub. This sensor is placed inside the nacelle protecting it against the environment and as such the sensor will more consistently give reliable data.

RPM Sensors: A wind turbine system in most cases has two types of *rpm* sensors: one measuring the *rpm* of the rotor blades. These sensor are placed on the inside of the nacelle, on the shaft, so it is not affected by the cold temperatures.

Fail-safe Operation Sensors: This is used to monitor the brake systems in the wind turbine. In the case the aerodynamic brakes are not working the mechanical brake will take over and vice versa. This is done in order to ensure that the wind turbine does not spin uncontrollably causing structural damage.

Torque Sensors: These sensors measure the torque on the rotor shaft. This sensor is placed inside the nacelle, where the sensor will not be affected by the cold climate.

Piezoelectric Sensors: These sensors allow for the size of vibrations to be tracked and thus for the system to be shut down if vibrational loads seem to exceed allowable limits. Furthermore, by keeping track of such information, fatigue loading can be derived and checked with design values to ensure safe operation. These sensors are implemented inside the blades. A spring is used to measure the vibrations. The material of the spring should withstand the cold temperatures.

Optical Ice Sensor: These sensors measure the amount of ice accumulated on its optical surface. An analogy can then be made with a reference state to determine the amount of ice in the blades.

Thermal couple: A thermal couple consists of two sensors measuring the temperatures. One is placed inside the nacelle and the other is placed outside on the shell.

16.2 Hardware and Software Block Diagrams

The control system is composed of actuators, sensors and the central processing unit (CPU) of a servo or monitoring system. So the CPU connects the hardware (sensors and actuators) with the software. The actuator is the part of control system that applies a certain force in order to change, for example, an angle or a length of a chain. They are the electric motors of the pitch system and nacelle opening, pulse actuator, pneumatic brake and back-up and dump switch. The sensors provide the information of the state of the wind turbine and of the environment mentioned above. The CPU is the component that 'closes the loop'. It controls the actuators with the information provided by the sensors.

The block diagrams for energy production system, de-icing system, cooling system, break system, batteries and backup system are presented in the Appendix L, with the battery control strategy shown in Appendix K.5.

17. Integration Plan

The integration plan, all actions taken from manufacturing until erection, for the wind turbines is presented in this chapter. According to *REQ-CO-1*, the wind energy system shall be operational on Antarctica before April of the year 2020. Thus, this integration plan of the wind turbines on Signy will be completed in 6 years. Section 17.1 describes the manufacturing plan for the rotor, nacelle and tower. The transportation plan for all components is covered in Section 17.2. Once the components are transported the wind turbines have to be assembled and erected on the designated location in a sustainable way that complies with the Antarctic conditions, described in Section 17.3.

17.1 Manufacturing Plan

In this section the manufacturing plans for the rotor, nacelle and tower are described in Subsections 17.1.1, 17.1.2 and 17.1.3, respectively.

17.1.1 Rotor Manufacturing

Since only few blades will have to be produced, the manufacturing process should be kept simple. This is to reduce the impact of the investment costs for the required tools. Therefore, the more complex processes like resin transfer molding or automated prepreg lay-up are not considered due to the very high initial costs involved. To simplify the manufacturing process, the internal stiffening box will be integrated into the aeroshells instead of producing it separately and assembling it later. This means that the shape of the blade will be very complex hence excluding production processes like pultrusion or filament winding. These two techniques are only useful for the construction of symmetric and simple geometries and are also relatively expensive. The final manufacturing technique that was chosen is vacuum bagging, which combines the cheap and easy manufacturing of the wet lay-up with the product quality and health advantages of vacuum assisted infusion [127]. Below the main steps in the manufacturing process are displayed:

1. Gelcoat is applied to upper and lower aeroshell molds
2. The outer resin-impregnated laminates are applied
3. The pre-milled balsa cores are applied
4. The cores are covered with laminates to obtain the required thickness
5. Both molds are covered with plastic bags and vacuum is applied to consolidate
6. Both aeroshells are exposed to a curing process
7. The two parts are removed from their molds
8. The two halves are bonded together and cured again
9. The outer surface is polished and inspected for defects

To reduce the costs and carbon footprint of the transportation of the blades, they can be manufactured by PE composites located in Isle of Wight, United Kingdom. The company has more than 10 years of experience in producing composite wind turbine blades and is located within 15 miles of Portsmouth, where the research ship will depart.

17.1.2 Nacelle Manufacturing

The nacelle and its subsystems have many different manufacturing techniques, since it consists of many components. The manufacturing technique and location of the manufacturer for each subsystem are stated below. The brake, hub and bedplate will be manufactured at the cheapest manufacturer, either in the UK or in northeast United States of America, since the research ship and the cargo ship depart from those two locations.

Generator and Shaft: The permanent magnet direct drive generator including shaft is 'off-the-shelf' customised for 143 *rpm* and 17 *kW* rated power and will be manufactured in China, since the leading manufacturers for permanent magnets are located there.

Bedplate: The bedplate will be constructed out of 3 plates of the same steel as is used for the tower, A537 Class 1 (Grade A), by casting. The plates will be welded together to form the requested I-beam. Manual shielded metal arc welding, which is one of the most used techniques in the world, will be used. It is a cheap and versatile process, particularly suited for steel, outdoors constructions. Due to the low required number of bedplates, the automated welding processes, as resistance or energy beam welding, are not used since they require very high investment costs. The bedplates can be manufactured by any metal construction factory located conveniently.

Shell and Cone: the shell and hub cone of the nacelle will be manufactured by the same company that produces the composite blades. The shell and cone can each be constructed out of one piece by applying the vacuum bagging technique which is also used for the blades in the United Kingdom.

Hub: The hub is a very complex shape due to the many cut-outs and thickness variations. To manufacture this steel part, it is first casted to obtain the general shape, after which machining techniques will be applied. Due to the lack of a symmetry axis, turning is not used. Instead, face milling will be applied to remove the necessary material and to create the cut-outs.

Braking System: The brake of the wind turbine will be casted from spheroidal graphite to form the solid disk that is required.

17.1.3 Tower Manufacturing

The tower manufacturing consists of the following steps to create a tower with a continuously decreasing radius from root to tip [128] [129]. The tower can be made out of one sheet of steel [130] with a new turbine tower welding technique, spiral welding [131] [11]. Figure 17.1 [11] shows how the turbine tower is manufactured with spiral welding. The manufacturer Keystone Tower Systems holds the patent on tapered spiral welded structures and is located in Sommerville, Massachusetts [132]. The foundation will be supplied by Maine Drilling & Blasting [133], who have expertise with placing rock anchor foundations in remote areas.

1. The dimensions of the steel sheet are determined and outlined
2. The steel sheet is flame cut and primed
3. The sheet is inserted into a machine with three rollers which will shape the sheet like a conical cylinder
4. The conical cylinder is then spiral welded to make a closed section
5. A holed ring is formed that will function as the connection between tower and anchor bolt cage
6. The ring is attached to the tower by submerged arc welding
7. The tower is placed into a painting and drying tunnel
8. Shot peening is applied to avoid the propagation of microcracks on a surface
9. After the shot peening treatment the paint is applied, also to protect the tower for corrosion
10. Pipe saddles are mounted on the inside of the tower near the tip and near the root for extending the cables coming from the nacelle

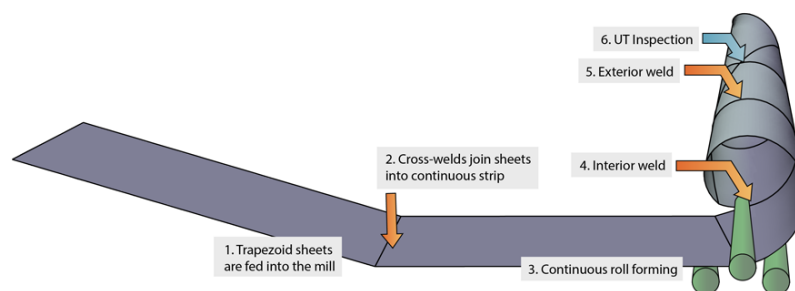


Figure 17.1: Spiral welding technique for turbine towers [11]

17.2 Transportation Plan

The components of the wind turbines are from all over the world. The blades are manufactured in the United Kingdom, the generator in China, the other nacelle components in Europe or in the northeastern states of the United States of America and the tower and foundation in the northeastern states of the United States. Subsection 17.2.1 discusses the transportation to Borge Bay, Signy Island. The transportation of the system components from the cargo ship to the wind turbines site on Signy Island is covered in Subsection 17.2.2.

17.2.1 From Manufacturers to Borge Bay

The blades are manufactured in Europe in the United Kingdom near port Portsmouth and will be transported by truck to Portsmouth, Great Britain. All nacelle subsystems except the generator are manufactured in Europe or northeast United States of America and will also be transported by truck to either Portsmouth or Boston. The generator is manufactured in China and will be transported by truck to the nearest port, from where it will be shipped to Portsmouth through the Suez Channel. From Portsmouth a research ship from the British Antarctic Survey will depart to Antarctica and Signy Island [134]. This research ship makes an intermediate stop at the Falkland Islands, which is British territory [135]. Naturally, the British Antarctic Survey research ship and the cargo ship which supports a project funded by the British government are allowed to berth at and leave from Port Stanley, Falkland Islands. The tower is manufactured in Massachusetts, United States of America, and the foundation components, including the grouting mixers, are supplied by a company in Maine, United States of America. The erection system and support structures come from Minneapolis, United States of America [136]. The tower, foundation and erection system components are transported over the road by trucks to the port of Boston. One cargo ship will transport the tower and foundation to the Falkland Islands.

At Port Stanley, Falkland Islands, the rotor and nacelle components will be unloaded from the research ship and loaded onto the tower and foundation cargo ship. From the Falkland Islands one ship, the cargo ship, will depart to Signy Island, Antarctica. There is opted for using another ship than the research ship from the British Antarctic Survey, because the foundation needs a month to harden. It is convenient to have the components and the assembly and erection workers near Signy when work needs to be done. The research ship has an already scheduled trip to several research stations located elsewhere on Antarctica for providing cargo and dropping off and picking up researchers. It is scheduling-wise not possible to use the research ship during the wind turbines system assembly and erection period at Signy Island.

The rotor and nacelle components are transferred from the United Kingdom to the Falkland Islands by a ship of the BAS. They have two research ships which can both hold cargo, the RRS Ernest Shackleton and the RRS James Clark Ross. The RRS Ernest Shackleton has an aft cargo hatch at the first bridge deck, a forward cargo hatch on deck A, and an aft and a forward main cargo hold on deck B and deck C. The aft cargo hatch on the first bridge deck is able to hold 2 ISO 20 *ft* containers. The forward cargo hatch on deck A is able to hold 4 ISO 20 *ft* containers. The dimensions of a 20 *ft* container are 20 *ft* in length, 8 *ft* in width and 8 *ft* in height. The main cargo holds on the lower decks are even larger, but are harder to reach. The main cargo crane can lift weights up to 30 *ton* with an arm of 20 *m*. The ship also has a helicopter deck. The RRS James Clark Ross can hold 4 ISO 20 *ft* containers aft on the deck and 1 ISO 20 *ft* container forward on the deck. The main cargo crane can lift weights up to 20 *ton* with an arm of 20 *m*. This ship also has multiple cargo holds, but again harder to reach with the cargo crane. The RRS Ernest Shackleton and the RRS James Clark Ross are shown in Figure 17.2a and 17.2b, respectively. One of these ships, depending on their departure date from port Portsmouth and their route in the Antarctic seas will be used to ship the components of the wind turbines to Signy Island. The costs and the carbon footprint will be reduced when making use of the research ship as transportation resource, since the research ship will travel to the Falkland Islands in any event. [137]

The tower, foundation, nacelle and erection mechanism components are transported from the port of Boston to the Falkland Islands by means of a small feeder cargo ship, the smallest type of cargo ships available. Such a ship is approximately 100 *m* long, has a width of 17 *m* and an average speed of 15 *knots* [138]. From the Falkland Islands this vessel will transport all the components to Signy Island.



(a) RRS Ernest Shackleton [137]



(b) RRS James Clark Ross [137]

Figure 17.2: BAS research ships

17.2.2 From Borge Bay to the Wind Turbines Site

Large ships cannot reach the Signy Research Station due to more shallow waters at Borge Bay. From Borge Bay to the research station, a smaller vessel with a platform is needed. A Meercat workboat [139] shown in Figure 17.3a, which supplier is located only 3 miles from Port Portsmouth, is used to transport the components of the wind turbines from Borge Bay to Factory Cove, where the research station is located. The workboat has to make several roundtrips in order to transport all components. The workboat will navigate from the suppliers location through the bay to Port Portsmouth. From there it will be attached to the side of the research ship. At the Falkland Islands the workboat will be lowered, navigate its way to the cargo ship and be attached to the side of the cargo ship.



(a) Meercat workboat [139]



(b) Foremost Husky 8 [140]

Figure 17.3: Transportation media

Once the components have arrived at the coast, they need to be transported to the site near the research station where the wind turbines will be erected. A Foremost Husky 8 with a cargo deck and a two man cabin can be used, shown in Figure 17.3b [140]. It can operate under extreme conditions and on a variety of grounds. The Husky can be readily equipped with an excavator, drilling rig and crane. This eliminates the need for separate machines [140]. The Husky 8 will be driven from Calgary, Canada to the port of Boston from where it will depart with the cargo ship.

17.3 Assembly and Erection Plan

When the cargo ship has reached Borge Bay the grout mixers, the Husky 8 with the foundation components and excavator, drilling rig and crane equipment will be transported to the Signy Island coast with the Meercat workboat which will have to make multiple roundtrips between cargo ship and land. The drilling tool prepares the cylindrical holes in which the anchor bolt cage, steel can and reinforcements will be placed. The excavator tool removes the loose rock from the foundation site. The foundation can be laid conform the procedures described below [101]. The grout is mixed at the site in the grout mixers. From the foundation sizing 2130 dm^3 concrete is needed. Two grout mixers which can hold 350 dm^3 , standard size, each will be used for the placing of the concrete.

1. Drilling the rock until it is loose
2. Removing the rock with an excavator
3. Drilling the self-drilling anchors in the rock bottom
4. Grouting the shafts where the anchors are placed
5. Placing outer cylindrical can in hole
6. Placing soil for layer in between rock bottom and concrete cap
7. Placing a first layer of concrete
8. Setting the anchor bolt cage
9. Placing concrete cap with reinforced steel
10. Tensioning the anchors

4 pipes are pushed into the surface of the concrete cap when it is still wet to create gutters where the wires are placed that conduct the current introduced in the system by lightning. The wires are insulated, but not at both ends. One end is connected to the tower once it is erected, the other end will be brought into contact with the rock anchors.

The nacelle subsystem are integrated into the shell at Signy Island. The rotor and nacelle are on the ground assembled to the 8.8 m high turbine tower. The blades are transported as separate components and assembled at the site. The

last step is to attach the rotor hub to the generator shaft. This is all assembled with the tower laying down on supports on the ground. A vertical gin pole wind tower raising system is used to erect the wind turbine. This structure can take up to 3 tons and erects towers up to 14 m [136].

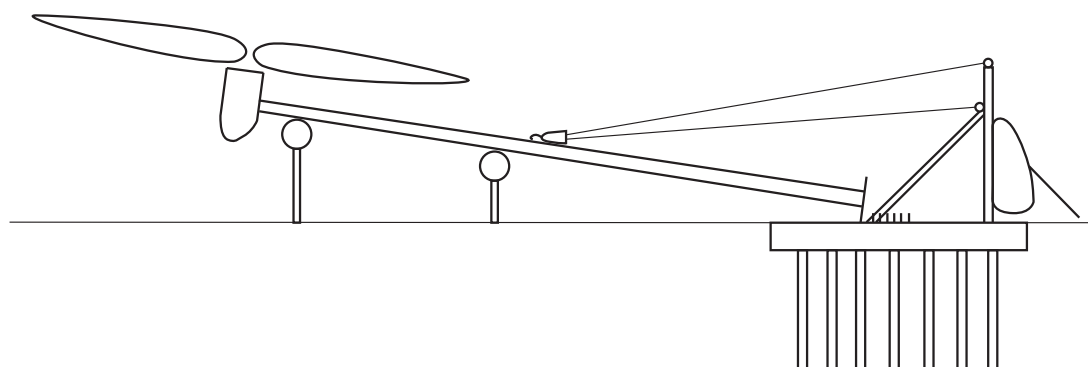


Figure 17.4: Wind turbine erection

Figure 17.4 presents the turbine erection lay-out with the fully assembled wind turbine on the ground. A tirfor sets the turbine upright. This erection strategy is not labour intensive. One person is needed to lever the tirfor, one person needs to check that all connection points are clear from obstruction and two persons need to check the state of the tower during the erection process of which one is supervising the erection.

During erection different loads are acting on the tower than during operation. When the cable from the tirfor is attached at half the tower height, 4.4 m, the bending moment at the lifting point is 54 kNm. The tower is designed to withstand a bending moment of 150 kNm at that lifting point location, so the tower will not fail during erection. [108]

When the tower is standing up straight, the tower is bolted to the rods of the anchor bolt cage extending above the concrete. The conductive wires for lightning strikes are then attached to the tower. Once all the above steps have been completed, the turbine system can be brought to operational readiness, where all electrical and mechanical connections are checked, and calibrated for energy production.

18. Operations, Maintenance and Logistics

This chapter will elaborate on the operational aspect of the wind turbine system, as well as the maintenance and logistics that are required for it. First of all, the performance monitoring system will be explained since this is of primary use for checking the operational performance of the wind turbine system and allows for investigating the proper working of the important systems in Section 18.1. Next, the operations will be described in detail, for different situations during the operational life in Section 18.2. In addition Sections 18.3 and 18.4 will present the maintenance procedures and logistical aspects that are required to ensure proper use of the wind energy system.

18.1 Performance Monitoring System

In order to monitor the wind turbine and its system, a semi-autonomous system is implemented which checks the status of several components and outputs. The performance monitoring system is part of the larger 'Performance Monitoring and Control System'. The monitoring process may be carried out online, to provide real-time feedback of condition; or offline in which data is collected at pre-defined time intervals using measurement systems. The monitoring system measures the performance of the wind turbine in terms of power and wind speed and also checks anomalies. Wind turbine performance depends on wind speed. This monitoring system measures the performance of the turbine in terms of power and wind speed and checks for anomalies.

The parameters that are measured are: power output, wind speed/direction, pitch angle, nacelle temperature, rotational speed and torque. Each of these parameters are measured with sensors that are described in Section 16.1. Redundant sensors are used to make sure the measurements are reliable. The three wind turbines will also be compared to each other to help in determining whether a component or a sensor is failing.

The performance of the turbine is checked by comparing the measured wind speed and power output data with the power curve. Every second the data is sent to the station, where a computer analyses the outputs. If the power output deviates by 5% from the power it should give for a certain wind speed for 2 days, an error light will go off in the station and a log of the data of the last 2 days will be sent to the UK specialist. The average power and wind speed data of a time period of 10 seconds is taken, to ensure that no gusts set off the failure system. The wind direction is also checked, to see whether the turbine is in maximum yaw. If the wind speed is coming from a direction to which the turbine cannot turn, the power output will not match the correct wind speed. This is because the wind speed is measured independent of the direction to which the turbine turns.

Several components are also monitored for anomalies:

- **Rotational Speed:** The rotational speed is checked to ensure it does not exceed a maximum.
- **Nacelle Temperature:** The nacelle temperature is monitored to observe the generator. The temperature should not surpass a predetermined maximum.
- **Torque:** The torque is also tracked to make sure it does not surpass the maximum torque the generator can handle.
- **Pitch Angle:** The pitch angle is monitored to check if the pitch control system is working. In case of a failure, no pitch angle change will be detected.

If the monitoring system detects an anomaly in any of these components, the station is warned by an error signal and the turbine is shut down. The UK specialist is informed and the data of the hour up until the failure is sent. Based on this data, the UK specialist will decide if the component needs to be repaired or replaced.

18.2 Operations of System

Although it might seem that the wind turbines are autonomous systems that provide power to the research station without the need of human interference, operational management is still needed to ensure safe and reliable power production. During normal operations of the wind turbines, one researcher will be appointed the task of 'Operations Manager' and will be trained accordingly. This person will be responsible for the daily management of the turbines, as well as the coordination of special situations like shut-down or start-up of the system.

During normal operations, the wind turbines will autonomously provide power to the research station and the on-board control systems will regulate the power production. However to evaluate if the system performs as desired, the performance monitoring system must collect the required data as stated above. The task of the Operations Manager is to send the data of the previous 24 hours to the responsible UK contacts, accompanied by a small log report stating possible anomalies or issues that were encountered. Thus the Operations Manager acts as a liaison and the actual performance evaluation of the system will be performed by a specialist in the UK. Additionally, the Operations Manager will perform an inspection of the site and wind turbines each week. The site inspection covers gates, fences, access tracks and electrical infrastructure. In addition to a checklist set up by the technicians, the Operations Manager can use visible, olfactive and auditive senses to perform the inspection. Finally, the Operations Manager is also in charge in case of an alert that emerges from the monitoring system. In case of a critical alert like overheating of the generator or failure of the pitch system, the Operations Manager will immediately contact the responsible technician crew in the UK for support and take the required actions from within the research station.

Apart from the daily operations, some other situations need to be considered as well. Since the station is currently only manned during summer, the wind turbines can be out of operation for approximately 8 months of the year since there will be (almost) no power demand during this period. Therefore, the entire system will be entered into a 'hibernating mode' before the scientists leave the station. This is achieved by pitching the blades towards the wind and locking the rotor into a fixed position to park the turbine (the yawing of the turbine will not be fixed). Since the de-icing system is only useful at the leading edge (where ice can build up during normal operations), it will not be turned on during the hibernating period. The control system inside the turbine will be shut off from within the system as required, and the performance monitoring system itself will enter a hibernating mode. This means that the system will not measure all the parameters nor will it measure every second. Only critical parameters will be measured from time to time, as for example the rotation of the rotor (which should be zero), the temperature inside the nacelle and the pitch angle. The measurements can be taken with ever increasing time intervals, if the trends show no significant changes in the parameters. In case of an anomaly (e.g. the blades start rotating, or the temperature in the nacelle increases significantly) or at the end of every week, the data is sent to the specialist in the UK who can safely monitor the integrity of the turbine. The required power for the hibernating mode will be provided by the battery station that is charged fully before leaving the station. With 1600 kWh of energy stored in the batteries, it is possible to provide 270 W of power continuously for 8 months, which will be amply sufficient for the monitoring system. On top of this, it is also better for the lead acid batteries to discharge them rather than not using them at all.

When the scientists return in the summer, the system is returned from its hibernating mode and the components are thoroughly checked before producing power again. The yearly maintenance session of the turbines will then also be performed, see Section 18.3. The central computer unit checks all the sensors inside the turbine and the Operations Manager performs the necessary inspections. When all systems are cleared for operation, the wind turbines are released from the parked position and they can enter the normal operations phase again.

18.3 Maintenance of System

To be able to ensure an operational lifetime of 15 years for the wind turbine system, it is important to perform proper maintenance, for which two types are distinguished. The first type is corrective maintenance which consists of repairing failed components, while the preventive maintenance is performed to avoid the system of having a breakdown and keep the equipment working properly [141]. The maintenance of the system shall be limited to 1 session per year (*REQ-TE-15*), mainly since it is expensive to transport a skilled maintenance crew to Signy Island. To limit corrective maintenance as much as possible, it is important to estimate the failure rates of the different components [142], as shown in Section 6.1. Using these failure rates, several components are given extra attention to reduce the risk of early failure. A thorough preventive maintenance session each year is also useful to limit the amount of corrective maintenance, so that some parts can be replaced before they lead to a system failure. Finally, the performance monitoring system can provide valuable insight into which components need extra attention during the yearly preventive maintenance system, thus reducing the need for corrective maintenance.

The preventive maintenance sessions will be performed at the start of every summer season. The first scientists will then arrive at the station with the research ship, accompanied by a maintenance crew. After performing the maintenance of the wind energy system, the maintenance crew departs again with the research ship to the other stations located in Antarctica to perform technical maintenance tasks there. Every five years, a more thorough maintenance session will be performed by externally hired maintenance experts. In Appendix M, a list of the required maintenance tasks for the yearly maintenance session is given. This task list is based on a schedule that was designed for offshore turbines in addition to the maintenance manual of the WT 6000, a reference wind turbine used at the Belgian Princess Elisabeth station [143].

18.4 Logistics

Logistics is defined as all the support provided to operate and maintain the turbines. The different support units will be determined and briefly explained. The spare parts that are produced and stored will also be shortly examined.

Support

The support is made up of several crews:

- **Operations Manager:** The Operations Manager is a scientist who has undergone training to provide on-base support for the turbine. He visually inspects the turbine and he is in charge of sending the data and reports to the UK specialist.
- **Technicians Crew:** The technicians crew is the team that accompanies the first group of researchers that arrives at Signy station in the summer. They will be trained appropriately to perform the yearly maintenance of the wind turbines, after which they go to the next stations along with the research ship.

The next persons are hired externally:

- **UK specialist:** The UK specialist analyses the data which is sent to him by the operational manager. Based on the data he determines what kind of maintenance needs to be done.
- **External maintenance crew:** The external maintenance crew is in charge of repairing and replacing critical failed parts and to do full system checks every five years (see Appendix M). In case of an unexpected failure, the specialist can inform the crew to immediately go to Signy Island for corrective maintenance.

Equipment

Several different tools and parts are bought and brought to the station. The erection system will remain on Signy and will be used when a turbine needs to be taken down to repair. Several small tools will also be stored at the station. All other tools that are needed for repairs will be brought by the maintenance crew with each visit. A small amount of spare parts is stored at the station. These consist only of parts that can be bought in bulk, e.g. brakes, which need to be replaced every year.

19. Sustainability Implementation and Environmental Impact

The sustainability and the environmental impact of the system are important factors when implementing the system. Section 19.1 discusses the sustainable development strategy. The optimised carbon footprint of the system, from manufacturing to the end-of-life disposal phase, is determined in Section 19.2. The noise and visual impact of the system on the environment on Signy Island are covered in Section 19.3. In Section 19.4 the carbon footprint of the wind turbines system is compared to the carbon footprint of the diesel generator currently used.

19.1 Sustainable Development Strategy

A widely used definition of sustainable development is obtained from the Brundtland Commission of the United Nations [144]. They describe sustainable development as *'the ability to make development sustainable to ensure that it meets the needs of the present without compromising the ability of future generations to meet their own needs'* [145]. With the definition of sustainable development in mind it is important to know how to incorporate this definition in the design of the wind energy system. In Subsection 19.1.1 the plan of addressing this definition in the design and life cycle is stated and the contribution of wind energy to sustainability is explained in Subsection 19.1.2.

19.1.1 Sustainable Development Plan

The sustainable development of the wind energy system at the Signy station is one of the key design objectives. This is also mentioned in the mission statement. Several requirements can be linked to this sustainable objective, in an environmental, social or economic way. The design process, production, utilisation, support and the disposal at the end of life should be executed as sustainable as possible. The long-term sustainable goals of the energy system are:

- Reduction of waste to limit the harm to the Antarctic environment;
- Reduction of the emissions to limit the contribution of the wind energy system to global warming;
- Be an example for other research stations in the Antarctic region considering sustainability

The sustainable development plan to achieve these long-term goals is defined by the requirements. Regarding the carbon footprint the carbon emission needs to be minimised during the process from design to end-of-life disposal and the use of fossil fuels needs to be limited. Furthermore, the noise and visual impact in the environment need to be minimised. During the planned actions particular attention should be given to the above mentioned goals.

19.1.2 Contribution of Wind Energy to Sustainability

Sustainability is largely influenced by three dimensions; environment, economic and social. Sustainability can be discussed in a structured way by considering these three domains [146]. The overwhelming consensus of scientific opinion is that human activities, particularly the emission of greenhouse gases, are the cause of global warming. The energy sector is by far the biggest source of these emissions. Also the limited fossil fuel reserves emphasize the need for sustainable and renewable sources of energy. The potential of wind power is enormous and offers many advantages concerning the three dimensions of sustainability. [147]

Environment Dimension: Turbines produce no particular emissions that contribute to the pollution of water and air. Wind power is pollution-free during operation and does not contribute to global climate change. Other power sources produce large amounts of greenhouse gases, while the gases are negligible for wind energy systems. Only during manufacturing, installation and maintenance of the devices emissions are produced. Additionally, wind is a renewable energy source that is inexhaustible in contrast to the exhaustible fossil fuels. Wind energy systems are more in harmony with the environment than most other energy sources.

Social Dimension: The use of wind turbines reduces the dependency on foreign fossil fuels of different regions and countries significantly. This locates the energy sector into the local economy. It also creates a larger diversity in the energy sources around the world. The use of wind energy on Antarctica will make research able to be done in a sustainable way. Other research stations or institutions in remote areas can learn from the wind turbine design on Signy Island and implement the design choices in a similar environment.

Economic Dimension: Wind is a freely available energy source. It does not need to be mined or transported and it limits the operational costs of the electrical generation. The cost of electricity from fossil fuels and nuclear power may fluctuate greatly while the wind energy cost are largely fixed. Wind energy projects create new jobs from engineers up to lawyers, for long and short periods.

19.2 Optimised Carbon Footprint

The total sets of greenhouse gas emissions of the manufacturing, transportation, erection and back-up system are transformed and summed to calculate the carbon footprint of the wind turbine. Among the renewable energy technologies, wind power is estimated to be among the lowest life cycle emitters of greenhouse gases. However, given the remote location of the Signy station, to achieve low values of carbon footprint a strategy to minimise waste has to be implemented. The requirements for the carbon footprint are that the wind energy system shall have a minimised carbon footprint and that a waste management plan shall be constructed for the entire life cycle of the wind energy system. The carbon contribution of manufacturing, transportation and erection are covered in Subsection 19.2.1 and the carbon footprint of the back-up generator in Subsection 19.2.2. The contribution of the end-of-life disposal is discussed in Subsection 19.2.3. Maintenance operations are not taken into account in the carbon footprint since they are unpredictable. Note that the carbon footprint is calculated for three wind turbines.

19.2.1 Carbon Footprint Due to Wind Turbines Integration

Manufacturing

The carbon footprint of the manufacturing processes of the wind turbine are roughly divided over the five main parts of the wind turbine, since they represent almost the entire carbon footprint of manufacturing. For every main part the carbon footprint created by manufacturing is subdivided into the carbon footprint created by the fabrication of the material and the fabrication of the part by using the fabricated material.

The foundation consists mainly out of concrete and steel. The total mass of concrete needed for the 3 foundations of the wind turbines is calculated to be 5760 *kg* this gives a carbon footprint of 3000 *kg CO₂*. The foundation consist also of an anchor bolt cage, rock anchors and numerous rebars. These steel parts of the foundation are estimated to weigh 800 *kg* per wind turbine, so 2400 *kg* for the three foundations. The manufacturing of these steel parts, considering tubes [148], creates 0.857 *CO₂* (*kg/kg*), so for the 3 foundations together this gives 2060 *kg CO₂*.

Another main part of the wind turbine system is the tower. The tower consist of primarily steel, with possibly some extra coating on the outside but this is neglected. The mass of one turbine tower is 738.5 *kg* so for the 3 wind turbines 2215.5 *kg*. The same value as for the foundation steel is used, 0.857 *CO₂* (*kg/kg*), this results in a total carbon footprint for the towers of 1900 *kg CO₂*.

The manufacturing of the rotors will also create a carbon footprint. The material used for the blades is "Carbon Flax Hybrid Composite with Super Sap 1100 53% Bio Based Epoxy", however for this specific material no information related to its carbon footprint is available. Therefore the most relevant information available to this type of material is the carbon footprint of carbon fibre reinforced polymer used in the automotive industry, with a value of 29.5 *CO₂* (*kg/kg*) [149]. The weight of the rotor is 75 *kg*. This gives for the 3 rotors in total a weight of 225 *kg* and results in a carbon footprint of 2215 *kg CO₂* for the three rotors.

The manufacturing of the generator is the most time and cost intensive process of the nacelle manufacturing. However, since no sources are available on the carbon footprint of the manufacturing of the nacelle and its subsystems, a factor of 25% of the total carbon footprint of manufacturing excluding the battery system will be applied for the generator manufacturing and equals 2300 *kg CO₂*.

The manufacturing of lead-acid batteries has a carbon footprint of 0.9 *kg CO₂* per *kg* battery [150]. This comes to 106,200 *kg CO₂* for when the battery stores energy for 3 days (back-up generator runs for 4 days a year) and 35,100 *kg CO₂* for when the battery stores energy for 1 day (back-up generator runs for 30 days a year).

Transportation

The transportation of the blades and tower from the manufacturer to the harbour are neglected since they are manufactured very close to the port in Boston or Portsmouth. The generator and shaft are shipped from China and with its 400 kg it has a carbon footprint of 390 kg CO₂ [151]. The Foremost Husky 8 is manufactured in Calgary, Canada. With a distance of 4000 km, a weight of 40,000 kg [140] and a carbon emission of 130 g CO₂ per tonne·km for transportation over the road by heavy trucks [152], the carbon emission is 20,800 kg CO₂. The foundation and the grout mixers are from Maine, United States of America. They have a weight of 5760 kg, since the foundation volume is 2130 dm³ in total from the foundation sizing and the concrete has a density and mass of 2.4 kg/dm³ and 900 kg, respectively. The anchor bolt cage and reinforcements weigh 2100 kg. A distance of 250 km results in 285 kg CO₂ emission. The erection system and support structures are from Minneapolis, United States of America and with a distance of 2250 km and mass of 900 kg [136] the carbon emission is 265 kg CO₂. The nacelle subsystems are manufactured in Europe. With a weight of 300 kg and an estimate of 1500 km the emission is 60 kg CO₂ for the transportation.

Ships will depart from Great Britain and one from Boston. The carbon footprint of the research ship that departs from Great Britain is not taken into account, since this trip is already scheduled and will also depart if it would not be used for the transportation of the wind turbine components. The route from Boston harbour to Signy Island is approximately 13,500 km. The speed of the small feeder is 15 knots which is 7.7 m/s. The ship runs on a diesel engine with a specific oil consumption of 174 g/kWh and a power output of 2525 kW. Burning oil results in 3.2 kg CO₂ per kg fuel burned. The CO₂ emission is the total fuel consumption for the trip times the CO₂ emission per kg fuel, and results in 637,000 kg of CO₂. The transportation of the system with the MeerCat and Husky 8 from the ship in Borge Bay to the wind turbines site is such a short distance that it is neglected in the carbon footprint calculation.

19.2.2 Carbon Footprint Due to Back-up Generator

Depending on the battery choice the back-up generator needs to run for different amount of days each year. If chosen for the battery where the back-up generator needs to be turned on for 4 days each year, the carbon footprint contribution of the diesel generator will be 37,440 kg CO₂ over 15 years. If chosen for the battery where the back-up generator needs to be turned on for 30 days each year, the diesel generator will generate 280,800 kg CO₂.

19.2.3 Carbon Footprint Due to End-of-life Disposal

At the end-of-life the wind turbine should be dismantled and the parts, with exception of the foundation, should be taken from Signy Island. There are currently three options for the disposal of the wind turbine. These options are landfill, incineration and recycling. [153]

Landfill represents the cheapest option. However, it is not sustainable. Landfills causes serious problems on the environment and contamination of groundwater and soil, but also on the atmosphere due to the methane generated by decaying organic waste. Incineration is the second option which produces energy by burning materials. However, incineration harms the environment due to the release of greenhouse gases and approximately 60% material remains as scrap that can be disposed in a landfill or recycled. Recycling is the most sustainable option, since materials are reused. Currently, there are two main methods of recycling wind turbines. The first one is mechanically, which greatly reduces the scrap size to produce recyclates. The second one is thermal processing, which breaks down the scrap material into materials and energy.

At the end-of-life of the wind turbine system the wind turbines need to be taken down and removed from Antarctica conform the Antarctic Environmental Protocol. The protocol also states that no visible traces may be left behind. Therefore, the foundation will stay on the same place, because more CO₂ is emitted by the necessary machines than by letting it stay. The research ship of the BAS will go to Antarctica as a scheduled trip. After visiting the research stations and dropping off the researchers and cargo, the ship makes another stop at Signy Island [137]. Workers will be brought by helicopter from Ushuaia, Argentina to the research ship which has a helicopter platform. The workers will dismantle the wind turbines by first lowering the wind turbines and then cutting the blades and tower up into pieces. The nacelle will also be dismantled. The anchors sticking out of the foundation will be cut off and grinded to remove sharp edges. All waste is loaded onto the research ship. The ship makes a stop at Cape Town [137]. Here, all the components are unloaded from the ship. The steel from the tower, foundation top part, bedplate, shaft and transformer will be brought to a steel recycling site.

It is assumed that the end-of-life recycling rate of steel is 99%. However, the steel used in the wind turbine is already from 59.4% recycled steel. This gives a net scrap percentage produced during life time of 39.6%. Roughly 1.787 tonne of CO₂ is saved for every tonne of scrap steel that is recycled. Therefore the entire carbon footprint created by the steel used in the wind turbines can be decreased by 1570 kg CO₂. [148]

The carbon-flax-fibre-reinforced polymer blades and the glass-fibre-reinforced polymer nacelle shell can be recycled mechanically, by cutting and milling. The recyclates are then categorised on their size and can be used as filler and reinforcement material in new composite fabrication [154]. The permanent magnets in the generator will be recycled and used in hardcore for road construction [155]. The rest of the generator can be recovered or modified and resold by specialised generator recycle companies.

Lead-acid batteries are for over 98% recyclable and consist of about 70% recycled lead and plastic. [156] Therefore, for the 1 day storage battery system a carbon footprint of 9800 $kg CO_2$ can be subtracted and for the 3 day storage battery system 29,700 $kg CO_2$.

19.2.4 Total Carbon Footprint

The total carbon footprint of the wind turbines system is based on the manufacturing of the system, the transportation of the system and tools and machines needed for integration, the contribution of the back-up diesel generator and the end-of-life disposal. Table 19.1 presents the contribution of the carbon for each contributor and the total carbon footprint. The total carbon footprint of the system for when the generator has to be turned on 4 days in a year, with the 3 day battery energy storage, is estimated on 782,600 $kg CO_2$, or 117 $g CO_2/kWh$, and for 30 days in a year, with the 1 day battery energy storage, 974,800 $kg CO_2$, or 146 $g CO_2/kWh$. The requirement on carbon emission is met for both battery options.

Table 19.1: Total carbon footprint

<i>Element</i>	<i>Carbon emission in $kg CO_2$</i>
<i>Manufacturing</i>	
Foundation	5060
Tower	1900
Generator	2300
Blades	2215
Battery: 1 day storage	35,100
Battery: 3 day storage	106,200
<i>Transportation truck</i>	
Husky 8	20,800
Foundation + grout mixers	285
Erection and support	265
Nacelle subsystems	60
<i>Transportation ship</i>	
Generator	390
Wind turbines system	637,000
<i>Back-up generator</i>	
4-days option	37,440
30-days option	280,800
<i>End-of-life disposal</i>	
Steel	-1570
Battery: 1 day storage	-9800
Battery: 3 day storage	-29,700
Total for 1 day energy storage	974,800
Total for 3 day energy storage	782,600

19.3 Noise and Visual Impact in Environment

A wind turbine has three noise sources; tonal, broadband and low frequency. Tonal sound is sound at discrete frequencies caused by gears, the generator, non-aerodynamic instabilities at the rotor blade surface and unstable flows at holes and slits and a blunt trailing edge. Broadband sound is a continuous distribution of sound pressure with frequencies greater than 100 Hz caused by interaction between atmospheric turbulence and the rotor blades. Low frequency sound is sound with a frequency between 20 and 100 Hz caused by local flow deficiencies at the rotor blades. The broadband sound is the most prominent sound. Impulsive sound is characteristic for downwind turbines, which is caused by the tower shadow. [157]

The sound pressure level L_p is a logarithmic measure of the effective sound pressure in dB . The sound pressure level varies with distance from the sound source. Since the most prominent sound will be above 100 Hz and below 250 Hz a weighting is used that approximates the response of the human ear to sounds of medium intensity. The human ear hears a lower sound pressure level than a measuring device. The A-weighting corresponds to the broadband sound. For a frequency between 100 and 250 Hz the A-weighting factor is -15 dB . This means that the sound pressure level observed by the ear is 15 dB lower than the actual sound pressure level [157]. From the initial requirements there is a constraint on the noise level. The acoustic noise resulting from the wind energy system operations shall not exceed 40 dB(A) at the research station [158]. Due to this requirement there is a maximum rotational speed at a certain distance from the research station according to Equation 19.1 [159], based on small wind turbines, where Ω is the rotational speed in rad/s , D the rotor diameter in m and R the distance from the hub in m . Since there are three wind turbines and Equation 19.1 is only correct for one wind turbine, the sound pressure level will be lowered from 55 to 50 dB . This is the equivalent sound pressure level for a little over 3 turbines and less than 4 turbines, since dB is a logarithmic unit.

$$L_p = 50\log(\omega) + 60\log(D) - 27 - 20\log(R) \quad (19.1)$$

The maximum rotational speed is 15 m/s and the maximum measured sound pressure level is 50 dB for a sound pressure level sensed by the human ear of 40 dB(A) . From Graph 19.1, where the red line corresponds to the right vertical axis and the blue line to the left vertical axis, it can be seen that the wind turbines have to be placed at least 70 m away from the research station. Since the design is based on pitch regulated blades, the blades will not stall, and thus there will be no noise contribution due to stalling. Furthermore, since the design is based on variable speed, the wind turbines will be quieter at lower wind speeds than a constant speed turbine. These two factors are favourable for a low sound pressure level. Even though the sound pressure level of the wind and background noise is over 40 dB(A) , the determination of the wind turbines location will still be based on these calculations to make sure the wind turbines will not be annoying noise source for the researchers. Next to the researchers the wildlife will also not be influenced by the wind turbine noise. The mammals and birds on the island communicate with higher frequency sounds [160].

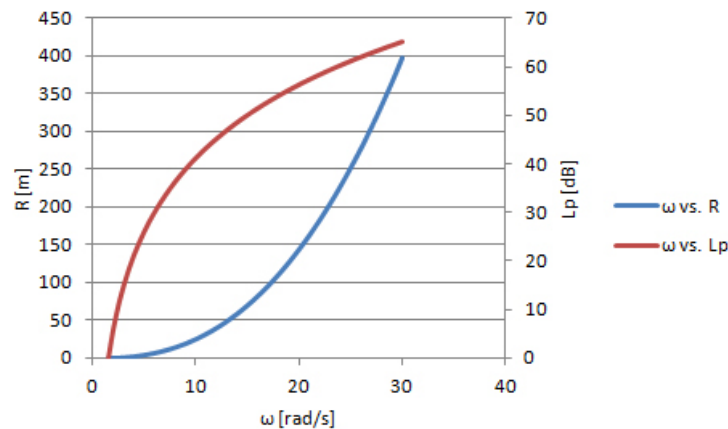


Figure 19.1: Distance from station and sound pressure level as function of rotational speed

For the visual impact potential shadow flickering is considered. The day with the longest daylight is considered, December 21 for in 2014. The wind turbines are placed south-south-west with respect to the research station, indicated with the red square in Figure 19.2 [12]. The black lines indicate the shadow direction and normalised shadow length. The wind turbines will not have a shadow on the station on the longest day. The other days throughout the year the sun will come less out of south-eastern and south-western direction. Therefore, the wind turbines will never leave a shadow, year-round, in the direction of the research station, and thus never on the research station. Shadow flickering will not occur.

19.4 Sustainability Comparison

If instead of the wind turbine system the diesel generator that is already present at the research station stays in operation, the carbon footprint of the power system would be much higher. A diesel generator generates 250 kg of CO_2 per MWh produced [161]. Taking an operational lifetime of 15 years, taking into account a diesel generator efficiency of 35% [162] and assuming that the wind turbines might have to operate during winter, the carbon emission of the diesel generator is $3,416,000\text{ kg } CO_2$ for the operational lifetime of 15 years.

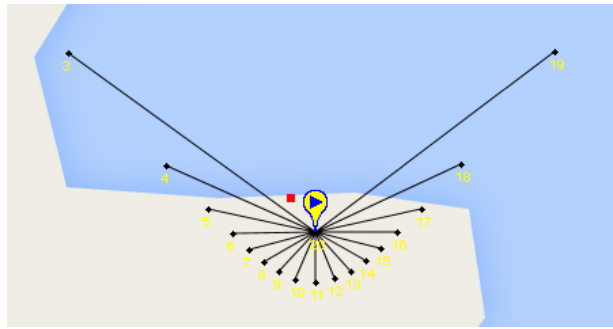


Figure 19.2: Normalised shadow of turbines [12]

The carbon footprint of the wind turbine system for when the back-up generator has to be turned on 30 days a year is estimated to be $974,800 \text{ kg CO}_2$ and for when the back-up generator has to be turned on 4 days a year it is estimated to be $782,600 \text{ kg CO}_2$. For both battery storage options it is at least 3.5 times more sustainable to implement the wind turbines system than to let the diesel generators run for 15 years, regarding the carbon footprint. For the determination of the carbon footprint a power output of 51 kW for the wind turbine system and 40 kW for the diesel generator has been used. Furthermore, even if the diesel generator only has to run during summer, the carbon footprint of the diesel generator is still over 1.75 times larger than to implement the new wind turbines system. It is the decision of the client to go either for the 1 day battery energy storage, which implies less costs, or for the 3 day battery energy storage option, which implies a lower carbon footprint and thus more sustainability.

20. Project Cost & Electricity Cost

The Signy station is controlled by the British Antarctic Survey. This organisation provides facilities to perform biological research on Antarctica and therefore there is no need to make profit out of the energy produced by the wind turbine system. To present the project to potential investors, the total project cost and the electricity cost are determined. The whole turbine investment should be captured by the price paid for the energy over the entire lifetime. As visible in Figure 20.1, the principal components required to determine the cost of energy per kWh include the levelised project cost and the expected annual energy production. Assessing the wind energy cost requires careful research which is performed below. In this chapter, the levelised project cost is determined in Section 20.1. The annual energy production is covered in Section 20.2. In Section 20.3 the electricity cost will be calculated and presented.

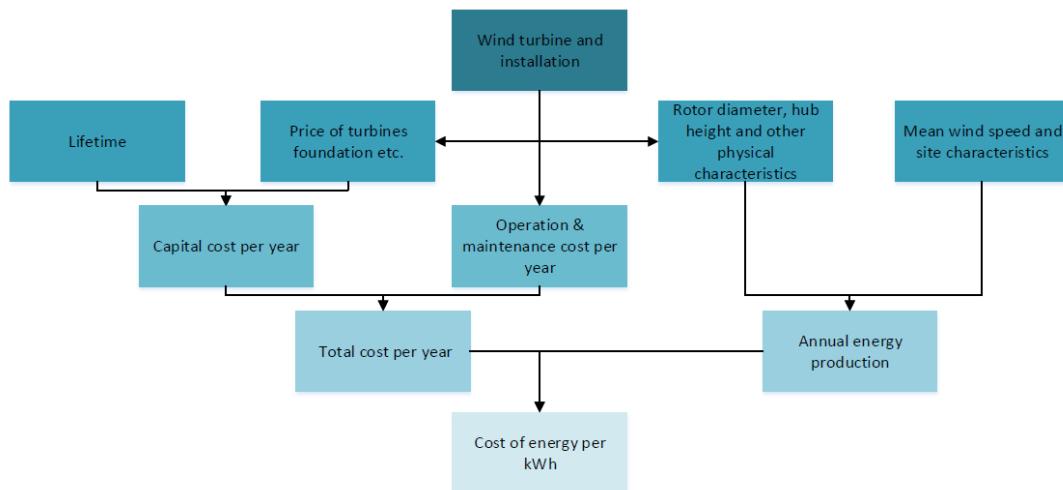


Figure 20.1: Key elements of costs of wind energy

20.1 Levelised Project Cost

This section will provide an overview of all the costs incurred during the entire lifetime of the wind turbine. At the end of this section, the value for the total project cost averaged over all the years of the lifetime will be given. This so-called levelised cost is of primary importance to determine the cost of electricity at a later stage. The key parameters that determine the levelised cost are the investment costs, the operations and maintenance costs and the lifetime of the wind system. Below, these parameters will be discussed in detail in order to quantify the total costs in the end. The first cost category comprises the upfront investment cost, commonly referred to as capital cost. This is a fixed, one-time expense that occurs in the beginning of the lifetime and is around 55% of the entire project cost. From reference data it is concluded that the capital costs for small wind turbines can be highly variable depending on the conditions that it is used in and the installation process. Combining the studies, the market analysis and a detailed estimation of separate components discussed in Appendix N.1, the capital cost per kW is estimated to be €6,882/ kW and €351,000 in total, which meets the requirements. The different shares that are included in the capital cost are listed below:

Wind Turbine Cost Share: This comprises the costs of all the components of the actual wind turbine and foundation, including production and possible sub-assembly. It accounts for approximately 80% of the total capital cost. In Figure 20.2 a visual representation is shown from the cost break-down of the different wind turbine components.

Civil Works Cost Share: This share includes the costs of transportation of the entire system, as well as its installation on the chosen site. Also the construction of the foundation and possible support infrastructures (e.g. transportation roads) are included. 15% Of the capital cost is required for this share.

Other Capital Cost Share: This comprises the miscellaneous costs involved, like development and engineering costs, consultancy costs, licensing costs, etc. 5% of the capital budget have to be reserved for these extra costs.

The next important parameter that determines the total cost is related to the operation and maintenance. Throughout the entire lifetime, the wind turbine will undergo maintenance checks which require trained personnel and specific tools, and spare parts as well. Additionally, the operations of the wind turbine itself increase the costs. The operations and maintenance costs typically account for 14% of the total costs of the entire project since the maintenance of the small turbines will probably not be too complex or resource consuming. In this case there are also batteries included in the total cost. The third parameter is the batteries and these are a main part of the total cost, as can be seen in Table 20.1. It accounts for 31% of the total costs.

Finally it is also important to consider the lifetime of the wind turbines to be able to describe the levelised cost. For the wind energy system designed in this report, the lifetime will be a minimum 15 years, meaning that the total cost will have to be divided by 15 in order to obtain the levelised cost.

By including all the previously estimated cost parameters, the total project cost is found to be €642,000 for the lifetime of 15 years. Dividing this by the entire lifetime, the levelised cost is determined to be €42,800. Consider also Figure N.1 in Appendix N to understand how the costs are actually divided amongst the years. At the beginning of life the investment cost is made, while the costs in the other years are governed by the operation and maintenance cost.

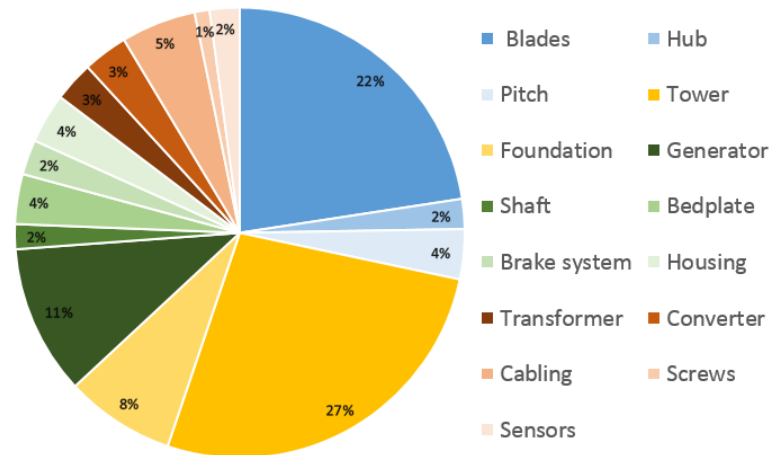


Figure 20.2: Cost break-down of the wind turbine components

20.2 Annual Energy Production

The annual energy production (AEP) is a measure of the total power produced during the whole year at the site. In order to compute the annual energy production, it is necessary to combine the power curve with a probability density function for the wind. The explanation of the method used to calculate the AEP can be found in Appendix N.2. Taking into account the electrical component losses of 5% and the yaw limitation losses of 15%, the AEP of one 17 kW turbine is calculated to be approximately 81,517 kWh. This is equivalent to a constant production of 9.3 kW during the whole year. The capacity factor of a power plant is the ratio of its actual output over a period of time, over its potential output if the plant would perform constantly at full capacity. For the design of the wind turbine, the capacity factor based on the Weibull distribution corresponds to 0.55. As is visible in the histogram of the wind data shown in Figure N.2 in Appendix N.2, a shoulder is present. Taking into account this phenomenon, the annual energy production of one turbine is 101,790 kWh and the capacity factor becomes 0.68. This value is high which can be explained by the enormously high wind speeds present at the Signy station. This proves that Signy Island is a perfect place to build wind turbines as power generation plant.

20.3 Electricity Cost

With all the information known from the sections above, the electricity cost can be determined. The estimated cost of wind power varies significantly, depending on the capacity factor, which in turn depends on the quality of the wind resource and the technical characteristics of the wind turbines. Usually the cost of wind energy is expressed as unit cost. It gives the relation between the levelised cost and the annual energy production. This parameter is defined in €/kWh. The electricity cost for the Signy station is estimated to be €0.1402/kWh based on the histogram distribution. In Table 20.1 a summary of the cost parameters that were described in this chapter can be found.

Table 20.1: Total cost

Total project cost incl. batteries		€642,000
	<i>Capital cost (55%)</i>	<i>€351,000</i>
	<i>Wind turbine (80%)</i>	<i>€279,000</i>
	<i>Civil work+construction (15%)</i>	<i>€54,000</i>
	<i>Other (5%)</i>	<i>€18,000</i>
	<i>Maintenance & Operations (14%)</i>	<i>€91,000</i>
	<i>Batteries (31%)</i>	<i>€200,000</i>
Levelised cost		€42,800
AEP		101,790(x3) kWh
Unit cost		€0.1402

21. Market Analysis

In this chapter the competitors and sales markets will be elaborated upon. Competitors that can provide the research station with energy are considered as well. In Section 21.1 different options are discussed that could be used on Signy Island to provide the research station with power. The current wind turbine solutions of competitors are discussed and compared to the Windpulse in Section 21.2. At last in Section 21.3 it is analysed in which other markets, apart from Antarctica, the Windpulse would be of added value.

21.1 Levelized Cost of Electricity

The Signy station has a relatively low power demand and therefore only several options are feasible. The options considered are the (bio)diesel generator, hydrogen fuel cell, offshore placement of the wind turbines and the wind turbine considered in this report. These options are compared with each other on the criteria cost and sustainability.

The total cost per unit of energy generated is expressed as the levelized cost of energy (LCOE) this LCOE is used to compare the costs of the different systems considered. It includes the costs of investment and the operations and maintenance costs. [163] The LCOE values are not known for all the systems considered. Different sources calculate it in a different manner for different time spans. Therefore [164] and [165] were used as a reference.

General LCOE values for biodiesel are not available, therefore the LCOE value of biomass is used since biofuels (biodiesel) are made from biomass. It should however be taken into mind that the LCOE value of biodiesel will probably be higher than that of biomass. The LCOE of biomass (which is assumed to be slightly lower than for biodiesel) and onshore wind are € 0.07 /kWh and € 0.08 /kWh, respectively [164] [165]. It can be concluded that onshore wind is considered the better option, since the biodiesel cost would be approximately the same as for onshore but it would be less sustainable. These values can also be compared to the LCOE of the Windpulse, which is € 0.14 /kWh. The reason that the LCOE of the Windpulse is higher than the value of onshore wind is the fact that the Windpulse is a small system and especially designed for the Antarctic environment. The option to use a diesel generator is considered as well. Its LCOE will be lower than the LCOE for biodiesel, but it is not a sustainable option and therefore it is discarded as a viable option.

The trade-off between offshore and onshore wind turbines can easily be done. On offshore locations wind energy is more costly, but has as benefit that it experiences better wind speeds which give a higher energy output. However Signy Island experiences already high enough wind speeds to produce the required amount of power and it is therefore cheaper and easier to implement the wind turbines onshore.

The option to use hydrogen fuel cells is also considered, but the technology is not yet advanced enough to implement it without risks on such a large scale. In addition, at the current stage of development it is still very costly.

If safety, sustainability and cost aspects are taken into account, onshore wind turbines are the best option for the remotely located Signy Island. In this way the windy conditions of Signy Island are used to an advantage when considering energy system designs.

21.2 Wind Turbines Competitors

In order to make sure the Windpulse will be selected as the wind turbine used for the BAS, a market analysis has to be performed in the form of a competitor research. This section will discuss the results of this research.

21.2.1 Competitor Map

In Figure 21.1 a map can be seen of the competitors that were found relevant and interesting for comparison. The competitors are located on a horizontal scale of rated power and a vertical scale of €/kWh. If specific data was not available, averages were assumed (an efficiency of 70%, a capacity factor of 0.3 and 5% maintenance cost per year).

It can be seen that the Windpulse performs superior with respect to the competitors. With respect to the other wind turbines optimised for Arctic environments it has a lot more power and lower price as well. The two real competitors are the Cyclone Green Power and the Aeolos-H. Although the specifications are comparable, these are not optimised for cold environments. As can be seen in [166] a cost increase of about 40% is needed to optimise a wind turbine for arctic environments. Therefore the Windpulse is the best solution for the BAS.

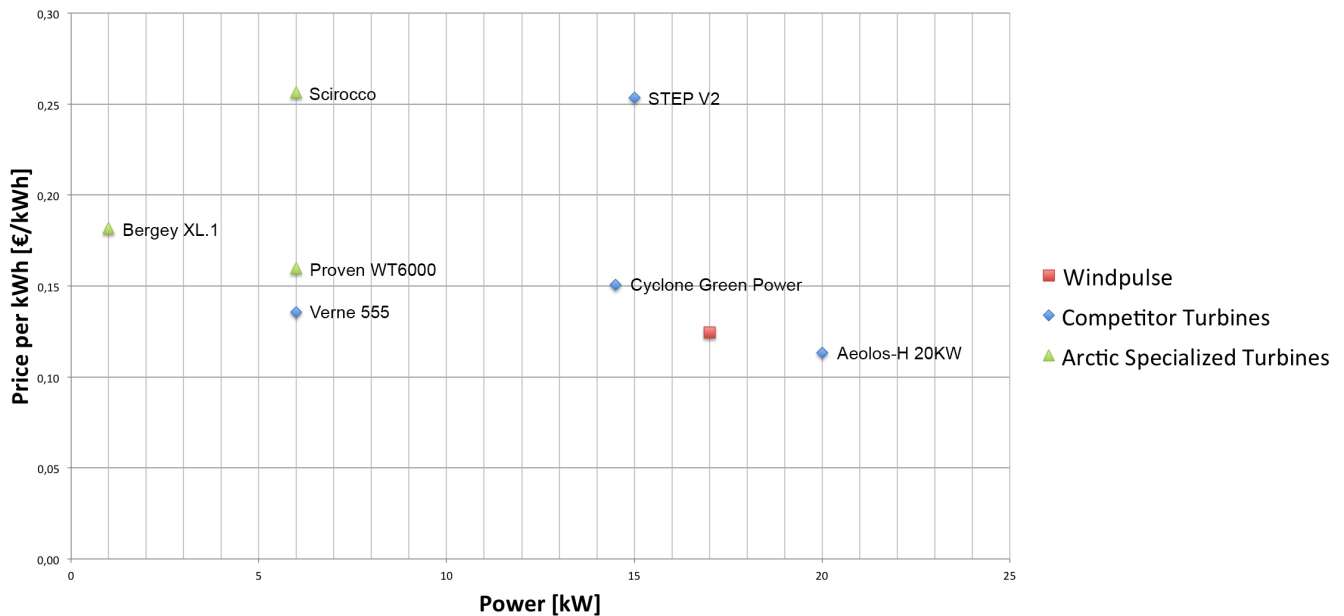


Figure 21.1: Competitor map placed with respect to rated power and price per kilowatt hour [13] [14] [15] [16] [17]

21.3 Sales Market

In order to improve the efficiency of the project, sales market research was performed to find alternative buyers. When the Windpulse has proven its mission on Signy Island it can be sold to two different markets: (Ant)arctic research facilities and the consumer market.

21.3.1 (Ant)arctic Research Facilities

Because the Windpulse proved to be the best solution if compared to its competitors, other research facilities will be interested in it as well. The operational ranges of the Windpulse are quite wide, which makes it suitable for different missions and (Ant)arctic locations. South Korea, China, India and Germany all erected new research stations in the last five years. China is currently planning to build two more research stations on Antarctica [167]. This shows that there certainly is a demand for Antarctic power production. The Windpulse should and can use this demand to its benefit, in order to increase both sales and reputation.

21.3.2 Consumer Market

The Windpulse is optimised for cold environments, which do not only appear on (Ant)arctic locations. Areas like Alaska, Northern Canada, Siberia, Scandinavia and Iceland are also interesting sales markets. But the Arctic itself is also becoming a more interesting sales market for consumers. The Arctic is becoming more accessible and therefore the USA is already starting with enforcing its stewardship [168]. The Windpulse should make use of this increasing demand on the Arctic for non-scientific stations, such as future oil and gas stations as well. Because the Windpulse produces about 90 *MWh* per year and an average household uses about 3.5 *MWh* per year, one single turbine could provide energy to 25 households or a small to medium enterprise (SME's). Therefore the Windpulse is very suitable for remote areas in cold environments. Because the European targets on sustainable energy production require that wind energy production doubles before the year 2020, the Windpulse can make use of this demand in these cold areas of Europe specifically. Scandinavia and Iceland can therefore be seen as potential buyers.

The Canadian Wind Energy Association states that it wants to increase the wind energy production from 3% to 20% of the domestic electricity demand before 2025 [169]. It is expected that therefore remote households will also start making use of wind energy more frequently and thus the Windpulse could provide wind energy in these cold environments.

22. Project Design & Development Logic

This chapter describes the activities that need to be executed in the post-design phases of the project. Figure 22.1 presents a block diagram of these activities.

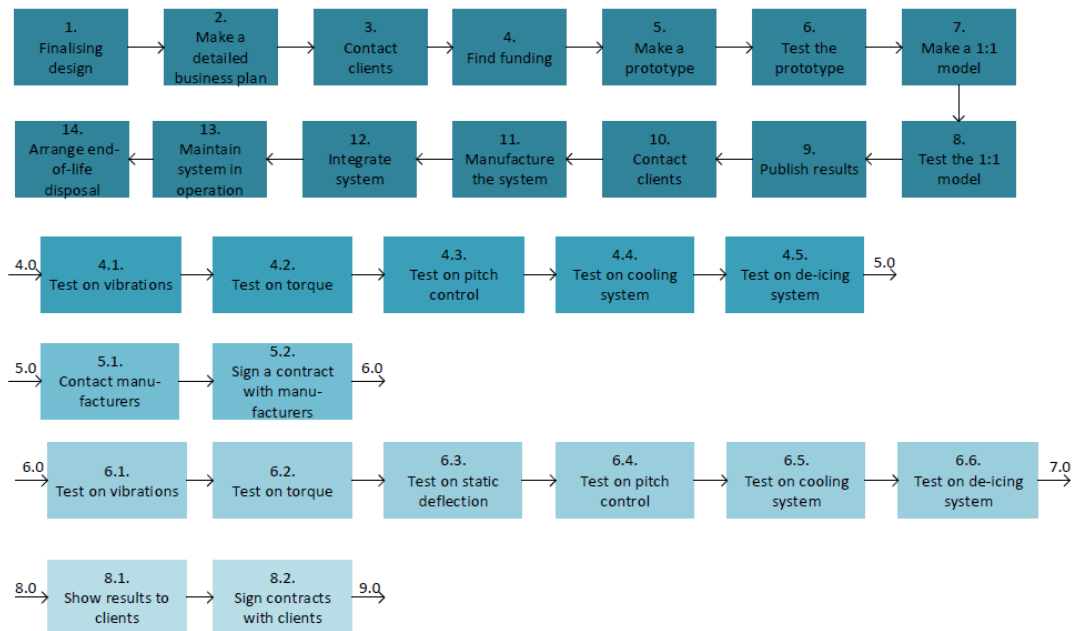


Figure 22.1: Post-design phases activities

The first activity is finalising the detailed design, for example designing the joints and bolts etc. After the design has been finalised a detailed business plan has to be made. This business plan must contain a description what the goals of the company are and the plan for reaching the goals, including where to find and how to approach potential clients. The business plan is followed by contacting potential clients for the wind turbine system. The potential clients should be informed about the Windpulse product. If one or multiple parties show interest in the product, funding needs to be found. This funding can come from institutions that stimulate technology, innovation and sustainable driven projects. Once funding is obtained a scale model prototype of the rotor can be made. The rotor prototype is tested in a wind tunnel under the extreme wind conditions present on Signy Island. The rotor will be tested on vibration modes, torque for the power output and the thermo-electrical pulsing de-icing system. For the de-icing system one blade will be frozen artificially and snowed upon to create a layer of ice on the surface. Then the pulses will run through the film on the blade to measure how long it takes to remove the ice and in what extend the system is suitable. When the scaled results for the rotor vibrations and torque are not similar to the results from the theoretical models, one needs to go back to the design phase. If the results then are similar another model, this time 1:1 scale, can be made, including tower and nacelle. Manufacturers to build one Windpulse are contacted and contracts are signed with the manufacturers. A blade of the full-scale model will be subjected to a static deflection test. The Windpulse will be integrated in an environment similar to the environment at Signy Island. There it will be subjected to tests on vibrations, dynamic deflection, power output, pitch control, cooling system and de-icing system. Once the Windpulse passes all these tests, the results can be published. These results are then shown to the clients to let them gain trust in the wind turbine design. A contract for the wind turbines to be placed on Signy before April 2020, is signed with the clients. Now the money is available to start the production of the whole system, from manufacturing, integrating, maintaining the system to arranging the end-of-life disposal, all described in this report. During all these activities a financial manager organises the financial aspects of the business and process. The 1:1 model can be placed after testing on the desired location from the client or can stay on the same location for future testing of improved systems.

There is a large uncertainty on the amount of fossil fuels still available on Earth. Furthermore, burning fossil fuels have a large impact on the increase in carbon in the air which causes extreme climate changes. Wind however, will always be available and is therefore a great energy source to power the world with. More money and time needs to be put into the research and development of wind turbines to help save this planet.

23. Conclusion

Within this report it was shown how the DSE group 20 of spring 2014 at TU Delft conducted the detailed design of a wind turbine system for the Signy area of Antarctica. Through the analysis of Signy Island, it was found that Signy experiences extreme weather conditions with a temperature range of $-38^{\circ}C$ to $10^{\circ}C$ and with maximum wind speed being found as 58 m/s . Taking these environmental conditions and the exceptional wildlife found on Signy Island into account led to the site layout and configuration of 3 horizontal wind turbines with a rated power of 51 kW ($3 \times 17\text{ kW}$). The turbines were placed 70 m from the research station and at a distance of 44 m apart in order to reduce noise level and mutual interference respectively. In order to fully evaluate if the design was a suitable system solution, designs were also assessed on the various risks that are imposed due to their specific implementation. Safety and reduction of risk was achieved by applying by both safe life and fail safe design methodologies, through the use of safety factors, conservative worst case calculation values, in conjunction with redundant components. This also includes reducing the risk bird impact which resulted in painting one blade of each wind turbine black. Moreover to protect the components and the structure of the wind turbine itself, the generator was cooled by using the cold environment where a variable opening in the nacelle leads to ventilation in the nacelle and an electro-thermal de-icing (PETD) system to implemented for the blades. In addition the control of the turbine consists of variable pitch, variable speed control and a passive downwind yaw regulation. Three blades of 4.4 m are placed on a tower of 8.8 m with a diameter of $0.64\text{ m} - 0.15\text{ m}$ from root till tip. The turbines are driven by a direct drive, permanent magnet generator. The operation of the turbines covers a performance monitoring system and a strategy to park wind turbines for 8 months while the research station is uninhabited . Once a year scheduled maintenance is performed by using a predefined check list. The energy supply system, in addition to the turbines consist of a Diesel generator that is already present on Signy and a lead acid battery system. Two options are presented: one day energy or a three day energy systems as battery size influences the costs of the project heavily. The total carbon footprint of the system for when the generator has to be turned on 4 days in a year, with the 3 day battery energy storage, is estimated on $782,600\text{ kg CO}_2$, or $117\text{ g CO}_2/\text{KWh}$, and for 30 days in a year, with the 1 day battery energy storage, $974,800\text{ kg CO}_2$, or $146\text{ g CO}_2/\text{KWh}$. These amounts are considerably less than the carbon footprint when using a diesel generator only. The maximum rotational speed is 15 m/s and the maximum measured sound pressure level is 50 dB for a sound pressure level sensed by the human ear of 40 dB(A) . Furthermore it was calculated that shadow flicker will not occur on the research station due to the turbine location layout. The price of electricity would be approximately 0.14 euros per kWh and the wind turbine system costs $\text{€}351,000$. It is shown that the Windpulse performs superior with respect to the competitors. With respect to the other wind turbines optimised for Arctic environments it has both higher installed power and lower price as well. More money and time needs to be put into the research and development of wind turbines in order to help contribute to the fight against climate change. Completing this report, the DSE group of the TU Delft has designed a wind energy system to meet the power demand of the Signy Research in a sustainable way, with future research to be focused on greater depth of detailed design and specific implementation.

Bibliography

- [1] N. Timmer. Project guide design synthesis exercise 2013-2014 - (ant)arctic wind turbines: A cold case. April 2014, TU Delft.
- [2] Horizontal axis wind turbines. <http://www.turbinesinfo.com/horizontal-axis-wind-turbines-hawt/>. Accessed on 30/04/2014.
- [3] Airborne wind turbine. <http://wordlesstech.com/2012/03/29/airborne-wind-turbine/>. Accessed on 30/04/2014.
- [4] Renewableuk - images. <http://www.renewableuk.com/en/news/media-galleries/>. Accessed on 30/04/2014.
- [5] Jet engine wind turbine is 4x more efficient, will hit market soon. <http://www.treehugger.com/corporate-responsibility/jet-engine-wind-turbine-is-4x-more-efficient-will-hit-market-soon-video.html>. Accessed on 30/04/2014.
- [6] W. Ray. British antarctic survey tech info for cde call, 2009.
- [7] W. Hodos. Minimization of motion smear: Reducing avian collisions with wind turbines. National Renewable Energy Laboratory. August 2002, University of Maryland.
- [8] James G. Smith Curtis Dodd, Thomas McCalla. How to Protect a Wind Turbine From Lightning. National Aeronautics and Space Administration.
- [9] Patrick and Henderson. Patrick and henderson rock anchor foundation. Powerpoint Presentation.
- [10] A.L. Rogers J.F. Manwell, J.G. McGowan. Wind energy explained: Theory, Design and Application. John Wiley & sons, LTD.
- [11] Keystone Tower Systems. Spiral Welding Solution. <http://keystonetowersystems.com/>. Accessed on 10/06/2014.
- [12] SunEarthTools. Sun Position. http://www.sunearthtools.com/dp/tools/pos_sun.php. Accessed on 19/06/2014.
- [13] Anna Lindquist. Wind power in antarctica a feasibility study for wasa. *Uppsala University, Sweden Division for Electricity and Lightning Research*, page 70, 2004.
- [14] All Small Wind Turbines.com. Step v2 small wind turbine by step energysystems gmbh. http://www.allsmallwindturbines.com/small_wind_turbines/95/83/STEP%20V2/STEP%20ENERGYSYSTEMS%20GmbH/. Accessed on 18/06/2014.
- [15] All Small Wind Turbines.com. Aeolos-h 20kw wind turbine small wind turbine by aeolos wind energy,ltd. http://www.allsmallwindturbines.com/turbine_detail.php?turbine_id=285&owner=38. Accessed on 18/06/2014.
- [16] All Small Wind Turbines.com. Verne 555 small wind turbine by enersud. http://www.allsmallwindturbines.com/turbine_detail.php?turbine_id=99&owner=72. Accessed on 18/06/2014.
- [17] All Small Wind Turbines.com. Eoltec scirocco 5.5-6 small wind turbine by weole energy. http://www.allsmallwindturbines.com/turbine_detail.php?turbine_id=379&owner=2122. Accessed on 18/06/2014.
- [18] C.M. Markussen B. Madsen M. Birkved, A. Corona. Selection of environmental sustainable fiber materials for wind turbine blades - a contra intuitive process? Department of Wind Energy, Section of Composites and Materials Mechanics, Riso campus, Technical University of Denmark, Denmark.
- [19] S. Navalkar. Control of variable speed wind turbines. Blackboard, windturbine design. 2014.
- [20] Twiflex. Twiflex product brochure. <http://www.ebibus.sk/content/products/strojarenstvo/twiflex/catalogs/Twiflex.pdf>. Accessed on 11/06/2014.
- [21] Jyri Outinen. Mechanical Properties of Structural Steel at Elevated Temperatures and After Cooling Down. Fire and Materials Conference, San Francisco, USA. 2006.
- [22] E. Moreno-Goytia G. Adam O. Anaya-Lara, D. Campos-Gaona. Offshore wind energy generation. Wiley. 2013.
- [23] D.G. Rethwisch W.D. Callister. Materials Science and Engineering, an Introduction. Wiley, eight edition.
- [24] O.C.J.J. Peters H.L. Bos, M.J.A. Van Den Oever. Tensile and compressive properties of flax fibres for natural fibre reinforced composites. *Journal of material science* 37.
- [25] M.J. Clifford D.U. Shah, P.J. Schubel. Can flax replace E-glass in structural composites? A small wind turbine blade case study. Division of Materials, Mechanics and Structures, Faculty of Engineering, The University of Nottingham, UK.
- [26] Tube properties. <http://www.carbonfibertubeshop.com/tube%20properties.html>. Accessed on 15/06/2014.
- [27] L. Pignatti F. Bottoli. Design and processing of structural components in biocomposite materials - Rotor blade for wind turbine cars. National Laboratory for Sustainable Energy, Riso DTU, Denmark.
- [28] Steels for Cryogenic and Low-Temperature Service. <http://steel.keymetals.com/Articles/Art61.htm>. Accessed on 1/05/2014.
- [29] AllAboutBatteries.com. Battery energy – what battery provides more? <http://www.allaboutbatteries.com/Battery-Energy.html>.
- [30] British antarctic survey signy research station, 2012.
- [31] British antarctic survey signy research station, April 2014.
- [32] British Antarctic Survey. Signy research station. http://www.antarctica.ac.uk/living_and_working/research_stations/signy/index.php. Accessed on 28/04/2014.
- [33] Edward W. Finucane. *Concise Guide to Environmental Definitions, Conversions, and Formulae*. CRC Press LLC, Boca Raton, Florida, 1999.
- [34] Matthews M.A. and Maling B.A. The geology of the south orkney islands. *F.I.D.S. Scientific Reports*, 25:43, 1967.
- [35] Thomson J.W. The geology of the south orkney islands: The petrology of signy island. *F.I.D.S. Scientific Reports*, 62:45, 1968.
- [36] L.N.Y. Wong S.J. Wang G.Y. Han X.P., Zhang. Engineering properties of quartz-mica-schists. *Elsevier: Engineering Geology*, 121:15, 2011.
- [37] Clark A. Benthic marine habitats in antarctica. *British Antarctic Survey*, page 11, 1995.

- [38] TRKOV J. Physical, mechanical and deformational properties of metabasalts, amphibolites and gneisses from ksdb-3 compared with surface analogues. *Acta Geodyn. Geomater.*, 2:9, 2005.
- [39] A.W. Meneilly B.C., Story. Petrogenesis of metamorphic rocks within a subduction-accretion terrane, signy island, south orkney islands. *British Antarctic Survey*, page 22, 1985.
- [40] Participating Countries. Protocol on environmental protection to the antarctic treaty. December 1959, Washington.
- [41] OpenEI. Wind turbine. http://en.openei.org/wiki/Wind_turbine. Accessed on 13/05/2014.
- [42] WiseGeek.com. What are the different types of wind turbine design. <http://www.wisegeek.com/what-are-the-different-types-of-wind-turbine-design.htm>. Accessed on 13/05/2014.
- [43] Beth Buczynski. 7 most impressive wind farms (and turbines) in the world. <http://www.care2.com/causes/7-most-impressive-wind-farms-and-turbines-in-the-world.html>. Accessed on 13/05/2014.
- [44] D Chiras. Wind power basics: a green energy guide. McGraw-Hill Print. 2010.
- [45] International Renewable Energy Agency. Renewable energy technologies: Cost analysis series. IRENA Working Paper. 2012.
- [46] Ir. Nando Timmer. Wind noise level conversation. Internal Communications. 2014.
- [47] Department of Planning Northern Ireland. Draft pps 18: Renewable energy annex 1 wind energy: Spacing of turbines. http://www.planningni.gov.uk/index/policy/policy_publications/planning_statements/pps18/pps18_annex1/pps18_annex1_wind/pps18_annex1_technology/pps18_annex1_spacing.htm. Accessed on 16/06/2014.
- [48] OpenEI. Wind energy: Land requirement. http://en.openei.org/wiki/Wind_energy1. Accessed on 16/06/2014.
- [49] OpenEI. Wind energy: Land requirement. http://en.openei.org/wiki/Wind_energy1. Accessed on 16/06/2014.
- [50] R. Curran E. Gill, G. LaRocca. Lecture: Ae3201-108-risk and reliability. February 2014, TU Delft.
- [51] hbpl.co.uk. Failure rates and outage times of wind turbine components. <http://offlinehbpl.hbpl.co.uk/NewsAttachments/0PW/data2.gif?HAYILC=INLINE>. Accessed on 17/06/2014.
- [52] Johan Ribrant. Reliability performance and maintenance - a survey of failures in wind power systems. http://faculty.mu.edu.sa/public/uploads/1337955836.6401XR-EE-EEK_2006_009.pdf. Accessed on 17/06/2014.
- [53] Michael Scholl. Availability and sensitivity analysis of smart grid components. <http://www.cse.wustl.edu/~jain/cse567-11/ftp/grid.pdf>. Accessed on 17/06/2014.
- [54] P.J. Tavner H. Arabian-Hoseynabadi, H. Oraee. Failure modes and effects analysis (fmea) for wind turbines. *International Journal of Electrical Power & Energy Systems*.
- [55] D. M. Rasmuson S. A. Eide, T. E. Wierman. Detailed study of emergency diesel generator performance using epix/rads database. <http://www.inl.gov/technicalpublications/Documents/4074909.pdf>. Accessed on 17/06/2014.
- [56] F.Spinato P.J. Tavner, J. Xiang. Reliability analysis for wind turbines. *Wind Energy*.
- [57] R. Curran E. Gill, G. LaRocca. Lecture: Ae3201-systems engineering methods. February 2014, TU Delft.
- [58] Sensitivity analysis. http://en.wikipedia.org/wiki/Sensitivity_analysis. Accessed on 21/05/2014.
- [59] British Antarctic Survey. Signy research station: Flora and fauna. http://www.antarctica.ac.uk/living_and_working/research_stations/signy/. Accessed on 08/05/2014.
- [60] G.R. Martin. Understanding bird collisions with man-made objects: A sensory ecology approach. *The International Journal of Avian Science*, vol. 153, p. 239-254. December 1959, Washington.
- [61] V.F. Petrenko. Pulse electro-thermal de-icer (petd). Elsevier: *Cold Regions Science and Technology*. June 2010.
- [62] Petd integrated. http://www.scribd.com/fullscreen/48596847?access_key=key-q72x15zc9os5huhvty5&allow_share=true&escape=false&view_mode=slideshow. Accessed on 15/06/2014.
- [63] Johathan Awerbuch. Pulse-electrothermal deicing of multi-mehawatt wind turbines: solving the problem of rotary electric power transmission. Thayer School of Engineering Dartmouth College Hanover, New Hampshire.
- [64] Aluminium in aircraft construction. <http://www.aluminiumleader.com/en/around/transport/aircraft>. Accessed on 22/05/2014.
- [65] Aluminium 7079. <http://www.steelforge.com/aluminum-7079/>. Accessed on 22/05/2014.
- [66] Optical ice sensors for wind turbine nacelles. <http://windsystemsmag.com/article/detail/75/optical-ice-sensors-for-wind-turbine-nacelles>. Accessed on 15/06/2014.
- [67] Lightning and surge protection for wind turbines. DEHN.
- [68] M. O. L. Hansen. *Aerodynamics of wind turbines*. Second edition. 2008.
- [69] Sal Spada. The Reliance on Wind Energy Depends on Advancements in Blade Pitch Control. ARC Advisory Group.
- [70] E.C. Fitch. Temperature stability of lubricants and hydraulic fluids. <http://www.machinerylubrication.com/Read/367/temperature-stability>. Accessed on 18/06/2014.
- [71] Downwind rotor. <http://www.hitachi.com/products/power/wind-turbine/feature/rotor/index.html>. Accessed on 15/06/2014.
- [72] Upwind turbine vs. downwind. <http://www.power-talk.net/upwind-turbine.html>. Accessed on 15/06/2014.
- [73] Danish wind industry association. Wind turbines: How many blades. http://www.motiva.fi/myllarin_tuulivoima/windpower%20web/en/tour/design/concepts.htm. Accessed on 22/05/2014.
- [74] O. Kovala B. M. Jatzeck, A. M. Robinson D. Estimation of the optimum rated wind velocity for wind turbine generators in the vicinity of edmonton, alberta. Online. May 1999.
- [75] F. Ghedin. Structural Design of a 5MW Wind Turbine Blade Equipped with Boundary Layer Suction Technology. Delft University of Technology. September 2010.
- [76] R. Nijssen P. Brondstedt. *Advances in wind turbine blade design and materials*. Woodhead Publishing Series in Energy.
- [77] SP Systems. The advantages of epoxy resin versus polyester in marine composite structures. Online.
- [78] F. Manwell A. Lacroix. *Wind energy: Cold weather issues*. University of Massachussets at Amherst, USA.

- [79] Jeff Sloan. Core for composites: Winds of change. <http://www.compositesworld.com/articles/core-for-composites-winds-of-change>. Accessed on 06/05/2014.
- [80] Anna Lindquist. Wind power in antarctica. Swedish Polar Research Secretariat. 2004.
- [81] Adams magnetic. Assemblies and magnetic devices. http://www.adamsmagnetic.com/magnetic_assemblies/permanent-magnets-vs-electromagnets.php. Accessed on 19/05/2014.
- [82] Berlet magnetics. Berlet magnetics. <http://www.berletmagnetics.ca/electromagnet-permanent-differences.php>. Accessed on 19/05/2014.
- [83] Z. Chen F. Blaabjerg. Power electronics for modern wind turbines. Morgan & Claypool publishers. 2006.
- [84] Ginlong. Ginlong generators. <http://www.ginlong.com>. Accessed on 20/05/2014.
- [85] PM generators. Pm generators product matrix. <http://www.pmgenerators.com/products/product-matrix>. Accessed on 20/05/2014.
- [86] Alxion. Alxion alternators. <http://www.alxion.com/products/stk-alternators/>. Accessed on 20/05/2014.
- [87] DVE tech. Dve tech pmg - permanent magnet generators. <http://dvetech.com/gfi-grid-feed-inverters/pmg-generators.html>. Accessed on 20/05/2014.
- [88] Det Norske Veritas, , and Wind Energy Department. Guidelines for design of wind turbines. DNV/Riso. 2002.
- [89] Erich Hau. Wind turbines, fundamentals, technologies, application, economics. Springer. 2013.
- [90] Sandeep Singh Klair. Design of nacelle and rotor hub for nowitech 10mw reference turbine. <http://www.diva-portal.org/smash/get/diva2:648694/FULLTEXT01.pdf>. Accessed on 18/06/2014.
- [91] <http://metals.about.com>. Steel history. <http://metals.about.com/od/properties/a/Steel-History.htm>. Accessed on 6/06/2014.
- [92] www.saburchill.com. Iron and steel manufacture. <http://www.saburchill.com/history/chapters/IR/037f.html>. Accessed on 6/06/2014.
- [93] World Steel Association. Steel Solutions in the Green Economy. <https://www.worldsteel.org>. Accessed on 1/03/2014.
- [94] Dan Ancona and Jim McVeigh. Wind Turbine - Materials and Manufacturing Fact Sheet. Princeton Energy Resources International. 2001.
- [95] www.materials.eng.cam.ac.uk. Strength - cost. http://www-materials.eng.cam.ac.uk/mpsite/interactive_charts/strength-cost/NS6Chart.html. Accessed on 6/06/2014.
- [96] Dr.Y.Yang. Recycling of Engineering Materials. TU Delft WB3320IO Lecture Slides. 2014.
- [97] www.azom.com. Steel recycling principles and practice. <http://www.azom.com/article.aspx?ArticleID=7979>. Accessed on 6/06/2014.
- [98] Introduction to wind turbine foundation design, March 2013.
- [99] Concrete Experts International. Freeze-Thaw Detoriation on Concrete.
- [100] W. Kilcollins. Maintenance Fundamentals for Wind Technicians. Delmar, Cengage Learning. 2013.
- [101] Patrick and Henderson. Patrick and henderson tensionless pier foundation. Powerpoint Presentation.
- [102] J. Zhao. Rock Mechanics. Powerpoint Presentation. Ecole Polytechnique Fdrale de Lausanne.
- [103] Dywidag Systems International. Mechanical Anchors and Rebar Rock Bolts. Brochure.
- [104] E.G. Nawy. Concrete Construction Engineering: Handbook. CRC Press: Taylor & Francis Group. Second Edition: 2008.
- [105] D.C. Wyllie. Foundations on Rock. E & FN Spon. Second Edition: 1999.
- [106] H. Famili A. Foroughi, S. Dilmaghani. Bond Strength of Reinforcement Steel in Self-compacting Concrete. University of Tabriz, Iran. Civil Engineering.
- [107] Fatigue (material). [http://en.wikipedia.org/wiki/Fatigue_\(material\)](http://en.wikipedia.org/wiki/Fatigue_(material)). Accessed on 11/05/2014.
- [108] Technical Committee PEL/88. British Standard: Wind turbines - Part 2: Design requirements for small wind turbines. Standard Policy and Strategy Committee. 2006.
- [109] Catalogue of european urban wind turbine manufacturers. http://www.urbanwind.net/pdf/CATALOGUE_V2.pdf. Accessed on 22/05/2014.
- [110] Thomas B. Reddy David Linden. Handbook of batteries. McGraw-Hill Print. 2002.
- [111] earth911. car-batteries. <http://www.earth911.com/recycling/car-batteries/>.
- [112] Battery Council International. National recycling rate study. BCI Recycling Rate Study Report. April 2014.
- [113] http://batteryuniversity.com/learn/article/lead_based_batteries. Accessed on 10/06/2014.
- [114] Belgian Antarctic Operator. Running on renewable energies. http://www.antarcticstation.org/station/renewable_energies/.
- [115] <http://www.energycentral.com/download/products/PT-7004-Maintenance.pdf>. Accessed on 11/06/2014.
- [116] Alstom. Emergency diesel generators for nuclear power plants. <http://www.alstom.com/power/nuclear/emergency-diesel-generators/>. Accessed on 11/06/2014.
- [117] dieselserviceandsupply.com. Role of diesel generators in the healthcare industry. http://www.dieselserviceandsupply.com/generators_healthcare.aspx. Accessed on 11/06/2014.
- [118] <http://equinoxlab.com/d-g-emission-monitoring/>. Accessed on 11/06/2014.
- [119] Abdul Qayoom Jakhrani. Estimation of carbon footprints from diesel generator emissions. <http://ieeexplore.ieee.org/xpl/articleDetails.jsp?reload=true&arnumber=6344193>. Accessed on 11/06/2014.
- [120] United Nations Center for Regional Development. Reduce, reuse and recycle (the 3rs) and resource efficiency as the basis for sustainable waste management. http://sustainabledevelopment.un.org/content/dsd/csd/csd_pdfs/csd-19/learningcentre/presentations/May20920am/120-20Learning_Centre_9May_ppt_Mohanty.pdf. Accessed on 11/06/2014.

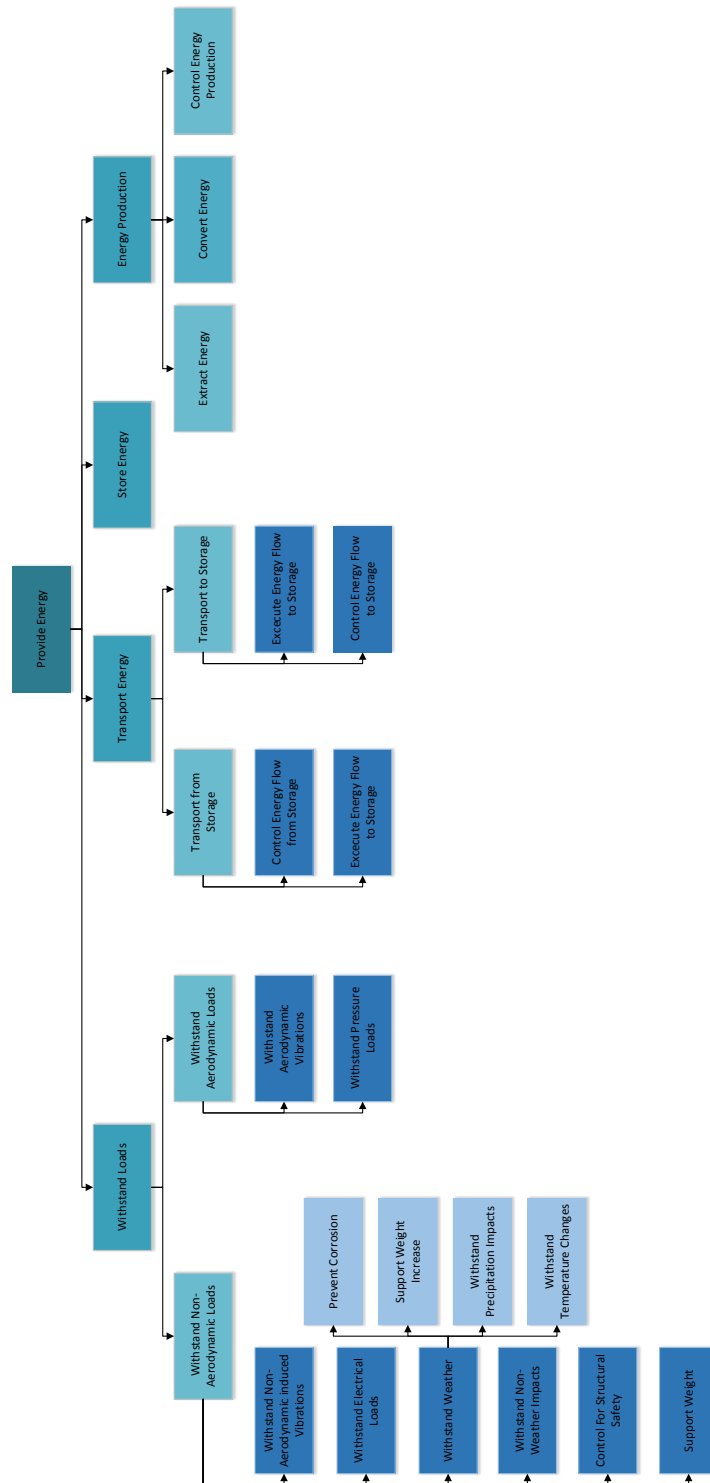
- [121] Larry Pryor. A comparison of aluminum vs. copper as used in electrical equipment. <https://www.geindustrial.com/sites/geis/files/gallery/White20paper20-20Aluminum20vs.20copper205-08.pdf>. Accessed on 12/06/2014.
- [122] doityourself.com. Copper vs aluminum wiring: Which to use? <http://www.doityourself.com/stry/copper-vs-aluminum-wiring-which-to-use#.U5mh1i8QISo>. Accessed on 12/06/2014.
- [123] differencebetween.net. Difference between aluminum and copper wire. <http://www.differencebetween.net/object/difference-between-aluminum-and-copper-wire/>. Accessed on 12/06/2014.
- [124] H. Wayne Beaty Donald G. Fink. Standard handbook for electrical engineers. McGraw-Hill Print. 1978.
- [125] Frank Alonso. Underground vs. overhead: Power line installation-cost comparison and mitigation. http://www.elp.com/articles/powergrid_international/print/volume-18/issue-2/features/underground-vs-overhead-power-line-installation-cost-comparison-.html. Accessed on 12/06/2014.
- [126] Vaisala wind set wa25. <http://www.vaisala.com/en/products/windsensors/Pages/WA25.aspx>. Accessed on 16/05/2014.
- [127] West Systems Epoxy. Vacuum bagging techniques. Gougeon Brothers Inc. 2010.
- [128] Gamesa. Wind Turbines: Manufacturing and Assembly Process. <http://www.gamesacorp.com/en/products-and-services/wind-turbines/design-and-manufacture/manufacturing-and-assembly-process.html>. Accessed on 22/05/2014.
- [129] J. Gong W. Jihang, Q. Fan. Optimization of Welding Joint between Tower and Bottom Flange based on Residual Stress Considerations in a Wind Turbine, 2010.
- [130] W. Husson M. Veljkovic. High-strength Wind Turbine Steel Towers. Elforsk rapport 09:11, 2009.
- [131] A. Myers A. Jay. Design of a Conical Steel Wind Turbine Towers Manufactured with Automated Spiral Welding. Northeastern University. Department of Civil Engineering and Environmental Engineering.
- [132] E. Smith. Tapered Spiral Welded Structure. <http://www.google.com/patents/US20110179623>. Accessed on 10/06/2014.
- [133] Maine Drilling and Blasting. Rock Anchors and Rock Bolting. <http://www.mdandb.com/maine-drilling-and-blasting-expertise.cfm>. Accessed on 10/06/2014.
- [134] British Antarctic Survey. List of Agents / Representatives Acting for BAS for Ship Port Calls. http://www.antarctica.ac.uk/living_and_working/research_ships/agents.pdf. Accessed on 08/05/2014.
- [135] Falkland Islands Government. Self governance falkland islands. <http://www.falklands.gov.fk/>. Accessed on 08/05/2014.
- [136] American Resource & Energy. Vertical Gin Pole Wind Tower Raising System. <http://www.arewindtowers.com/raising-systems/vertical-gin-pole>. Accessed on 22/05/2014.
- [137] British Antarctic Survey. Research ships. http://www.antarctica.ac.uk/living_and_working/research_ships/index.php. Accessed on 07/05/2014.
- [138] MAN Diesel. Propulsion Trends in Container Vessels. 2009.
- [139] Meercat Workboats Ltd. The Meercat Range. <http://www.meercatworkboats.com/>. Accessed on 10/06/2014.
- [140] Formost. Nodwell 110 Specifications. <http://www.foremost.ca/products/nodwell-110-0>. Accessed on 08/05/2014.
- [141] W. Bierbooms E. Lourens. Offshore wind farm design lecture slides. <http://blackboard.tudelft.nl>. Accessed on 08/05/2014.
- [142] Institute for Wind Energy. Typical Design Solution for OWECs, Faculty of Civil Engineering and Geoscience, Delft University of Technology. http://www.offshorewindenergy.org/reports/report_017.pdf. Accessed on 20/05/2014.
- [143] N. Amin. Princess elisabeth antarctica station. <http://www.polarpower.org/examples/PrincessElisabeth/index.html>. Accessed on 29/04/2014.
- [144] Brundtland Commission. Our common future. United Nations Report. 1987.
- [145] Thomas M. Parris Robert W. Kates and Anthony A. Leiserowitz. What is sustainable development? goals, indicators, values, and practice. <http://www.environmentmagazine.org/Editorials/Kates-apr05-full.html>. Accessed on 1/05/2014.
- [146] S. Uren S. Parkin, F. Sommer. Sustainable development: understanding the concept and practical challenge. Online. February 19, 2003.
- [147] Windustry. Why wind energy. <http://www.windustry.org/wind-basics/why-wind-energy>. Accessed on 01/05/2014.
- [148] . The carbon footprint of steel. http://www.tatasteelconstruction.com/en/sustainability/carbon_and_steel/. Accessed on 16/06/2014.
- [149] Sujit Das. Life cycle assessment of carbon fiber-reinforced polymer composites. Springer-Verlag. February 2011.
- [150] M.C. McManus. Environmental Consequences of the Use of Batteries in Low Carbon Systems: The Impact of Battery Production. Elsevier: Applied Energy . 2011.
- [151] Climate Friendly. Calculate Freight Emissions with Our Carbon Footprint Calculator. <http://www.climatefriendly.com/Business/Calculators/freight/>. Accessed on 16/06/2014.
- [152] G. Termeer M. Vastbinder. Handboek CO₂ - Prestatieladder 2.2. Stichting Klimaatvriendelijk Aanbesteden en Ondernemen. April 2014.
- [153] Recycling of wind turbine blades. http://www.appropedia.org/Recycling_of_wind_turbine_blades. Accessed on 21/05/2014.
- [154] M. Overcash E. Asmatulu, J. Twomey. Recycling of Fiber-reinforced Composites and Direct Structural Composite Recycling Concept. Journal of Composite Materials. February 2013.
- [155] E. Goodier. The Recycling and Future Selection of Permanent Magnets and Powder Cores. Arnold Magnetic Technologies. October 2005.
- [156] U.S. Environmental Protection Agency. Battery Recycling. <http://www.epa.gov/osw/conserves/materials/battery.htm>. Accessed on 18/06/2014.
- [157] S. Wright A.L. Rogers, J.F. Manwell. Wind Turbine Acoustic Noise. page 26, 2006.
- [158] Ministry of Environment: Ontario. Development of noise setbacks for wind farms. page 23, 2009.

- [159] D.H. Wood. Noise measurement and prediction for small wind turbines. *Proceedings of Solar 97: Australian and New Zealand Solar Energy Society*, (153):6.
- [160] D. Kastak B.L. Southall, R.J. Schusterman. Acoustic Communication Ranges for Northern Elephant Seals. *Aquatic Mammals*, Vol. 29. 2003.
- [161] The Scottish Government. Calculating Potential Carbon Losses & Savings from Wind Farms on Scottish Peatlands. Technical Note. August 2011.
- [162] R. Taghavi. Fundamentals of Reciprocating Engines. University of Kansas: AE 571. 2014.
- [163] Commission of the European Communities. Second Strategic Energy Review: An EU Energy Security and Solidarity Action Plan. Commission Staff Working Document. 2008.
- [164] Renewable energy technologies: Cost analysis series. http://www.irena.org/DocumentDownloads/Publications/RE_Technologies_Cost_Analysis-WIND_POWER.pdf. Accessed on 12/06/2014.
- [165] Levelized Cost and Levelized Avoided Cost of New Generation Resources in the Annual Energy Outlook 2014. http://www.eia.gov/forecasts/aeo/electricity_generation.cfm. Accessed on 22/06/2014.
- [166] Shimon Awerbucht, Søren Krohn, and Poul-Erik Morthorst. The Economics of Wind Energy. *The European Association for Wind Energy*, 2009.
- [167] More research stations planned for antarctica. http://usa.chinadaily.com.cn/china/2013-04/10/content_16387948.htm. Accessed on 16/05/2014.
- [168] NOAA releases arctic action plan. <http://www.arctic.noaa.gov/features/action-plan.html>. Accessed on 17/05/2014.
- [169] CWEA. Vision/mission Canadian wind energy association. <http://canwea.ca/about-canwea/visionmission/>. Accessed on 18/06/2014.
- [170] Canada Ministry of Environment. Development of noise setbacks for wind farms. Online. September, 2009.
- [171] British Antarctic Survey. Rothera research station. http://www.antarctica.ac.uk/living_and_working/research_stations/rothera/index.php. Accessed on 29/04/2014.
- [172] AWI. Neumayer-station iii. Online. January 10, 2012.
- [173] Australian Antarctic Division Australian Government, department of the Environment. Australian antarctic division: Leading australia's antarctic program. <http://www.antarctica.gov.au/living-and-working/station-life-and-activities/power-generation>. Accessed on 29/04/2014.
- [174] International Polar Foundation. Running on renewable energies princess elisabeth antarctica station. http://www.antarcticstation.org/station/renewable_energies/. Accessed on 29/04/2014.
- [175] D.Blake T.Tin, B.K.Sovacool. Energy efficiency and renewable energy under extreme conditions: Case studies from antarctica. Online. October 14, 2009.
- [176] Australian Antarctic Division Australian Government, department of the Environment. Energy efficiency and renewable energy under extreme conditions: Case studies from antarctica. <http://www.antarctica.gov.au/living-and-working/stations/mawson/living/electrical-energy>. Accessed on 29/04/2014.
- [177] A. Lindquist. Wind power in antarctica - a feasibility study for wasa. Online. Uppsala University, Sweden, 2004.
- [178] Bill Splinder. The mcMurdo wind farm. <http://www.southpolestation.com/trivia/00s/windfarm.html>. Accessed on 29/04/2014.
- [179] S. Gouws. Wind energy utilisation in antarctica. <http://research.ee.sun.ac.za/sanap/about.html>. Accessed on 29/04/2014.
- [180] Adrian Ilinca. Analysis and mitigation of icing effects on wind turbines. InTech. Wind Energy Research Laboratory, Universit du Quebec Rimouski Canada.
- [181] R. Cattin. Icing of wind turbines. *Vindforsk*. April 2010.
- [182] Pilot friend. Icing conditions in flight. http://www.pilotfriend.com/safe/safety/icing_conditions.htm. Accessed on 09/05/2014.
- [183] D. Sweet. Giving ice the boot; understanding pneumatic de-icing. <http://utcaerospacesystems.com/cap/systems/sisdocuments/Ice%20Detection%20and%20Protection%20Systems/Understanding%20Pneumatic%20De-icing%20White%20Paper.pdf>. Accessed on 09/05/2014.
- [184] Thayer School of Engineering at Dartmouth. Pulse electro-thermal de-icing. <http://engineering.dartmouth.edu/research/pulse-electro-thermal-de-icing/>. Accessed on 09/05/2014.
- [185] A.L. Rogers J.F. Manwell, J.G. McGowan. Wind Energy Explained. University of Massachusetts, USA.
- [186] T.H.G. Megson. Aircraft Structures: for Engineering Students. Elsevier. 2013.
- [187] S. Kichhannagari. Effects of extreme low temperature on composite materials. University of New Orleans Theses and Dissertations. August 2004.
- [188] E.J. Biss A.T. Nettles. Low temperature mechanical testing of carbon-fiber/epoxy-resin composite materials. Marshall Space Flight Center, Alabama. November 1996.
- [189] Johan Morren Henk Polinder. Developments in wind turbine generator systems. 2005.
- [190] Wei Qiao Dingguo Lu, Xiang Gong. Current-based diagnosis for gear tooth breaks in wind turbine gearboxes. online. 2012.
- [191] B. Fox e.a. Wind power integration; connection and system operational aspects. The Institution of Engineering and Technology. 2007.
- [192] Akers. Product data. <http://www.akersrolls.com/upload/Product%20data%20sheets/CORE/Core.pdf>. Accessed on 11/06/2014.
- [193] E. Hau. Wind Turbines: Fundamentals, Technologies, Application, Economics. Springer-Verlag. 2006.
- [194] Meng Ran Ma HongWang. Optimization Design of Prestressed Concrete Wind-turbine Tower. Science China: Technical Sciences. 2013.
- [195] Ferrous Metals:Low Temperature Steel. <http://www.matbase.com/material-categories/metals/ferrous-metals/low-temperature-steel/>. Accessed on 1/05/2014.

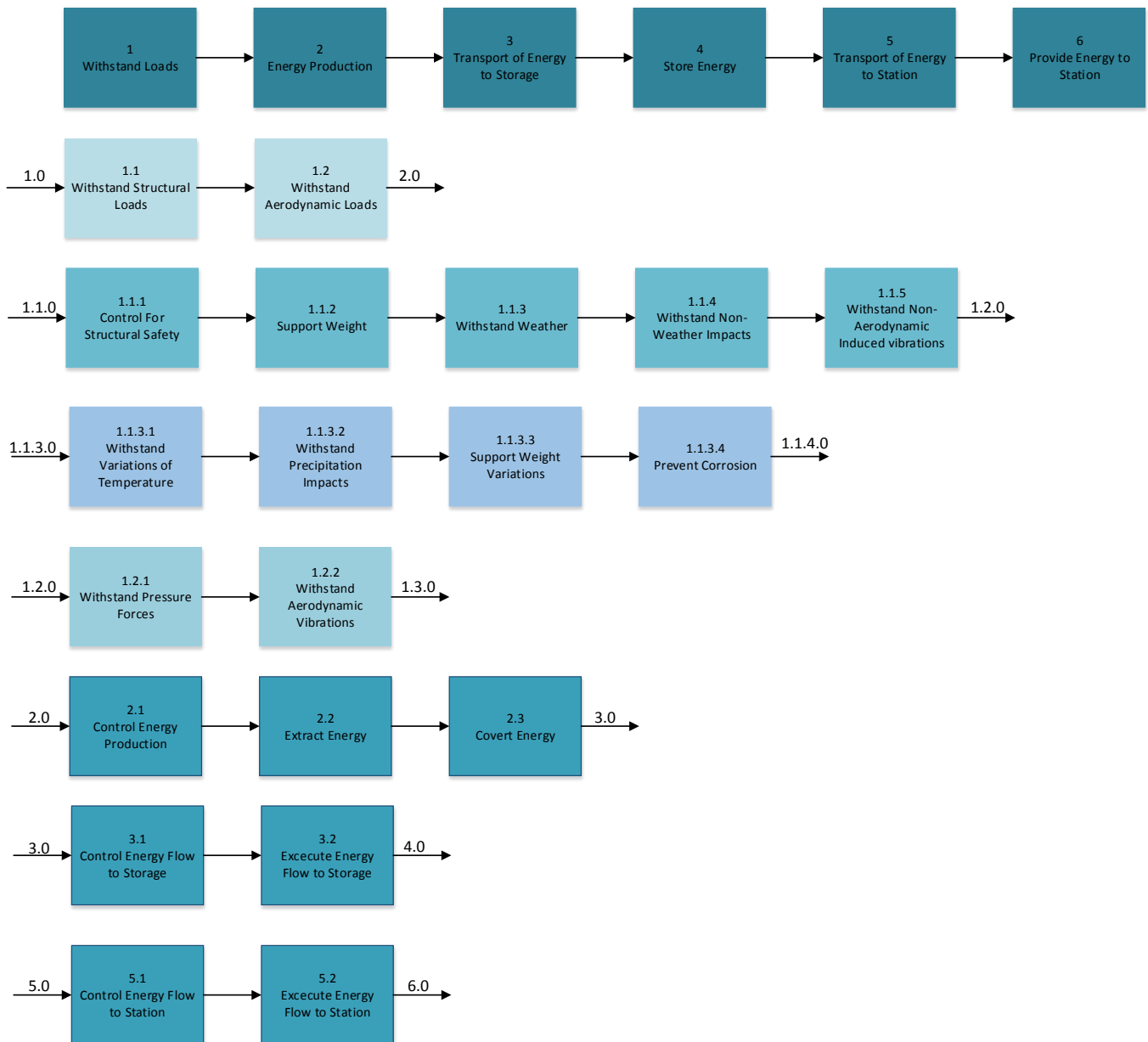
- [196] Effects Of Low Temperature on Performance of Steel & Equipment. <http://www.spartaengineering.com/effects-of-low-temperature-on-performance-of-steel-equipment/>. Accessed on 1/05/2014.
- [197] <http://www.meps.co.uk/WorldCarbonPrice.htm>. Accessed on 6/06/2014.
- [198] Purdue University. The Theorem of Least Work. https://engineering.purdue.edu/~ce474/Docs/The%20Theorem%20of%20Least%20Work_2012.pdf. June 2013.
- [199] M. Laney. Developing efficient wind turbine foundation designs through seamless team delivery. <http://ds.terracon.com/2014/04/developing-efficient-wind-turbine-foundation-designs-through-seamless-team-delivery/>. Accessed on 1/05/2014.
- [200] M. Zaaier. Introduction to Wind Energy: Dynamics. Powerpoint Presentation. 2013.
- [201] Y.Slavchev G.Venkov J.Genov, B.Gilev. Modeling and Control of Wind Turbine Tower Vibrations. Applications of Mathematics in Engineering and Economics: Conference Paper.
- [202] D.-P. Molenaar J. van der Tempel. Soft-Soft, Not Hard Enough? Conference Paper. 2002.
- [203] D.-P. Molenaar J. van der Tempel. Wind Turbine Structural Dynamics A Review of the Principles for Modern Power Generation, Onshore and Offshore. Wind Engineering DUWIND. 2002.
- [204] Isidor Buchmann. Discharging at high and low temperatures. http://batteryuniversity.com/learn/article/discharging_at_high_and_low_temperatures.
- [205] <http://www.tadiranbat.com/index.php/product-overview>. Accessed on 11/06/2014.
- [206] allbatterysalesandservice.com. Lithium & lithium thionyl. <http://www.allbatterysalesandservice.com/browse.cfm/2,1096.html>.
- [207] <http://www.altestore.com/howto/Solar-Electric-Power/Design-&-Components/Deep-Cycle-Batteries-Introduction/a85/>. Accessed on 11/06/2014.
- [208] <http://www.frost.com/sublib/display-market-insight.do?id=11607369>. Accessed on 11/06/2014.
- [209] <http://www.tadiranbatteries.de/eng/products/applications/>. Accessed on 11/06/2014.
- [210] http://battery council.org/?page=Safety_Reliability. Accessed on 11/06/2014.
- [211] Hans Streng. Mindboggling consequences in wake of battery price drops. <http://cleantechnica.com/2013/12/27/mondboggling-consequences-wake-battery-price-drops/>.
- [212] <http://www.backwoodshome.com/articles/thomsen28.html>. Accessed on 11/06/2014.
- [213] http://www.dieselserviceandsupply.com/Diesel_Fuel_Consumption.aspx. Accessed on 11/06/2014.
- [214] P. Herzog P. Zelenka, W. Cartellieri. Worldwide diesel emission standards, current experiences and future needs. Online. September 14, 1996 , Engine Engineering Diuision, Graz, Austria.
- [215] Agencia de Noticias Brasil-rabe. Brazil uses biofuel to generate power in antarctica. Online. January 10, 2012.
- [216] sugarcane industry association Unica. Ethanol-powered generators in antarctica: Export potential for sustainable technology. <http://english.unica.com.br/noticias/show.asp?nwsCode=%7BD76FD732-9233-4254-B638-D9DEAF2A5532%7D>. Accessed on 30/04/2014.
- [217] J. van Buijtenen A. G. Rao, B.Zandbergen. Ae2203 propulsion and power. Online, Blackboard. 2012, TU Delft.
- [218] fuelcellmarkets.com. Advantages & benefits of hydrogen and fuel cell technologies. http://www.fuelcellmarkets.com/fuel_cell_markets/5,1,1,663.html?FCMHome. Accessed on 11/06/2014.
- [219] Andrew Bhevan. The challenge of hydrogen storage. <http://www.thenakedscientists.com/HTML/content/interviews/interview/2210/>. Accessed on 11/06/2014.
- [220] HyperPhysics. American wire gages (awg) sizes and resistances. <http://hyperphysics.phy-astr.gsu.edu/hbase/tables/wirega.html>. Accessed on 12/06/2014.
- [221] Mark Bowman. American wire gauge conductor size table. <http://web.fscj.edu/Mark.Bowman/handouts/American20Wire20Gauge20Conductor20Size20Table.pdf>. Accessed on 12/06/2014.
- [222] Electricians Toolbox. Useful formulas. <http://www.elec-toolbox.com/Formulas/Useful/formulas.htm>. Accessed on 12/06/2014.
- [223] legislation.gov.uk. The electricity safety, quality and continuity regulations 2002. <http://www.legislation.gov.uk/uksi/2002/2665/regulation/27/made>. Accessed on 12/06/2014.
- [224] Anders Carlsson. The back to back converter. Department of Industrial Electrical Engineering and Automation Lund Institute of Technology. 1998.
- [225] Siemens AG. Efficient transformers for the grid integration of wind power. Siemens AG. 2011.
- [226] progressivedyn.com. Battery basics. http://www.progressivedyn.com/battery_basics.html. Accessed on 08/05/2014.
- [227] progressivedyn.com. How a battery works. <http://zing.ncsl.nist.gov/nist-icv/battery/battery/BatteryCare2.html>. Accessed on 08/05/2014.
- [228] Faculty of Civil Engineering and Geoscience. A Typical Design Solution for an OWECs. Institute for Wind Energy, Faculty of Civil Engineering and Geoscience, Delft University of Technology.
- [229] WT6000 Manual. Proven Energy Ltd.
- [230] International Renewable Energy Association. Renewable energy technologies: Cost analysis series vol 1: Power sector. Online. June 2012.
- [231] Levelized cost of energy report. http://www.nrel.gov/emails/wind/utws_newsletter_2012-06.html. Accessed on 12/06/2014.
- [232] Understanding costs for wind-turbine drivetrains. <http://www.windpowerengineering.com/design/mechanical/understanding-costs-for-large-wind-turbine-drivetrains/>. Accessed on 12/06/2014.

A. Requirements & Functional Evaluation

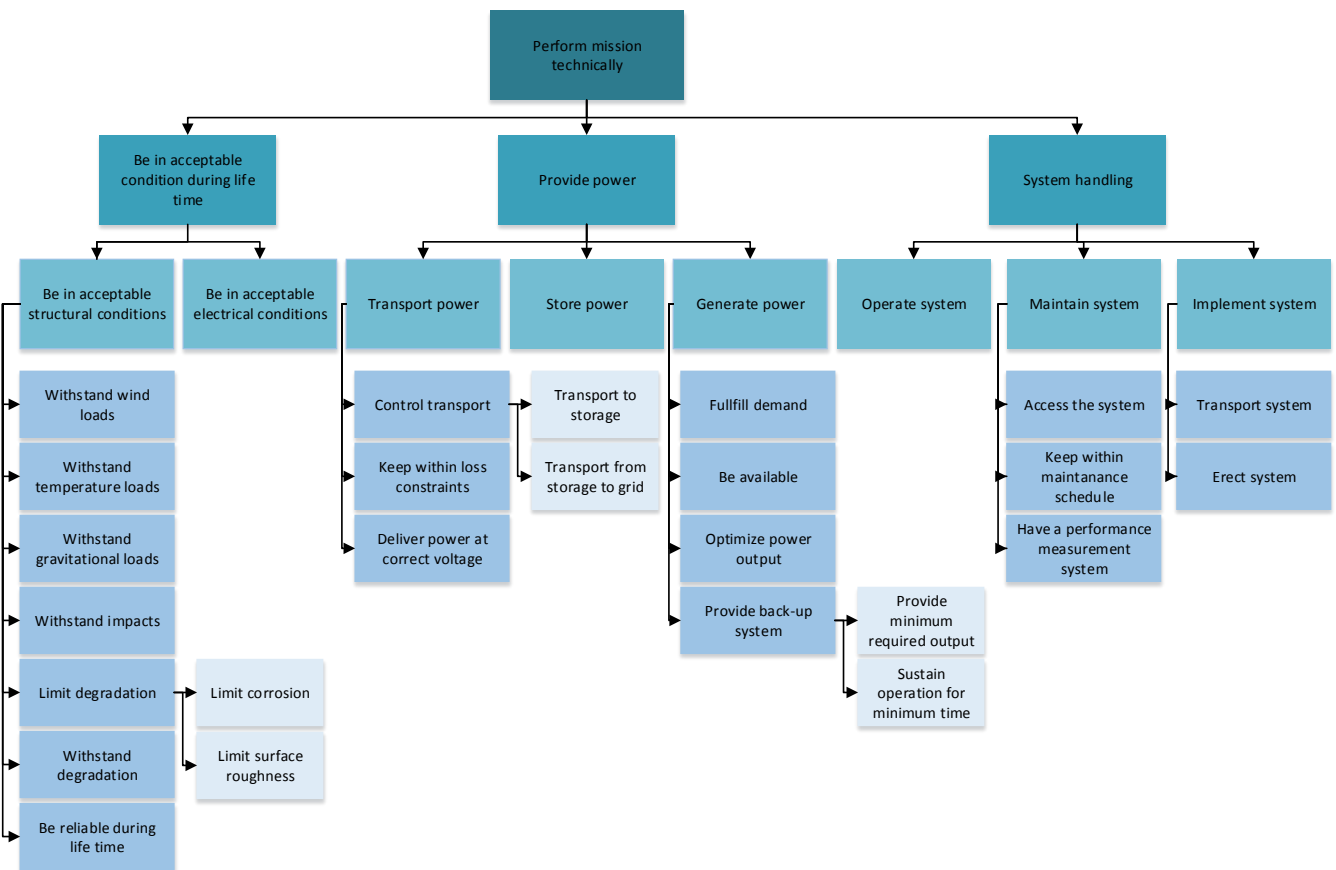
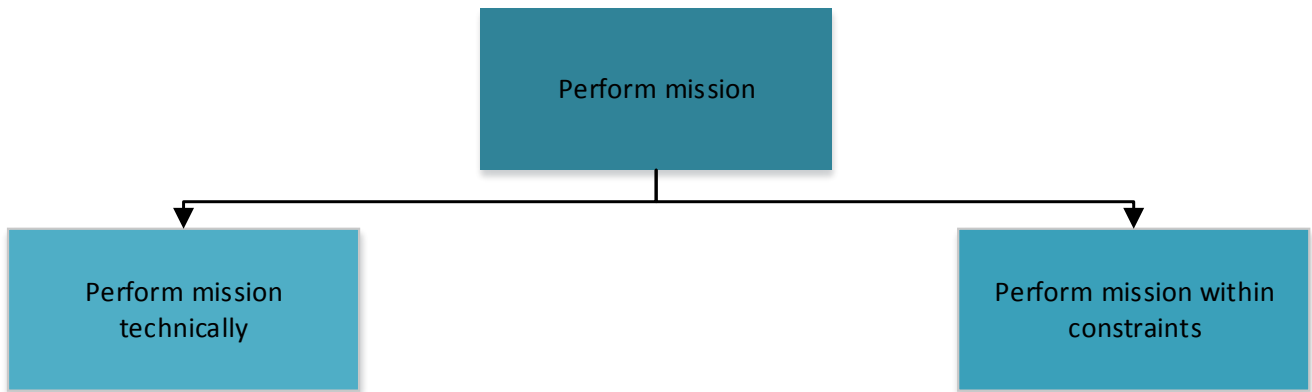
A.1 Functional Break-down Structure (FBS)

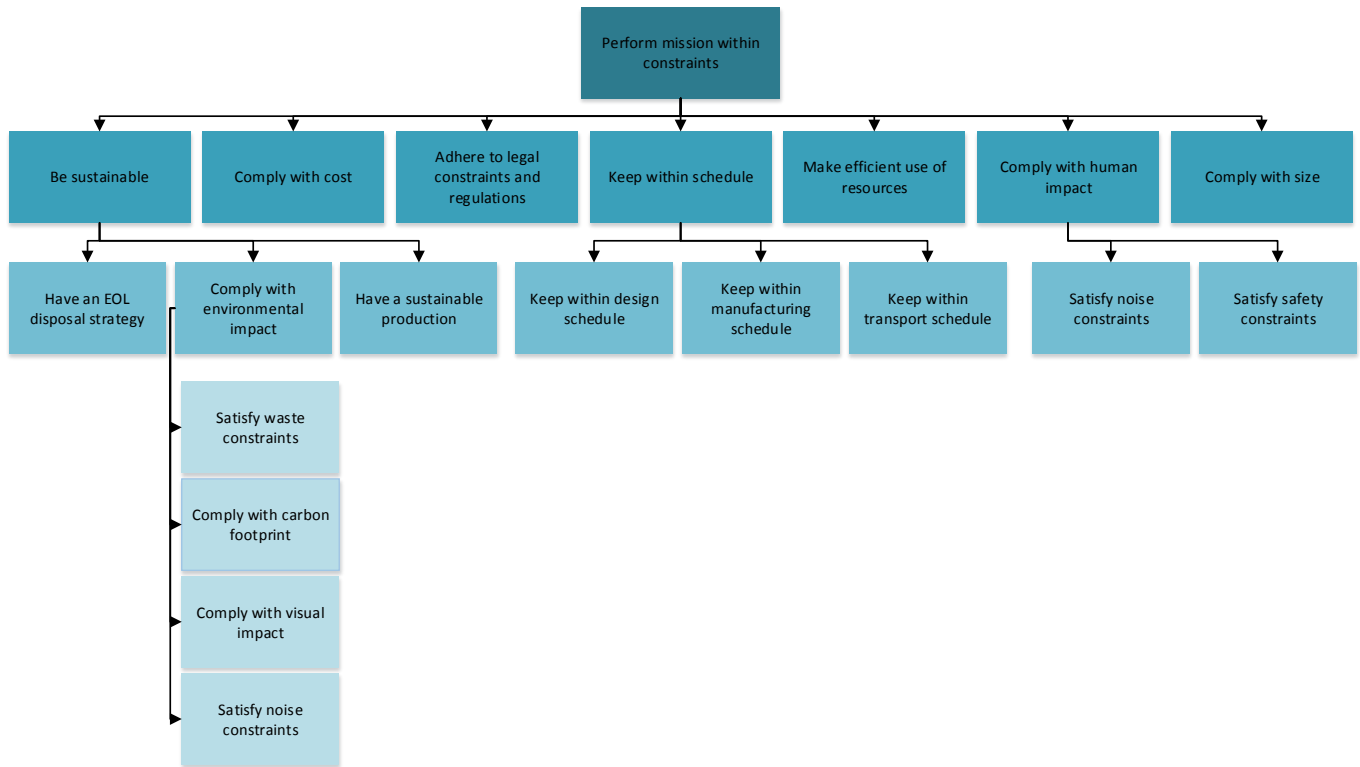


A.2 Functional Flow Diagram (FFD)



A.3 Requirements Discovery Trees (RDT)





A.4 Requirements

This section will present the formal description of the requirements coming from the requirements discovery tree. It is however important to note that not every subdivision in the tree leads to a specific requirement, since some of the subdivisions are covered by another requirement or would produce a non-verifiable requirement. These requirements are properly constructed according to the VALID criteria. The VALID criteria serve to create a validated set of requirements by considering if the requirements are verifiable, achievable, logical, integral and definite. The requirements are listed below and are grouped according to the initial dichotomy of the requirements discovery tree. As a result, the requirements related to the mission constraints are labelled with "REQ-CO-", while the technical requirements are given the label "REQ-TE-". Regarding the constraints on the mission, the following requirements can be recognized:

- **REQ-CO-1:** The wind energy system shall be operational on Antarctica before April of the year 2020.
- **REQ-CO-2:** The wind energy system shall adhere to the legal constraints and regulations imposed by the British government.
- **REQ-CO-3:** The wind energy system shall adhere to the legal constraints and regulations imposed by the Protocol on Environmental Protection to the Antarctic Treaty.
- **REQ-CO-4:** The wind energy system shall leave no visible trace above the surface on the Antarctic continent after its end-of-life.
- **REQ-CO-5:** A waste management plan shall be constructed for the entire life cycle of the wind energy system.
- **REQ-CO-6:** The wind energy system shall have a carbon footprint with a CO_2 equivalent smaller than the current power system averaged over its entire life cycle.
- **REQ-CO-7:** The total cost of the wind energy system shall not exceed €500,000, excluding battery systems.
- **REQ-CO-8:** The wind energy system preliminary design phase shall be contained within the allocated schedule time of 10 weeks.
- **REQ-CO-9:** The wind energy system shall have a minimum lifetime of 15 years under normal operations on Antarctica.
- **REQ-CO-10:** The acoustic noise resulting from the wind energy system operations shall not exceed 40 dB(A) measured at the research station.

- **REQ-CO-11:** Fragments emerging from the wind energy systems shall under no conditions damage the BAS resources.

The technical aspects of the mission stipulate the following requirements:

- **REQ-TE-1:** The wind energy system shall be able to continuously meet the power demand of the Signy Research Station.
- **REQ-TE-2:** The structure shall withstand the aerodynamic loads obtained at an average wind speed of 15 m/s with gusts of maximum 75 m/s during its entire lifetime.
- **REQ-TE-3:** The structure shall withstand temperature variations of minimum $-50^{\circ}C$ and maximum $20^{\circ}C$ during its entire lifetime.
- **REQ-TE-4:** The structure shall withstand the gravitational loads during its entire lifetime.
- **REQ-TE-5:** The structure shall provide a bird strike prevention system.
- **REQ-TE-6:** The effect of surface degradation of the structure shall not reduce the output power of the energy system below the peak power load between two succeeding maintenance sessions.
- **REQ-TE-7:** The structure shall withstand the entire range of operational vibrations during its entire lifetime.
- **REQ-TE-8:** The time for a crack to grow from detectable length until non-repairable length shall at least be the time between two succeeding maintenance sessions.
- **REQ-TE-9:** The back-up power generating system shall be able to provide a minimum power of 35 kW .
- **REQ-TE-10:** The wind energy system shall have a power generation control strategy.
- **REQ-TE-11:** The wind energy system shall have a power transport control strategy.
- **REQ-TE-12:** The wind energy system shall have an energy storage system capable of providing power at 65% of the average power for three consecutive days.
- **REQ-TE-13:** The wind energy system shall have the ability to be operated from within the polar station.
- **REQ-TE-14:** The wind energy system components shall be accessible at all times.
- **REQ-TE-15:** The maintenance of the wind energy system shall be limited to one session per year.
- **REQ-TE-16:** The back-up generator shall not be used to provide power during maintenance sessions under normal operations.
- **REQ-TE-17:** The wind energy system shall have a continuously operating performance measurement system.
- **REQ-TE-18:** The wind energy system shall be transportable by means of a transport system that is able to reach the Signy station.
- **REQ-TE-19:** The wind energy system shall have a sustainable erection plan complying with the Antarctic conditions.

By inspecting the formal requirements stated above, it can be inspected that some of these requirements are quantified by specific values. These values are the result from research into reference systems or preliminary analysis including safety factors. In this paragraph the reasoning behind some of the quantified requirements will be briefly discussed. The cost requirement was based on an estimation for the cost per produced kW by the system. Applying a safety factor of 1.5 resulted in the budget limit of €500,000. Regarding the noise annoyance resulting from the wind energy system, a Canadian study ([170]) showed that the noise annoyance level corrected to the sensitivity of the human ear for wind energy systems within 30 m is 40 $dB(A)$. The technical requirements related to the wind speeds and temperature variations were based on scientific data obtained from the British Antarctic Survey. The other technical requirements that are given a value were constructed based on initial calculations using reference data mainly of the Princess Elisabeth Antarctica station. [143]

A.5 Requirements Compliance Matrix

Requirement	Compliance	Requirement	Compliance	Requirement	Compliance
REQ-CO-1	✓	REQ-TE-1	✓	REQ-TE-11	✓
REQ-CO-2	✓	REQ-TE-2	✓	REQ-TE-12	✓
REQ-CO-3	✓	REQ-TE-3	✓	REQ-TE-13	✓
REQ-CO-4	✓	REQ-TE-4	✓	REQ-TE-14	✓
REQ-CO-5	✓	REQ-TE-5	✓	REQ-TE-15	✓
REQ-CO-6	✓	REQ-TE-6	✓	REQ-TE-16	✓
REQ-CO-7	✓	REQ-TE-7	✓	REQ-TE-17	✓
REQ-CO-8	✓	REQ-TE-8	✓	REQ-TE-18	✓
REQ-CO-9	✓	REQ-TE-9	✓	REQ-TE-19	✓
REQ-CO-10	✓	REQ-TE-10	✓	REQ-TE-20	✓

B. Gantt Chart

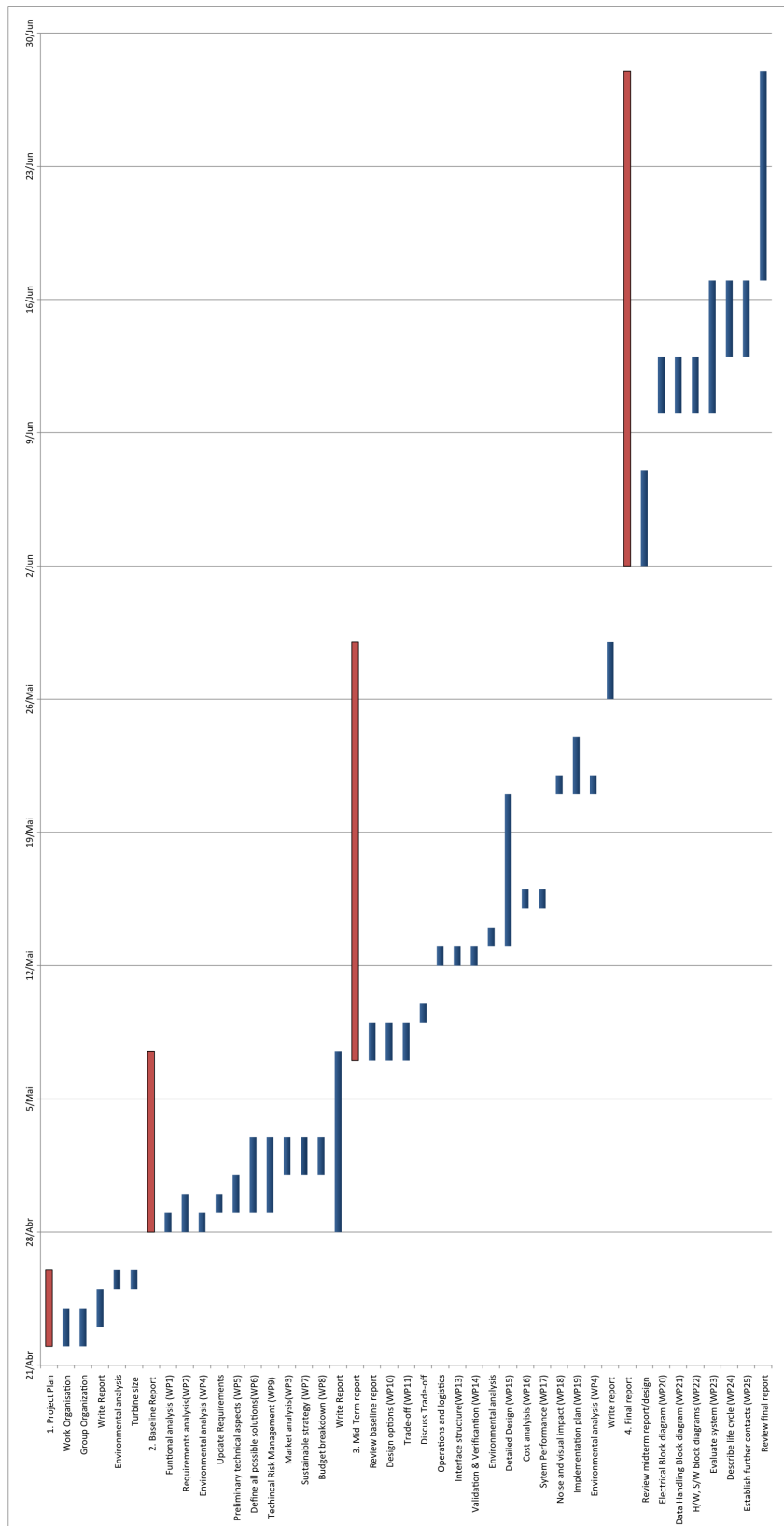


Figure B.1: Gantt chart

C. Lay-out Wind Energy System

In this Appendix, tables supporting Chapter 5 can be found. The trade-off table and reference information can be found. Also the summary of the designed wind energy system are presented in this Appendix.

C.1 Trade-off Wind Energy Configuration

The values used for design trade-off are shown below in Table C.1.

Table C.1: Trade-off table design options

<i>Criteria</i>	<i>Normalised weight</i>	<i>Horizontal</i>	<i>Vertical Lift</i>	<i>Vertical Drag</i>	<i>Vertical Drag & Lift</i>	<i>Jet Engine</i>	<i>Airborne</i>
Feasibility	0.18	5	4.5	4	3.5	3.5	3
Reliability	0.16	5	3	2	2	1	1
Sustainability	0.14	4	4	5	4	4	3
Availability	0.14	4	4	4	4	4	5
Maintainability	0.12	4	5	5	5	4	3
Cost	0.11	5	5	4	4	3	1
Complexity	0.09	4.5	5	5	4.5	3	4
Size	0.07	4	3	2	3	5	5
Total	1	4.48	4.17	3.89	3.69	3.32	2.98

C.2 Summary Wind Energy System

HAWT	
# Turbines	3
Power output	3x17 kW
Rotor	
# Blades	3
Radius	4.4 m
Tower	
Height	8.8 m
Diameter	0.64-0.16 m
Foundation	
Type	Rock Anchor
Depth	2m
Radius	1.28 m
Nacelle	
Generator	Direct drive permanent magnet
Dimensions	1x1.1 m
Control	
Upwind/downwind	Downwind
Power control	Variable pitch, Variable speed
Direction control	Downwind yaw system

Battery	
Type	Lead Acid
Capacity	1600 kWh
Back-up	
Type	Diesel Generator
Power output	40 kW
Material	
Blade Box	Carbon/flax with bio-based epoxy
Blade Aeroshell	Glass with bio-based epoxy
Tower	Low temperature Carbon Steel
Bedplate/Shaft	Low temperature Carbon Steel
Nacelle housing	Glass with bio-based polyester
Cost	
Total	€642000
Electricity	€0.1402
Weight	
Turbine	1248.2 kg

C.3 Power Rating & Number of Turbines

In Table C.2 and C.3, information about the wind energy system of reference Antarctic research stations is shown. This information is used to justify the decided power rating and number of turbines.

Table C.2: References turbine sizes

<i>Research station</i>	<i>Country</i>	<i>Rated power in kW</i>	<i>Max crew</i>
Princess Elisabeth [143]	Belgium	100	48
Rothera [171]	Great Britain	200	100
Neumayer [172]	Germany	345	45
Davis [173]	Australia	250	120

Table C.3: Total power, number of turbines and power per turbine for reference research stations

<i>Research station</i>	<i>Total wind power in kW</i>	<i>Number of turbines</i>	<i>Power of one turbine in kW</i>
Princess Elisabeth [174]	54	9	6
Neumayer [175]	150	5	30
Mawson [176]	600	2	300
Dumont D'Urville [177]	12	1	12
McMurdo/Scott Base [178]	990	3	330
Sanae IV [179]	60	3	20

D. Risk Analysis

Within this section additional discussion on system risks can be found in Section D.1 and D.2 as well as values of the system component failure rate shown in Section D.3. Finally, the distance achieved by fragments during a catastrophe is analysed on Section D.4.

D.1 Risk

Risk can be defined as the "uncertainty of attaining a specific goal or requirement"[50]. Thus the risks associated with a specific design solution are essential to the success or failure of the system.

Risk can also be seen to stem from the interaction of the likelihood of failure and the severity/consequence of a given failure, which can be represented visually in the form of a risk map. If likelihood of failure is very high and the consequence of such a failure is also very high then risk is seen to be very large. An expansion on the two concepts is given here.

Likelihood of Failure: This relates to the probability that a given concept or component will fail. This can be generally seen to originate from the level of maturity of the given technology. If the component is only conceptualised in literature, then the likelihood of failure is considered very high. On the other side of the scale, if the component or design is already been used in industry for long periods, then the design is assumed to have a lower likelihood of failure. The separation of the level of maturity of a given concept can be separated into the following categories, from most likely to least likely: *feasible in theory, working laboratory model, based on existing non-wind engineering, extrapolated from existing wind engineering design, proven design*. It should be noted that the use of statistical knowledge of specific component failures can be used to estimate the likelihood of failure, e.g the frequency of failures in wind turbine systems that are due to gearbox failures.

Severity of Failure: This is seen as how a given failure type effects the mission requirements, and thus the success of the mission. If the severity of a given failure simply causes a minor inconvenience, then the consequence is deemed as low. On the other extreme, if the consequence of a given failure is a complete break-down of the system, then the severity of failure is considered very high, as now the system is unable to complete its mission. The separation of the level of severity of given failures can be separated into the following categories, from least severe to most severe: *negligible, marginal, critical, catastrophic*.

It must be noted when using the above for risk analysis as and that maintainability possibilities of the system are also to be considered, including how they affect the risk map of a given design. This is of vital importance as one may be confronted with the situation that a given component has a catastrophic consequence and high likelihood for a given failure, but can easily be mitigated through very simple maintenance procedures, whereas another component may have critical consequences of failure of a given component but no measures in terms of simple maintenance can be applied to ease the problem. Thus maintainability must be used in conjunction with risk, in order to give a more complete picture.

D.2 System Risks

- **Mechanical Risks:** This group incorporates risks found in the gearbox, shafts and brakes of a system. A more complex system will bring more mechanical risks. However, other risks such as sensitivity to fatigue, material toughness, maximum allowable stresses, and temperature resistance of the mechanical parts must be considered when examining risks to a system. As a direct drive system is used large portion of the mechanical risks are mitigated as no gearbox is present. There are still risks however that oscillatory loading on the shaft will cause failure of the component and subsequent failure of the generator and the turbine systems as a whole. In addition a complete failure of the mechanical brake could cause the rotor to spin uncontrollably after cut-out wind speed and as such overload the generator. This is, however, extremely unlikely as such an event would also have to coincide with a failure in both the aerodynamic break and the fail safe spring within the brake system.
- **Risks in Aerodynamic Elements:** These risks encompass all possible risks to the aerodynamic elements of the system, defined as the elements that have direct interaction with the airflow for the purpose of extracting

energy from the airflow. The possible risks include, but are not limited to, corrosion, impact deformation, possible formation and growth of cracks through vibrations or environmental conditions, all of which are intrinsically related to the chosen design and location of implementation. Due to the very large range of winds and changes in wind speed found on Signy Island, failure due to fatigue growth on the blades leading to structural failure is of concern, however a safety factor of 10 is applied to the design stress in order to minimise this risk as much as possible. Furthermore disconnection of blades from the rest of the turbine due failure of connection with the hub is a possible risk. This is due to the range of temperatures that the system is exposed to causing expansion and contraction and as such leaving the locations where two or more material types are joined particularly vulnerable. Moreover failure of the whole system can occur if a blade is damaged due to bird impacts, although such risks are mitigated as the anti-collision system implemented.

- Risks in Structural Elements:** These risks encompass all risks to the structure, defined as the components which have a primary goal of handling the physical loads of the system and the environment. These risks depend on how the design is exposed to and is dealing with, weight, load variations, possible fatigue, impacts, and environmental interaction such as corrosion formation. These risks are related to the structural design of the system, including its geometry and the materials used. The likelihood of damage to the tower due to bird impact is extremely low as the tower is visible to birds. However similarly to the aerodynamic elements, due to the large wind range fluctuations experienced risk of fatigue growth is of a concern in addition to problems with component connections due to thermal expansion and contraction.
- Risks in Electrical System:** These include risks that exists in the electrical cables, transformers and generators. These risks are related to the weather conditions a given design exposes the electrical systems to and these risks are related to the complexity of the electrical system itself. Any one of the many electrical components, including the generator, transformers, battery terminal, or monitoring system can break due to sudden electrical fluctuations or enviromental stimuli causing the wind turbines to not be able to provide power to the system. If the electrical system effects a local component then the other two turbines are still capable of providing energy. However if the problem occurs in a central system such as the batteries or the monitoring system, then all three turbines will be offline and the research center will be running on simply the back-up generator. Such failure can occur due to the very low temperatures that electrical components experience in the antarctic location, and thermal differences causing fatigue in soldered connections. In addition if the batteries are not kept thermally insulated and above a temperature of -20 degrees Celsius, then there is a risk that the electrolyte will freeze, cracking the battery casing and rendering the batteries inoperable. Furthermore, not only the low temperatures of Antarctica are a problem to the electrical systems but also there is a risk that the generator cooling system fails and as such the generator overheats due to high temperatures, leading to the turbine being offline. Finally there is a risk that the electrical components can become short circuited if components are not completely sealed from the rain and as such allow water to build up inside the various components.

D.3 Component Failure Likelihood

In Table D.1 the likelihood values for component failure rates are found.

Table D.1: Annual failure frequency

Component	Failure frequency [-][51] [52] [53] [54][55]
Electrical System	0.045
Pitch control	0.035
Sensors	0.04
Yaw damper	0.005
Rotor blades	0.05
Mechanical Brake	0.01
Rotor Hub	0.001
Generator	0.021
Supporting Structure/housing	0.01
Shaft	0.005
De-icing	0.05
Back-up	0.004

D.4 Distance Achieved by Fragments During a Catastrophe

During a catastrophe, if the were to turbine disintegrate, it should ensure that no fragments will hit and consequently damage the station as required by *REQ-CO-11*.



Figure D.1: Damage on a wind turbine

As can be seen in the FigureD.1, several fragments of different sizes can be released from the wind turbine. A calculation was conducted for different sizes, with a wind speed of $75m/s$. The equations are derived assuming that drag has a linear relation with velocity, and so the force in x-direction and y-direction are given as:

$$F_y = m \cdot g - c \cdot V_y \quad (D.1)$$

$$F_x = -c \cdot V_x \quad (D.2)$$

Where F , m , g , c , v are the force for each direction, mass of the fragment, constant of gravity, drag constant and velocity at each direction respectively. The drag constant is calculated by knowing that drag force is:

$$F_D = c \cdot V = \frac{1}{2} \rho V^2 C_D A \quad (D.3)$$

By integrating the force equations, the velocity of a fragment at a certain time is found. Integrating those equations also, the position of the fragment can be determined and the ultimate equation for velocity and position are found as:

$$x = V_{0x} B \cos(\theta) (1 - e^{-\frac{g \cdot t}{B}}) \quad (D.4)$$

$$V_X = V_{0x} \cos(\theta) e^{-\frac{g \cdot t}{B}} \quad (D.5)$$

$$y = \frac{B}{g} (V_{0y} \sin(\theta) + B) (1 - e^{-\frac{g \cdot t}{B}}) - B \cdot t \quad (D.6)$$

$$V_Y = V_{0y} \sin \theta e^{-\frac{g \cdot t}{B}} - B ((1 - e^{-\frac{g \cdot t}{B}})) \quad (D.7)$$

Where B equals to mg/c . The maximum distance reached by the fragments is $62.3841m$, thus not hitting the research station.

E. Investigation on De-icing Systems

This appendix will elaborate on the different de-icing systems that were considered for the wind energy system.

E.1 Black Coating

Black coating is often used in combinations with an ice-phobic coating. Black paint is a passive de-icing system and is very cheap. When the solar intensity during icy periods is very high a black coating can be used as a de-icing system. This method is sufficient for sites with temperatures around $0\text{ }^{\circ}\text{C}$. However, it will not prevent all icing on lower temperature sites. [180]

E.2 Special Coating

Coatings are passive anti-icing surfaces. Coatings rely on their hydrophobic property that prevents the water from settling on the surface and thus it reduces the ice formation. However, studies from the Fraunhofer IFAM institute showed that hydrophobicity is only one determining factor of anti-ice properties. A hydrophobic coating is not necessarily an anti-icing coating. An increase in ice formation occurs under specific angles. There are many coatings tested in the lab, but there are only a few field tests, mainly for hydrophobic coatings. For the coatings where anti-freeze proteins are coupled to the coating, the coating which makes use of chemical freezing point depression, the coatings that contain hydrophilic centres in a hydrophobic environment and many others have not yet been proven to be very effective. The advantage of special coatings is that they are of low cost and that they do not require much maintenance compared with de-icing systems that require mechanical parts. However, coatings can become porous and therefore can lose their ability to repel the ice. [181]

E.3 Electrical Heating

The electrical heating uses an electrical resistance embedded inside the membrane or laminated on the surface. The idea is to create a water film between the ice and the surface. Once this film is created, centrifugal forces will throw the ice away. The heating element covers only the leading edges of the blades and does not affect the aerodynamics. The ice detector and blade surface temperature are used to control the operation of the heating system and additional temperature sensors are installed to protect the blade from permanent damage induced by over-heating. This method has been installed but there is no mass production yet, it is still in the prototype phase. Most recent results have proven that this method uses 5% of the rated power. [180]

E.4 Hot Air

Hot air is blown into the rotor blade at standstill with special tubes. Blowers located in the root of each blade or inside the hub, produce the hot air. The heat is transferred through the blade shell in order to keep the blade free of ice. A water film is developed between the surface and the ice and the centrifugal forces will throw the ice off. The aerodynamics and the lightning protection system will not be affected. It has a relatively high energy consumption at high wind and temperatures around $0\text{ }^{\circ}\text{C}$. However waste heat of the generator can be used. It consumes 1% of the total electricity production, although this relation increases with the size of blade. [180] A passive hot air system was designed for the wind turbine, taking the advantage of the losses of the generator to heat the blade surface. However when modeled it was proven that there was not enough energy to heat the entire length of the blade. In Figure E.1 the temperature on the blade surface and air existing between leading edge and wingbox along the length, when the radius of a circular hole on the front of the nacelle is 16 cm , with external temperature of -10 ° and freestream velocity of 10 m/s is shown. To model the temperature on the root of the blade the conservation of energy and mass for the control volume, the interior of nacelle, is considered. In the blade it is considered that there is convective heat transfer between the external air and the external part of the leading edge and the internal air, between leading edge and wing box, and the internal part of the leading edge. Next to conservation of energy there is conservation of mass.

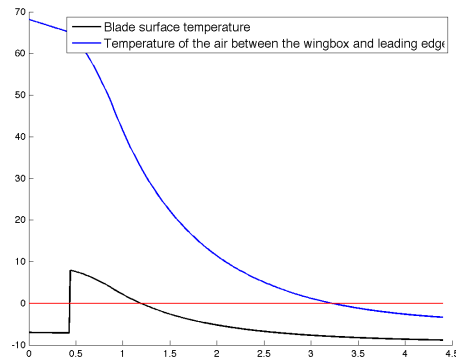
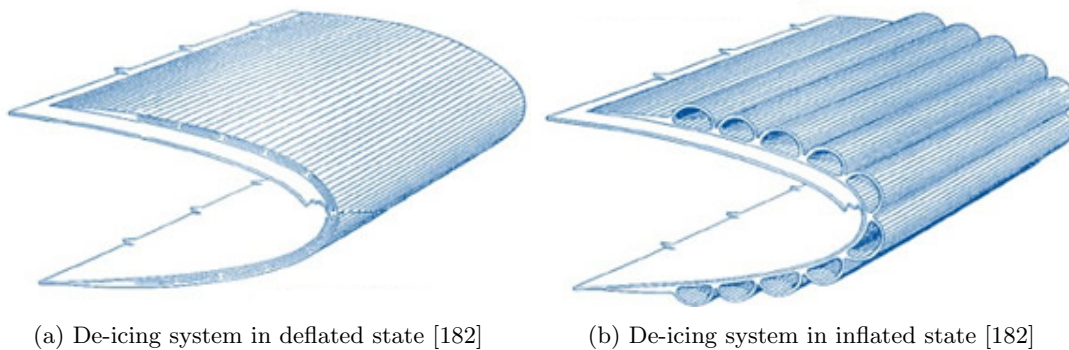


Figure E.1: Temperature on the blade

E.5 Inflatables

Inflatable parts are an often used de-icing system to reduce the ice on aircraft wings. These parts inflate when compressed air is pumped into the de-icer. Due to this the ice will break and is removed from the surface. The pneumatic boots are ideally used after the build up of 6 to 13 *mm* of ice. [180] They consist of multiple layers of rubber, neoprene/polyurethane and nylon. Images of pneumatic boots in deflated and inflated state are shown in Figures E.2a and E.2b, respectively.



(a) De-icing system in deflated state [182]

(b) De-icing system in inflated state [182]

Figure E.2: Inflatable de-icing system that can be implemented on the wind turbine

Pneumatic de-icing systems are light-weight, require low power, are often used and have low costs [183]. The main disadvantage is the need for intensive maintenance [180], which is difficult on Signy Island. The boots also increase the drag and produce noise when inflated. However the total time needed for the removal of the ice is just a few seconds and so the drag and noise are not a permanent problem. After the removal of ice a vacuum is applied to deflate the parts. Ice expulsion can be a potential problem of this de-icing system, because chunks of ice are removed. [180]

E.6 Pulse Electro-thermal De-icing

Pulse electro-thermal de-icing (PETD) is an ice removal method using electrical pulses directly applied to an ice-covered surface. A thin electrically-conductive film is applied to the frontal surface, with respect to the wind direction, of the wind turbine blades as in Figure E.3a. A milliseconds-long pulse of electricity heats the film which melts a micrometer-thin layer of ice. PETD is a nearly perfectly efficient de-icing system. The blades can be constantly kept free of ice by applying the pulses regularly. An advantage of PETD is that the power consumption is low. Figure E.3b shows qualitatively the temperature distribution along substrate, melted layer of ice and the ice layer. [184], [61]

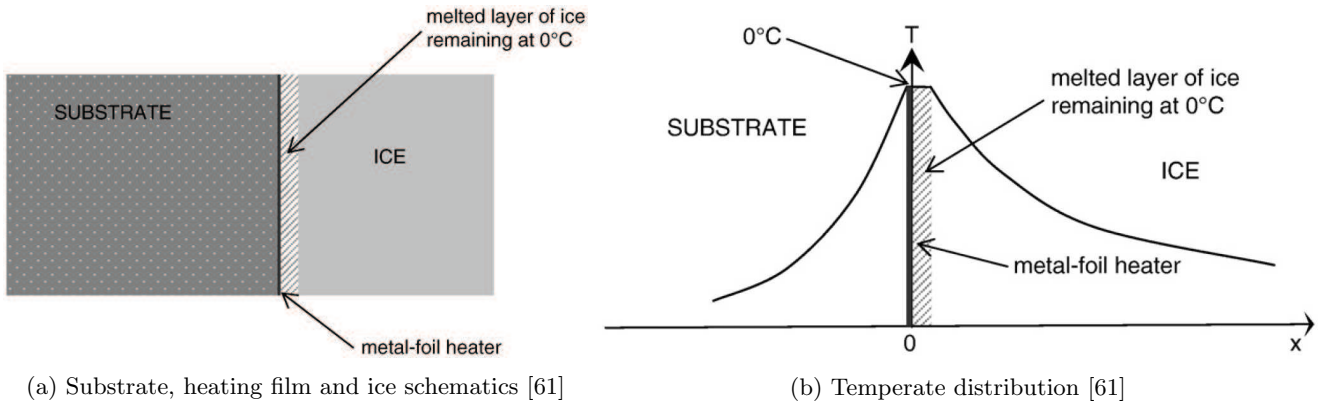


Figure E.3: Pulse electro-thermal de-icing system

E.7 Trade-off

The methods described above are presented in the trade-off matrix given below.

	<i>Influence on aerodynamics</i>	<i>Influence on structural design</i>	<i>Feasible in environment</i>	<i>Costs</i>	<i>Sustainability</i>	<i>Maintenance</i>
Special coating	0	0	+/-	+	+/-	+/-
Black coating	0	0	-	++	+/-	+
Inflatables	-	0	+/-	+/-	+	-
Hot air	0	-	++	-	-	-
Electrical heating	0	0	+	-	-	-
PETD	0	0	+	+/-	+	+

Influence on aerodynamics All the methods do not influence the aerodynamics of the blades to which a '0' is allocated, except the inflatables. However, these are often used in aircraft, so the influence will be acceptable.

Influence on structural design The structural design is also not a decisive property since most methods do not influence the structure of the wind turbine, so again a '0' is allocated. Only the hot air has influence since tubes need to be placed inside the blades. This is not favourable for the structure, so a '-' is given.

Feasibility in environment The extreme climate on Signy could influence the performances of the de-icing systems. The black coating is the least feasible in the Arctic environment when compared to the other systems followed by the special coating. Black coatings work are the most effective for temperatures around zero °, while the temperature range on Signy most often lies at much lower temperatures. Then, the special coating works on hydrophobicity, which may not work as efficiently for the large amounts of ice. The PETD is proven to be effective, but the hot air is the most effective and feasible since the blades are constantly heated above 0 °C, so no ice can attach to the blades.

Costs: The coatings itself are not expensive and the application is without advanced production technique so these methods score the best in the trade-off. The inflatables are widely used, so the production technique will not be very costly since the application is easily applied. The PETD scored equally to the inflatables, since small and only a few components are needed. The hot air and the electrical heating methods are the most expensive because these systems are relatively large, require extra integrated components that affect the structure and are the systems are at an early stage of development.

Sustainability It is important that de de-icing system does not pollute the environment, so a sustainable method should be chosen. Hot air and electric heating require constant power supply, so this systems are not sustainable, so '-' is allocated to both these systems. The coatings are substances that are not sustainable, but these do not require any power. The inflatables and PETD are considered to be sustainable since the material is recyclable and no power is required.

Maintenance As is mentioned, the inflatables require much maintenance. Also, the heating systems may degrade the material and the condition of the blades which needs to be checked regularly. These three systems score therefore the least at this criterion. The special coating gets porous, so this must be renewed relatively often when compared to the black coating. The PETD is a proven technology in icy climates, so this method will not be demanding in maintenance sessions which is very advantageous on Signy.

F. Blade Design

In this Appendix, the methods used to end up with the final blade design are explained in detail. This appendix is complement to Chapter 10. Each decision is based on an extensive analysis consisting of multiple steps. The used formulas and calculation flow can be found in this chapter.

F.1 Airfoil Trade-off

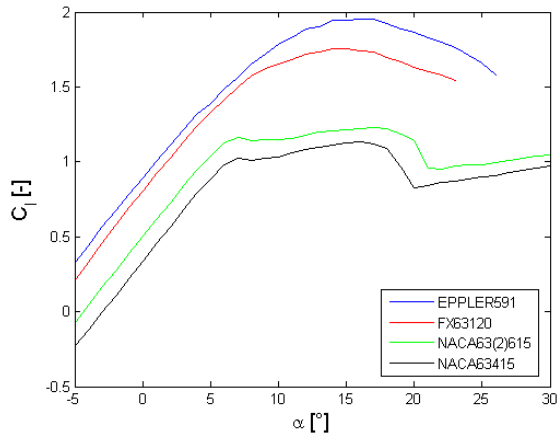
To determine the best suitable airfoil for this project, an airfoil trade-off is performed. Airfoils like S8, DU, FFA or Ris ϕ are considered as well as NACA, Wortmann and Eppler. The data of these airfoils is gathered by Xfoil and compared. Due to the different aerodynamic requirements of the tip and root, separate trade-offs are performed for the two parts. At the root, the operational Reynolds number is estimated to be 879902 as for the tip the Reynolds number is taken to be 456388.

The airfoils S8, DU, FFA and Ris ϕ are designed to be insensitive to roughness and to have a high maximum lift-to-drag ratio. However, at the low Reynolds numbers for a small wind turbine, these airfoils do not present a good performance. As an example, the airfoil S822 in clean conditions has a non-linear relation between the lift coefficient with the angle of attack and stalls early and very sudden. Another disadvantage of these airfoils is that they are not free to be used, with the exception of the DU airfoils. This means that limited information is available from measurement data and only programmes like Xfoil can be used to estimate the performance of these airfoils. However, this software is not accurate in predicting flow separation and thus the resulting polars might not be reliable.

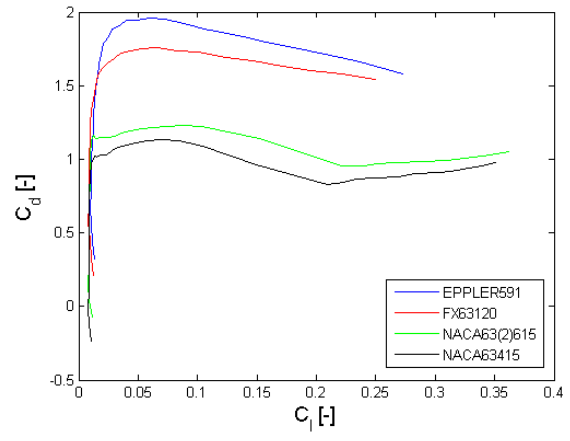
The remaining airfoil families are the Eppler, Wortmann and NACA families. For the tip E591, FX63120, NACA 63615 and NACA 63415 are considered while for the root the E858, FX84W218, NACA2424 and NACA23024 are compared. These airfoils are selected based on the good lift-to-drag ratio (major concern for tip airfoils) and a good stall behaviour (major concern for root airfoils). Since also the roughness sensitivity is very important, the lift and drag polars are displayed for both a clean and rough configuration (Figure F.1 to F.4). The roughness of the airfoils is simulated by forcing transition at the leading edge of the airfoils, which would also happen if the airfoil was contaminated.

When examining the polars, it can be noticed that the NACA airfoils have a poor performance when compared with the Eppler and Wortmann families, since the maximum lift coefficient and stall angle are significantly lower and the drag is higher. Additionally, it can be noticed that the relation between C_l and α at the root is non-linear and that the stall behaviour is not ideal for wind turbines. Based on this reasoning the NACA airfoils are excluded from the airfoil trade-off.

When comparing the Wortmann and Eppler airfoils, it can be observed that the minimum drag is similar for both the tip and root and that the maximum lift coefficient of the Eppler airfoil is larger. Although this is a good indicative, the maximum C_l/C_d ratio is higher for the Wortmann airfoils. This is also reflected in a better stall behaviour for the tip and a later stall for the root. The FX63120, analysed for the tip, has a high relative thickness of 12% and presents a leading edge stall. The separation bubble only bursts at really high angles of attack (30°). When comparing the sensitivity to roughness, it can be seen that the Wortmann airfoils do not lose so many performance as compared to the Eppler airfoils. This can be explained by analysing the relative position of the maximum thickness. For the tip the maximum thickness of FX63120 occurs at 30.8% of the chord while for E591 it is at 25% of the chord. For the root, FX84W218 has its maximum thickness at 33.9% while for E858 it is at 26.6% of the chord. An airfoil with the maximum thickness near the leading edge leads to the fact that transition and stall occur earlier than expected; for the airfoil with maximum thickness at a large distance of the leading edge the streamlines still follow the airfoil shape without creating high adverse pressure gradients. By the reasons presented before, the airfoil FX63120 turned out to be the most suitable for the tip and the airfoil FX84W218 for the root.

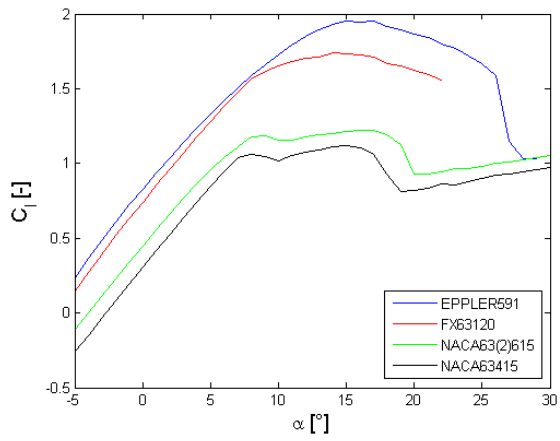


(a) Cl- α

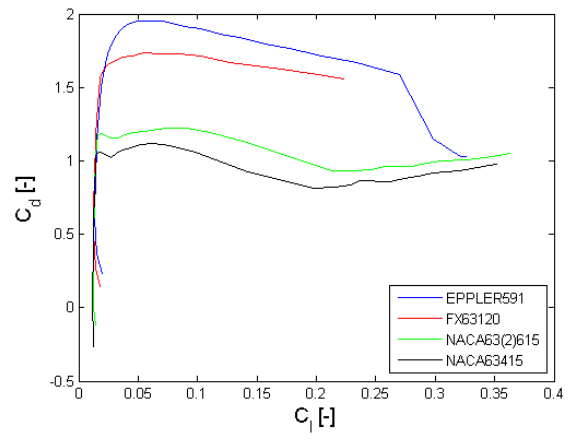


(b) Cl-Cd

Figure F.1: Polars of tip airfoils for clean configuration at $Re = 456388$

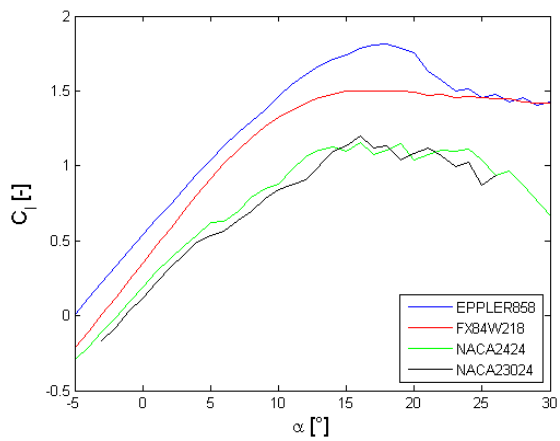


(a) Cl- α

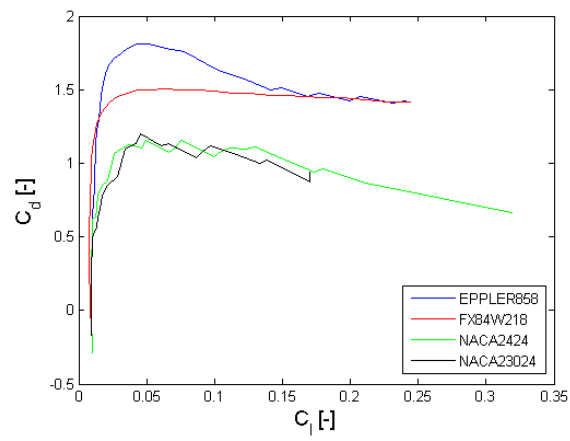


(b) Cl-Cd

Figure F.2: Polars of tip airfoils for rough configuration at $Re = 456388$



(a) Cl- α



(b) Cl-Cd

Figure F.3: Polars of root airfoils for clean configuration at $Re = 879902$

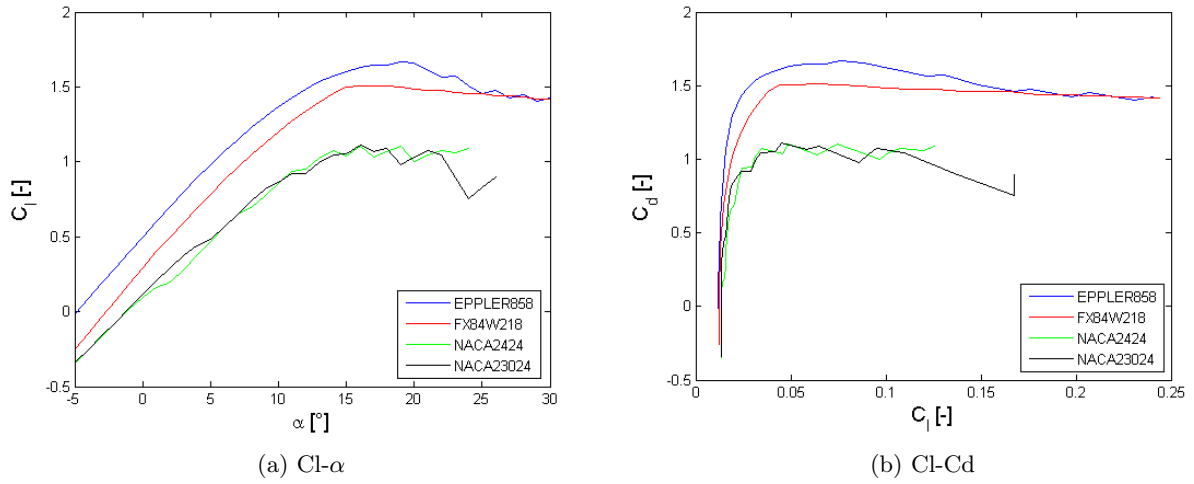


Figure F.4: Polars of root airfoils for rough configuration at $Re = 879902$

F.2 Airfoil Selection

The airfoils for the Windpulse are selected to be FX63120 at the tip and FX84W218 at the root part of the Wortmann family. In Figure F.5 and F.6 the lift and drag graphs are shown.

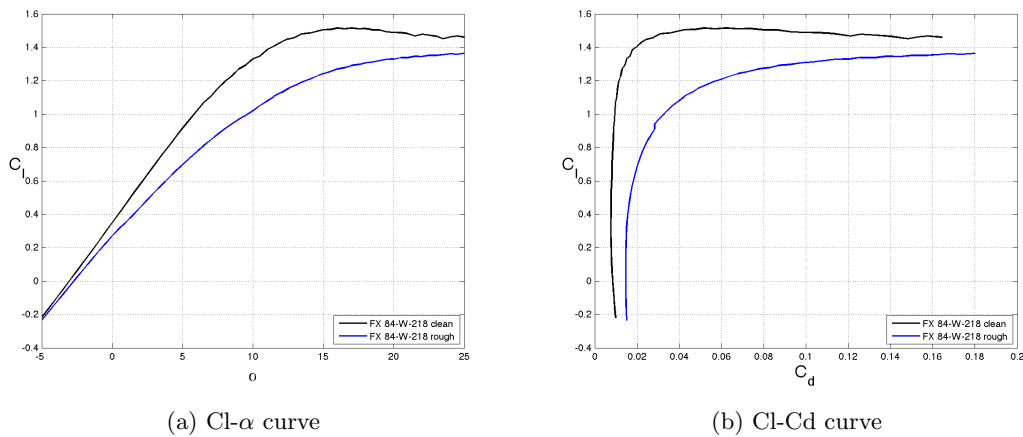


Figure F.5: Airfoil curves for the root part of the blade at $Re = 879902$ in clean and rough configuration

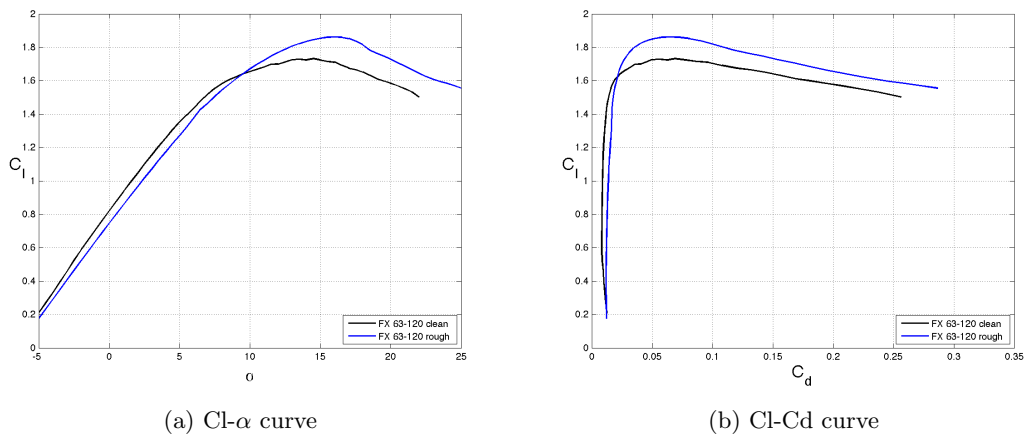


Figure F.6: Airfoil curves for the tip part of the blade at $Re = 456388$ in clean and rough configuration

The plotted data is extracted from the software Rfoil. Measurement data are much more accurate to obtain the lift and

drag coefficients however for the operational Reynolds numbers of the Windpulse no measurement data is available. The comparison of the measurement data and the Rfoil data is explained in detail during the validation. The errors shown in Table F.1 are applied on the Rfoil data of the tip and root airfoils at the correct Reynolds numbers. For the middle airfoil, the average between the tip and root errors is obtained. For the tip airfoil the performed procedure is visualised in Figure F.7.

Table F.1: Error applied on the Rfoil data for the tip, root and middle airfoil

<i>Airfoil location</i>	<i>Operational Reynolds number [-]</i>	<i>Lift correction [-]</i>	<i>Drag correction [-]</i>
Tip	456388	$-0.0038(\alpha + 8.04) - 0.0014$	0.1232
Middle	879902	$-0.00378(\alpha + 1.9) - 0.0102$	0.0566
Root	681444	$-0.00379(\alpha + 4.97) - 0.0058$	0.09

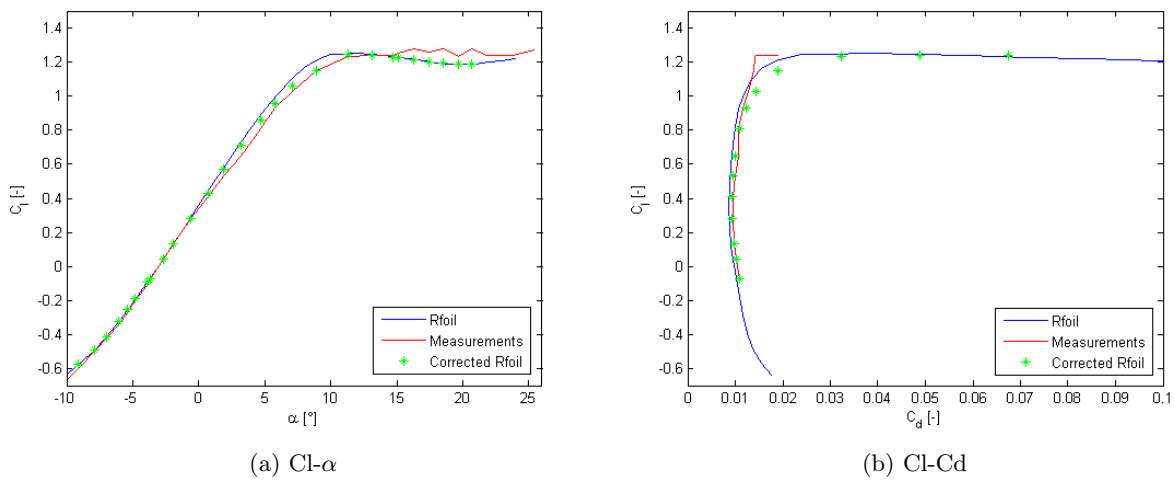


Figure F.7: Polars of FX84W218 at a Reynolds number of 700000 for Rfoil data, measurement data and corrected Rfoil data

F.3 Rated Velocity

The values of the rated wind velocity at which a wind turbine will produce its maximum average power has to be determined. The method for determining the optimum rated wind velocity was based on the procedure explained in [74]. The method relies on the average power calculation shown in Equation F.1 [74]. Therefore the power for each wind speed and the probability of a certain speed should be known. The output power of the wind turbine being considered is expressed by Equation F.2 [74]. The probability density function of the wind velocities is given by a Weibull distribution based on measurement data. The a and b variables (equation F.3) are calculated by the MATLAB software during the environmental analysis. To finally determine the optimum rated velocity for the Signy case, the derivative of the average power with respect to the rated velocity is set equal to zero. Since this derivative is a function of both the rated velocity, the cut-in speed and the cut-out speed, the number of variables was reduced by estimating V_{in} and V_{out} as 0.3 and 3 times the rated velocity, respectively [74].

$$P = \int_0^{\infty} P(V) \cdot g(V) dV \quad (F.1)$$

with:

$$P(V) = \begin{cases} 0 & \text{for } 0 < V < V_{in} \\ P_R \cdot \frac{V-V_{in}}{V_R-V_{in}} & \text{for } V_{in} < V < V_{rated} \\ P_R & \text{for } V_{rated} < V < V_{out} \\ 0 & \text{for } V_{out} < V \end{cases} \quad (\text{F.2})$$

and:

$$g(V) = \frac{b}{a} \cdot \left(\frac{V}{a}\right)^{(b-1)} \cdot e^{\left(\frac{-V}{a}\right)^b} \quad (\text{F.3})$$

F.4 Chord Distribution

To find the optimum chord distribution, Equation F.4 from [68] is considered. The optimum distribution means that when this distribution is used, there will be a minimum loss of kinetic energy due to wake rotation. The used method allows the twist and chord distribution of a blade to be determined that would provide Betz limit power production. The only unknown parameters in the equation are the axial induction factor a , the Prandtl tip loss factor F and the angle Φ . The third order polynomial that gives the optimum relationship between the local tip speed ratio x and axial induction factor a can be solved for a . This relation ends up with three a values of which the value closest to $1/3$ is chosen, based on the Betz limit. The corresponding optimum value for the tangential induction factor a' can now be calculated. With a and a' known, the flow angle Φ can be easily determined from trigonometry of the velocity triangle. Normally, the larger the number of blades, the smaller the chord and the variation in the chord with respect to the radial distance will be.

The flow angle Φ is the sum of the section pitch angle θ_p and the angle of attack α . From this relation the optimum twist θ_T can be calculated assuming that at rated speed, the blade operates at operational angle of attack. The blade twist angle is defined relative to the blade tip taking into account the blade pitch angle at the tip $\theta_{p,0}$. The formulas are shown in F.6 adopted from [185].

$$\frac{c(x)}{R} = \frac{8\pi a x \sin^2(\Phi)}{(1-a)BC_n\lambda} \quad (\text{F.4})$$

where:

$$C_n = C_{l,opt} \cos(\Phi) + C_{d,opt} \sin(\Phi) \quad (\text{F.5})$$

$$\Phi = \theta_p + \alpha \quad (\text{F.6})$$

where:

$$\theta_p = \theta_T - \theta_{p,0} \quad (\text{F.7})$$

F.5 BEM Code

To calculate the power output of a certain wind turbine, the aerodynamic loads should be known. With The Blade Element Momentum (BEM) model it is possible to calculate the steady loads and thus also the thrust and power for different settings of wind speed, rotational speed and pitch angle. A lot of problems and required outputs may be solved by adapting this code. It is thus important that the code is compatible for multiple problems and written in a general form.

Since the wind turbine is not always running in optimum conditions, the third order polynomial which gives an optimum relationship between a and a' is not longer valid. This is why the BEM-method is introduced. The BEM-method

couples the blade element theory and the momentum theory. The essence of the code is to calculate the axial and tangential induction factors in an iterative way. These two parameters depend on the flow angle and vice versa. The iteration continues until the differences between the updated values for a and a' and the previous values are smaller than ϵ , which is set to 0.0001. The algorithm can be summarized as eight steps. [68]

- Step 1: Initialize a and a'
- Step 2: Compute the flow angle Φ
- Step 3: Compute the local angle of attack α
- Step 4: Calculate C_l and C_d corresponding to α
- Step 5: Compute C_n and C_t
- Step 6: Calculate a and a'
- Step 7: If a and a' have changed more than a certain tolerance, go to step 2 or else proceed
- Step 8: Compute the local loads on the segments of the blades

Since it is assumed that the different control volumes are independent, each section can be treated separately. The eight steps can thus be performed subsequently for each individual radial section. To implement the BEM-method, two corrections should be added to the code. The first correction is called the Prandtl's tip loss factor. Since the momentum theory assumes an infinite number of blades a correction should be introduced. The second correction is the Glauert correction. When a becomes larger than a critical value, the simple momentum theory is no longer valid. The momentum theory predicts a decrease in the thrust coefficient for large values of a , which is however not true. Experiments have shown that C_T keeps on increasing with a . Therefore empirical relations, the linear Wilson/Walker relation and the third order polynomial Glauert relation, exist to account for the deficiency of the momentum theory.

The necessary input parameters of the BEM-code are the number of blades B , the chord distribution $c(r)$, the twist angle distribution $\beta(r)$, the pitch angle θ_p , the lift coefficient $C_l(\alpha)$ and drag coefficients $C_d(\alpha)$, the radius R , the rotational speed ω , the wind speed V_0 and finally the air density ρ . The tangential and normal load distribution of all the control volumes are the outputs of the BEM-code. With these outputs, the total shaft torque may be calculated by summing all the moment contributions along one blade multiplied by the number of blades. Finally the output power can be computed.

F.6 Blade Geometry and Loading

Due to the varying chord length along the wind turbine blades, the inner box will be tapered in width and height and will become smaller towards the tip of the blade. The width and height of the box will be 0.4 and 0.1 times the chord length respectively. Since the root sections of the blades are subjected to the highest loads and since these sections are designed mainly for structural instead of aerodynamic reasons, the root sections of the blade will be modelled as a rectangular shaft with a width of 60% of the maximum chord which is connected to the blade through a tapered section. For the structural design, it is also assumed that this shaft is not loaded by the aerodynamic forces as is the case for the other sections. The dimensions of the box are visualised in Figure F.8.

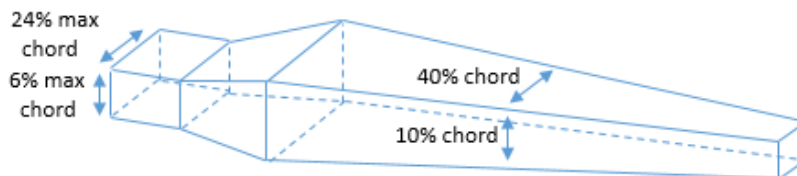


Figure F.8: Schematic representation of the structural box dimensions

It is important to know the different loads acting on the blade, so that the blade can be properly sized in order not to fail under the applied stresses. Two of the most important loads are given by the BEM-code, namely the tangential load and the normal load (normal and tangential to the rotor plane). These loadings are distributed along the blade length and are the driving force behind the power extraction of the wind turbine. In addition to the normal and tangential loads, the blade is also subjected to the weight and the centrifugal forces, the latter being caused by the rotation of the blades. Due to the varying rotational position of the blades, it is important to consider how the effect of the weight changes with the position of the blade. If the blade is in the upward or downward position, the weight is only exerting a normal force on the blade, causing it to be in compression and tension respectively. At 90° of these positions, the weight is only exerting a bending moment on the blade, and no normal force. In fact, the weight component in the direction of the blade is given by Equation F.8, while the component normal to the blade is described

by F.9. In these equations, γ depicts the rotational position of the blade with respect to the upward position.

$$W_{\text{tangential}} = W \cdot \sin(\gamma) \quad (\text{F.8})$$

$$W_{\text{normal}} = W \cdot \cos(\gamma) \quad (\text{F.9})$$

In order for the design to be conservative and able to sustain the high loads, safety factors are applied. Since the BEM-code provided the normal and tangential loads for all the sections and for all the velocities, the maximum values for all the sections are used in the structural designing tool after being multiplied with a factor of 1.36, given by [108]. The weight of each section was multiplied by 3 to account for the material that is needed to construct the outer contour of the section and add-ons like the de-icing system. The maximum allowed Von Mises stress of the chosen composite was divided by 10, to come up with a robust design with respect to the fatigue, [108] (see Section 13.2 for more information on this factor). Finally, the design value for the angle γ was set to 90° since this position (together with 270°) yields the highest stresses on the structure. In addition to the loads sustained during operations, the load case during maximum wind speeds was also considered. In that case, the blades are pitched towards the wind to minimize the forces acting on it. After analysis, it was found that it was best to pitch the blade so that the tip has zero degree angle of attack, which gives the root a -16° angle of attack. If that is done, the stresses achieved in the blade are still much lower than the maximum allowed value and the deflections remain within limits.

F.7 Stress Calculations

A tool is constructed that finds the minimum thickness distribution of the blade needed to withstand the stresses induced by the varying loads acting on it. The Von Mises stress at many points along the blade is calculated for different values of the material thickness. Then, the maximum Von Mises stress is compared with the allowed value. Finally, the weight is calculated for all the boxes that satisfy the maximum stress constraint and the solution with the lowest weight is chosen. Also note that the width and height of the box were adjusted in order to increase the stiffness. However this approach was limited by the thickness of the airfoils. The decision was made to not change the airfoils to thicker types for the sake of structural stiffness, mainly since the selection of airfoils was done by keeping the airfoil thickness in mind already. Symmetry is assumed for the thickness of the top and bottom skin, as well as the thickness of the front and rear webs. These assumptions cause the shear centre to be located in the middle. Because of the three dimensional taper of the inner box and because of the varying loads along the blade length, the thicknesses will be different along the blade length. Therefore, the thickness distribution for the skins and the webs will each be described by a factor that is multiplied with the local chord length. These two factors will be the variables that are used (in the loops) to find the optimal box structure. Due to the different geometry of the shaft at the root of the blades, the thickness factors at the root will be different than the ones used for the tapered box that comprises the rest of the blade. Therefore, the numerical tool will first determine the optimum thickness factors that ensure that the actual blade will not fail under the applied load, after which the optimum factors for the shaft are determined separately. The factors for the shaft will be values that need to be multiplied with the ones for the blade part, so the thickness at the shaft will be a multiple of the thickness at the blade. The reader is referred to Figure O.1 of Appendix O for a flowchart of the created numerical tool.

Discretisation: The actual stress calculations in the numerical code are performed by discretizing the box into a finite number of elements. In each of those elements or sections, the loads and stresses will be computed. The calculations will start at the tip and will advance towards the root, since the loads acting on the previous sections are relevant to calculate the stresses in the current section. The sections are the same as the ones used in the BEM-code for the aerodynamic design. The reason for this is that the loads resulting from the BEM-code are defined in those particular sections. For the sake of simplicity, the geometric parameters and loads are assumed to be constant for the entire section. To have a conservative design, the loads at the end of each section will be calculated, since they are highest at this location.

Idealisation of structure: After the discretization and the determination of each sections geometry, the elements are idealised using booms. This means that the webs and skins are replaced by lumped areas called booms. These areas consist of a contribution from both skins that are adjacent to each specific boom. The use of booms allows for easier calculations of cross sectional properties and stresses in each section. The boom areas can be determined by the following equations:

$$B_1 = \frac{t_D \cdot b}{6} \cdot \left(2 + \frac{\sigma_2}{\sigma_1}\right) \quad (\text{F.10})$$

$$B_2 = \frac{t_D \cdot b}{6} \cdot \left(2 + \frac{\sigma_1}{\sigma_2}\right) \quad (\text{F.11})$$

In these equations, σ_1 and σ_2 are the normal stresses at the booms, t_D is the thickness of the skin and b is the width of the skin between the booms. These equations are derived from equating the bending moments caused by normal stress on an actual skin and on an idealized skin [186]. In the numerical tool, the assumption was made that the stress ratio $\frac{\sigma_1}{\sigma_2}$ is equal to one, which is valid if the number of booms used is large enough (e.g. 50 booms on each side). With this assumption, it is possible to calculate the boom areas already before knowing the actual stresses acting on the cross section.

Loads and Stresses: After idealizing all the sections it is possible to obtain the normal forces, shear forces and bending moments acting on the section. A right-handed coordinate system located in the tip is used, with the y-axis pointing in blade direction towards the root and the x-axis pointing towards the blade leading edge. In this case, the normal force (in y-direction) consists of the relevant weight component and the centrifugal force. The shear forces in x-direction are caused by the weight component and the tangential force from the BEM-code, and the shear forces in z-direction are the result from the normal force coming from the BEM-code. The bending moments are only in x- and z-direction since there is no torque acting on the wind turbine blade.

When the loads on each section are defined, the normal stress and shear stress at each of the booms in every section is calculated. The normal stress is caused by the bending moments and normal forces that are exerted on the box. The shear stresses are the result of the shear forces explained above. To calculate the bending stress, the assumption was made that engineering bending theory is valid. The shear stresses in the sections are found by calculating the shear flow and dividing this by the thickness. In order to properly compare the stress values at all the booms with a specified failure stress, the Von Mises stress is computed at all the booms. This is done by combining the shear stress and normal stress in all section. Below several plots showing the stress distributions throughout the blade are given, in addition to the deflections under design loads. The plots for maximum stresses during the life time are shown, as well as the ones sustained during the maximum wind speed case of 75 m/s with blades fully pitched towards the wind.

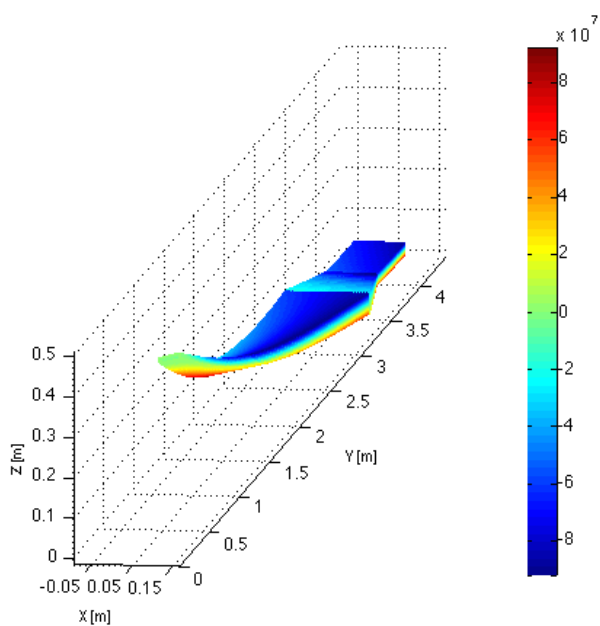


Figure F.9: Normal stress throughout the internal box (Pa), for the design loads considered. Blade twist and deflections are also included.

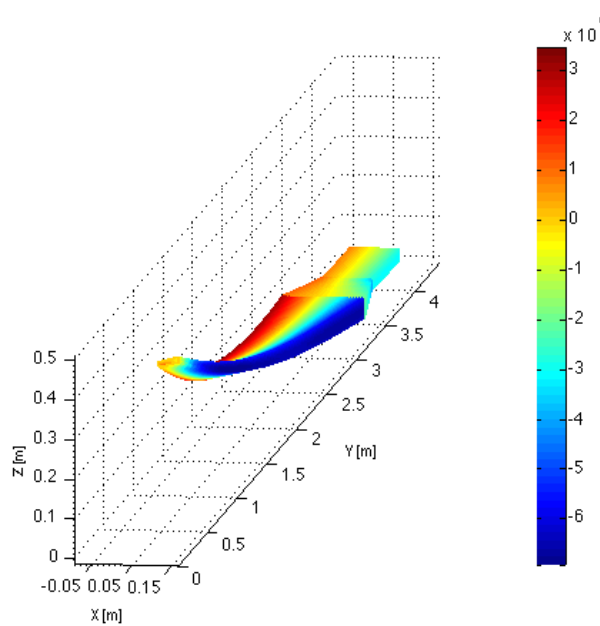


Figure F.10: Shear stress throughout the internal box (Pa), for the design loads considered. Blade twist and deflections are also included.

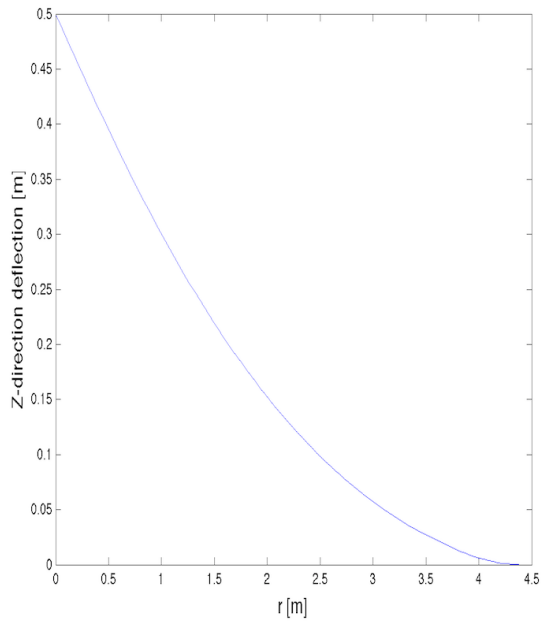


Figure F.11: Z-deflection of blade under design loads with safety factor 2. The zero-value on the x-axis corresponds with the blade tip.

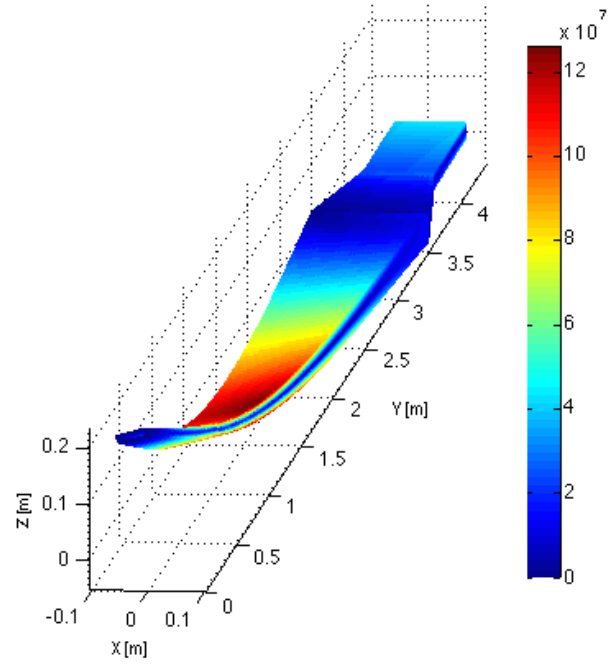


Figure F.12: Von Mises stress throughout the internal box (Pa), for the loads sustained at maximum wind speed of 75 m/s with blades pitched towards the wind. Blade twist and deflections are also included.

F.8 Deflection Calculations

To calculate the static deflections of the wind turbine box, which is modelled as a cantilever beam, a numerical algorithm is constructed. To calculate the deflections of a discretized cantilever beam exposed to an external loading, the bending stiffnesses around the two principle axes, the twist angles, the internal forces and moments have to be known at each discrete position. With this information, the deflection can be computed by considering the curvature of the beam and consequently the angular deformations. Equations F.12 and F.13 show the equations for calculating the curvatures about the principal axes. The decomposition of these curvatures in the z- and x-direction is given by Equations F.14 and F.15. Finally, the deflection angles and the deflections are determined by Equations F.16 to F.19.

$$\kappa_1 = \frac{M_1}{EI_1} \quad (\text{F.12})$$

$$\kappa_2 = \frac{M_2}{EI_2} \quad (\text{F.13})$$

$$\kappa_z = -\kappa_1 \sin(\beta + \nu) + \kappa_2 \cos(\beta + \nu) \quad (\text{F.14})$$

$$\kappa_x = \kappa_1 \cos(\beta + \nu) + \kappa_2 \sin(\beta + \nu) \quad (\text{F.15})$$

$$\frac{d\theta_x}{dy} = \kappa_x \quad (\text{F.16})$$

$$\frac{d\theta_z}{dy} = \kappa_z \quad (\text{F.17})$$

$$\frac{du_z}{dy} = -\theta_x \quad (\text{F.18})$$

$$\frac{du_x}{dy} = \theta_z \quad (\text{F.19})$$

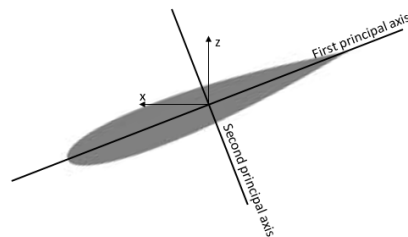


Figure F.13: Orientation of principal axes

F.9 Blade Materials

This appendix provides more information on the design decisions made when selecting the material for the blades. The first section provides additional information on the selection procedure for the internal box of the blades. The second section considers the effects of the cold temperatures on the chosen material.

F.10 Material Selection

In the table below, several properties are stated for the four considered materials for the internal blade box, Glass fiber-epoxy matrix, Carbon fiber-epoxy matrix, Aluminium 2024-T3 and Flax fiber-epoxy matrix, as well as a hybrid material consisting of 60% Carbon fibres and 40% Flax fibres.

Table F.2: Properties of the different materials considered [23], [24], [25], [26] [18]. The composites have a fiber volume fraction of 60%. The cost values were averaged from available ranges and can differ for each manufacturer. They should be considered as relative values for cost.

<i>Material</i>	<i>Density</i> [kg/m^3]	<i>E-modulus</i> [GPa]	<i>Ultimate Strength</i> [MPa]	<i>Specific Cost</i> [$$/kg$]
E-Glass fiber-epoxy matrix	2100	70	1600	25
Carbon fiber-epoxy matrix	1700	220	1700	75
Aluminium Alloy 2024-T3	2770	75	480	15
Flax fiber-epoxy matrix	1800	65	1500	50
Carbon/Flax fiber-epoxy	1740	158	1620	60

These properties are used together with the created numerical tools to support the material selection process. First the stress tool was used to determine the designs in terms of thickness distributions (dependent on ultimate strength). Then the deflections of the blades were checked (dependent on E-modulus) and the designs were altered so that they would meet the maximum tip deflection requirement of 50 cm. This was done for the Glass fibre, Carbon fibre, Flax fibre and Aluminium designs (the hybrid solutions is explained later).

The designs after the stress calculations had to be altered in such a way that the flexural stiffness became high enough to limit the deflection. Increasing the stiffness was first done by increasing the width and height of the blade box. However, this procedure was limited by the geometrical shape of the airfoils that were used. The decision was made to not alter the chosen airfoils, thus the remaining stiffness increase had to be achieved by increasing the material thickness. When this was done, it became clear that three out of four designs were infeasible, since the material thickness at the root was larger than the actual height of the blade box. The only remaining design was the one using carbon fibres, mainly due to the high E-modulus of the composite. Table F.3 shows the results of running the numerical tools with the properties of the different materials. Even though the Glass, Flax and Aluminium designs have infeasible thickness's, their cost is represented for the sake of completeness.

Although the Carbon fibre design satisfies the requirements and has a relatively low cost (even lower than Glass fibre, if that design was considered feasible), it still has a high environmental impact and requires a large amount of energy to be produced, as shown in table F.3. Studies in [18] and [27] have therefore analysed the feasibility of hybrid composite wind turbine blades, making use of a combination of Flax and Carbon fibres. In [27] the energy consumption to produce different types of blades was calculated and the conclusion was drawn that the hybrid Carbon/Flax solution provides the best compromise between performance, cost and environmental impact. The study in [18] showed that the ideal fiber solution, in terms of environmental sustainability is the fiber composition having the lowest resin demand and the lowest overall energy demand. The authors then concluded that a Carbon/Flax hybrid is indeed the most environmentally sustainable solution, and not e.g. a fully Flax blade. This is because the Flax fibers require a high resin content while resin still has a heavy environmental burden (this is also why the Flax composite has a similar density to the Carbon composite, while Flax fibres themselves have a much lower density). Thus by combining Carbon and Flax, the environmental disadvantages of both fiber types are balanced by both types' advantages. The 60 – 40 Carbon/Flax ratio was determined based on information from [18] showing that up until

40% of Flax fibres, the blade cost is almost not increased, as visualised in figure F.14. To have an even more environmentally sustainable design, the Flax fibre content can be increased up to 70%, however at the expense of high costs. According to the same study, the glass fibre solutions perform worst on the environmental aspect due to the environmentally burdensome production process of the fibres, and the low specific stiffness resulting in a higher end-mass.

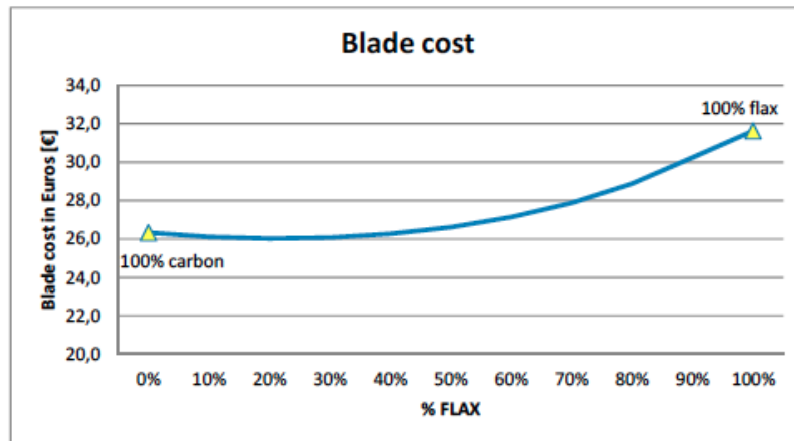


Figure F.14: Blade cost for small wind turbine blade with different Carbon/Flax ratio's. [18]

Table F.3: Resulting designs for the different materials. The energy consumption values result from analysing different types of blades as described by [27]. The values are to be considered relatively for comparison of the different materials. No values were available for Aluminium 2024-T3. The value for glass blade was based on comparisons described by [18]. The composites have a fiber volume fraction of 60%.

<i>Material</i>	<i>Weight [kg]</i>	<i>Cost [€]</i>	<i>Specific Production Energy Required [MJ/kg]</i>	<i>Production Energy Required [MJ]</i>
E-Glass fiber-epoxy matrix	24	607	115	2790
Carbon fiber-epoxy matrix	7	521	115	798
Aluminium Alloy 2024-T3	32	480	—	—
Flax fiber-epoxy matrix	21	1064	5	106
Carbon/Flax fiber-epoxy	9	560	67	625

Table F.3 indeed supports the idea that the combination of Carbon and Flax results in a suitable compromise between performance (weight), cost and environmental impact. It must be noted that to reduce the environmental impact of the blades even further, a bio-based epoxy will be used. According to [18] and [27] this has environmental advantages in every case of fiber type.

F.11 Temperature Effects

The Antarctic cold climate poses an additional challenge to any designer of structural components. Therefore, the effect of cold temperatures on the composite materials that were used to construct the blades are important to consider. As stated earlier, the main research focus of temperature effects on composites deals with the high temperature region. However, cryogenic (temperature below -150 degrees Celsius) effects on composites have been investigated, mainly for space applications.

According to [187], the shear strength of GFRP's and CFRP's increases at low temperatures. As a conclusion, the author stated that cryogenic temperatures do not deteriorate the mechanical properties of a composite but will in fact increase the shear strength. However, the author also highlighted the possible issue of micro-cracks. Since the

matrix and fibers have a different coefficient of thermal expansion (the matrix can have an order of magnitude higher), decreasing the temperature will lead to unequal contraction. This will then induce residual or internal stresses which can cause micro cracking. However, the research in [187] mainly focussed on changing temperatures and on the effect of so-called cryogenic cycles, which is not the case for the Signy Area (the temperatures are not cryogenic, nor do they change very fast).

More applicable research was done in [188], where the effect of micro-crack occurrence when the material is loaded at cold temperatures is investigated. The researchers concluded that the cryogenic temperatures in fact inhibited the formation of micro-cracks when the material is loaded in this cold temperatures (so the microcracks are now due to loading and not due to the cryogenic cycling). This is in line with the observations that the toughness decreases for decreasing temperature and the material becomes more brittle. Since toughness is an indicator for how well the material can absorb energy and since energy can be absorbed by creating micro-cracks, it makes sense that lower temperatures inhibit the formation of micro-cracks due to mechanical loading. Also stated in [188] is the fact that the temperature does not affect the ability of the matrix to transfer the applied loads to the fibers.

Based on the existing research on cryogenic temperature effects, the conclusions were drawn that the chosen composite materials would be able to cope with the cold environment at Signy Island. The temperatures that occur there are never as low as in cryogenic applications, nor do they vary quickly (as is the case for cryogenic cycles). The decreasing toughness was highlighted as the major concern for the chosen material, however the mechanical properties are not affected negatively and the blade was designed in such a way to limit the deflections and thus deformations.

G. Nacelle Design

In this appendix, additional information can be found about the nacelle. Section G.1 elaborates about the structural components and gives the results of the dimensions and acting stresses. The generator trade-off is given in Section G.2 and the selected brake is presented in Section G.3.

G.1 Bedplate & Shaft Design

As mentioned in the report, the bedplate is the main structural part of the nacelle and the shaft connects the rotor to the generator. The design process for both the bedplate and the shaft is similar since they both cope with the same forces. For the bedplate, it was determined to use two I-beams to transfer the loads into the tower. After a torque analysis it was found that the torque resistance of the two I-beams needed to be increased. A solution was found to connect the two I-beams in order to create a torsion box.

G.1.1 Design Process

In order to determine the optimal dimensions of these I-beams, a MATLAB program was written that calculates the Von Mises stresses in the whole I-beam for given dimensions. This program relies on the same kind of equations as the program of the tower optimisation. The reader is referred to Appendix H for elaboration of these structural equations. A shell was written around this program that applies a parameter sweep to find the optimal solution with respect to weight. The flow chart can be seen in Figure O.2 in Appendix O.

Optimisation Shell: The shell is the part where the parameter sweep takes place. It loads the whole program for different dimensions of the I-beam and it will converge to an optimal design. Together with the given time span for the project, it was determined to use such an algorithm.

Static Relations: Before the forces acting on each section can be calculated, first the general forces acting on the beam need to be determined. These forces comprise of the weights of both bearings and the forces and moment of the tower.

Moments of Inertia: This block calculates the moments of inertia and centroid locations of the sections.

Discretize: The layout of the I-beam needs to be converted into a FEM model. This block determines the location of all the points in the I-beam.

Loads on Section: In order to calculate the stresses acting on each section, first the loads acting on those sections need to be determined. Most of the loads are distributed loads, so only a certain percentage of all loads act on each section.

Von Mises Stress: Using a loop, the Von Mises stress of all sections are determined. The bending stress, normal stress and shear stress are combined in this calculation. A safety factor of 10 was used, in order to make sure the fatigue requirements are also met. This means that the maximum allowable stress is 62 MPa .

Column Buckling Check: Aside from the failure mode mentioned above, the I-beam can also fail on column buckling. Therefore it needs to be checked if the given solution can also withstand this failure.

G.1.2 Results I-beam

In Figure 11.3a in the report the results of the optimisation can be found. The width of the flanges are set to the width of a foot of the generator and brake, which is 50 mm . The shear force, normal force and moment diagrams are presented in this section.

After this optimisation a small research was performed to check if it was possible to reduce the height of the I-beam. A smaller I-beam results in less friction on the nacelle's shell, because the frontal area becomes smaller. As can be seen in Table G.1, the weight increase is quite acceptable until a height of 110 mm . At this height the I-beam is 1.1 kg heavier than the optimum dimensions. The total weight of the bedplate is 6.5 kg .

Table G.1: Optimisation results I-beam

h (mm)	$t1$ (mm)	$t2$ (mm)	$t3$ (mm)	W (N)	<i>Increase</i> (%)
230	1	1	1	12.88	0
200	1	2	1	13.63	5.8
180	3	1	1	14.77	15
150	2	3	2	17.44	35
140	2	2	2	18.54	44
130	3	2	2	19.64	52
120	3	2	2	21.52	67
110	3	3	3	24.04	87
100	4	4	3	28.36	120

Figure G.1 shows the Von Mises stresses acting on the bedplate. The shear and normal forces and bending moments result in the corresponding stresses. As mentioned, the Von Mises stresses is a combination of these stresses, so the shear and normal force diagrams and the bending moment diagrams can be used as explanation for the Von Mises diagram. This means that the slope and sign changes seen in Figure G.1 are similar to Figure 14.4.

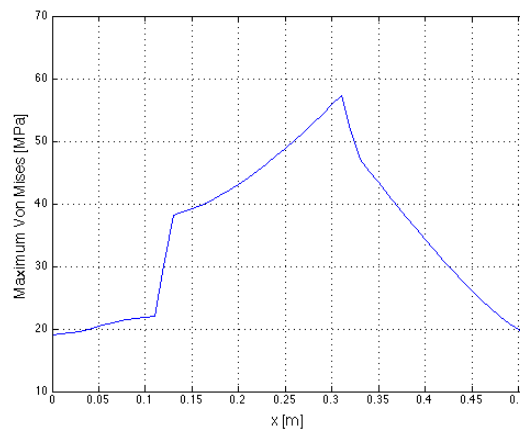


Figure G.1: Maximum Von Mises stress acting on each section

G.1.3 Torsion Box

For simplicity, it is assumed that the added material to create the torsion box is not contributing to the resistance of the bending and compression loads. Therefore, in this section there will only be a check to see if the torsion box can cope with the applied torsion. The extra shear stress due to the applied torsion appeared to be 11 MPa, using basic calculations. Adding this to the existing stresses, resulted in a maximum Von Mises stress of 75 MPa, including the safety factor. This is just higher than the allowable yield stress of the material (62 MPa). Because a safety factor was included in the calculations and the flanges of the I-beams were neglected, this solution is still deemed acceptable. See Figure G.2 for a general impression of the bedplate.



Figure G.2: Impression of the bedplate

G.1.4 Shaft

The shaft is designed using the same tool as for the bedplate. In Figure G.3 the maximum Von Mises stress on the shaft is displayed.

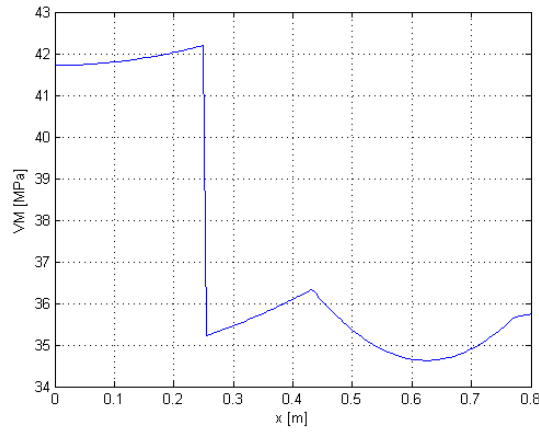


Figure G.3: Maximum Von Mises stress acting on the shaft

G.2 Generator Trade-off

For the wind turbine on Signy Island, four types of generators are considered, the constant speed (CS), the doubly-fed induction generator (DFIG), the variable speed direct drive (DD) and the variable speed with gear (GFC). All the generators should be operating optimally with a pitch controlled power control. The power level of the DFIG and GFC is larger than 1.5 MW and larger than 2 MW respectively. Since the wind turbine on Signy Island will be 17 kW, these generators are quickly eliminated. The CS is suitable for wind turbines with a power level smaller than 1.5 MW and the DD can be applied to all power levels. [19] The performance of the CS and the DD will be examined by means of a trade-off. The layout of the CS can be seen in Figure G.4a. Between the rotor and the generator, there is a gearbox and the gearbox connects the low-speed shaft to the a high speed shaft. Due to the gearbox, a standard (most commonly 1500 rpm) squirrel cage induction generator can be used. [189]

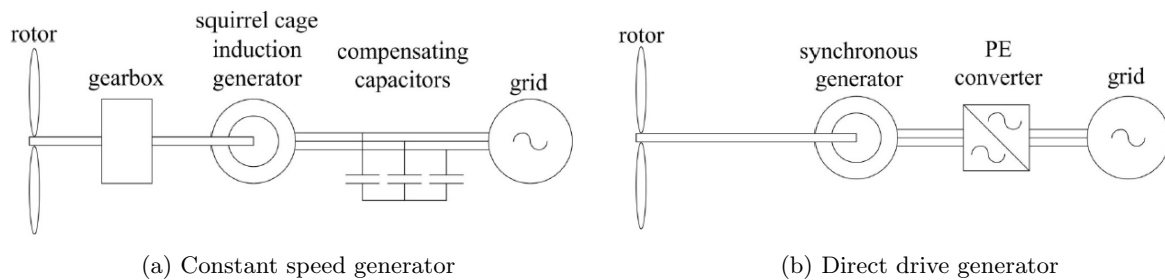


Figure G.4: Generators in trade-off [19]

The variable speed direct drive generator, see Figure G.4b, does not need a gearbox because the generator operates at low rotational speeds. It is, however, more difficult to select the right generator as the rated rpm of the generator needs to be equal to the rated rpm of the rotors. [189] The trade-off matrix between the CS and the DD is presented in Table G.2. Criteria that deliver a significant contribution to the performance are applied on the two types. When one type performs better on that criterion, a '+' is allocated. When the performance has only a slight difference, a '+/-' is allocated.

Table G.2: Trade-off CS and DD

<i>Criteria</i>	<i>CS</i>	<i>DD</i>
Cost/size/weight	+	-
Noise	-	+
Reliability	-	+
Complexity	+	+/-
Maintenance	-	+
Power output	+/-	+

Cost/size/weight: The DD is more expensive than the CS because it requires a specific design, while the CS has standard configurations. The DD generator has a larger diameter, however does not need a gearbox which lowers the

used space and weight. Most of the DD generators make use of permanent magnets and are therefore heavier.

Noise: Mechanical noise is generated mainly by the gearbox and generator. The gearbox has the largest contribution in the noise level, the vibration of the drive train, e.g. gearbox and shafts, are transmitted to supporting structure, which causes the noise. A CS generator causes significantly more noise because of the gearbox.

Reliability: The gearbox is considered the most troublesome part in modern wind turbines due to the high mechanical loads. [190] The CS requires a gearbox but the DD is not geared. Therefore, the DD is considered to have a much better performance on reliability than the CS. In a DD wind turbine the mechanical stresses are reduced and the gusts of wind can be absorbed. [191]

Complexity: Although the DD generator does not make use of a gearbox, it is considered more complex than the CS generator. This is mainly due to the fact that the generator will be operating at a variable rotational speed, thus requiring complex electronic equipment and control mechanisms.

Maintenance: Failure of a gearbox is likely to have a great impact on wind turbine availability owing to a long time needed to remove the failed gearbox from the nacelle for repair or replacement. [190] The maintenance is only scheduled once a year, so it is important that the generator operates optimally during the entire year. The CS requires a gearbox so a '-' is allocated and a '+' is allocated to the DD because of the absence of a gearbox.

Power output: The system efficiency is increased when using a DD variable speed generator in comparison with the CS generator. In the DD generator the turbine speed is adjusted as a function of wind speed to maximise the power output. [191] Moreover, the power quality of a variable wind speed generator is better and the operation at the maximum power point can be realised over a wide power range. Due to reduced torque pulsations the electrical power variations are reduced. [191]

For the Signy research station, both maintenance and reliability are important criteria. In low temperature climates gearboxes are the most troublesome part of the turbine. Additionally, less moving parts are required in the Antarctic climate [80]. Therefore, a DD generator is considered more suitable for the cold climate at Signy island.

G.3 Brake and Disk

The mass moment of inertia of the rotor-shaft structure is determined to be 250 kgm^2 , see section G.3.1. With a maximum angular rotation of 15 rad/s and a maximum braking time of 15 s , it is determined using equation G.1 that the braking torque on the shaft needs to be 250 Nm .

$$Q = I \cdot \alpha \quad (G.1) \qquad r_{disk} = \frac{250Nm}{2600N} = 0.096m \quad (G.2)$$

In Figure G.5 the chosen disk brake is showed. This figure also shows the needed disk diameter as a function of the braking torque.

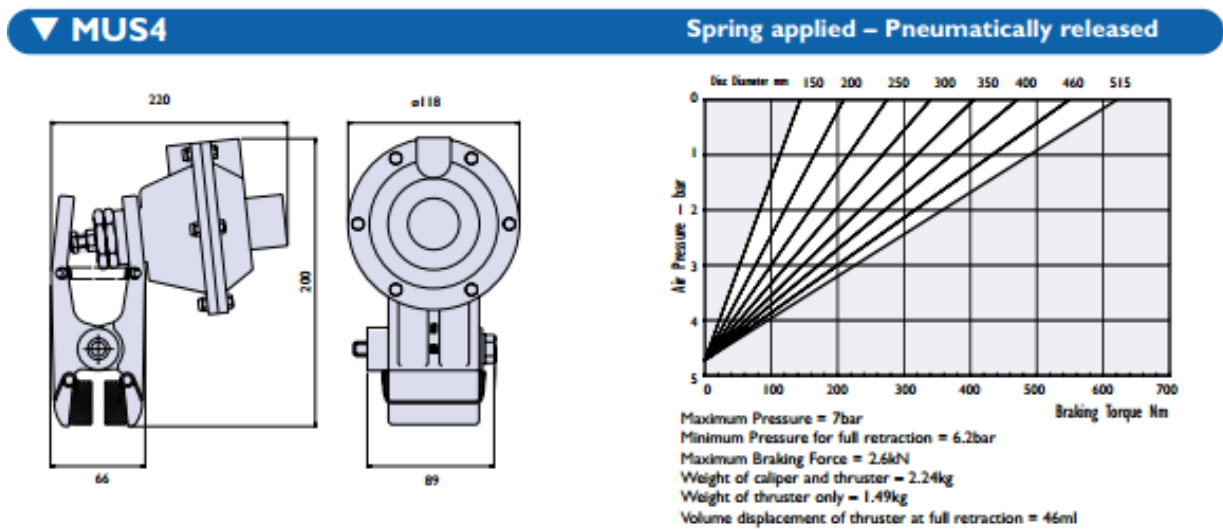


Figure G.5: Disk brake layout [20]

The disk and disk brake properties are showed in Table 11.1

Table G.3: Parameters generator

Parameter	Variables
Disk radius	0.096 <i>m</i>
Disk Thickness	8 <i>mm</i>
Weight Disk	1.56 <i>kg</i> [192]
Weight Braking system	3.8 <i>kg</i>

G.3.1 Mass Moment of Inertia

The mass moment of inertia (MMOI) was determined by making the assumption that the wing box of the blades result in the predominant MMOI and the MMOI of the aeroshell can be neglected. Also the wing box is assumed to be a straight box, instead of having taper. The MMOI of a solid cuboid can be calculated using equation G.3. The MMOI of the shaft can be calculated using equation G.4.

$$I = \frac{1}{12}m(w^2 + d^2) \quad (\text{G.3})$$

$$I = \frac{mL^2}{12} \quad (\text{G.4})$$

H. Tower and Foundation Sizing

The tower accounts for approximately 34% of the total costs [193]. The challenge is to reduce the tower costs while still having a tower that will perform conform to requirements. Within this section the various aspects considered during the tower design process will be expanded on.

H.1 Tower Structure Type

For the tower there are several options regarding the type of the structure. The lattice tower and the tubular tower are the most common tower structure types. The advantages and disadvantages of the lattice tower and tubular tower in the environment on Signy Island are presented in Table H.1.

Table H.1: Advantages and disadvantages of lattice tower and tubular tower

	<i>Lattice tower</i>	<i>Tubular tower</i>
Advantages	<ul style="list-style-type: none"> • Less material needed • Transportable in smaller parts 	<ul style="list-style-type: none"> • Cables are protected • Yaw omnidirectional stress sizing • More simple assembly • Widely used → reliable and less computational effort
Disadvantages	<ul style="list-style-type: none"> • Multiple structural connections → temperature sensitive regarding expansion • Cables are not covered • More complex/time consuming assembly • Wildlife may sit on the trusses → higher endangerment of wildlife and interference with environmental natural behaviour • Maintenance intensive due to many parts 	<ul style="list-style-type: none"> • More materials needed → higher mass and material costs

Due to the harsh environment on Signy Island, the cables for control, power transmission and storage need to be covered in order to not get damaged by both weather and wildlife. Thus if the lattice tower is opted for, the costs for cable insulation will increase significantly. Furthermore due to the many truss segments, the lattice tower would require intensive maintenance due to the connections being sensitive to temperature differences. This is because of possible differences in expansion and compression rates at the connection points, causing a higher likelihood of failure and longer maintenance check times. In addition, a lattice structure would create places for birds and other wildlife to sit on. This both increases the danger to the birds themselves and to the structure and interferes more with the environment, which should be minimised when trying to observe the behaviour of birds in their natural environment. Also it should be considered that a truss structure will require more parts to be connected together and thus require a longer assembly time during erection. This can be avoided with pre-assembly of the truss, however this would mean that the truss structure no longer has the advantage of being transportable in smaller parts. Moreover a tubular structure is widely used within the wind turbine community and as such there are more optimisation approaches and reference materials available. Finally, a tubular structure can more easily be analysed. This allows for more resources to become available for optimisation of the structure, and reduces the probability of unforeseen modes of failure occurring. Therefore, a tubular tower design has been selected and implemented in structural models. The interaction of wildlife with the lattice structure and possible cable damage were of particular concern when selecting between the two options.

H.2 Tower Material Type

In order for the tower to be correctly sized and constructed a material for the design must be selected. Steel is currently widely used as main material for the manufacturing of wind turbine towers. Of all wind turbine towers 90% are tubular steel towers [93] and an even higher percentage is made out of steel when considering only small wind turbines [94]. Another material used in the construction of wind turbine towers is pre-stressed concrete. However, such concrete tower constructions are only used for large scale wind turbines, since it allows for the possibility of installing turbines with diameters larger than 4.3 meters (transportation constraint) with lower construction cost than for a steel tower

[194]. For this reason the primary material considered for tower construction will be steel.

Steel alloys however can vary greatly in terms of material properties and thus specific alloying types must be considered in order to withstand the harsh environmental conditions in Antarctica. The first possible problem encountered when using steel is due to the wide temperature ranges that the material will be exposed to when implemented on Signy Island. The material properties of steel vary depending on operating temperatures. Figures H.1 and H.2 are used as an example showing common temperature variation characteristics of steel [21].

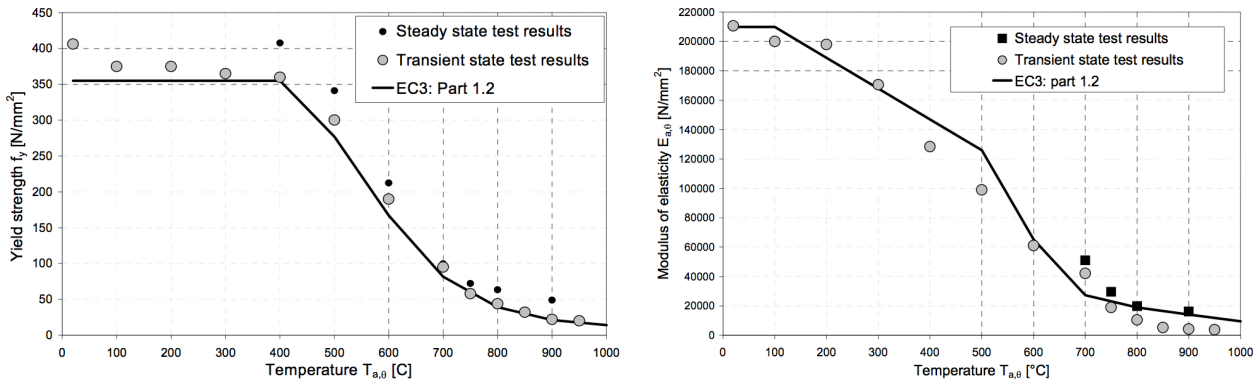


Figure H.1: Yield strength of structural steel S355 at temperatures 20 °C - 950 °C [21]

Figure H.2: Modulus of elasticity of structural steel S355 at temperatures 20 °C - 950 °C [21]

As can be seen from the example Figures H.1 and H.2, material property variance over the positive range of operating temperatures in the Antarctic location will not be an issue as the material properties only significantly change at high temperatures, which the structure will not be exposed to during usual operation. However, when considering the negative temperature range, the changing material properties start to become a problem. Many common steels become brittle near zero degrees Celsius and so can not be used for this application [195] [196] [28]. In order to combat such problems, specific low temperature grade alloys must be considered. Possible options are shown in Table H.2 [28].

Table H.2: Low temperature steel alloys properties [28]

<i>Designation</i>	<i>Lowest usual service temperature, °C</i>	<i>Minimum yield strength, MPa</i>	<i>Tensile strength, MPa</i>
A537 Gr. A	-60	345	483 - 620
A537 Gr. B	-60	414	551 - 690
A203 Gr. A	-60	255	448 - 531
A203 Gr. B	-60	276	482 - 586
A203 Gr. D	-101	255	448 - 531
A203 Gr. E	-101	276	482 - 586
A533 Gr. 1	-73	345	552 - 690
A533 Gr. 2	-73	482	620 - 793
A533 Gr. 3	-73	569	690 - 862
A543 Gr. 1	-107	586	724 - 862
A543 Gr. 2	-107	690	793 - 931

Furthermore, the recyclability of steel is extremely high. Currently steel recycling is near its theoretical maximum, dependent only on the amount of steel that previous generations implemented into the mineral cycle [96]. Moreover by using steel, which does not lose its material properties upon being recycled, 642 kWh of energy, equivalent to 1.8 barrels of oil can be saved with every ton of steel recycled [97].

In conclusion, there are many aspects to consider when selecting an adequate material for the construction of the tower. Temperature properties and recycling opportunities must be considered to select the optimum material. The low temperature steel group of which some are shown in Table H.2 are considered the group of materials from which a selection will be made. In addition to considering the temperature, and recyclability properties, the cost to strength ratios and fabrication costs should also be considered when making a trade-off. In terms of cost to strength ratios, steel is very high as indicated with the extensive use of the material in wind turbine towers globally [93] [94] [95]. Furthermore, due to the decades of steel in industrial use, production and manufacturing techniques are at a high level of maturity and so a reliable material to use for such a project [91][92]. The specific steel alloy selected was A537

grade A, giving a yield stress of the material is 345 MPa and has a Young's modulus of 200 GPa. This alloy was selected as it has an operating temperature of -60 °C, thus meeting the environmental needs of the Antarctic. A537 was selected over the other lower temperature alloys, as such alloys become more expensive and are generally only used for high pressure applications [28]. A537 was selected over A203 as A537 has a higher strength to weight ratio given that the alloys have equal densities. Furthermore, it allows for a tower of smaller radius to be designed and as such reduces possible tower shadow effects. A537 Grade A was selected over A537 Grade B as the top of the tower was already considered small enough to meet requirements and thus the extra costs incurred for higher strength material would not add structural benefits due to minimum radius restrictions. The raw material costs of low temperature carbon steel are considered to be 768 US dollars per tonne (currently 564 euros), given by averaging world carbon steel commodity prices for structural sections and beams over 12 months [197].

H.3 Forces, Moments and Load Cases

To structurally analyse the tower, the forces and moments acting on the tower need to be known. Figure H.3 shows the drag forces due to the rotor, the nacelle, the tower, the gravity forces due to the rotor, the nacelle and the tower, and the thrust force due to the rotor spin.

The various forces can be calculated using the following Equations H.1, H.2, H.3 and H.4.

$$Thrust = 0.5 \cdot \rho \cdot V^2 \cdot C_T \cdot A_{Disk} \quad (H.1)$$

$$Drag_{Nacelle} = 0.5 \cdot \rho \cdot V^2 \cdot C_{D_{Nacelle}} \cdot A_{FrontalNacelle} \quad (H.2)$$

$$Drag_{Tower} = 0.5 \cdot \rho \cdot V^2 \cdot C_{D_{Tower}} \cdot A_{FrontalTower} \quad (H.3)$$

$$dDrag_{Blades} = 0.5 \cdot \rho \cdot V^2 \cdot C_{D_{Blade}} \cdot dA \cdot N \quad (H.4)$$

With C_T , $C_{D_{Nacelle}}$ and $C_{D_{Blade}}$ being the thrust coefficient, the nacelle drag coefficient and the blade drag coefficients, respectively. Furthermore V , ρ and N represent the local velocity, local air density and the number of blades, respectively. In addition A_{Disk} , $A_{FrontalNacelle}$, $A_{FrontalTower}$ and dA are the representative disk/swept area of the blades, the frontal nacelle area, the frontal tower area and the blade area, respectively. All units are in equivalent SI units.

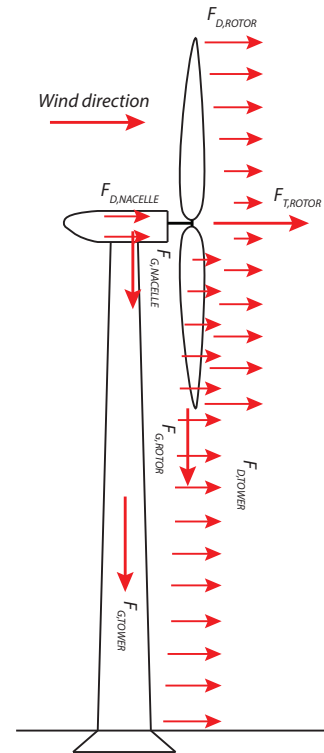


Figure H.3: Forces acting on wind turbine

The equations above show linear behaviour regarding all parameters bearing the local wind speed, where the force is proportional to the local velocity squared. When considering the drag force due to the wind on the rotor along the span of the blade, this non-linear behaviour can be observed as the relative airflow at the tip is higher than the speed of the airflow at the hub due to the rotations of the blades. Furthermore it can be seen that the drag force on the tower is reliant on the frontal area of the tower and thus will subsequently change along the tower if the given design has varying diameter along the height. The various magnitude of the moments acting on the tower segments depend on the given segment being analysed and on the initiating force. The various moments that need to be considered are listed below and are defined as positive in the clockwise direction.

- Moment due to nacelle weight
- Moment due to nacelle drag
- Moment due to rotor weight
- Moment due to rotor drag
- Moment due to thrust force
- Moment due to tower drag

The combination of nacelle and rotor center of gravity, if placed in line with the center of the given tower segments would result in the minimisation of the moment at the root of the tower due to the moment arm being reduced to zero and thus not contributing to increased stress. Furthermore the moment caused by the nacelle and rotor combined can be used to counteract the moment caused by the thrust, if the nacelle assembly's center of gravity is to the left of the tower (towards the rotor). However this counteracting moment is only of benefit when thrust and drag are also acting on the tower, else the tower structure must compensate.

The various forces and moments are of great importance to the tower and foundation sizing. The overturning moment caused by the forces are of great significance for both the foundation design and play a major role in the bending stresses introduced into the tower. The weight of the assembly is also of significance when considering static compressive stresses and buckling criteria of the tower. Furthermore the tower characteristics derived from the above stresses will effect the vibrational behaviour of the tower assembly and thus must also be considered for fatigue loading.

The various load cases, failure modes and how these loads are used to obtain the sizing of the tower will be addressed within the structural methods section of this chapter, with the reader being advised to refer back to this section and Figure H.3 for visualisation of the forces on the tower for the two cases.

H.4 Load Cases

The discretised MATLAB tower model was analysed for two load cases in order to account for the most extreme boundary conditions of design. These two cases were in themselves the extreme boundary conditions for their given modes of operation, pre-cut-out and post-cut-out, as explained below.

- **Pre-Cut-Out:** The most extreme condition for the pre-cut-out wind speed range is when the moment caused by the thrust acting on the tower and the moment due to the drag of the nacelle is maximum. Due to the fact that the thrust of the rotor changes with varying wind speed and also the drag on the nacelle changes non-linearly across wind speeds, an iteration of all wind speeds is conducted in order to find the most critical design conditions where the combination of these moments are maximum. The thrust, tower and the nacelle drag contribute to the moment through their respective moment arms relative to tower segments. The initial shear force V_0 relative to the first tower segment is the summation of the thrust and nacelle drag for this load case.
- **Post-Cut-Out:** The most extreme condition for post-cut-out wind range is when the turbine rotor is stationary, thus no thrust, combined with the drag on the rotor, nacelle and tower at survival wind speed of the wind turbine system. The drag of the various components contribute to the moment through their respective moment arms relative to the tower segments. The initial shear force V_0 relative to the first tower segment is the summation of the blade and nacelle drag for this load case.

It should be noted that the moments caused by the weights of the various components such as the nacelle and blades are considered and are the same for both load cases. With the various moments being defined within the force and moment section of this report.

H.5 Bending Stress

The first failure mode considered by the MATLAB model analysis is failure by bending stress. The program uses various iterations in order to come to a final distribution for both the radius and thickness of the tower with the method explained below.

Firstly, the tower is split up into a number of n segments along the tower height. For each segment the moments and shear forces acting upon the segment are calculated, with the details of this calculation described later within this section. Once the moments acting upon the various segments have been calculated the required thickness of each section is derived. This is done by iterating through various sizes of diameters and calculating the required thickness in order to keep the stress in the segment equal to the maximum allowable stress, including a safety factor of 3. The program then selects the combination of radius and thickness that minimises weight, with the constraints of minimum thickness and minimum and maximum diameter size. It should be noted that when the required thickness for a given diameter is lower than the minimum thickness allowable, the program assigns the diameter for the minimum thickness available. The method used for the final model assesses the moments at each location using Equation H.5 to H.8 and Figure H.4.

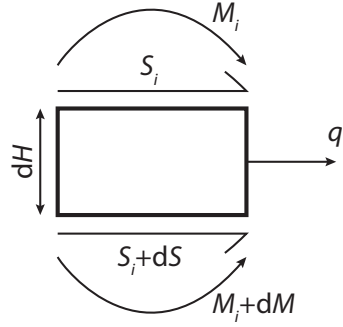


Figure H.4: Forces and moments on a tower segment

$$dS = q_i \quad (\text{H.5})$$

$$dM = S_{i-1} \cdot dH + dS \cdot \left(\frac{dH}{2}\right) \quad (\text{H.6})$$

$$S_i = S_{i-1} + dS \quad (\text{H.7})$$

$$M_i = M_{i-1} + dM \quad (\text{H.8})$$

With the initial M_0 and S_0 calculated based on the two load cases described above and q representing the drag force on the element itself. Furthermore M_i and S_i are seen as the moments and shear forces acting on the given segment respectively.

As can be seen in Figure H.4, the drag of each segment is modelled as a point load acting at the center of the segment. As the drag of each segment contributes to the moment values at the other segments a number of iterations must be conducted in order for the model to converge to a final solution. This is done by first setting the drag of the tower to zero and calculating the given radii and thicknesses for the tower. These radii are then used to calculate the drag q on each segment. The model then recalculates the necessary radii and thicknesses when such drag forces are present, this in turn leads to the drag being recalculated for the new radii. This process continually loops within the program until the change in radii of the sections is found to be less than 5%, and thus seen to have converged. The necessary thickness for a given radius of a segment is calculated with Equations H.9 and H.10. It should be noted that in the following equations the thin walled assumptions have been used to simplify the moment of inertia, and thus higher order terms of thickness are neglected.

$$I = \frac{M \cdot R}{\sigma} \quad (\text{H.9})$$

$$t = \frac{I}{\pi \cdot R^3} \quad (\text{H.10})$$

H.6 Buckling Load

Once the bending stress has been calculated and the tower thicknesses and radius have been defined using the weight optimisation approach described above, the structure must also be checked for the possibility of failure through buckling. This is done by calculating the necessary thickness the tower must have in order to buckle under the weight of the structure when considered as a point load, comprising of the nacelle and rotor assembly, and including a safety margin of 1.5. If the required thickness is smaller than the sized thicknesses derived from bending stress calculations, then the structure is seen to be sufficient for buckling, with no further actions required for this failure mode. However if the required thickness needed to prevent buckling is larger than the derived thickness for bending stress, then an iteration of the process is conducted. This iteration sets the minimum required thickness in the bending stress model equal to the required thickness for buckling, with the model being re-run in order to optimise the structure for this new thickness. Equation H.11 is used for determining the required thickness for buckling.

$$t_{buckle} = \frac{W_{buckle} \cdot H^2}{n^2 \cdot \pi^2 \cdot E \cdot R^3} \quad (\text{H.11})$$

With H , W_{buckle} , E and R , being the height of the tower, the weight of the rotor-nacelle assembly with safety factor, Young's modulus and tower diameter respectively. Furthermore with n being the bending mode and set to one when considering a simply supported beam. It should be noted that the calculations give an conservative value for the required thicknesses. This is because the beam model implemented, takes the smallest diameter segment of the tower tip and assumes that the tower is this size through the entire height. Thus the actual thickness for which the tower structure would buckle under the given loads would be lower than those calculated using the above equation when considering a tower which gets wider from top to bottom.

H.7 Static Compressive Stress

Once both bending and buckling have been considered and the tower has gone through possible design iterations to converge to an optimised distribution, a static compressive stress (SCS) test calculation is conducted as a simple check on the validity of the results. The static compressive stress is then compared to the maximum allowable stress including a safety factor. If the SCS calculated is lower than the maximum allowable stress then the design can be checked for maximum deflections as described in the subsequent section, else the design calculations must be checked to find the source of the error and new iterations for the segment dimensions must be conducted until the SCS test also gives satisfactory results. The SCS is considered at two points for each load case. The first point is at the top of the tower where the radius is minimum and the weight is equal to the weight of the rotor and nacelle assembly weight. The second point is at the bottom of the tower where the radius is maximum but the weight includes the weight of the tower itself in addition to the weight of the rotor-nacelle assembly. The resulting stresses were all found to be below the maximum allowable stress including safety factor and are shown in the table below. Thus sizing is seen to be much more greatly effected by the stress caused by the bending moments rather than the static compressive stress, as the bending stress are order of magnitudes higher. The SCS is calculated using the equation of normal stress, with stress equal to force divided by area on which the force is acting upon.

H.8 Tower Deflection

Within this section the two methods used for calculating tower deflection are described, namely simplified beam theory and Castigliano's method respectively.

H.8.1 Beam Theory

The maximum tower deflection is of importance for the rotor performance. The airflow around the rotor changes with increasing deflection and leads to a non-optimally performing rotor. Therefore, there is a constraint on maximum tower deflection. The maximum deflection occurs at the tip of the tower and is computed with Equation H.12 [186]. The deflection is analysed for both the cases where the rotor is spinning and not spinning, since the deflection is also important for fatigue characteristics of the tower. M is the moment contribution in Nm from the nacelle drag, tower drag, nacelle weight, tower weight, and thrust for the spinning rotor and rotor drag for the non-spinning rotor. H is the height of the tower at the given point in m , E is the Young's Modulus of the tower material in Pa and I is the second moment of area of the tower's cross-section in m^4 . It should be noted that the mean thickness and mean radius is used to calculate the equivalent moment of inertia needed for the equation below.

$$\delta = \frac{MH^2}{2EI} \quad (\text{H.12})$$

H.8.2 Castigliano Method

The second method used to determine the deflection of the tower is Castigliano's Second Theorem. Castigliano's Second Theorem calculates the deflection by taking the partial derivative of the total internal energy of the tower with respect to the forces applied [198]. The deflection is determined for two cases with this method: the operational condition with the thrust of the rotor and the extreme drag case after cut-out, the latter being the most influential case. The beam is modelled as a linear tapered circular cantilevered beam with only one point force acting on the tip of the beam. The point force represents for each situation the load cases mentioned above. Equation H.13 represents the internal energy U of the tower and Equation H.14 is used to determine the deflection. The simplified beam model is presented in Figure H.5. In the equations v is the deflection in m , F is the force applied in N , E is the Young's modulus in Pa , α is the changing taper gradient, D_t is the top diameter in m , t is the thickness of the tower in m and x represent the position on the tower in m .

$$U = \int_0^L \frac{M^2}{2EI} dx \quad (\text{H.13})$$

$$\Delta v = \frac{\delta U}{\delta F} = \frac{F}{E} \int_0^L \frac{x^2}{\left(\pi \cdot \left(\frac{\alpha x + D_t}{2}\right) \cdot t\right)} dx \quad (\text{H.14})$$

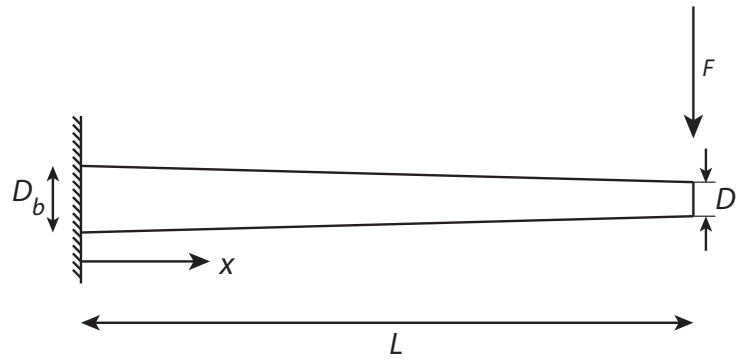


Figure H.5: Simplified model of tower for deflection analysis with Castigliano's Theorem

H.9 Geotechnical Research

The type of foundation design is highly dependent on the ground at the site of the wind turbine. The ground characteristics at the Signy Research Station are researched. The bottom mainly consists of the metamorphic rock amphibolites. [34][35] Amphibolite has a high hardness and is therefore suitable as structural foundation [39]. The stratigraphy, composition, strength, compressibility and stiffness of the ground are properties that need to be researched to come up with a suitable design for a specific bottom. Besides an analysis of the rock type bottom, it needs to be ensured that no caves are present beneath the wind turbine site. When the rooftops of such caves collapse, the layers on top of the cave will slowly collapse over time and this retrogressive process will eventually lead to failing of the foundation and thus of the entire wind turbine system [98]. The amphibolite rock bottom is very compact. There is a change that a cavity beneath the wind turbine site exists. Measurement systems exist to detect cavities beneath a surface. Research on the designated site for the wind turbine system can be done before placing the wind turbines. However, since the amphibolite rock bottom is so compact and strong, it is very unlikely for the rock bottom to collapse.

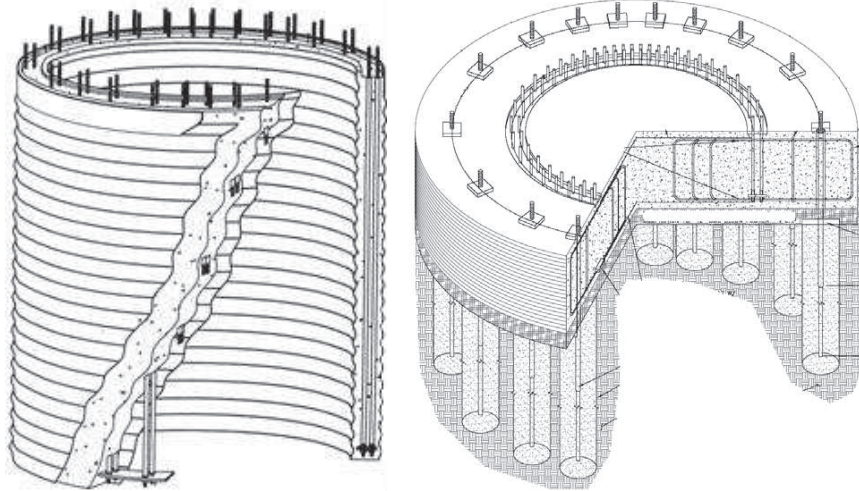
H.10 Rock Foundation Types

There are two types of foundations that are suitable in a bedrock bottom. These types are the rock socket or tensionless pier foundation and the rock anchor foundation. Both foundations require a shallow strong bedrock and rely on the strength of the rock. The tower connection to the foundation for both the rock socket and the rock anchor foundation is an anchor bolt cage [98]. The principle of the rock socket foundation is shown in Figure H.6a and of the rock anchor foundation in Figure H.6b.

The rock socket foundation is basically a concrete tower extension beneath the ground's surface. This foundation type is hard to implement [199]. A deep hole has to be excavated to input a cylindrical metal can, a cage of piers and an inner cylindrical metal can. This is not an environmentally friendly option, since a large volume of the bedrock bottom has to be removed for this foundation. Furthermore, it requires a large volume of concrete. The rock anchor foundation is basically multiple piles anchored into the rock bottom with a concrete cap on top of the anchors. The gap, filled with weaker soil, between anchors and cap allows post-tensioning and retensioning of the anchors. The soil may shift during the year because of the extreme seasonal changes on Signy Island, such as changes in water content and temperature, rain- and snowfall, seasonal freeze and thaw cycles. Under normal conditions the rock anchor foundation needs tensioning of the piers annually [100]. Maintenance on the foundation on Signy Island will be more extensive and more frequent due to the extreme environment. However, since the foundation has to deal with relatively small turbines and its reliability due to its worldwide implementation, the rock anchor foundation type will be used as foundation for the wind energy system on Signy Island.

H.11 Rock Foundation Sizing

The optimal rock anchor length, diameter and number of anchors are determined with through a trial and error process with Equations H.15 [105], H.16 [102] and H.17, based on rock mechanics. l_a is the anchor length in m , A_b the cross-sectional area of the anchor in mm^2 , σ_y the specified yield strength of the non-pre-stressed reinforcement of $500 MPa$ [103], σ_{uc} the specified compressive strength of the grout of $20 MPa$ [106], D the borehole diameter of $75 cm$, L_b the length of the grouted anchor bond of half the anchor length in m , τ_{ult} the ultimate grout bond strength of $15 MPa$ [106] and W_{sys} the weight of the entire system of $12.24 kN$.



(a) Rock socket foundation [101]

(b) Rock anchor foundation [9]

Figure H.6: Rock foundation types

$$l_d = 2 \frac{0.019 A_b \sigma_y}{\sqrt{\sigma_{uc}}} \quad (\text{H.15})$$

$$Q_a = \frac{1}{2} \pi D L_b \tau_{ult} \quad (\text{H.16})$$

$$N = \frac{W_{sys}}{Q_a} \quad (\text{H.17})$$

I. Vibrations

In order to check the possible resonant conditions, the natural frequencies of the structure are plotted with the excitation frequencies. This is done in a Campbell diagram. The lead-lag, flap and tower natural frequencies are checked for resonant conditions. Within this appendix the calculations used to approximate the natural frequencies of the system are found.

Flap & Lead-lag

The lead-lag and flap natural frequencies change when the rotor operates at different operational speeds. They are calculated using Equation I.1:

$$\omega_{n,rotating}^2 = \omega_{n,non-rotating}^2 + K_n \Omega^2 \quad (I.1)$$

Where $\omega_{n,rotating}$ is the natural frequency when the rotor is rotating, $\omega_{n,non-rotating}$ is the non rotating natural frequency, K_n is the Southwell coefficient (which is typically between 1.17 and 1.25) and Ω is the rotational speed. For both the lead-lag and flap frequencies, a Southwell coefficient of 1.22 is chosen.

The natural frequencies for the flap and lead-lag are calculated by taking an initial load, calculating the corresponding deflection, determining the natural frequency and using that natural frequency to calculate the new load. This procedure is repeated a few times until the frequency stays constant. The non-rotational natural frequencies can be seen in Table I.2

Drive Train

The drive train is modelled as a two-disc torsional system, with one disk representing the rotor and the other representing the generator. The natural frequency of the drive-train is calculated using Equation I.2:

$$\omega_n = \sqrt{\frac{K_t(I_{rot} + I_{gen})}{I_{rot}I_{gen}}} \quad (I.2)$$

Where K_t is the stiffness of the shaft, I_{rot} is the rotor mass moment of inertia and I_{gen} is the generator mass moment of inertia. The stiffness of the shaft can be calculated using Equation I.3:

$$K_t = \frac{GJ}{l} \quad (I.3)$$

Where G is the shear modulus of the A537 Class 1 (Grade A) steel alloy, J is the second moment of area of the shaft and l is the length of the shaft. The G and l are 80 GPa and 0.8 m , respectively. The J can be obtained using Equation I.4:

$$J = \frac{\pi D^4}{32} \quad (I.4)$$

Where D is the diameter of the shaft and is equal to 0.067 m . Now inserting all the values in Equation I.3 results in a K_t of $2,428$.

The moment of inertia of the rotor was calculated in Section G.3.1 and is equal to $250 \text{ kg} \cdot \text{m}^2$. The moment of inertia of the generator (modelled as a disk) can be calculated using Equation I.5:

$$I = \frac{mR^2}{2} \quad (I.5)$$

Where m is the mass of the generator and R is the radius of the generator these are 400 kg and 0.275 m , respectively. Filling in these values, a mass moment of inertia for the generator of $60.5 \text{ kg} \cdot \text{m}^2$ is obtained.

All values are now known to compute the natural frequency of the drive train and it is found to be 9.17 rad/s .

Tower

The tower is simplified to a beam with a mass at the top. This mass is the nacelle and rotor mass plus 22.7% of the tower mass [200],[201],[202],[203]. The addition of the 22.7% of the tower mass is an approximation since the tower is modelled as a mass-spring system. The natural frequency of the tower is computed with Equation I.6 [201],[202],[203]:

$$\omega_{n,tower} = 1.744 \sqrt{\frac{EI}{(m_{rotor+nacelle} + 0.227m_{tower})H^3}} \quad (I.6)$$

Where E is the Young's modulus of 200 GPa, I the second moment of area of $8.15 \cdot 10^{-4} m^4$ at the bottom, $1.11 \cdot 10^{-5} m^4$ at the top and a mean value of $2.61 \cdot 10^{-4} m^4$, $m_{rotor+nacelle}$ the rotor and nacelle mass of 509.7 kg, m_{tower} the tower mass of 738.5 kg and H the tower height of 8.8 m. Table I.1 presents the natural frequencies for the three cases. Normally, for a more accurate result, the spring stiffness of the tower is determined through experiments.

Table I.1: Tower natural frequency

Output	Unit	Value
$\omega_{n,bottom}$	rad/s	32.8
$\omega_{n,mean}$	rad/s	17.8
$\omega_{n,top}$	rad/s	3.8

The different natural frequencies can be found in Table I.2.

Table I.2: Natural frequencies

Parameter	ω_n [rad/s]
Flap (non-rotating)	5.13
Lead-lag (non-rotating)	15.04
Drive train	9.17
Tower	17.8

The final input for the Campbell diagram is the operational range. The minimum rotational speed is determined from the cut-in wind speed and the maximum is fixed by the noise constraint. The operational range will be between 5.6 and 15 rad/s. The Campbell diagram can be seen in Figure I.1a

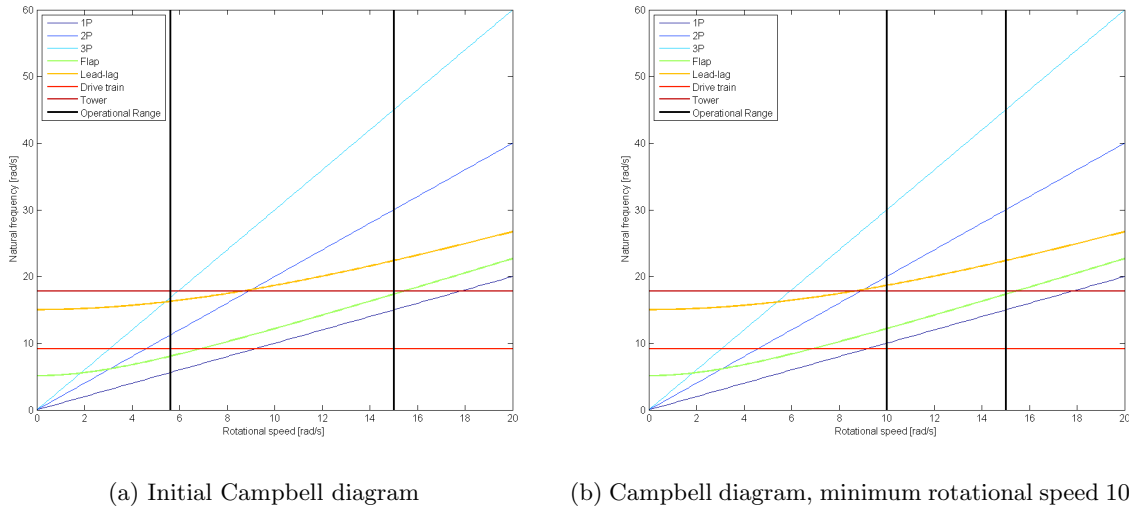


Figure I.1: Campbell diagram

From the initial Campbell diagram it can be concluded that several resonant conditions exist. Almost every deflection, except for the flap-wise, will be excited in the operational range of the turbine. This is mainly due to the large operational range of the turbine. It can be seen that if the minimum operational speed is limited to 10 rad/s, no excitation causes resonance. If the turbine is kept at a constant rotational speed of 10 rad/s from the cut-in of 3 m/s till 5.5 m/s (which resembles the minimum wind speed for which the optimum tip speed ratio of 8.25 can be maintained), the AEP goes down with only 0.2 %.

J. Verification and Validation

In this chapter the tables with the comparison of the numerical and analytical tools can be found. The chapter is subdivided into the results of the blade, nacelle and tower.

J.1 Rotor Blades

Table J.1 and Table J.2 show the verification of the BEM-code and the structural code, respectively.

Table J.1: Verification data between the developed and provided BEM code

$V0$ [m/s]		λ [-]		Q [Nm]		P [W]	
Developed	Provided	Developed	Provided	Developed	Provided	Developed	Provided
4.5	4.5	9.63	9.63	13.77	13.3	15.53	15
5	5	8.67	8.67	16.07	15.4	26.24	25
5.5	5.5	7.88	7.88	18.23	17.6	37.98	38
6	6	7.22	7.22	20.2	19.8	49.54	51
<i>Differences[-]</i>							
0.0%		0.0%		3.3%		1.3%	

Table J.2: Comparison numerical and analytical results structural blade analysis

<i>Variables</i>	<i>Numerical</i>	<i>Analytical</i>	<i>Differences</i>
Blade chord [m]	0.2	0.2	0.0%
A [m^2]	2.38E-04	2.34E-04	1.8%
I_{xx} [m^4]	2.07E-08	1.91E-08	8.3%
I_{zz} [m^4]	1.78E-07	1.68E-07	6.0%
I_{xz} [m^4]	-4.37E-24	0	0.0%
S_z [N]	322.7605	322.7267	0.1%
S_x [N]	104.868	104.6831	0.2%
S_y [N]	0	0	0.0%
M_z [Nm]	80.5117	80.6897	0.2%
M_x [Nm]	-241.8404	-241.844	0.0%
M_y [Nm]	-12.9091	-12.9091	0.0%
σ [Pa]	-1.50E+08	-1.50E+08	0.0%
q [N/m]	-1.492E+04	-1.4895+04	0.2%
u_z [cm]	30.68	30.58	0.003
<i>System Test</i>			
σ [Pa]	-9.8958E+07	-1.1456E+08	7.6%
q [N/m]	-1.49E+04	-1.57E+04	5.2%

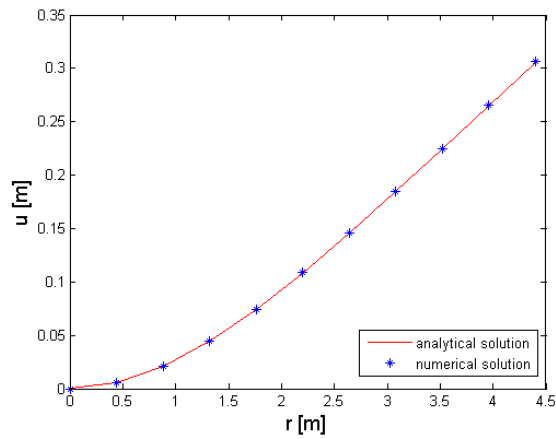


Figure J.1: Deflection of a beam with constant stiffness and a uniform loading

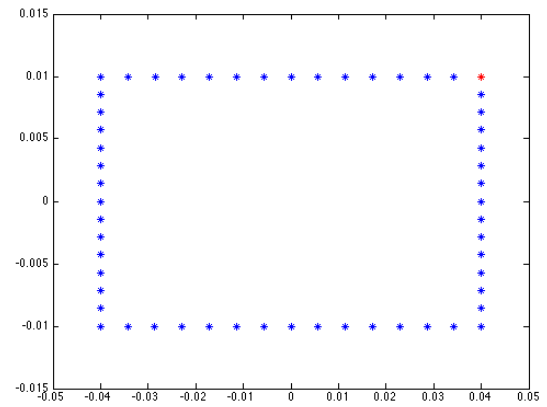


Figure J.2: Visual representation of the booms of the cross-section

J.2 Nacelle

Table J.3: Comparison numerical and analytical results structural bedplate analysis

<i>Variables</i>	<i>Numerical</i>	<i>Analytical</i>	<i>Differences</i>
Compressive force acting on tower	2498 <i>N</i>	2498 <i>N</i>	0.000%
Shear force acting on tower	23.6 <i>kN</i>	23.6 <i>kN</i>	0.000%
Moment acting on tower	107.4 <i>N</i>	107.4 <i>kN</i>	0.000%
Moment of Inertia	1.189E-6 <i>m</i> ⁴	1.240E-6 <i>m</i> ⁴	4.113%
Von Mises Stress section 27 center	32.0 <i>MPa</i>	32.0 <i>MPa</i>	0.000%
Weight	93.4 <i>N</i>	94.7 <i>N</i>	1.267%
Discretisation points	2496	2496	0.000%
Normal force on section 27	6.5 <i>kN</i>	6.5 <i>kN</i>	0.000%
Shear force on section 27	450 <i>N</i>	450 <i>N</i>	0.000%
Moment on section 27	15.6 <i>Nm</i>	15.6 <i>Nm</i>	0.000%

J.3 Tower

Table J.4: Comparison numerical and analytical results tower analysis

<i>Variables</i>	<i>Numerical</i>	<i>Analytical</i>	<i>Differences</i>
Drag on Tower	1.383E+03 <i>N</i>	1.383E+03 <i>N</i>	0.000%
Buckling thickness	1.193E-04 <i>m</i>	1.196E-04 <i>m</i>	0.250%
Deflection	4.400E-02 <i>m</i>	4.600E-02 <i>m</i>	4.550%
Static Compressive Stress	2.487E+01 <i>Pa</i>	2.487E+01 <i>Pa</i>	0.000%
Natural Frequency	8.570 <i>rad/s</i>	8.570 <i>rad/s</i>	0.000%

K. Energy Supply System

This section provides a more detailed analysis on the design of the various sub-component groups within the energy supply system including the relevant electrical load strategy required for the system.

K.1 Battery Type Options

There are various types of batteries that can be used for the system must be considered. Some of the common battery options are shown below:

Table K.1: Battery properties [29]

<i>Battery Type</i>	<i>Cost \$ per Wh</i>	<i>Wh/kg</i>	<i>J/kg</i>	<i>Wh/liter</i>
Lead-acid	\$0.17	41	146,000	100
Alkaline long-life	\$0.19	110	400,000	320
Carbon-zinc	\$0.31	36	130,000	92
NiMH	\$0.99	95	340,000	300
NiCad	\$1.50	39	140,000	140
Lithium-ion	\$0.47	128	460,000	230
Li-SOCl	\$1.16	700	2,000,000	1100

Other than the energy information of batteries shown in the above table, it is also of vital importance to consider the standard temperature operation range of such batteries due to the extreme conditions found in the Antarctic. In general batteries tend to increase their internal resistance and thus decrease their capacity in a linear manner at colder than operating temperatures [204]. The standard temperature problems of such batteries are given in below [204]:

- **Lithium-based:** batteries tend to perform better in hotter temperatures than in colder ones due to the internal resistance increase effect. The dry solid polymer types require operating temperatures of 60-100 °C, however Li-polymer batteries use a moist electrolyte for conductivity and can operate at lower temperatures. At -20 °C, most Lithium based batteries stop functioning.
- **Nickel-based:** batteries degrade very quickly at higher temperatures, able to lose 20 percent of operating capacity with a ten degree increase in temperature. In addition operating at high temperatures decrease the operational life of such batteries. At -20 °C, most nickel based batteries stop functioning. NiCd batteries can operate at -40 °C, however this is at very low discharge rate.
- **Lead-based:** batteries have the danger of the electrolyte freezing at low temperatures, possibly cracking the casing and at -20 °C, most lead based batteries stop functioning.
- **Specialist Lithium:** batteries such as specialist Li-ion batteries can operate at -40 degrees with a reduced discharge rate and only in the discharge mode. Li-SOCl batteries can operate in extreme temperatures, with a temperature range of -55+150 °C [29].

When considering all the above information Li-SOCl emerges as a good candidate for the energy storage system due to its high energy density and suited temperature range. The battery however has two major downsides. Firstly, this type of battery is significantly more expensive than both the alkaline and lead acid types, and only rival the NiCad batteries when considering costs. Furthermore, Li-SOCl have been mainly developed mainly for military, aerospace, and sensitive equipment. This development has been focused on very small batteries and not storage on a large scale, thus a vast amount of batteries must be used in combination for application to the wind turbine system [205].

Lead-acid batteries can also be seen as a very good candidate when considering both the relatively cheap costs of such systems, and the relatively large sizes that are manufactured as standard. Such an option however would require that the area in which the batteries are stored to be heated in order to keep them in the required operational temperature ranges. It should be noted that such an option would seem to be feasible as it is already implemented in Antarctica at the Belgium research station [114].

In terms of recyclability, lead acid batteries can be relatively easily be recycled, with industrial techniques developed due to their extensive use within the automotive industry [111]. Li-SOCl can also be recycled at specialist centers and

require specific handling procedures bringing the cost of recycling to around five dollars per pound of such batteries [206].

In terms of cycle discharge properties, lead acid batteries are used in many deep cycle operations where low maintenance is required such as photovoltaic systems [207][208], whereas Li-SOCL batteries are used for very high energy density (in terms of size) applications [209]. However, it should be noted that lead acid batteries have decreased lifetimes when used in large discharge applications and as such must be sized accordingly.

In conclusion although Li-SOCL is a very good candidate in terms of operating temperatures they are simply too expensive at nearly 7 times as much as lead acid. In addition, lead acid is also seen as an extremely reliable technology due to the enormous world wide use [110][210]. Furthermore lead acid is extremely recyclable and as such the sustainable choice for an energy storage system [112]. Although lead acid will require an insulated operating area, the multiple benefits described above outweigh such a cost and so lead acid will be used for the system. It should also be noted that battery prices tend to be falling rapidly each year in response to the large investments from automotive companies wishing to produce electric cars, and as such future systems may be able to incorporate a lithium based solution in order to increase cycle life [211].

K.2 Back-up Energy System

The three "off the shelf" back-up generator types considered for the back-up system are summarized below, with the selected design discussed in the body of the report.

Diesel Generator: These types of generators are widely used. In comparison with other fossil fuel generators, the diesel generator is very fuel efficient [212][213]. Diesel is a conventional power source and as such this type of generator has a long life time and high reliability [115]. The main disadvantage is the noise produced by the generator and the emissions [118]. A generator which uses diesel produces NO_x , HC and CO [214][118]. On the majority of the research stations located in Antarctica this type of power generation is currently used as main energy system. The few research stations which mainly use a wind power system have diesel generators as back-up systems.

Biofuel Generator: This is a sustainable option for providing energy. Two types of fuel are currently on the market, biodiesel and ethanol. An ethanol-fuelled generator is already installed on the Brazilian Navy Station in Antarctica [215]. At this station the generator is used along with two diesel generators, however it can power the entire operating and scientific needs of the station [215]. Ethanol has a low freezing point which is an advantage for a system situated in the Antarctic. The greenhouse gasses emissions are reduced by 68% in comparison with a fossil fuel generator [216]. A disadvantage of using biofuel for the back-up system is that the production of this fuel is in an early stage, and such generator system will be experimental and may be less reliable than a conventional diesel system.

Hydrogen Fuel Cells: Fuel cells use fuel (hydrogen) and an oxidizer (air) to provide energy. In the cell two electrodes and one electrolyte are sandwiched. When oxygen passes over the cathode and hydrogen passes over the anode two reactions are initiated. These reactions generate electricity, water and heat. Hydrogen fuel cells can deliver high power rates, between 10 – 15 kW [217]. The major advantage of these cells is the lack of greenhouse emissions, and so it is a very sustainable option [218]. In addition during operation, fuel cells are quiet and will not harm the environment [218]. The fuel should be stored carefully as hydrogen can be ignited easily and so can be dangerous. The main disadvantage of an integrated fuel cell and storage system is the difficulty in storing the hydrogen at high pressures with high reliability and the large costs associated with such systems [219][219].

K.3 Cabling

In order to determine the required thickness of the different cables, the maximum power loss will be investigated. A maximum cable power drop of 3 % from power source to station is allowed. Several load paths are analysed, each having the maximum allowable drop of 3 %:

- **Wind Turbine Generator to Station:** This consists of the Wind Turbine generator to transformer, transformer to controller, controller to battery and battery to station. All losses are summed across all connections in percentage form in order to give a conservative value of the total loss of the given path.
- **Back-up to Controller:** The back-up is linked to the controller to control the charging of the battery by the back-up system, and then once again from controller to battery and battery to station. The back-up is also linked directly to the station to ensure power is available for the station in case of a controller failure, however as these cables are already installed at the station they will not be further analysed.

All losses are summed across all connections in percentage form in order to give a conservative value of the total loss of the given path.

In order to come up with a thickness for each cable, the American Wire Gauge (AWG) wire sizes are used [220][221]. For a given thickness of a wire this gauge gives the maximum allowable current able to safely pass through the wire. Furthermore the voltage drop over a given wire is calculated with the equation below [222]:

$$Vd = \sqrt{3} \frac{P}{V} R_c l \tag{K.1}$$

With P , V , R_c and l being the power, the voltage, the resistance per meter of copper and the length of the cable respectively. A specific thickness is selected by matching the minimum thickness required for maximum allowable power loss, while simultaneously able to safely handle the required current flow given by the AWG tables [220][221]. The voltage across all wires is assumed to be 240 volts in order to conform with British standard electrical configurations and eliminates the use of additional transformers [223]. The use of additional step-up and step-down transformers would be considered beneficial if the distances to the station were drastically increased, however due to the proximity of inhabitants and wildlife, and in order to reduce complexity, a safer operating voltage of 240 volts is selected. The power across a given connection are taken to be the worst case, highest power values and are given in Table K.2. The results of the above analysis are given in the main body of the report in Section 15.3. Keep in mind that the cabling from the wind turbines to the controller is made up of three different cables, all running through the same insulated tube.

Table K.2: Cabling

	Distance [m]	Cable thickness [mm]	Power [kw]	Power loss [%]
Wind Turbine Generator - Station	86	4.6-8.3	51	2.63
Wind turbine Generator - Transformer	10	4.6	17	0.52
Wind Turbine Transformer - Controller	70	6.5	17	1.83
Controller - Battery	5	8.3	51	0.05
Battery - Station	1	8.3	51	0.25
Back-up - Controller	5	7.3	40	0.24

K.4 Electronics

The electrical output frequency of the generator varies, however with a variable frequency power converter the grid frequency can be kept constant. The AC is transformed to DC and the DC needs to be inverted to the required AC of 50 Hz.

The variable frequency power converter exists of a rectifier at the generator side, an inverter at the grid side and a DC-link in between. At the generator side, two different rectifiers were considered: a diode-based rectifier or a Pulse Width Modulated-VSC (PWM-VSC) as can be seen in Figure K.1a and K.1b respectively. At the grid side, a PWM-VSC is used for both systems.

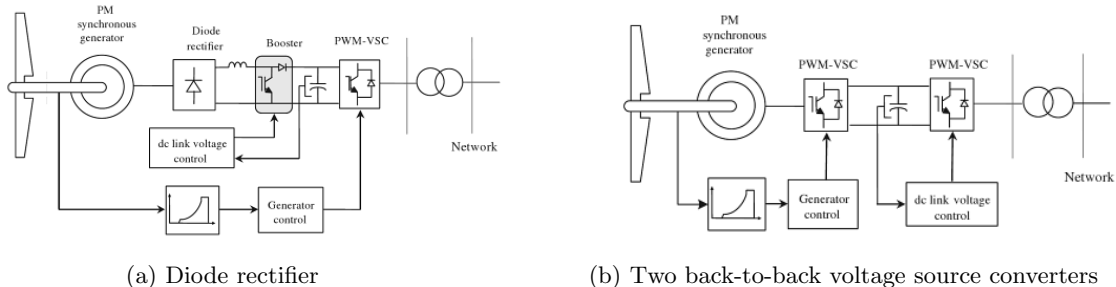


Figure K.1: Permanent magnet synchronous generator electrical scheme [22]

One drawback of conventional variable speed drives, is the large content of low frequent line-current harmonics due to the diode rectifier on the generator side. For a wide use of variable speed drives, care must be taken to limit these low order harmonics in the utility grid. The two back-to-back system suffers in a much lower extent from this problem, so

this system will be installed in the wind turbines. [224]

The electronics are installed at the bottom of the tower, in a well insulated housing. It is important that the sensitive electronics are protected against the cold which is better achieved when situating the electronics in a separate box. Additionally, this is favourable for the service and maintenance as is mentioned in Section 11. Each wind turbine needs its own transformer. These are placed near the wind turbines. The transformers can be bought off the shelf [225], but with material adjustments to cope with the extreme cold climate. The components made of steel shall be replaced with low temperature steels as are used in the nacelle and the tower. The transformer requires cooling, which the environment can supply by incorporating a fan. Dry-cooled transformers are being increasingly used, the windings of which are cast in resin. The design is more compact and less susceptible to fire hazards. [89]

K.5 Energy Supply Control Strategy

This section will explain how the energy supply to the research station is regulated by the performance control system. It is defined that the state of charge (SoC) should not drop below 50 percent or exceed 95 percent to avoid damage to the batteries/storage [226][227]. The energy control strategy is visualized in the diagram below followed by explanatory text.

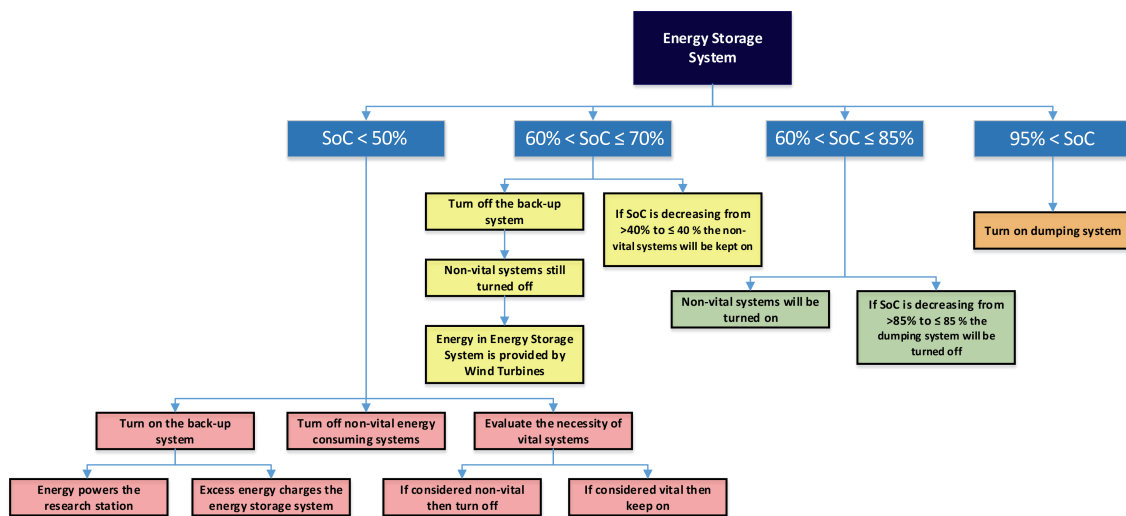


Figure K.2: Energy storage system

SoC < 50%: When the SoC of the battery drops below 50 percent, the back-up generator is turned on. All designated non-vital systems consuming energy will be turned off. Furthermore all designated vital systems consuming energy should be re-evaluated to ensure that their priority status has not changed, thus allowing for them to be turned off. The power provided by the back-up generator will be used to meet the energy demand of the research station. As the energy produced by the generator can not vary from second to second (for some types of back-up system this may not vary at all) all excess energy will go towards charging the battery.

60% < SoC ≤ 70%: Once the battery has been recharged and crosses the 60 percent SoC point, the back-up generators are turned off. It should be noted that if the battery SoC is below 60 percent and increases over this boundary, then the non-vital energy consuming systems remain turned off. If however the SoC was above 60 percent and then crosses this boundary, then the non-vital systems remain on and will only be turned on if once the battery level falls below 50 percent as stated in the paragraph above.

70% < SoC ≤ 85%: During this band all non-vital systems can remain on, or if the battery has been increasing and crossed the SoC boundary from below the 70 percent mark, then the non-vital systems can be turned on. Within this band the batteries are being charged by the wind turbine system and the back-up generator remains in the off status. It should be noted that if the SoC of the battery crosses the 85 percent boundary from above, the energy dumping systems must be turned off.

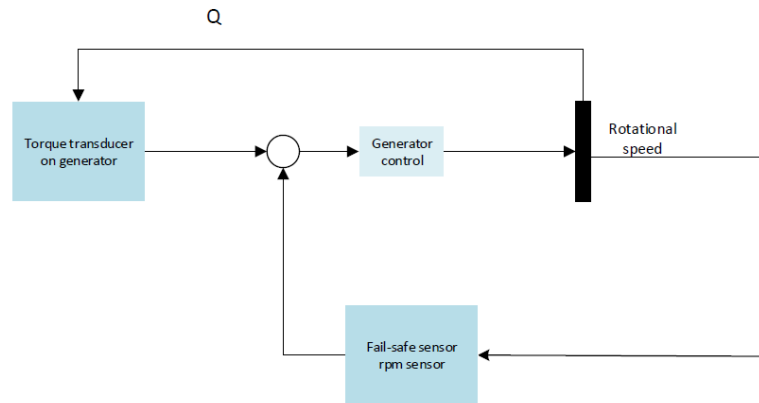
85% < SoC ≤ 95%: Below this band dumping is turned off and above this band dumping is turned on. Also within this band the back-up generator remains off, and both vital and non-vital systems can remain on. This band can be seen as a buffer between the energy dumping and normal mode, in order to prevent fluctuations.

95% < SoC: Once the batteries SoC have reached above 95 percent, the battery system must start to dump energy so as not to overload the batteries or other components within the system. The control will at first try to dump energy in useful systems. These could be in the form of extra experiments that could be run on the station such as Lidar experiments or other experiments deemed useful for BAS, or possible water heating. In the case that all useful applications are used and there is still excess power being produced, energy will be dumped in resistive blocks.

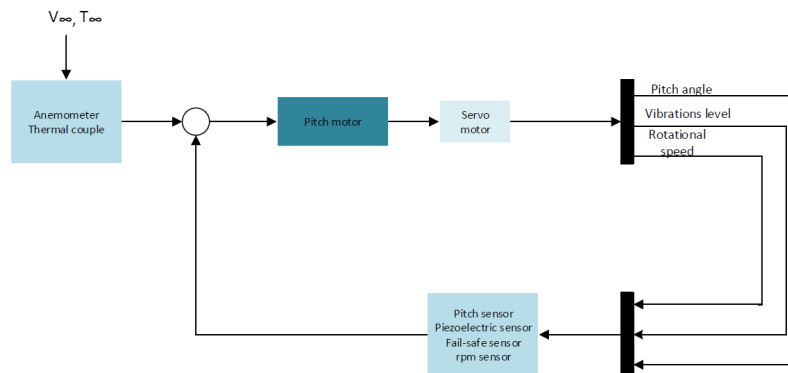
As can be seen from the various bands, the energy control system is designed to avoid constant fluctuations. Such fluctuations are avoided as they could cause damage to electrical systems due to constant switching from on and off. Furthermore the back-up system in particular will have a given response time when being turned on and off and thus such changes should be limited. This is done by providing buffer ranges as stated above and also progressively turning systems back on once they have been turned off rather than all at once, thus also avoiding sudden spikes of power required.

L. Hardware & Software Diagram

Below the simple control schemes are presented. These show the relations between sensors (blue blocks) and actuators (dark blue blocks) through the CPU (light blue blocks) for energy production system, de-icing system, cooling system, break system and batteries and back-up system.



(a) Overview of rotational speed control



(b) Overview of pitch system

Figure L.1: Overview of energy production until rated velocity L.1a and after rated velocity L.1b

In Figure L.1a the control scheme of rotational speed control is displayed. Until the maximum rotational speed (15 rad/s) is reached, the wind turbine runs at different rotational speed with constant pitch angle in order to achieve the optimal tip speed ratio. To control the rotational speed the torque produced by the wind turbine is measured on the generator, after which the magnetic field on the generator is changed, if necessary, correcting the rotational speed of the wind turbine. At the rated velocity a certain amount of torque is produced; when this torque is achieved, the pitch system is turned on (Figure L.1b), and so the pitch angle is changed for each different torque measured. Before cut-in and after cut-out velocities the pitch angle is the one at which the aerodynamic loads are smallest. For both systems, if something fails the fail-safe system turns on the brake system. It will also notify the monitoring system.

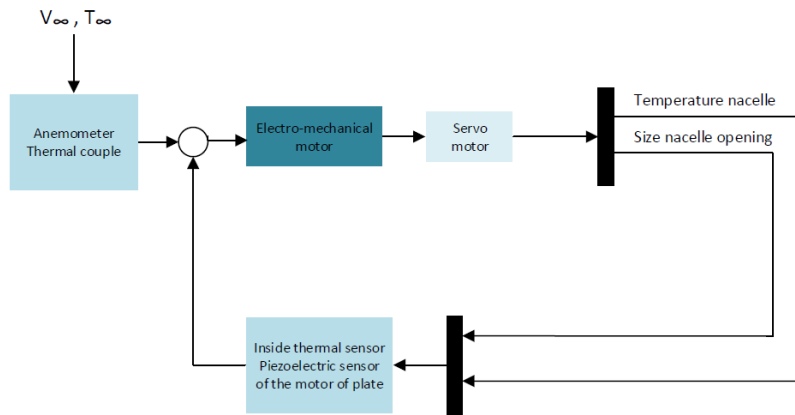


Figure L.2: Overview of cooling system

The cooling system of the nacelle, showed in Figure L.2, has as input the wind velocity, external and internal nacelle temperatures and the position of the plate (measured by the force made by the plate with piezoelectric sensor). The electromechanical actuator will be controlled by the servo to change the size of the opening in order to have a constant temperature of $30\text{ }^{\circ}\text{C}$ inside the nacelle, when the wind velocity is larger than 30 m/s - cut-out velocity - the opening is completely closed.

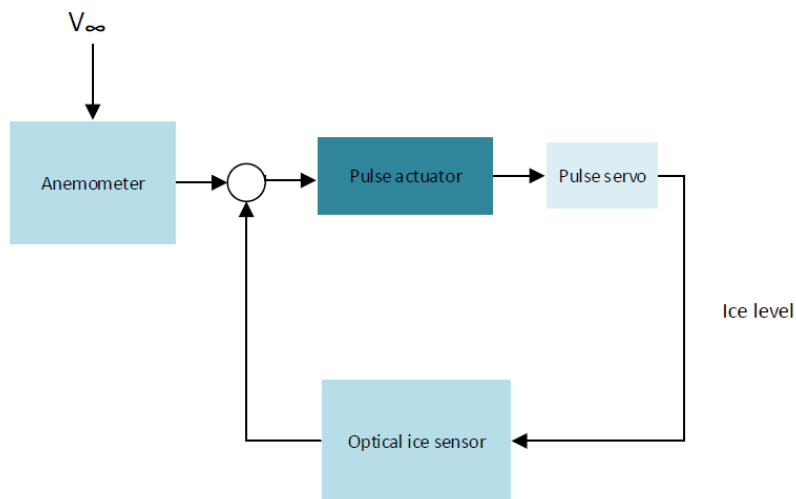


Figure L.3: Overview of de-icing system

The de-icing system, Figure L.3, is switched on when the ice level reaches a certain value, however when the wind velocity is lower than 3 m/s or larger than 30 m/s the system is turned off.

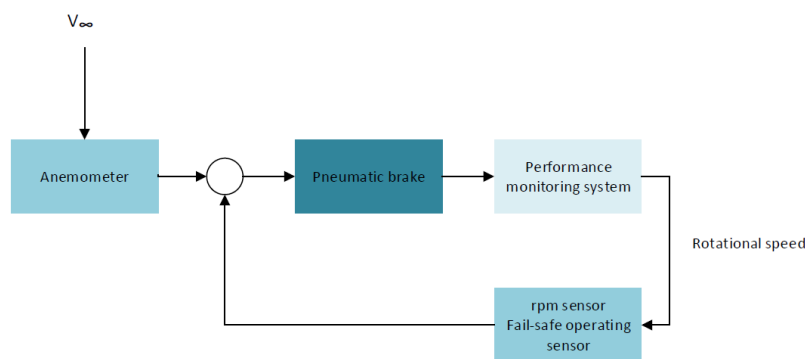


Figure L.4: Overview of brake system

The pneumatic brake, Figure L.4, is switched on when crossing the cut-in wind speed boundary from above for more

than fifteen minutes, or when crossing the cut-out wind speed boundary from below for a duration of more than a fifteen minutes. When the system fails, the fail-safe operating sensor will notify the monitoring system and the brake can be manually turned on.

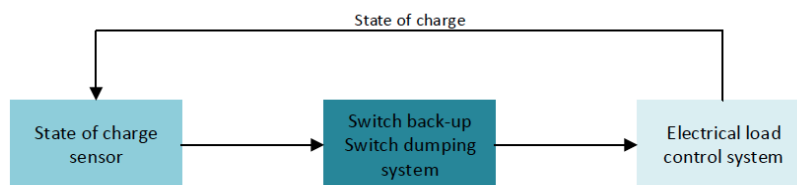


Figure L.5: Batteries & back-up system

The relation between the batteries and back-up system can be seen on the section K.5. In parallel with batteries & back-up control system shown on Figure L.5, in case of the aerodynamic brake (pitch control) and mechanic brake fail, the back-up system and batteries are disconnected automatically, in addition there are manual brakes for each of the wind turbines. Also the batteries, the back-up system and the station can be disconnected from each other in case of an emergency.

M. Maintenance Task List

Below, the task list is shown that will be used to perform the maintenance sessions each year. This list was based on an offshore maintenance schedule[228] and the manual of the WT 6000 wind turbine, also used on Antarctica[229].

Table M.1: Preventive maintenance of the wind turbine subsystems

System	Component	Action	
		1 year	5 years
Blades	Outer surface	V	
	Bolt connection	V	
Blade pitch	Blade bearings	V, G	P
	Shaft bearing	G	P
De-Icing		V, F	
Main shaft	Thrust bearing	G	P
	Oil distribution box	V	
Braking system	Emergency stop	F	
	Mechanical brake	F	
	Brake linings	V, X	X
Generator	Shaft bearings	G	
	Windings		V
Nacelle	Bed plate, hub	V	R
	Nacelle cover	V	
Tower		V	
Yaw system	Yaw bearing	V, G	P
Transformer		V	
Cables		V	
Control system		V	

V Visual inspection

G Greasing

P Measurement of bearing play

X Exchange of components if necessary

N. Project Cost & Electricity Cost

In this chapter additional information is given about the project costs and electricity price. The methods used to perform the calculations will be presented and the reasoning about obtained numbers is explained. This chapter is subdivided into the capital cost and the annual energy production.

N.1 Capital Cost

For the analysis of the current market, comparable wind energy systems are analysed. Multiple wind turbines are already present in the harsh Antarctic conditions to power research stations. The market analysis is performed based on research papers and existing wind turbines.

According to the American Wind Energy Association (AWEA), the capital cost per kW and the cost of energy produced by small wind turbines is still higher than for large scale turbines [230]. These costs vary significantly depending on the competitiveness and the different factors influencing installation, and generally lie within the range of $\text{€}2000/kW$ and $\text{€}4500/kW$ for small wind turbines. A feasibility study at the Uppsala University of Sweden revealed that the averaged cost for wind turbines that could be used in Antarctica is $\text{€}2000/kW$, however these turbines were not specifically designed for a particular customer and have been built frequently. The same study showed that the company 'Wind Steam Power Systems' is able to develop a new turbine for specified Antarctic conditions at the price of $\text{€}7000/kW$ to $\text{€}9000/kW$. From a performed market analysis a cost figure of $\text{€}7000/kW$ was determined based on similar research stations.

In the market analysis the Princess Elisabeth Station (Belgium), Mawson Station (Australia), McMurdo Black Island (United States of America), Scott Base (New Zealand), Neumayer (Germany) and Sanea IV (South Africa) are also considered. A target cost was made based on statistical data obtained from these wind energy systems. However, since only a relatively small amount of information is available about wind energy systems on the Antarctic continent, the analysis is expanded with up-scaled cost values for small wind turbines within the same power range. The price estimations obtained from these references are combined, resulting in a price estimation of $\text{€}6657/kW$.

Table N.1: Wind turbine component cost

Rotor		€79,000.00
	<i>Blades</i>	€63,000.00
	<i>Hub</i>	€6,000.00
	<i>Pitch</i>	€10,000.00
Tower		€97,000.00
	<i>Tower structure</i>	€75,000.00
	<i>Foundation</i>	€22,000.00
Nacelle		€62,000.00
	<i>Generator</i>	€30,000.00
	<i>Shaft</i>	€5,000.00
	<i>Bedplate</i>	€10,000.00
	<i>Brake system</i>	€7,000.00
	<i>Housing</i>	€10,000.00
Other		€41,000.00
	<i>Transformer</i>	€8,000.00
	<i>Converter</i>	€9,000.00
	<i>Cabling</i>	€15,000.00
	<i>Screws</i>	€3,000.00
	<i>Sensors</i>	€6,000.00
Total wind turbine		€279,000.00

Additionally, based on references, estimations are made for each component of the project cost [164],[231],[232]. The capital cost is subdivided in the wind turbine cost itself, the civil work and construction cost and additional costs such as development and engineering costs, consultancy costs, licensing costs, etc. The wind turbine cost share generally accounts for 75 – 94% of the total capital cost for onshore turbines. For the wind turbine designed in this project,

this percentage is estimated to be 80%. The estimation is based on the fact that the wind turbine complexity will be generally lower than the large-scale commercial turbines that are currently installed. Additionally, it is expected that only a small grid will be used for the wind energy system considered in this report, the grid connection will be relatively simple as compared to the connections for the larger wind farms. Recall that the system being described will make use of a battery storage system, which is not considered in the wind turbine cost. Therefore the costs of this system is excluded from the current cost analysis. Regarding the percentage of civil works cost of the total investment cost, it is possible to state that this percentage will be high compared to a conventional installed wind turbine that is placed in a less harsh and remote environment. Generally, the civil works account for 4 – 16% of the capital cost, so this number is assumed to be 15% for the case of this wind energy system. This is mainly the consequence of the relatively inaccessible location of the site and the harsh environment in which the turbine operates. The last 5% of the capital costs are induced by miscellaneous costs. Generally, this number lies between 4% and 10% for onshore turbines, but since this wind energy system is designed using low cost tools and without the use of expensive resources, the 5% value seems acceptable. In Table N.1, the detailed cost break-down is shown and in Figure N.1 a visual representation to understand how the costs are actually divided amongst the years can be found.

N.2 Annual Energy Production

The annual energy production (AEP) is a measure of the total power produced during the whole year at the site. In order to compute the annual energy production, it is necessary to combine the power curve with a probability density function for the wind.

The probability density function of the wind speeds at the Signy site is derived from the wind speed data gathered by the British Antarctic Survey over several years. The probability function shows the probability that the wind speed lies in a certain range. Usually a Weibull distribution is obtained to present the data as a smooth function. The Weibull function is modelled through a scaling factor A and a form factor k . The parameters A and k are determined corresponding to the best fit of the local meteorological data, using Matlab. However, due to the deviated form of the Weibull distribution with respect to the histogram, both will be used to calculate the AEP. In Figure N.2 the probability density function of the Signy wind speeds is displayed.

The power curve found from the blade design, describes the power as a function of the wind speed. The rated velocity and rated power are respectively 10.16 m/s and 17 kW . These values are based mainly on the fact that it is required to deliver for a long period of time a constant power rather than having a maximum energy output over the year. As explained before, the cut-in and cut-out speed are set to be 3 m/s and 30 m/s respectively. The power curve is shown in Figure 10.4.

By now multiplying the power curve with the wind speed probability density function and the total amount of hours in a year, the annual energy can be obtained. The AEP of the wind energy system for the Signy station can be obtained using the Equation N.1 [68], where T is the total amount of hours in a year, V_{in} and V_{out} are the cut-in and cut-out wind speed, $P(V)$ is the power for a certain wind speed and $f(V)$ is the probability of a certain wind speed.

$$AEP = T \int_{V_{in}}^{V_{out}} P(V) \cdot f(V) dV \quad (N.1)$$

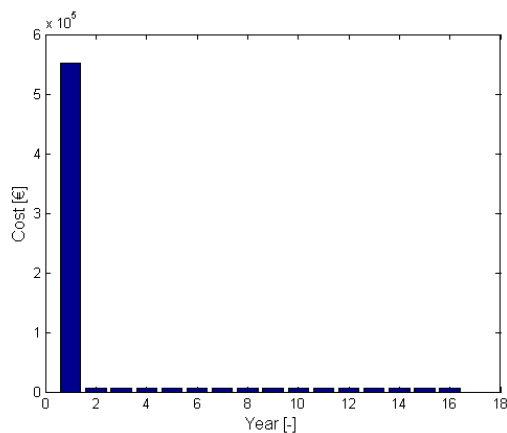


Figure N.1: Costs throughout lifetime

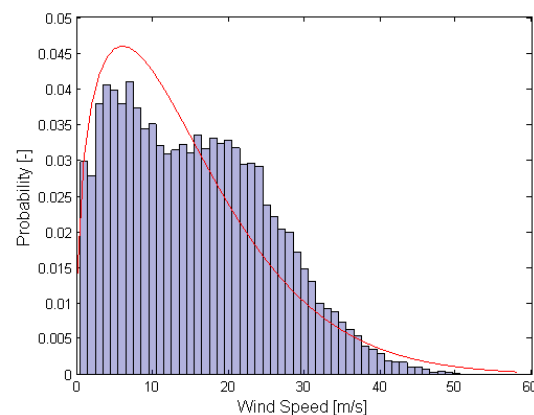


Figure N.2: Wind speeds at the Signy station

O. Model Flow Charts

Within this section the computational model flowcharts are shown in order to give the reader an additional overview of the MATLAB code layout. The flow diagrams are split into three parts representing the major turbine system component models, being models of the blades, nacelle and tower respectively.

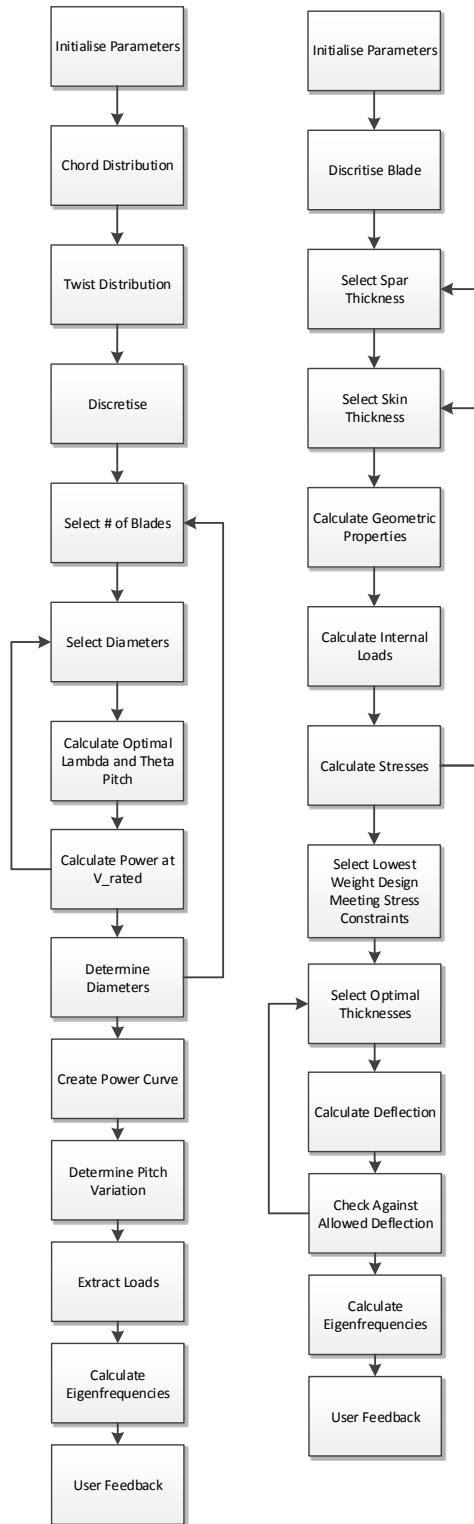


Figure O.1: Blade computational model flowchart

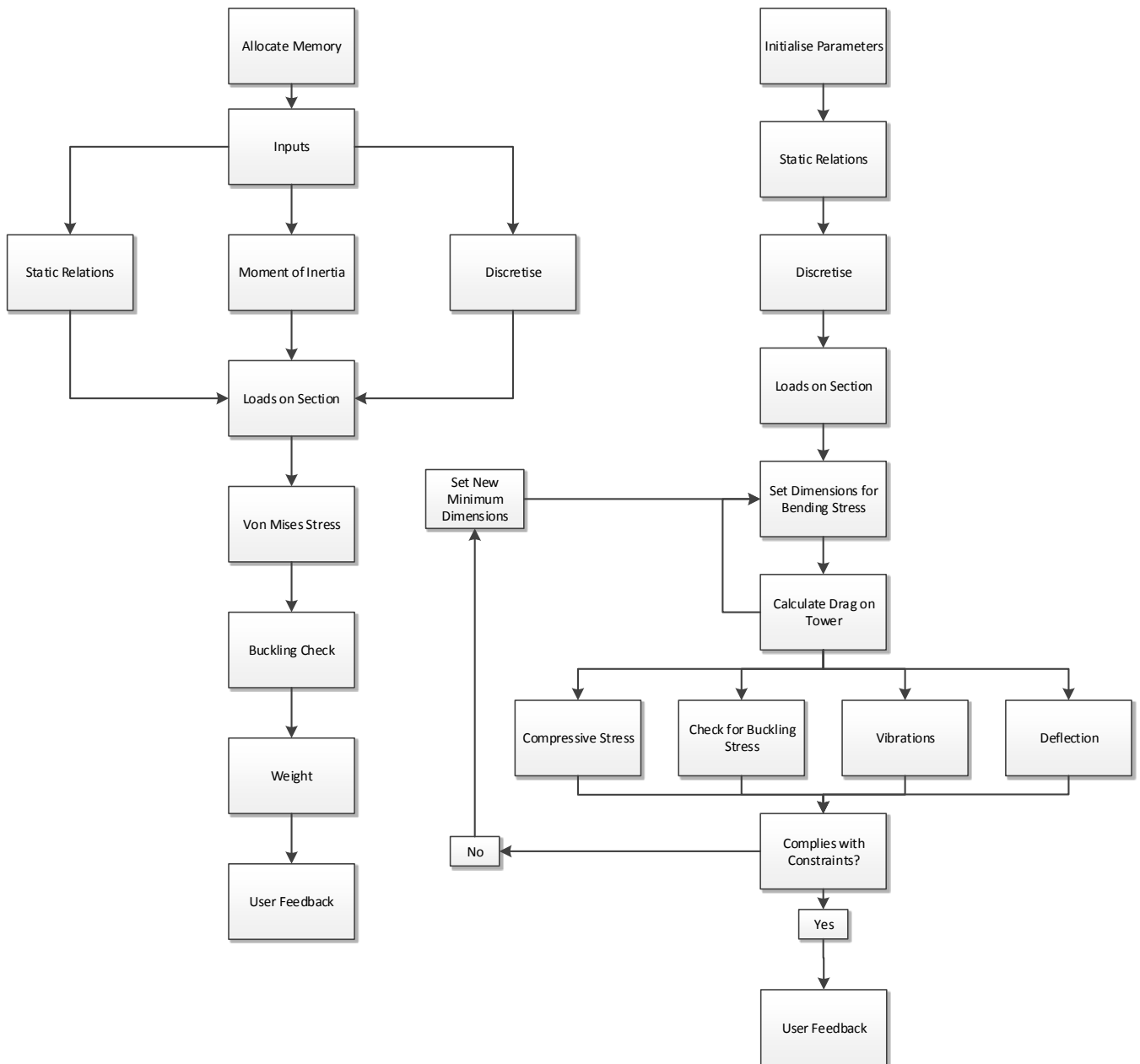


Figure O.2: Nacelle (left) and tower (right) computational model flowchart

P.3D Catia



Figure P.1: 3D CATIA Model